STUDIES IN THE BEHAVIOUR OF MOLECULAR BEAMS

THESIS

submitted for the degree of

DOCTOR of PHILOSOPHY

of the

UNIVERSITY of GLASGOW

by

JOHN J. McCARROLL B. Sc.

November, 1967.

ProQuest LLC.
789 East Eisenhower Parkway
P.O. Box 1346
Ann Arbor, MI 48106 – 1346

Acknowledgments

I would like to thank my supervisor, Dr. S. J. Thomson, for suggesting the problem which is the object of this thesis. His advice and unflagging encouragement have been deeply valued throughout this work.

I also wish to express my gratitude to the technical staff of the Chemistry department. In particular, I thank Mr. J. Hardy for his assistance with the many electronic problems encountered, the glassblowers under Mr. J. Connolly, the staff of the general workshop under Mr. J. Rae, and Mr. A. McQuarrie and Mr. A. Ritchie for laboratory assistance. In addition, I would like to thank those who helped me to analyse data - Mr. D. Lister who compiled the computer programme used and Miss F. Green. I thank Dr. D. L. Adams, Dr. K. C. Campbell, Dr. G. Webb and my colleagues of this laboratory who have been responsible for much helpful discussion.

The Science Research Council I thank for a maintenance grant for part of this work.

Finally, I would like to thank my wife for typing this thesis.

Contents

Abstract

This thesis describes the design, construction and development of a molecular beam apparatus for the study of interactions of gases with solid surfaces in systems of catalytic interest. The apparatus has been used in an investigation of the displacement, from palladium surfaces, of the surface species resulting from the adsorption of ethylene C-14 by beams of acetylene and ethylene.

The apparatus produced ultimate static vacua of about 5×10^{-9} torr. The palladium was in the form of a film, freshly deposited in vacuo, to which was admitted ethylene C-14 at a pressure of greater than 5×10^{-2} torr, known to provide saturation of the surface with adsorbed species. The fate of the isotopically labelled surface species was followed in vacuum desorption and in beam-displacement reactions. The detector for radioactivity was, in the final form of the apparatus, a lithium-drifted silicon solid-state detector mounted close to the target inside the beam system.

The maximum flux intensity which could be directed on to the surface was 2.5×10^{13} molecules/cm^2/sec as against a background of scattered beam material of 4.1×10^{13} molecules/cm^2/sec. The beam was produced from a source whose pressure was 2×10^{-3} torr and whose temperature could be varied between 15°C and 350°C. The temperature of the target was variable between 15°C and 90°C.

The displacement of surface species by beams of acetylene and ethylene has been observed. The effects of changing surface and beam temperatures, and beam intensities, on the rate of displacement by acetylene beams, have been studied. Increased rate of displacement resulted when target temperature, or beam intensity, was increased, but not when beam temperature was increased. With

beams of ethylene, whether or not displacement occurred appeared to depend on the amount of vacuum desorption which had occurred prior to the introduction of the beam.

In both the displacement and vacuum desorption experiments three phases of surface species were clearly visible. A fast desorption or displacement step was followed by a slower step, while a third phase was retained on the surface. In all cases of desorption and displacement where it could be discerned, the kinetic order of the rate of loss of each phase from the surface was unity with respect to the surface concentration of that phase. We observe, typically, a $t_{\frac{1}{2}}$ value of 18.3 minutes for displacement of the more slowly removed surface species, at a surface temperature of 60°C, by a beam of acetylene, with a flux of 2.5×10^{13} molecules/cm^2/sec.

The relative amounts of retained and displaceable species could be correlated with the vacuum conditions in which the films were prepared. A film contaminated by oxygen displayed a lack of displaceable phases and consequently a high percentage of the retained phase. A typical film, prepared in a residual vacuum of about 3×10^{-7} torr, resulted in values for the quantities displaced in the fast and slow displacement phases of 15% and 20% respectively, with 65% of the initially observed surface species retained.

Approximate values of the activation energies for both desorption phases (6.1 k cal/mole and 8.3 k cal/mole), and for the slow phase of acetylene displacement (5.4 k cal/mole), have been calculated.

Attempts have been made to construct a model, which is necessarily speculative, of the surface species to fit the three-

fold heterogeneity displayed in these studies. The model evolved has been compared with the results produced by others in conventional catalytic studies.

The results are particularly meaningful in the context of surface heterogeneity and its effect on the rates of catalytic reactions. Not only can it be said that the surface was heterogeneous, in that it displayed an active and an inactive fraction, but also that the active fraction was itself heterogeneous in nature.

The study is, we believe, the first attempt to study systems of direct catalytic interest using the molecular beam method.

Chapter 1
Introduction

It has been the intention during the course of this work to design and build an apparatus with which the molecular beam method can be employed to study systems of interest in the catalytic field and to demonstrate its potential as a method of investigating surface/gas systems. To this end an apparatus has been developed and used in a variety of systems.

It is pertinent to ask the question - "why use the molecular beam method in surface studies?" What advantages can be gained by using this method over the more conventional methods of study of surface chemistry and catalysis? The answers lie in the characteristics of molecular beams.

Molecular beams are well-defined, uni-directional streams of matter travelling, of necessity, through a vacuum, the generic term "molecular beams" applying to beams of both atoms and molecules. The basic advantage achieved is that the effective temperature of the beam may be altered independently of the temperature of the solid surface on which it impinges and vice versa. Energy separation of the two phases, gas and solid, comprising the reaction system can thus be achieved.

Their directional characteristics can be used in reflection and diffraction studies from surfaces. Use can be made of their localised character in surface diffusion and mobility studies as well as in condensation studies. They may, to facilitate interpretation, be made mono-energetic by velocity selection, though this is achieved only with loss of signal strength and consequent detection problems. Finally, they offer a method of admitting small amounts of material continuously to a surface,

maintaining a constant effective "pressure" of gas on the surface - a situation which cannot be duplicated by admitting aliquots of gas to a closed system.

In the following chapters we shall examine the uses to which the molecular beam method has already been put in the study of the interaction of surfaces with gases and gaseous matter and discuss the selection of the systems studied in this work; trace the design and evolution of the apparatus used in the present study; describe its operation and performance; discuss the results achieved and their implications; and look at the future potential of the method.

Chapter 2

Background and Approach to the Study

(1) A Review of Molecular Beam/Surface Interactions

Whilst the main areas of research in which the molecular beam method has been used were and are studies of reactive and non-reactive scattering, investigations of the Maxwell-Boltzmann distribution of velocities and the determinations of nuclear spins, the work in this thesis is concerned with surfaces. Thus it is proposed to review in this section surface studies.

The first molecular beam was produced by Dunoyer [1] in 1911. His apparatus consisted of an evacuated glass tube with two constrictions. In one end of the tube he placed sodium metal which, when heated, produced a dark deposit at the far end of the tube; it covered only that area which could be reached by sodium atoms which had passed in a straight line through the two constrictions to condense on the glass wall of the apparatus. His object was to demonstrate the linear motion of atoms in vacuo, and his study fell into the first of the four categories into which the field of molecular beam interactions with solid surfaces can be separated. These are:

(1) detection of the presence and position of a molecular beam by condensation on, or chemical reaction with, a solid surface;
(2) studies of reflection or diffraction from surfaces;
(3) studies of condensation phenomena;
(4) in which the interaction is of specifically chemical interest.

The first category includes such work as the original Stern-Gerlach experiment [2], in which a neutral beam of silver atoms

was deflected by a magnetic field, to be collected as an oval-shaped deposit on a glass plate where in the absence of a magnetic field a linear deposit is observed. Previously Stern [3] had deposited a beam of silver atoms on to a rotating glass plate to demonstrate the Maxwell-Boltzmann distribution of atomic and molecular velocities. More recently several workers [4-6] have used the deposition detection technique to determine the nuclear spins and moments of radioactive atoms. This method is confined to those systems in which a high and constant sticking coefficient is evidenced; i.e. in which a high fraction of the beam falling on the detector is condensed.

The surface ionisation detector [7] also falls into this category. In this detector a hot tungsten filament or ribbon is used to ionise the atoms or molecules impinging on it with almost complete efficiency. The ions are then collected on a negatively charged plate and the positive ion current is used as a measure of beam intensity. This method has been used successfully for the detection of the alkali metals, their compounds and a few other elements, such as gallium and indium. Several detection systems have been developed of a chemical nature: atomic hydrogen beams have been detected by the reduction of yellow molybdenum oxide to the blue oxide [8] and Simons and Glasser [9] have used a tellurium oxide detector which reacts with atomic hydrogen, oxygen and the halogens. In all of these systems the study of the interaction of the beam with the surface was secondary to its use as a detector measuring beam intensity and position.

The specular reflection of molecules from surfaces (i.e. in which the angle of incidence and the angle of reflection are the same) was first demonstrated by Knauer and Stern [10] in 1927, using beams of hydrogen and helium with metal surfaces and later with cleavage surfaces of sodium chloride. Later Johnson [11]

and Kerschbaum [12] showed the same phenomenon for beams of atomic hydrogen. Estermann and Stern [13] provided the first proof of the diffraction of molecules at surfaces, using beams of hydrogen and helium in interaction with cleavage surfaces of lithium fluoride; diffuse maxima were observed due to Maxwellian distribution of velocities in the incident beam. Estermann, Frisch and Stern [14] refined the early study by using velocity selected beams, confirming the associated wave nature of matter.

Lately reflection and diffraction studies have again been carried out under the impetus of space research. In these the interest has lain not in the phenomena per se but rather as a guide to the better understanding of the surfaces under investigation. Crews [15, 16] has studied the reflection of helium and argon from cleavage planes of lithium fluoride, finding no evidence of diffraction for argon. Smith [17] has studied the scattering of helium, neon, argon, krypton and deuterium from nickel and, with Fite [18], of hydrogen from tungsten. He finds the superimposition of a cosine distribution and a preferred, though pseudospecular, distribution (i.e. between the specular angle and the normal to the surface) in the reflection pattern. With Saltzburg [19] he has demonstrated the diffraction of helium from clean gold films and shown its dependence both on surface cleanliness and crystal orientation; with argon pseudospecular reflection is observed which is not affected by the presence of adsorbed gas molecules on the surface. Moore, Datz and Taylor [20, 21] deduce, from their observations of the scattering of deuterium and helium by platinum foils, information on residual species on the surfaces being studied. The velocity distribution of scattered beams of potassium from various surfaces has been examined by McFee and Marcus [22], who found that at low surface temperatures the scattered beams had Maxwellian distribution of velocities

characterised by the surface temperature.

Attention has been sustained over a long period of time on the condensation of metal atoms on cold surfaces [23-28]. Theoretical models [29-31] have been evolved to cover the results obtained on surface nucleation, sticking coefficients and the effects of temperature, surface cleanliness and surface migration. An excellent review by Wexler [32] covers this material in great depth.

In the three categories already mentioned - which can be classified as surface physics - a great deal of work, some of it overlapping in content, has been published in the last forty years. By comparison, the fourth category - surface chemistry - contains little published work - and what there is is comparatively recent.

Lifetimes of adsorbed species were studied by Holst and Clausing [33] and Veszi [34] in the late twenties. More recently they have been the object of study by Leonas [35] and by Dewing and Robertson [36]. The former showed lifetimes for argon, nitrogen and carbon dioxide with incident energies of approximately 1 eV on copper, iron and tantalum of between 10 and 30 microseconds; the latter showed retention times of the order of 1 millisecond for molecular hydrogen on nickel and observed changes which they related to the cleanliness of the surface. Radiotracer measurements of silver desorptions from, and lifetimes on, molybdenum have been carried out by Goeler and Peacock [37]. Similar studies of gold on molybdenum and gold and copper on tungsten have been performed by Goeler and Luscher [38] and Godwin and Luscher [39] respectively. They have inferred details of the nature of the bonding process between adsorbate and substrate and speculated on the effects of surface heterogeneity on their results. Scheer and Fine [40] have studied the desorption of alkali metals from

rhenium at high temperatures and proposed a model to describe the interactions observed.

McKinley [41] has studied the translational energy accommodation in the nickel-chlorine surface reaction, finding that, at surface temperatures in excess of 1100°K, between 20% and 40% of the chlorine reacts on the surface. Anderson and Boudart [42] have investigated the interaction of oxygen beams with germanium surfaces using a supersonic beam, deducing that oxygen molecules must lie flat on the germanium surface prior to adsorption. Madix and Boudart [43] refined the picture by using an effusive beam of precisely known temperature rather than the unpredictable supersonic beam technique. Hollister, Brackman and Fite [44,45] have studied the interaction of atomic hydrogen and oxygen and molecular hydrogen, oxygen, nitrogen and water with solid surfaces, being particularly interested in the recombination of atoms on the surfaces. Beeck [46] has determined the accommodations of hydrocarbons relative to argon on nickel surfaces. Dalins [47] has linked the techniques of molecular beams and field emission microscopy to study the adsorption, desorption and migration of caesium on tungsten, in the first instance, under ultra-high vacuum (u.h.v.) conditions. It should be noted that in addition to the direct surface chemical studies above the recent reflection experiments mentioned earlier have often been used to probe surface cleanliness and are thus of indirect interest.

Various review articles and books [48-53] have contributed to the general picture of the use of the molecular beam method.

(2) The Potential Problem and the Experimental Configuration

The work already described was to be only of indirect interest to us in the field in which we proposed to use the molecular beam method - the surface chemistry of catalysts. What did emerge from the literature was an insight into the practicalities and difficulties of the beam method. From this insight came the experimental configurations used in this study. The problems to which the molecular beam method was applied came from our interest in surface chemistry and catalysis. In this section we discuss the advantages and limitations of the method in our field, the type of problem to which it could best be applied and the general experimental configuration adopted.

It is a condition, sine qua non, that molecular beam studies can only be carried out in vacuo. Furthermore, the flux of a typical molecular beam is between 10^{13} and 10^{14} molecules/cm^2/sec and the pressure to which this is equivalent is about 10^{-7} torr. It is thus impossible to duplicate the conditions under which the formation of monolayers of adsorbed species on clean surfaces is observed. Such studies are performed typically in the pressure range 10^{-4} torr to 1 torr. Growth in surface concentrations of adsorbed layers using the molecular beam method cannot therefore be interpreted in precisely the same way as in classical adsorption systems, though obviously such studies would be of great interest. Nor was it our intention to use data from reflection experiments to gain information on the nature of surfaces.

We turned to the displacement of adsorbed species on metals by a second species in the gas phase - which could be introduced by the beam. Typical of the species in which we are interested are ethylene, acetylene, propylene, hydrogen, oxygen and mercury;

displacement reactions of various combinations of these species on metal surfaces have previously been studied in this laboratory. The main advantages seen at the outset in the proposal to use the molecular beam method were, as already stated, the ability to vary separately beam gas and surface temperature and the facility of continuous and constant gas flux on the surface, with no chance of any species desorbing from the surface reacting again with that surface - it is pumped away. The pre-adsorbed surface species must of course be stable in vacuo or at least be desorbed only slowly with time. The species listed above had already displayed this pre-requisite condition in studies in this laboratory.

Having decided to study the reactions of an adsorbate on a metal surface with a beam species, decisions were made which were to settle the experimental configuration adopted. The type of surface and the interrogatory method employed to obtain information about the surface processes were considered and selected at an early stage. They did not change to any extent throughout this work.

Surface roughness, on a macro-scale, precludes the study of powders and metals supported on powdered or granular substrates. Foils are difficult to prepare such that they exhibit clean surfaces, whilst single crystals, although almost uniquely guaranteeing the crystallographic orientation of the metal, are similarly difficult to clean. Freshly evaporated metal films, on the other hand, can easily be prepared in a relatively clean state. For comparison of results the data available for films exceeds in quantity that for foils and single crystals. Our choice therefore fell on films.

The use of the molecular beam method places a severe

restriction on the area of metal which can be studied, viz. 1 - 10 cm^2. A beam to cover a larger area at high beam intensities requires higher pump speeds to cope with the additional gas inflow. Experimental difficulties rise in proportion. For a given, constant pump speed a larger area of film can be covered only at the expense of reducing beam intensity - thus increasing the difficulties of detecting the beam or its effects. This restriction on the area of the surface which can be studied places, in turn, restrictions on the choice of interrogative method which can be employed.

Various methods, already mentioned, have been used in which the direct study of a beam reflected from a surface has been used to elucidate the nature of the surface. For example, a mass spectrometer has been used [20] to detect phase shifts of reflected, chopped beams, as well as follow the angular distribution of the reflected beam. From the resultant data deductions could be made about surface contamination by adsorbed species. Such information cannot, however, be called quantitative. In our case it was felt that following the behaviour of the pre-adsorbed species itself would more easily provide information on the surface reactions we wished to study. This entails following in detail changes in the concentration of surface species on an area of film of the order of 5 cm^2 - a total amount of adsorbate of about 10^{15} molecules. Conventional pressure measurements are, of course, useless. Such techniques as gas-liquid chromatography would entail the abstraction of desorbed material from the system - and in any case their limits of detection are not low enough. Direct spectroscopy of the adsorbed species is difficult both experimentally and to interpret. Only the best mass spectrometers could be used to detect the stated quantity and then only if the rate of transfer to the instrument is rapid. With a low rate of transfer no detection would be possible.

Direct study of the surface with its adsorbed layer is possible. Low energy electron diffraction can only be used with single crystals, which we have already rejected, whilst field-emission microscopy is only possible with certain combinations of metals and adsorbed species. Field-ion microscopy is incompatible with the molecular beam method, requiring as it does the presence of a gas - usually helium. The technique adopted was the radio-tracer method, involving the labelling of the adsorbed species with a radio-active isotope. The method is relatively simple and independent of the surface under study. The number of disintegrations detected is directly proportional to the concentration of the labelled adsorbed species. The method, of course, restricts the adsorbed species used to one which can be obtained labelled with an unstable radioactive isotope. Carbon compounds, mercury and hydrogen can be obtained which satisfy this condition, the isotopes used being ^{14}C, ^{203}Hg and ^{3}H respectively. The radio-tracer method thus allows us to use the compounds in which we have previously stated our interest.

The feasibility of the method was calculated, for a possible substrate, postulating that at least 3 counts per second (cps) must be observed in the over-all system of counter and adsorbed species to follow changes in surface concentration with time. Ethylene C-14 is available from the Radiochemical Centre, Amersham, with a specific activity of approximately 50 mC/mM (milli-curies per millimole). An activity of 1 Curie is defined as 3.7×10^{10} disintegrations per second (dps). If we postulate that we can achieve a detection efficiency of 1% we require a rate of disintegration from the surface of 300 dps. This requires an amount of ethylene equal to $300/50 \times 3.7 \times 10^{10}$ mM, i.e. approximately 2×10^{-7} mM or 1.2×10^{14} molecules, which is much less than the value already quoted as the expected surface amount.

The radio-tracer method seemed, from the outset, the most promising interrogative technique available and was adopted.

As it was envisaged that carbon-14 compounds would be used as the surface species, the detector system had to be chosen with care. Carbon-14 emits β-particles of low energy (E_{max} = 156 keV) and a sensitive detector of low background and good resolution is necessary. (With tritium (E_{max} = 18 keV) the problems are much greater). An internal detector - as against an external counter such as a Geiger counter detecting γ emissions from ^{203}Hg through glass - must therefore be employed. A gas-filled ionisation detector such as a Geiger or proportional counter has to have a window to contain the counting-gas filling but which is thin enough to pass as many particles as possible to its sensing volume. This window would have had to be strong enough to withstand the pressure differential between its inside and the vacuum in which it would operate. While such detectors have been constructed, it was felt that there was the possibility of gas leakage across the window. A scintillation-detector head with a high transparency to carbon-14 β-particles and a robust vacuum window was evolved and used initially.

As this method of interrogating the system would detect the effects produced by a beam rather than the beam itself, it is important that the beam flux on the target surface produce effects distinguishable from those of the flux due to the presence of random gas molecules in the target area - caused by normal operation of the beam. We arbitrarily fixed the ratio of beam: background flux at which to aim at 1 : 1. This would enable the effect of changing beam temperature to be seen amongst the constant-temperature background flux. This meant, in essence, the provision of high speed pumping for the proposed apparatus.

(3) The Choice of Problem

Having selected as substrates evaporated metal films, and chosen the radio-tracer technique to follow the concentration of pre-adsorbed surface species, we faced the selection of the chemical system to be studied. Cormack, Thomson and Webb [54] had shown that a variety of supported metal catalysts exhibited heterogeneity of a pre-adsorbed surface species in hydrogenation and displacement reactions. Only a fraction of a pre-adsorbed ethylene monolayer, varying from metal to metal, was removed from the metal in such reactions. Thomson and Wishlade [55] showed similar features for evaporated metal films, while Cranstoun and Thomson [56] had witnessed slow desorption of hydrogen in vacuo and by mercury displacement, in addition to retention of hydrogen, on nickel films. These studies provided the basis on which this work was conceived.

The system which was of greatest interest to us was the interaction of ethylene with metal films, its vacuum desorption and displacement by other gases, such as acetylene. The particular metal film of interest was palladium which Cormack et al. had shown to occupy an anomalous position with respect to the other metals which they studied - platinum, nickel, rhodium and iridium - with respect to the high fraction of adsorbed ethylene not removed by reaction or vacuum treatment. By altering the temperature of both the adsorbed species and the beam, or by altering the temperature of the surface or the beam, we hoped to elucidate something of the kinetics of displacement reactions. For a 10 Centigrade degrees change in temperature a reaction with an activation energy of 10 k.cal/mole should have its rate affected by a factor of 2. Which had the greater effect, gas (beam) or surface temperature change, we wished to investigate. It should be pointed out that,

since the higher energy particles in a beam source have a greater chance of escaping through the source exit, the root mean square velocity of molecules in a molecular beam is 1.16 times that of the molecules in the source. The beam temperature is thus effectively higher than the source temperature. The beam temperature from a source at $300^{\circ}K$ is $395^{\circ}K$ - temperature being proportional to the square of the velocity.

The second aspect of the chemical system which was obviously going to be of interest was the question of surface heterogeneity - already revealed in the systems we wished to study. By surface heterogeneity we mean the variable topography of any given metal surface, whether due to the presence of different crystallographic orientations or to the presence of physical aberrations such as edge defects. In the work of Thomson and his co-workers (54-56) it had been demonstrated that only part of the surfaces studied was active in exchange reactions - strong evidence for surface heterogeneity.

An experimental configuration to study the interaction of a beam of acetylene with a layer of ethylene C-14 chemisorbed on palladium would have involved the use of high speed diffusion pumps to obtain a beam : background flux ratio on the target of 1 : 1 - already postulated as a good working ratio. At the beginning we had little experience of high speed pumping or of obtaining pressures in the range 10^{-8} - 10^{-9} torr which was also entailed. High speed pumping of condensable species by liquid nitrogen cold-traps is however a relatively simple matter. To gain experience in vacuum technology before building a system to handle beams of permanent gases, we decided to build a system to handle condensable gas beams - specifically of mercury - in which we were also interested. Beams of mercury could have been used to study

the displacement of hydrocarbons, tritium or ^{203}Hg from metal surfaces. The choice of initial adsorbate fell on ^{203}Hg. This is a β,γ emitter with a β E_{max} of 210 keV, and posed less of a problem in detection than carbon-14 (156 keV) or tritium (18 keV).

It was intended to follow this study with mercury displacements of carbon-14 labelled compounds and then construct an apparatus to extend the study to displacement reactions by permanent gas beams. In the event the mercury/^{203}Hg displacement reaction proved intractable. Difficulties were encountered in the use of the target system initially used as well as with the scintillation counter. It was decided that after these difficulties were overcome we should omit the intermediate studies of displacements by mercury and proceed to the problems we most wished to study - the displacement of ethylene C-14 by beams of gases such as acetylene.

An account of the apparati used follows in chapters 3 and 4.

Chapter 3
Apparatus

(1) Introduction

The chronological sequence of events in the evolution of the beam system has been as follows:

1) construction of an apparatus with the capability of studying Hg/^{203}Hg exchange reactions on metal films,
2) evolution of counters and targets using this first apparatus as a test system whilst designing for
3) an apparatus with a capability for handling permanent gases in the beam.

The description of these apparati will follow this order, after the criteria of performance and the reasons for the choice of certain materials have been stated.

Any molecular beam system has the following features (fig. 3.1):

1) a source of gas or vapour which emerges through some form of slit or hole into
2) a collimation region which has a second point of exit, the collimator, which forms the beam passing into
3) the work region. This part is invariably evacuated separately from the collimation region.

The following requirements should be observed:

1) the vacua through which the beam passes should be such that a negligible fraction of the beam is dissipated by collision with those gas molecules remaining in the vacuum chamber, i.e. that the mean free path of the beam

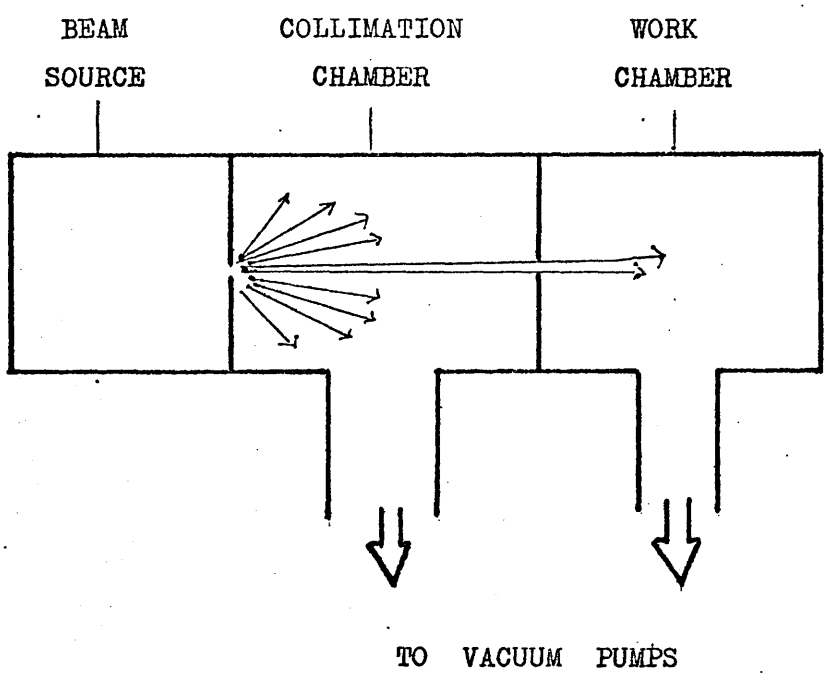
BEAM
SOURCE
COLLIMATION
CHAMBER
WORK
CHAMBER
TO VACUUM PUMPS

FIG. 3.1

particle is greater than the path it has to travel.

2) that the signal obtained from the beam in the work region should be high relative to the signal produced by the residual gas so that its presence or effects should be unequivocally seen.

These points will be considered in detail in the section on apparatus design.

It is obvious that the prime requisite for experimental work is the provision of high speed pumping for each chamber. In the case of condensable species, such as mercury, this can be provided by means of liquid nitrogen cold traps. For non-condensable species this speed can only be provided by diffusion pumps or ion pumps. In our case, diffusion pumps have been used throughout.

(2) Materials

The description of the apparatus must include a discussion of why the particular material, Quickfit Visible Flow (QVF) Pyrex glass pipeline units, was chosen to provide the basic building units. The best possible material for pipeline-type vacuum construction is, without question, stainless steel. The apparatus could have been built from standard stainless steel units available from various manufacturers or by making units in our own workshops. Our basic objection to a metal system was, and is, our lack of welding and brazing facilities. Purchase of metal units would have meant lack of flexibility and high cost.

An all glass-blown system was considered but this would have lacked the advantages of demountability and robustness: this latter was a necessity as it was envisaged that heavy sub-units would be attached to the main line.

A compromise was reached with the use of QVF glassware units. These are of thickwalled glass, 3 mm thick, with flanged, ground glass ends and they can be bolted together, with a gasket pinched between the ground glass faces, to form large, rigid and robust assemblages. Demountability and robustness are achieved at far less cost than for a metal system and yet flexibility in unit design is achieved: up to 3" diameter QVF can be handled with comparative ease by our glass-blowers when modification is required. The method of assembly is shown in fig. 3.2.

The only material supplied by Messrs. Quickfit Ltd. as a gasket material is Neoprene. This was tried and found unsuitable owing to its high outgassing rate. The best vacua attainable after baking at 70-80°C for 48 hours and applying relatively high

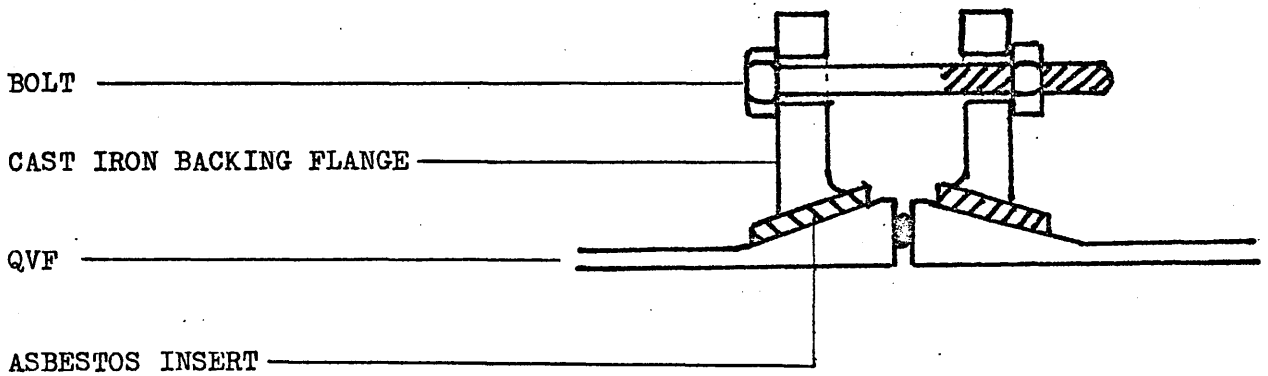
BOLT
CAST IRON BACKING FLANGE
QVF
ASBESTOS INSERT

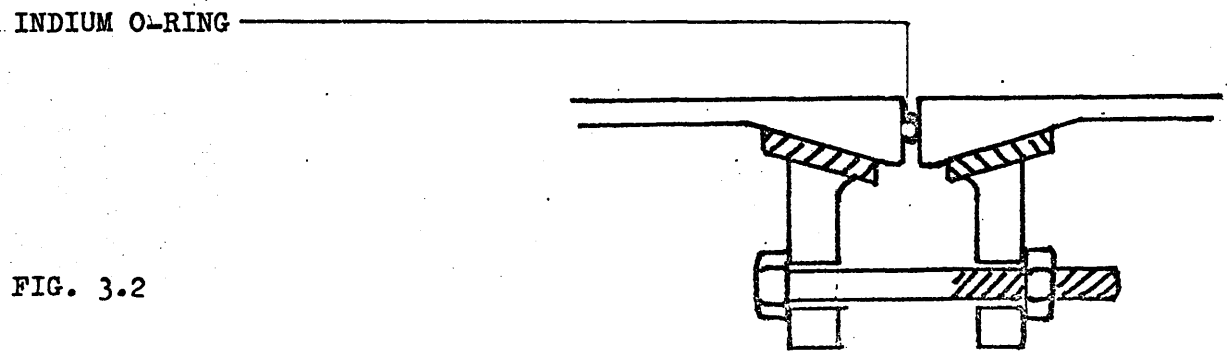
INDIUM O-RING

FIG. 3.2

pump speeds to small systems were of the order of 10^{-5} torr. The material finally used for gaskets was 1/16th in. diameter indium wire supplied by Johnson Matthey & Co. Ltd. This was used as shown in fig. 3.3. The wire is laid on the ground glass face of one unit, the other unit brought up and the two bolted together. The overlapping wires cold weld under pressure to form a perfect vacuum seal. Before use the wire is cleaned of surface grease and dust by being rubbed with tissue soaked in chloroform, and then allowed to dry.

The backing flanges used are of cast iron, the inserts asbestos. Plastic backing flanges, though lighter, frequently snapped under strain, and rubber inserts tended to adhere strongly to both the backing flange and the glass, making dismantling a tedious process.

Initially it was found that the QVF units tended to crack around the flanged end, under the backing flange, when under strain. This was prevented by annealing the units at 530°C. No unit given this treatment has yet failed. Indium sealed assemblies have been baked to 150°C repeatedly without incident.

Other materials used in construction had also to be chosen with care. Porcelain beads rather than plastic insulators have been used to cover electrical leads where necessary. Silver solder rather than soft solder has been used in almost all circumstances. Where this is impossible the amount of soft solder used is kept to the minimum, to present the smallest surface area liable to outgas. Where materials not commonly used in ultra-high vacuum work have had to be used, e.g. Apiezon N vacuum grease and Araldite, these have been carefully outgassed during pre-run pump-downs.

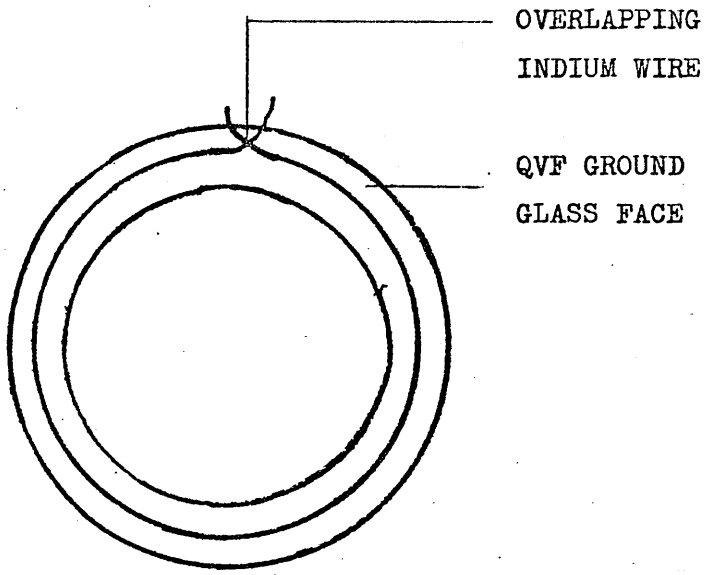

FIG. 3.3

With such a mixed glass and metal system it has been necessary to use a specialised leak detector - a Balzers H.L.G.1 halogen-leak detector. Here the method of operation is to spray the test gas, Arcton 22 (CF_2Cl_2), on to the outside of the vacuum system. Any leak draws the gas into the system over the gauge head, which detects the presence of halogen atoms as the gas is cracked on a hot filament. With this unit leak rates of approximately 10^{-5} l torr /sec. (estimated from pressure rise measurements) have been located with ease. Slow fouling of the gauge head filament occurs with time - oil vapour being the culprit. This can be rectified by running the filament hot, in air, for 24 hours.

(3) Apparatus for Hg/^{203}Hg Replacement Studies

What now follows is a description of an apparatus built, as a test system, to study displacement reactions on metal films. It was intended for use only with condensable species, not for permanent gases. Following the description is a calculation on its performance for mercury as the beam gas. The performance of the apparatus is discussed in section 4 of this chapter, together with the lessons learned from it.

The apparatus is shown in fig. 3.4. It consisted of a two-chamber assembly, the chambers being separated by the Viton A collar. The source was a twin-oven assembly with oven A, containing liquid inactive mercury, determining the pressure in the source and oven B determining beam temperature. A plug of glass wool was placed at the entrance point from oven A to ensure that thermal equilibrium was achieved. Mercury emerges from oven B into the collimator chamber through a slit in the collimator face.

The collimator, which is shown in detail in fig. 3.5, together with its method of mounting between two QVF flanges, is made of nickel and carries stainless steel slits, each 5 x 10^{-3}cm wide and 1.8 cm long at each end. The slits were fitted, and aligned, by the Scientific Apparatus Division of A.E.I. Ltd. The collimator was pumped through a hole of 1" diameter cut in the underside. It was intended to further perforate the nickel wall to increase the pump speed which could be applied to the chamber. For various reasons this was not carried out. The chamber was pumped by a 1" mercury diffusion pump with large liquid air traps adjacent to the chamber: these provided the effective pumping for mercury. The wall of the chamber was a 2" bore QVF tee-piece. Vacuum sealing between this chamber and

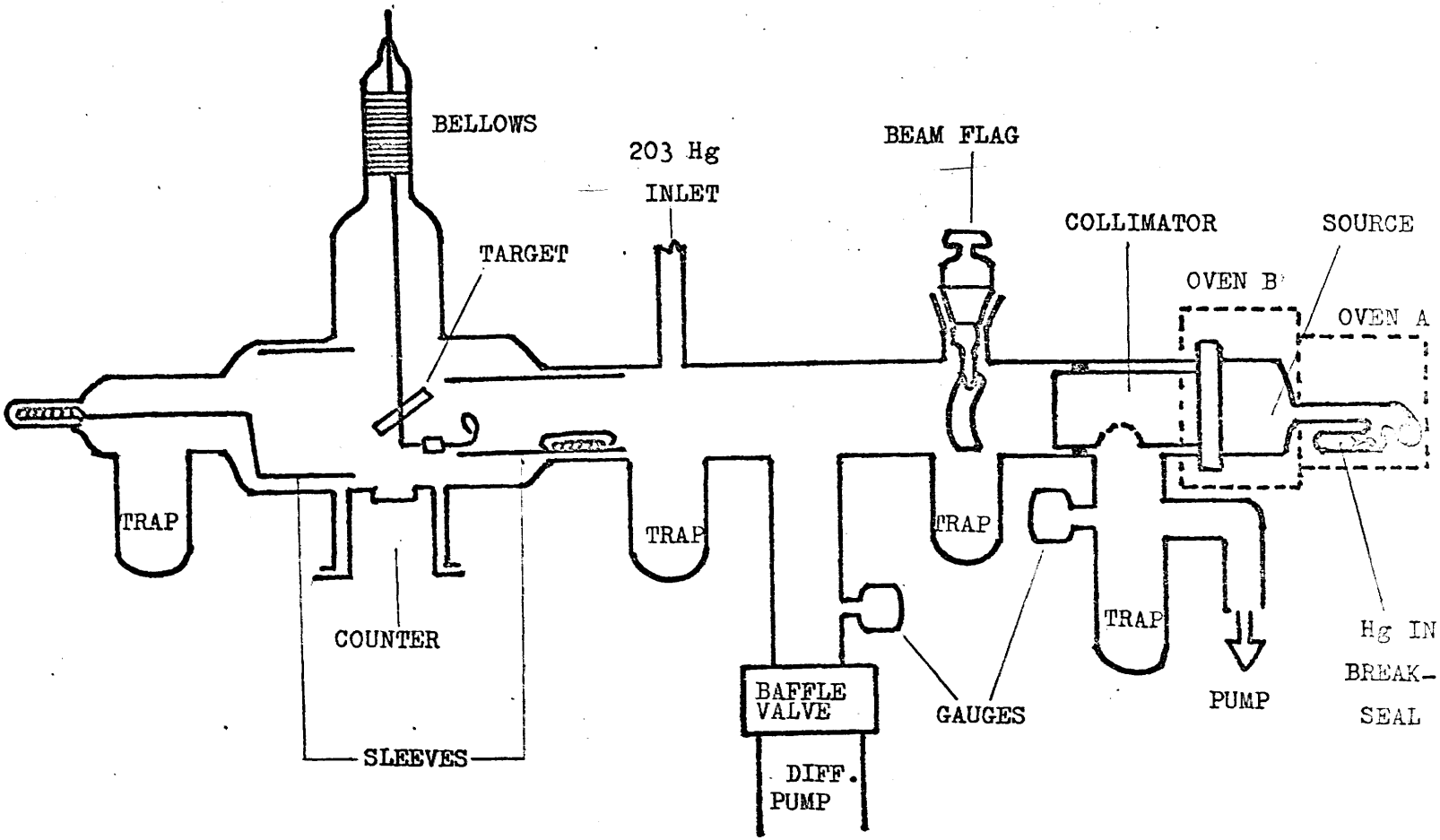
BELLOWS
203 Hg
INLET
BEAM FLAG
COLLIMATOR
SOURCE
TARGET
OVEN B
OVEN A
TRAP
TRAP
TRAP
TRAP
COUNTER
BAFFLE
VALVE
GAUGES
PUMP
Hg IN
BREAK-
SEAL
SLEEVES
DIFF.
PUMP

FIG. 3.4

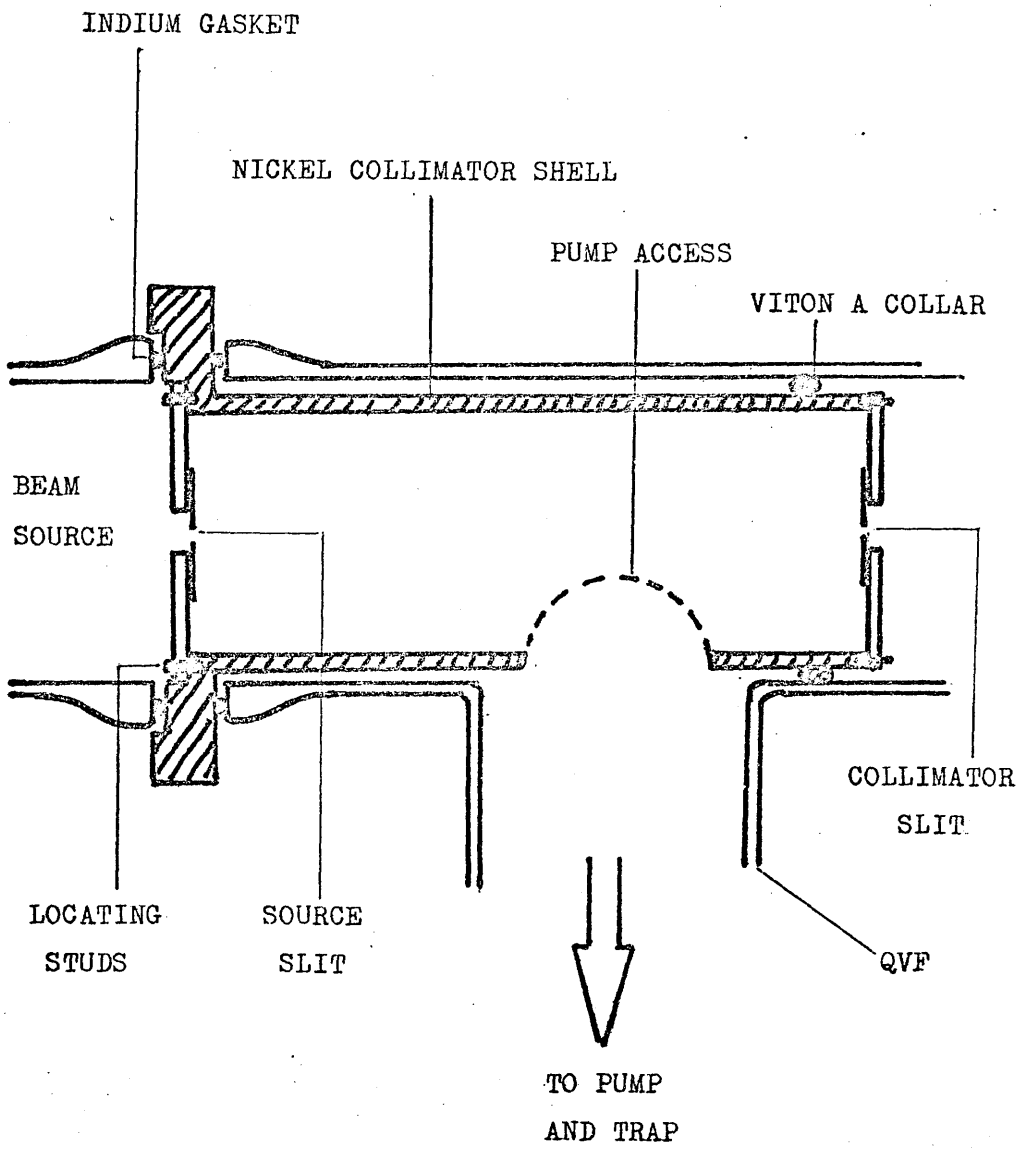
INDIUM GASKET
NICKEL COLLIMATOR SHELL
PUMP ACCESS
VITON A COLLAR
BEAM
SOURCE
COLLIMATOR
SLIT
LOCATING
STUDS
SOURCE
SLIT
QVF
TO PUMP
AND TRAP

FIG. 3.5

the target chamber was provided by a collar of Viton A rubber filling the annular space between the collimator and the chamber wall. This was held in place on the collimator cylinder by Araldite. To ease the fitting of the collimator into place the rubber collar was oiled with Silicone 704 vacuum oil.

The target chamber, pumped by a trapped and valved 2" Edwards oil diffusion pump, was essentially a tube constructed from QVF units, each of which carried at least one service to the chamber. The beam flag was a curved strip of aluminium, fixed by Araldite to a glass rod. This was carried initially, as shown, through a B34 cone and socket joint mounted on a 2" tee-piece. This was later changed to a 2" cross-piece carrying in addition a liquid nitrogen trap on the lower arm. Gas inlet and pump access facilities were carried on separate 2" tee-pieces. Next in line came a 2" to 3" pipeline adaptor, mating into the target chamber - a 3" QVF cross-piece. Inside the gas inlet tee-piece and the pipeline adaptor lay a glass cylinder closely fitting the walls of the system. This could be moved backwards and forwards by the action of an external magnet on a thin rod of iron held in a sealed section of tight-fitting glass tubing which was fixed by Araldite to the wall of the cylinder. This tube, bevelled at one end, could be slid up to shield the target chamber during evaporation.

The target chamber carried the target (fig. 3.6), the counter (fig. 3.7) which sits directly under the target, and another shield. This second shield was a cylinder of aluminium fixed by Araldite to a glass arm which terminated in an encapsuled iron slug. The arm, and the shield to which it was attached, could be moved backwards and forwards along a wide-bore glass tube protruding from this end of the apparatus. This tube

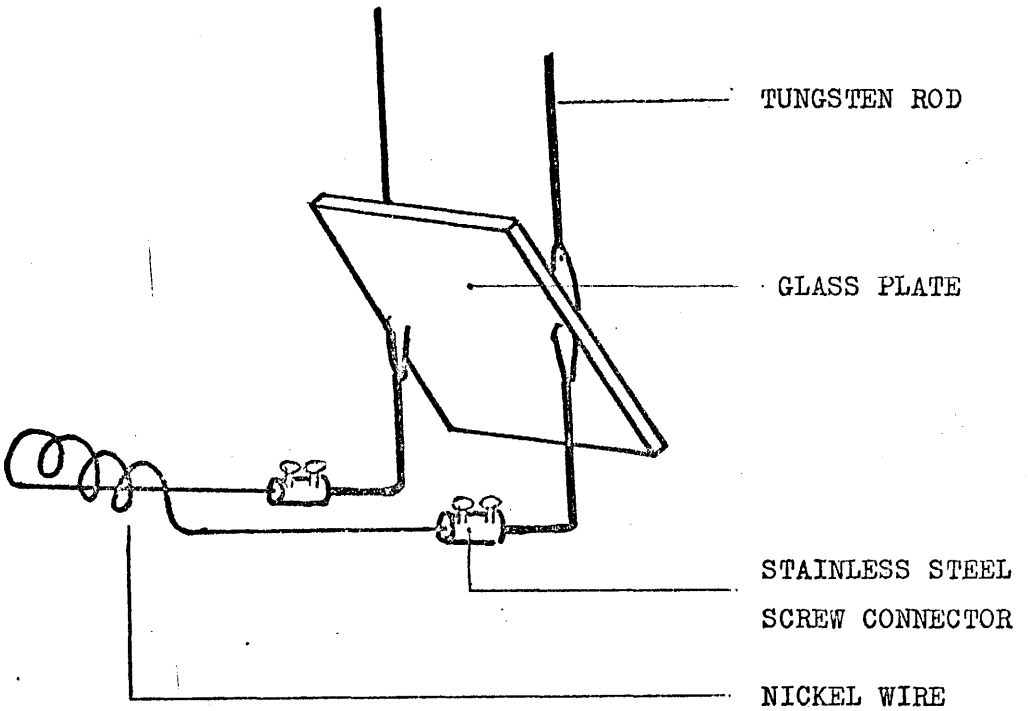
TUNGSTEN ROD
GLASS PLATE
STAINLESS STEEL
SCREW CONNECTOR
NICKEL WIRE

FIG. 3.6

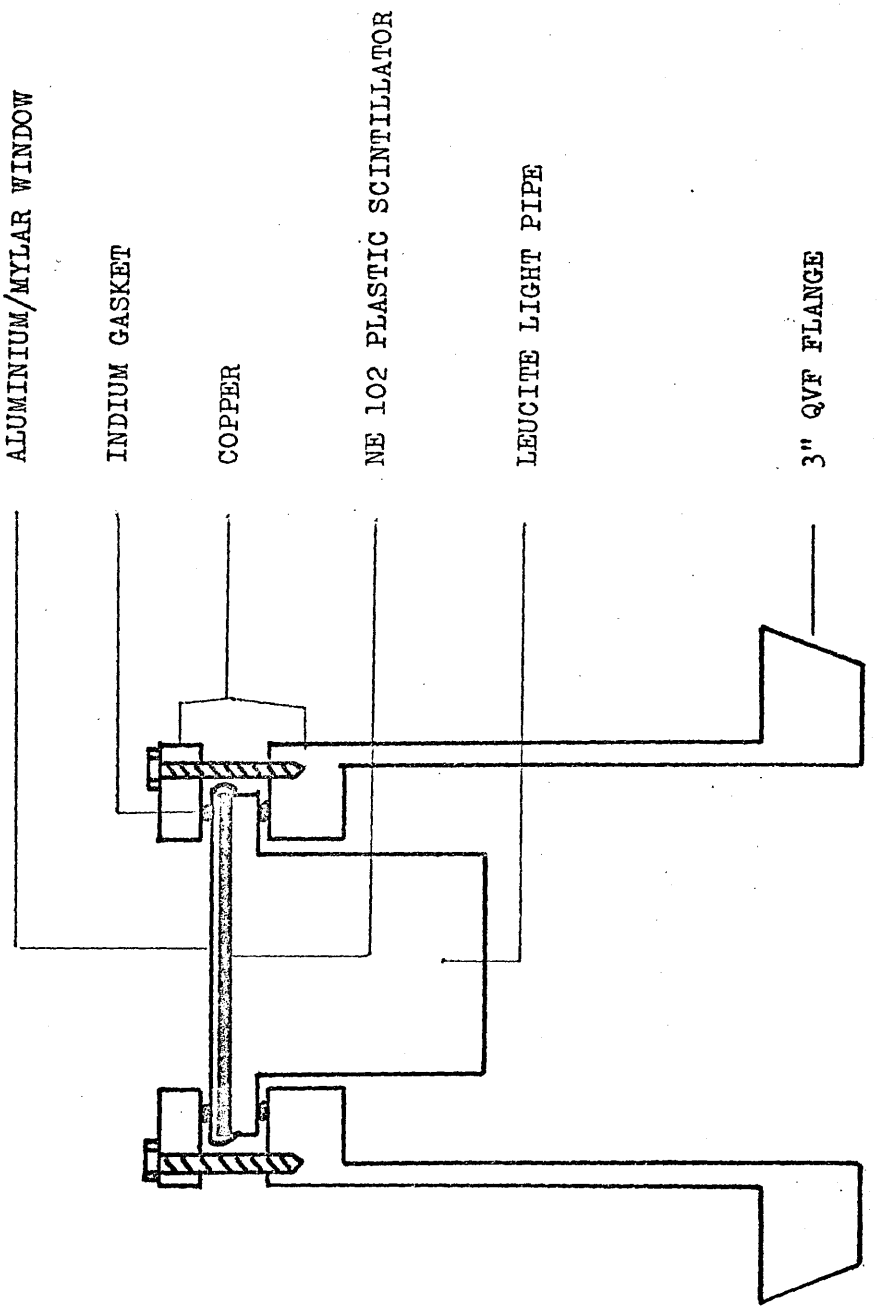
ALUMINIUM/MYLAR WINDOW
INDIUM GASKET
COPPER
NE 102 PLASTIC SCINTILLATOR
LEUCITE LIGHT PIPE
3" QVF FLANGE

FIG. 3.7

also served as the entrance to yet another trap.

The target consisted of a small (2 cm x 2 cm) square glass plate suspended through a metal bellows by two tungsten rods sealed into the plate. These rods also carried the current to heat the filament which was attached across the bottom of the rods with stainless steel screw connectors. The bellows unit was made by silver soldering a brass B24 cone to each end of an Edwards 1" pipeline bellows - the bottom cone fitting into a specially made 3" QVF to B24 adaptor, the top cone fitting into the glass socket end of a tube carrying the two tungsten rods sealed into Pyrex glass. The joints were made vacuum tight with Apiezon W wax ("black" wax). By moving the top of the bellows the target could be moved forwards, backwards and sideways. The target hung at an angle of 45° directly above the counter to afford reasonable geometry for radioactivity counting.

The counter was contained within a copper re-entrant tube which was machined to be mated to a 3" QVF flange. At the top of this tube a tee-section Leucite light pipe was held in position by a flange ring, the seal between Leucite and copper being made by an indium O-ring. Pressure to vacuum seal the assembly was maintained by four Allen screws. To the top of the Leucite was bonded a NE 102 plastic scintillator, 0.01" thick. Over this lay a Mylar film 0.0025" thick coated on each side with a film of aluminium 0.1 micron thick. The aluminium/Mylar film shields the scintillator assembly from light. Light sealing between the copper flanges was provided by a sleeve of aluminium foil held in place by a Viton A O-ring. The interior of the whole assembly contained an E.M.I. 6097 S photomultiplier tube - optically coupled to the Leucite light pipe with Silicone 704 oil. The scintillator/light pipe unit was prepared by Nuclear

Enterprises Ltd. and machined in our workshops.

The electronics consisted of a cathode follower, high voltage supply, amplifier, analyser/discriminator and scaler, all supplied by Ecko Electronics Ltd.

The alignment of target with beam was carried out by removing the QVF end-pieces of the apparatus and placing a 500 watt bulb in a reflector behind the source slit of the collimator. The target was then swung from side to side to ensure that the beam would cover all of it. This was done, by eye, by viewing the image of the source slit, seen through the collimator slit, and ensuring that it was visible when the target was swung fully to each side, crossing the path of the beam as it did so. It also ensured that the beam flag did indeed interrupt the beam.

Vacuum measurement was carried out using Philips cold cathode ionisation gauges E4.551.59 which operated from 2×10^{-3} torr to 10^{-5} torr and W.4.303.64 operating from 10^{-4} torr to 10^{-8} torr on collimator and target chambers respectively. These were controlled by a Philips P.W. 7902/00 unit. Backing pumps to each of the diffusion pumps used were Edwards 1 SC 50B rotary pumps, connected to the diffusion pumps by Edwards vacuum pipeline coupling units. Blank flanges on the backing lines were left to allow connection of the Balzers leak detector head sensing unit when needed. Vacua obtained in both chambers with all traps full were in the range $1-3 \times 10^{-6}$ torr, this being the useful limit of the W.4.303.64 cold cathode gauge.

The vacuum performance of the system was calculated using the following formulae.[57] The pump speed applicable to remove gas from a system is given by $1/S_E = 1/S_N + 1/C_1 + 1/C_2 + 1/C_3$ .....

where

S_E is the effective applicable pump speed, in l/sec.

S_N is the nominal pump speed, in l/sec. (for air, the rated pump speed quoted by the manufacturers; for mercury, the pumping effect produced by traps).

C_1, C_2, etc. are the conductances in l/sec of the various parts of the connecting pathway between pump and system.

The pumping speed produced by a trap is given by $S = 75 \times (29/M)^{\frac{1}{2}} \times (1 - P_2/P_1) \times A$ l/sec. where

M is the molecular weight of vapour

P_1 is the partial pressure of the vapour within the system

P_2 is the pressure of the saturated vapour at the trap temperature (for mercury at $-196^{\circ}C$, $P_2 = 10^{-27}$ torr).

A is the effective surface area of the trap in square inches.

For mercury this formula simplifies to $30 \times A$ l/sec.

The values of conductances are given by the formulae

$C = 79 \times D^3/L$ l/sec, for a circular pipe, and

$C = 75 \times A$ l/sec, for an orifice,

where D and L are the diameter and length, in inches, of the pipe and A the area, in square inches, of the orifice.

The conditions for free molecular flow from the source slit of the molecular beam oven are as follows: (48)

1. that the width of the slit be very much smaller than or equal to the mean free path of the molecules in the source
2. that the thickness of the jaws is negligible.

The maximum operating temperature of the source oven is $150^{\circ}C$ - set by the limitations on the baking of indium seals. A typical operating source pressure (set by oven A) would be 1 torr.

Under these conditions the mean free path of mercury atoms is 4.87×10^{-3} cm.[58] The first condition was thus fulfilled as the source slit was 5×10^{-3} cm wide. The second condition was fulfilled by having the slits made with bevelled edges.

Under these conditions the total rate at which molecules emerge from the source is given by $Q = \frac{1}{4}n\bar{v}A_s$,[48] where

n is the gas density in the source in molecules/cc

$\bar{v}$ is the mean velocity of the gas molecules in cm/sec

A_s is the area of the source in cm^2.

This can be more conveniently expressed as

$Q = 1.118 \times 10^{22} \times \pi \times p_s \times A_s / (M \times T)^{\frac{1}{2}}$ molecules/sec where

M is the molecular weight of the source gas

T is the temperature of the source gas in ^oK

p_s is the source pressure expressed in mm of mercury (torr).

The intensity of the beam falling on a target at a distance L cm from the source is given by

$I = 1.118 \times 10^{22} \times p_s \times A_s \times A_d / L^2 (M \times T)^{\frac{1}{2}}$ molecules/sec where

A_d is the area of the detector or target used in cm^2.

Thus in our circumstances (fig. 3.8) with a source pressure of mercury of 1 torr at a temperature of 150°C and with a slit 5×10^{-3} cm wide and 1.8 cm long

$Q = 1.118 \times 10^{22} \times \pi \times 1 \times 5 \times 10^{-3} \times 1.8 / (208 \times 423)^{\frac{1}{2}}$ molecules/sec

$= 1.07 \times 10^{18}$ molecules/sec

$= 3.04 \times 10^{-2}$ l torr/sec.

Effectively all of this material must be pumped out of the collimator chamber. Here the effective pump speed is given by:

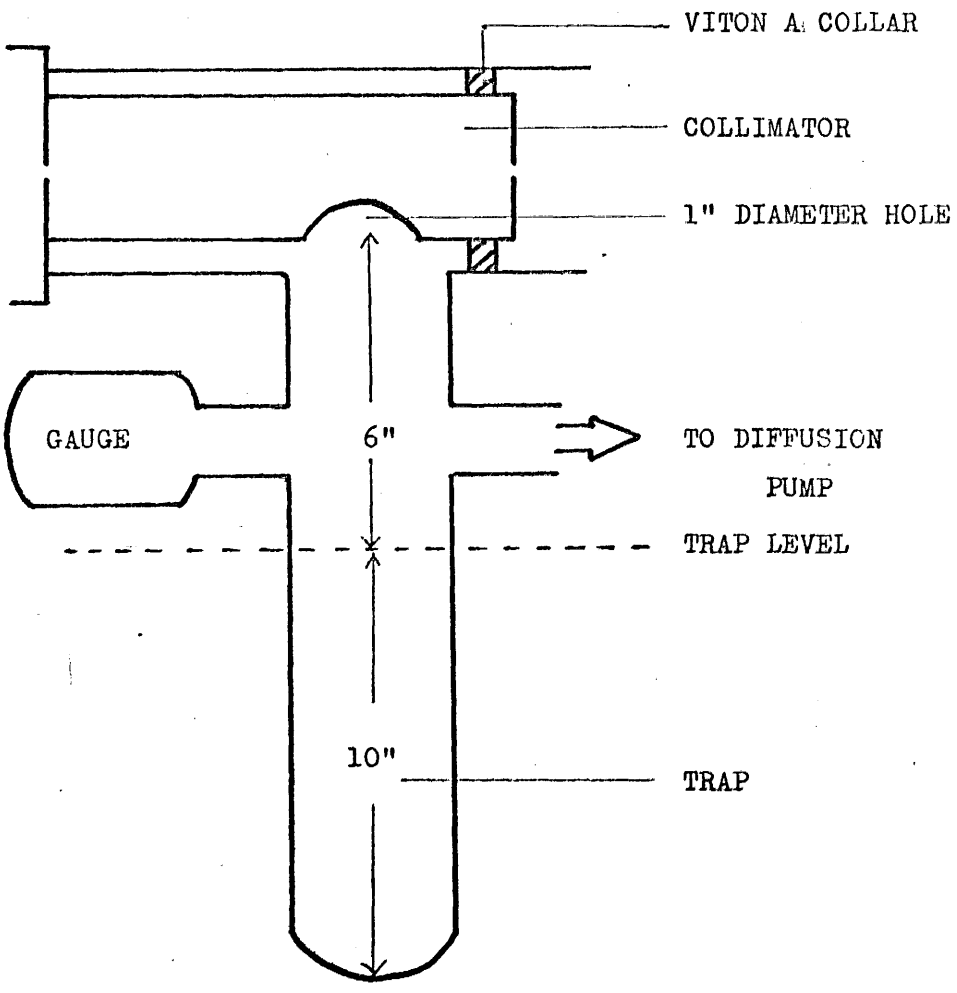
VITON A COLLAR
COLLIMATOR
1" DIAMETER HOLE
GAUGE
6"
TO DIFFUSION PUMP
TRAP LEVEL
10"
TRAP

FIG. 3.8

$1/S_E = 1/S_N + 1/C_1 + 1/C_2$ where

S_N is the pump speed of a liquid air trap 10 in. long and 2 in. in diameter, having an area of 40π in.^{2} and a pump speed for mercury of 1200π l/sec.

C_1 is the conductance of an aperture 1 in. in diameter.

C_1 thus equals $75 \times 0.25 \times \pi$ l/sec

$= 58$ l/sec.

C_2 is the conductance of the 2 in. diameter pipe leading from the trap to the chamber. The length of the pipe was 6 in. The conductance was thus $79 \times 8/6$ l/sec

$= 105$ l/sec.

As $1/S_N$ is trivial compared to $1/C_1$ and $1/C_2$, it can be neglected.

Thus $1/S_E = 1/58 + 1/105$

Thus $S_E = 37$ l/sec.

Against an inflow of 3.04×10^{-2} l torr/sec this would have provided a residual pressure of 8.2×10^{-4} torr. The mean free path of mercury atoms in this residual pressure would have been 5.1 cm. (58) This would have caused serious dissipation of the beam in the collimator chamber - the path length the beam would have had to travel in this chamber being 17 cm. It was realised and intended that the collimator tube should be opened up (fig. 3.9) and incorporated in a 2" QVF cross-piece with a trap mounted as shown. This trap would have had an effective surface area of at least a disc with a diameter of 2 in. and a pump speed of 235 l/sec. This would have been in addition to the pumping action of the trap formerly used, which would now have had a pump speed approximately equal to the conductance of the tube linking it to the collimator chamber, i.e. 105 l/sec. The combined pump speed would thus have been 340 l/sec. Against an inflow of 3.04×10^{-2} l torr/sec this would have resulted in a pressure of

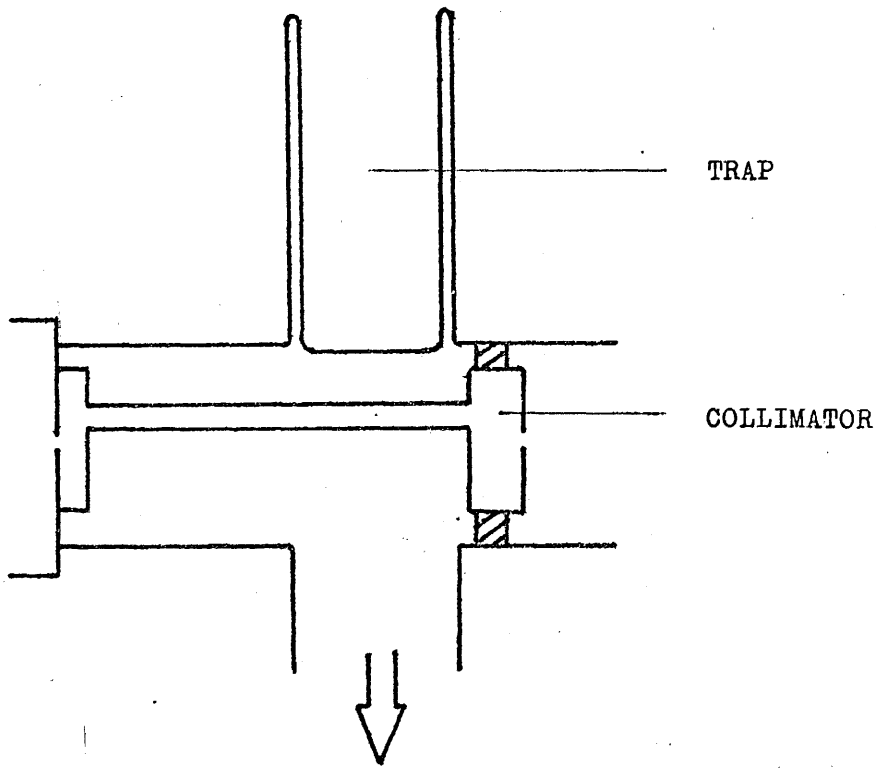

FIG. 3.9

8.9×10^{-5} torr - in which the mean free path of mercury atoms was now approximately 50 cm.[58] Comparatively little dissipation of the beam would have occurred in the collimator chamber.

We must now consider how a beam of mercury would have affected the target chamber. The flow of mercury into this chamber resulted from a combination of two separate influxes - that diffusing through the collimator slit from the collimator chamber and the beam flux itself. To evacuate this chamber we had available a series of traps with a combined effective pump speed of at least 1,000 l/sec.

The flux resulting from diffusion is given, as before, by

$Q = 1.118 \times 10^{22} \times p_c \times A_s \times \pi / (M \times T)^{\frac{1}{2}}$ where

p_c is the pressure of mercury in the collimator chamber in torr
$= 8.9 \times 10^{-5}$ torr

A_s is the area of the slit separating the two chambers in cm^2

T is the temperature of the mercury in the collimator chamber
$= 300^{\circ}K$

Thus $Q = 1.13 \times 10^{14}$ molecules/sec
$= 3.2 \times 10^{-6}$ l torr/sec.

The flux produced directly by the beam is given by calculating the rate at which molecules emerging from the source pass through the collimator slit, i.e. by the equation:

$I = 1.118 \times 10^{22} \times p_s \times A_s \times A_c / L^2 (M \times T)^{\frac{1}{2}}$ where

$p_s = 1$ torr

$A_s = 1.8 \times 5 \times 10^{-3}$ cm^2

$A_c = 1.8 \times 5 \times 10^{-3}$ cm^2

$L = 17$ cm

$M = 208$

$T = 423^{\circ}K$

Thus $I = 1.116 \times 10^{13}$ molecules/sec
$= 3.2 \times 10^{-7}$ l torr/sec.

Assuming that effectively all of this material must be pumped away, the total amount of mercury to be removed from the target chamber was 3.5×10^{-6} l torr/sec. Applying a pump speed of 1,000 l/sec to this amount would leave a residual pressure of 3.5×10^{-9} torr.

The number of molecules striking a surface at a given residual pressure can be calculated using the same equations as before, but imagining that we are calculating the number of molecules emerging from a source of that pressure through an aperture of area 1 cm^2.

i.e. the number of molecules striking a surface
$= 1.118 \times 10^{22} \times \pi \times p_s / (M \times T)^{\frac{1}{2}}$ /cm^2/sec.

In this case $p_s = 3.5 \times 10^{-9}$ torr
$M = 208$
$T = 300^{\circ}K$.

Thus the number of atoms of mercury striking a surface at 3.5×10^{-9} torr
$= 5.6 \times 10^{11}$ /cm^2/sec.

This figure can now be compared with the beam intensity.

The beam intensity, in terms of molecules hitting unit surface area in unit time, is given by:

$I = 1.118 \times 10^{22} \times p_s \times A_s \times A_d / L^2 (M \times T)^{\frac{1}{2}}$ where

A_d is the area of the detector
$= 1 cm^2$ in this calculation

$L = 120$ cm

$M = 208$

$T = 423^{\circ}K$

p_s = 1 torr

$A_s = 1.8 \times 5 \times 10^{-3}$ cm^2

Thus $I = 2.35 \times 10^{13}$ atoms mercury/cm^2/sec.

It should be noted that this intensity would have been achieved on only a small part of the target. Only by opening up the collimator slit would this intensity have been attained over the whole surface. It should also be noted that no account has been taken of the reduction of beam intensity by scattering in the collimator chamber.

(4) Performance and Criticism

We have now described the apparatus intended for use in Hg/^{203}Hg exchange reactions and predicted its performance from the vacuum aspect. In the case of mercury there was no possibility of precisely measuring the pressure of mercury in all sections of the apparatus. Pressure in the source was set by the temperature in the oven A, which was measured by a thermometer. Pressure in the collimator chamber could be measured accurately by the cold cathode ionisation gauge. In the target chamber the partial pressure expected from mercury vapour was so low - in the revised design it was expected to be 3.5×10^{-9} torr - that it would not have been detected in a background pressure of between 1 and 3×10^{-6} torr of residual permanent gases. Calculations of the performance of this apparatus were thus the best way of testing its performance - short of mounting a detector capable of scanning the target chamber for the beam. It was hoped to detect the beam by the chemical effects of its interaction with the target.

This stage was never reached. The apparatus was not used for its designed purpose. The reason for this lay basically in the selection of ^{203}Hg as the adsorbed species on films. This flaw became obvious at an early stage of the testing of the counter under experimental conditions. The counter assembly was pre-tested with both ^{203}Hg and ^{14}C, the first amalgamated on copper foil, the second in the form of ^{14}C-methyl methacrylate polymer providing a known rate of radioactive disintegration. It was not possible to operate the scintillation assembly in normal room-lighting conditions - the front foil apparently having minute cracks through which light could pass. When the assembly was darkened the efficiency for ^{14}C detection was measured as being

approximately 7% with a total background of 400 cpm, both in vacua and in air. The first runs were carried out by depositing a film of nickel and then admitting ^{203}Hg vapour from a break-seal vial attached to the gas inlet unit with the counter electronics pre-set to the optimum for counting ^{203}Hg from preliminary calibrations with the ^{203}Hg amalgamated copper foil. The background here was approximately 300 cpm. With the target directly above the counter the count rate after exposure of the surface to ^{203}Hg vapour was about 1,000 cpm. With the target swung forward, away from the counter, the count rate fell - but only to 600 cpm - the background appeared to have increased.

The apparatus was then dismantled and each unit of the target chamber checked for radioactivity with a commercial thin-window Geiger counter. Radioactive material - ^{203}Hg - was found on the copper and aluminium of the counter assembly as well as on the nickel film. This was found in spite of no cleaning of the counter assembly having been attempted prior to installation. All surfaces were deliberately left "dirty" to discourage ^{203}Hg adsorption. More disturbing still was the discovery of ^{203}Hg, though in smaller amounts, on glass surfaces where no nickel film could possibly have been thrown.

An attempt was then made to introduce ^{203}Hg in such a way as to increase the chance of it adsorbing specifically on the nickel film. This was done by introducing a QVF section (fig. 3.10) carrying a capillary pointing at the target and admitting the ^{203}Hg through this capillary. A nickel film was again thrown in vacuo inside the shields; these were drawn back and ^{203}Hg admitted via the capillary. The results achieved were similar to those in the previous attempts to adsorb ^{203}Hg on nickel - the ^{203}Hg adsorbed indiscriminately on glass and metal

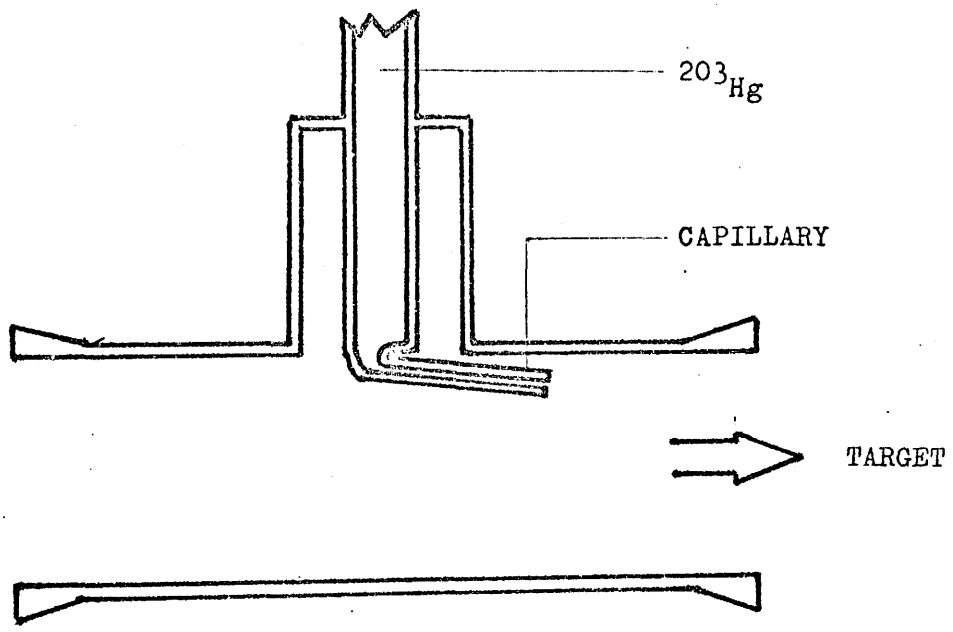

FIG. 3.10

throughout the target area. This effectively prevented the use of ^{203}Hg as the adsorbate on the target.

The second aspect which was unsatisfactory was the design of the target and the necessity of swinging it through the beam. This in effect meant that any part of the target only saw the beam intermittently. Opening up the collimator slit would have enabled complete coverage of a static target, though necessarily increasing the background flux at the same time. For example, if the collimator slit were opened up to 0.14 cm it would have allowed complete coverage of a static target with the dimensions 1 cm wide by 2 cm high at the full beam intensity, for mercury, of 2.35×10^{13} atoms/cm^2/sec. The background would have gone up in proportion: thus, by increasing the collimator slit from 5×10^{-3} cm to 0.14 cm, the increase would have been by 28 times, to 1.56×10^{13} atoms/cm^2/sec which would have approached the beam intensity. This figure, though not unacceptable, could have been reduced with comparative ease by fitting further cold traps to the system and it would still have been possible to attain beam : background intensity ratios of at least 10 : 1. Yet this ratio would still only have been attainable for condensable species such as mercury, water, etc., with vapour pressures, at liquid nitrogen temperature, below 10^{-8} torr. Permanent gases could not be handled with this apparatus.

Other unsatisfactory aspects were the arrangements for evaporation of the filament and shielding of the target chamber during evaporation. The shields were first of all clumsy and awkward to operate. Secondly, they could not be moved far enough away from the counter to ensure that no contribution was made to the observed count by radioactive material adsorbed on the film deposited on the shields.

The counter itself gave increasing trouble in two ways. Cracking of the Leucite between the copper flanges which held it in place produced vacuum leaks which initially were sealed by liberally spreading Araldite around the cracked regions. This problem recurred and eventually we were faced with deciding whether to continue with this design or to adopt another form of counter altogether. The decision to abandon the design completely was hastened by a progressive deterioration in the background count level of the counter from approximately 300 cpm to approximately 4,500 cpm. This was not due to contamination by radioactive material nor, apparently, to deterioration of the photomultiplier tube. It was therefore attributed to progressive deterioration of the light-sealing characteristics of the Mylar/aluminium window which bowed into the vacuum system each time the system was evacuated.

The vacuum characteristics of the system also left something to be desired. The inability to measure the low background pressure of mercury in the residual vacuum in the target chamber, approximately 10^{-6} torr, meant leaving estimation of background flux on the target to the calculations performed in section 3 of this chapter. The pressure during evaporation of metal films rose typically to 10^{-5} torr - leaving little doubt that we were not working on clean films. It was felt that evaporations should be carried out in lower vacua if possible.

With the above criticisms in mind, it was decided to design and construct an apparatus which had the following features:

1. it should be capable of handling permanent gases;
2. it should provide a beam : background flux ratio on the target of approximately 1 : 1;
3. ultimate vacua produced should enable pressure rises;

attributable to the beam to be clearly identified and measured, and be as low as possible to enable cleaner films to be thrown ;

4. pressure measurements should be made in all sections of the apparatus ;
5. a static target, which is covered entirely by the beam and whose temperature could be controlled and adjusted over even a limited range should be used ;
6. a method of evaporating films should be adopted which could not leave any suspicion that adsorption on stray film not covered by the beam was affecting results ;
7. a different design or type of detector should be used to eliminate the shortcomings in the detector previously used ;
8. a wider range of source temperatures should be available than the limited range (room temperature to 150°C) at our disposal with the arrangement already discussed.

These improvements were put in hand in two stages. Firstly, improvements to target, evaporation technique and detector were attempted and proved using parts of the existing apparatus as a test-system. Secondly, the other requirements were met by an over-all redesign and ordering and making new parts where necessary whilst the development work was being carried out.

(5) Interim Improvements

In this section we shall describe, in detail, the improvements made in target, evaporator and counter design to meet the requirements outlined at the end of the last section. The arrangement of the three items in the target chamber was envisaged as in fig. 3.11, where the three units are in position for evaporation. This takes place on to an angled target face as before, but the film to be studied is thrown as a spot in the centre of the glass face. The target, which is mounted through a greased cone and socket, can then be turned to face the counter, and is also in alignment with the beam. The three units are mounted on three arms of an adapted 3" QVF cross-piece, the fourth allowing entry of the beam, and with a fifth arm, projecting into the plane of the diagram, connected to a diffusion pump. All arms of this unit, made to our specification by Messrs. QVF Ltd., terminate in standard 3" QVF flanges, except that carrying the target which terminates in a B.55 ground glass socket.

The target used initially was a square glass plate on the end of a glass stalk. This was superseded by the fully thermostated design shown in fig. 3.12. Water is circulated through this from an external thermostated tank, being carried by the inner tube to the front face. The temperature at the face was measured by a pre-calibrated copper-constantan thermocouple, using a Doran thermocouple potentiometer to measure the E.M.F. produced. It was found that up to 70°C the difference between the temperature of the external water bath and that of the target, as indicated by the thermocouple, with the whole target unit inserted into the vacuum system, is zero. At 80°C bath temperature, the target temperature is 79.5°C. In use,

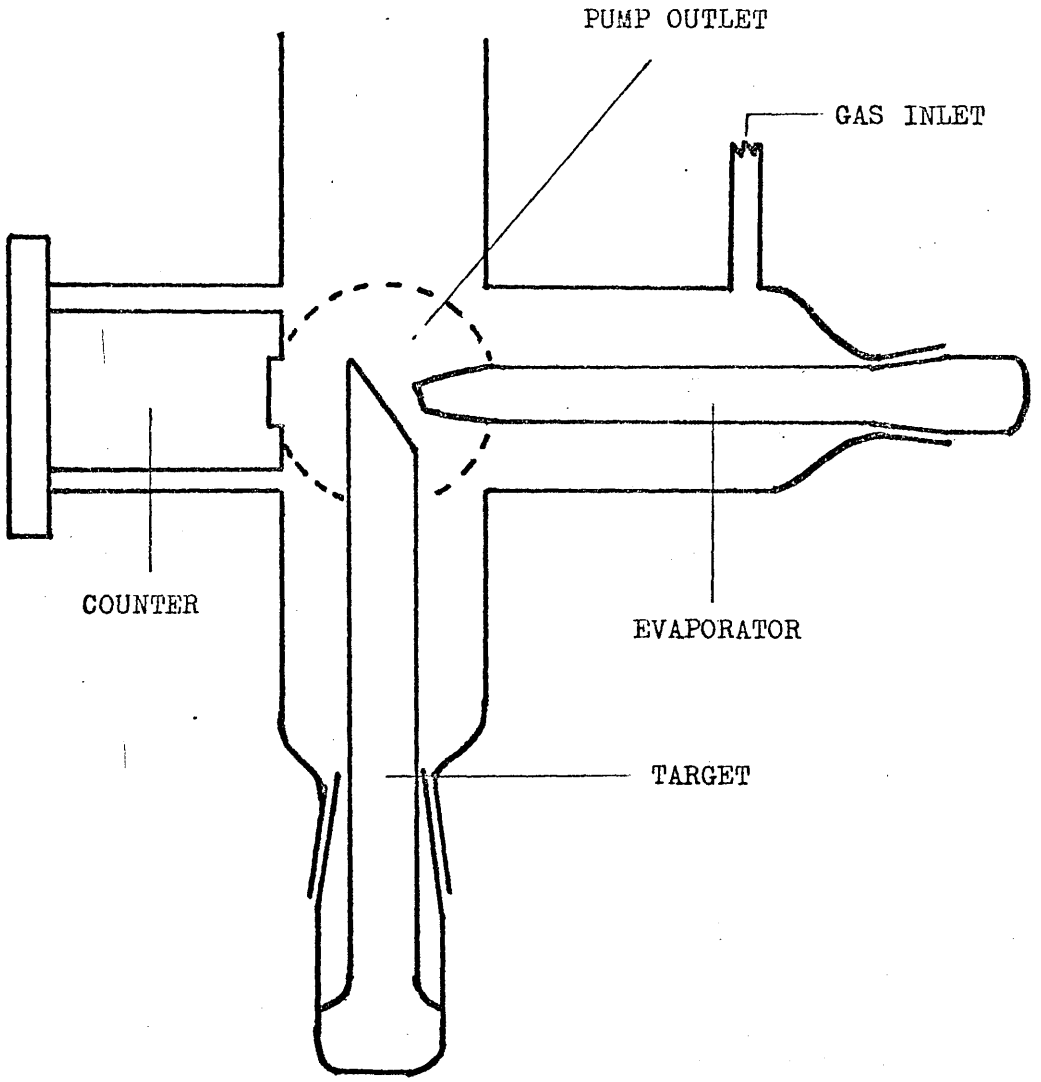

FIG. 3.11

FIG. 3.12

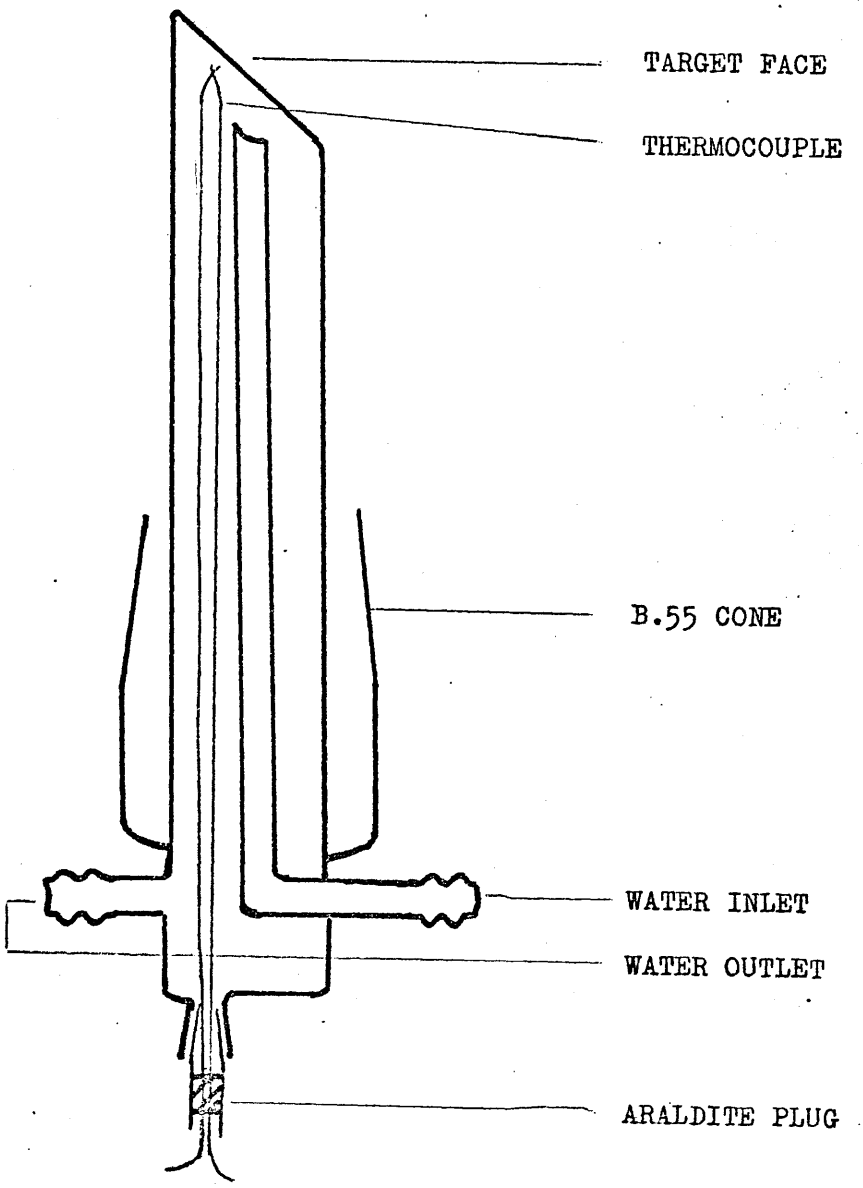
TARGET FACE
THERMOCOUPLE
B.55 CONE
WATER INLET
WATER OUTLET
ARALDITE PLUG

temperature measurements of the target are therefore taken by measuring the bath temperature - a much more convenient practice. The thermocouple is itself a plug-in unit, entering the target unit via a B.7 joint. The thermocouple wires have glass jackets and are sealed into the B.7 cone by an Araldite plug.

The evaporator (fig. 3.13) is mounted through a B.34 cone and socket joint which is attached to a 3" QVF flange for mating to the body of the target chamber. This unit carries a side-arm through which gas admission to the target chamber takes place. The evaporator consists of a tube carrying two 2 mm diameter tungsten rods which are sealed through Pyrex glass. To these rods is attached, by stainless steel screw connectors, the filament of the metal which will form the film - in our case palladium. The end of the tube is detachable for access to replace filaments, this being achieved by a dry B.24 cone and socket. The evaporator sits in a horizontal position and the rigidity of the tungsten rods ensures that the filament, when hot, does not touch the walls of the glass tube. Heating the filament is carried out by passing current from a step-down transformer through it via the tungsten rods, current being measured with an Avometer. The tip of the evaporator is narrowed to an open ended cone - the aperture being angled to match the target - which forms the film spot on the target. The metal not forming the film collects on the inside of the evaporator tube. When the target, with its spot of film, is turned to face the counter it completely screens the counter from radioactive material adsorbed on the inner walls of the evaporator.

The problems which were overcome in the counter field were of a more difficult and prolonged nature. Once the decision had

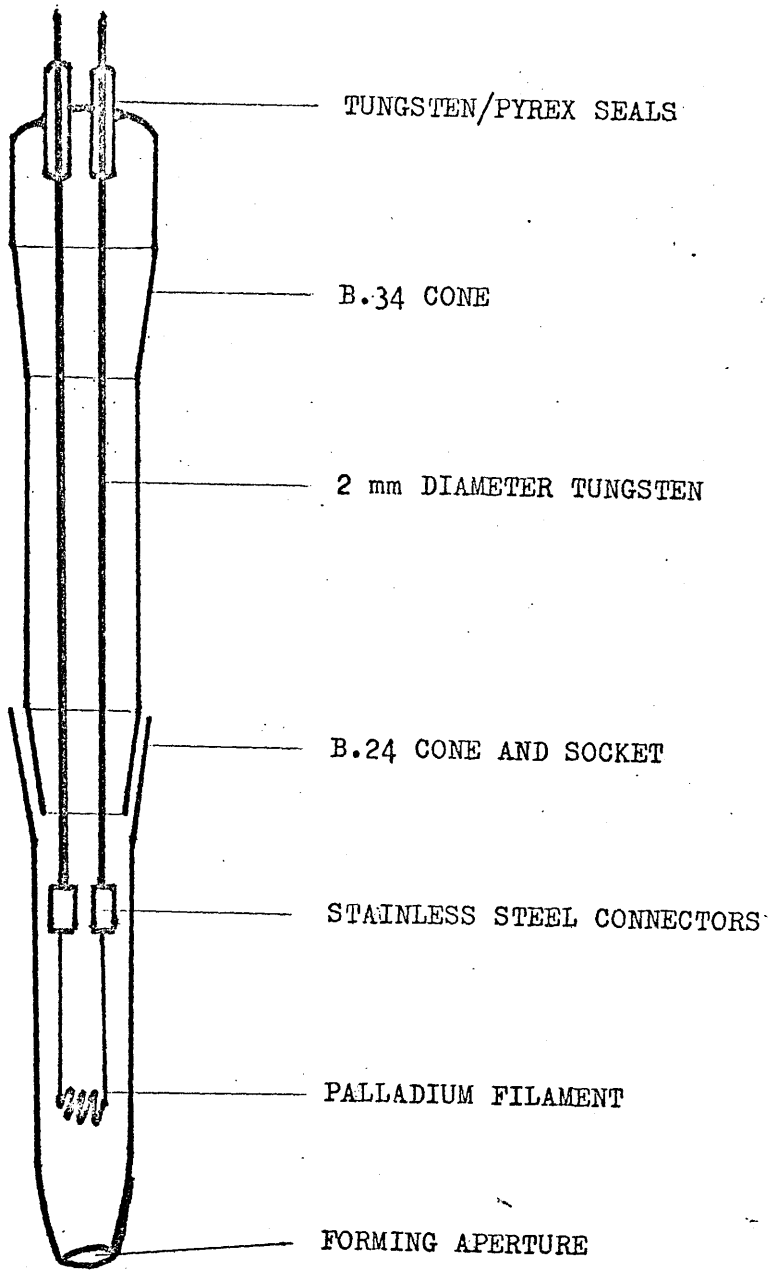
TUNGSTEN/PYREX SEALS
B.34 CONE
2 mm DIAMETER TUNGSTEN
B.24 CONE AND SOCKET
STAINLESS STEEL CONNECTORS
PALLADIUM FILAMENT
FORMING APERTURE

FIG. 3.13

been made to jettison the original photomultiplier design we were faced again with the choice between Geiger-Muller and scintillation assemblies. The next design studied was of a scintillation assembly employing a glass scintillator as shown in fig. 3.14. This would have involved hot rolling a thin section of glass scintillator (a heavily lithium-doped glass) to soda-glass, Pyrex being incompatible with the scintillator glass. This glass sandwich disc would then have been sealed to the end of a soda glass tube which in turn would have been connected to a 3" QVF flange via a soda/Pyrex graded seal. The inner face of the soda disc would have needed to be optically flat and be coupled to a photomultiplier tube by a silicone oil. Other scintillation assemblies were also considered - including one in which the photomultiplier tube itself was mounted within the vacuum system together with a glass scintillator. Both glass scintillation units would have presented us with problems of mounting: the first in the construction of the window; the second in the number of electrical leads into the vacuum system. In addition, both units would have been subject to the low detection efficiency of glass scintillators. Geiger-Muller detectors were again ruled out, as they had been initially, because of the possibility of gas-leakage at their fragile windows.

At the time at which the decision had to be made there appeared on the commercial market solid-state particle detectors with low enough background characteristics to make them usable, at room temperature, for the detection of ^{14}C β-particles. These offered great advantages of operation in vacuum systems - only two leads to the detector itself being necessary - together with no window problems and high detection efficiency, though, like scintillation assemblies, they are light sensitive. In addition, the materials from which they are constructed have

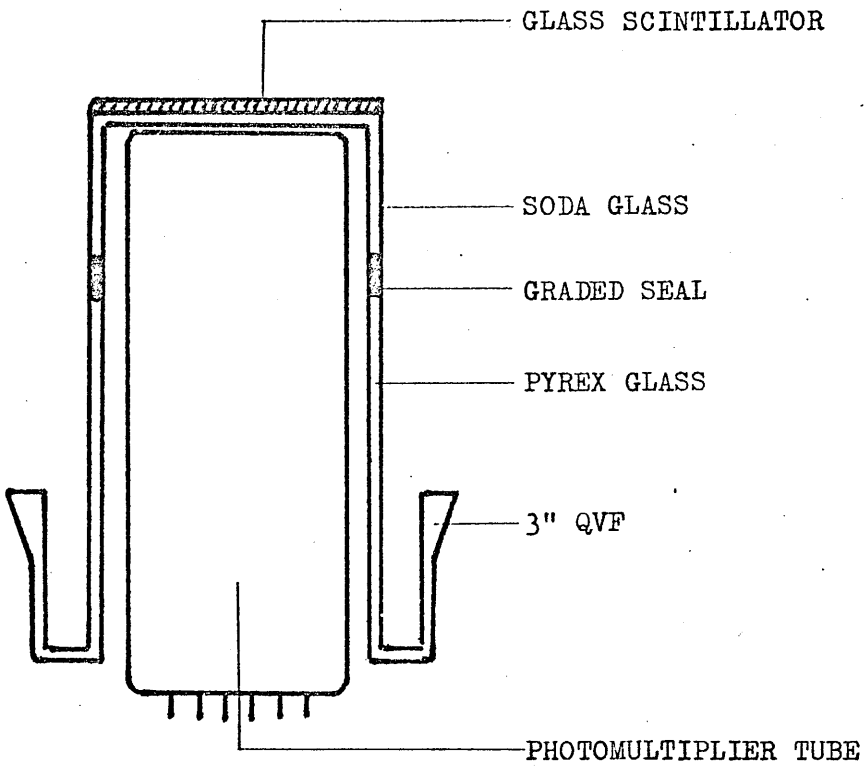
GLASS SCINTILLATOR
SODA GLASS
GRADED SEAL
PYREX GLASS
3" QVF
PHOTOMULTIPLIER TUBE

FIG. 3.14

excellent vacuum properties, e.g. low vapour pressures. The promise of high efficiency and ease of operation in vacuo offered by such detectors made us decide to abandon the scintillation technique entirely.

The solid-state detector chosen for use was a lithium-drifted silicon unit manufactured by Simtec Ltd. of Canada. In this the sensing volume is a region, 0.5 mm deep, in which normally p-type silicon of high resistivity is compensated by diffusing or drifting into it lithium which would form n-type material. When a charged particle passes through this material it produces charge pairs along its track, which separate under the influence of an applied electric field to be collected at the electrodes, (see fig. 3.15), in a way comparable to the production of ion pairs in any gas-ionisation type counter. The number of current carriers produced is proportional, within limits, to the energy of the incident particle. Charge collection is very fast, of the order of a few nanoseconds, and the dead time of a counting system is then set by the subsequent amplifier and other electronics. Windows still exist, as in gas filled counters, in the sense that the incident particle must first pass through a dead layer in which energy is dissipated before entering the detection region. This reduces somewhat the efficiency of the counter over-all. The stopping power of the solid detector means that much higher detection efficiencies are achieved than with gas detectors, for the same given depth of detector.

The main drawback lies in the small size of the signal current produced, necessitating a high degree of amplification and low noise electronics. The noise levels at room temperature are due mostly to thermal production of ion pairs, only 3.6 eV

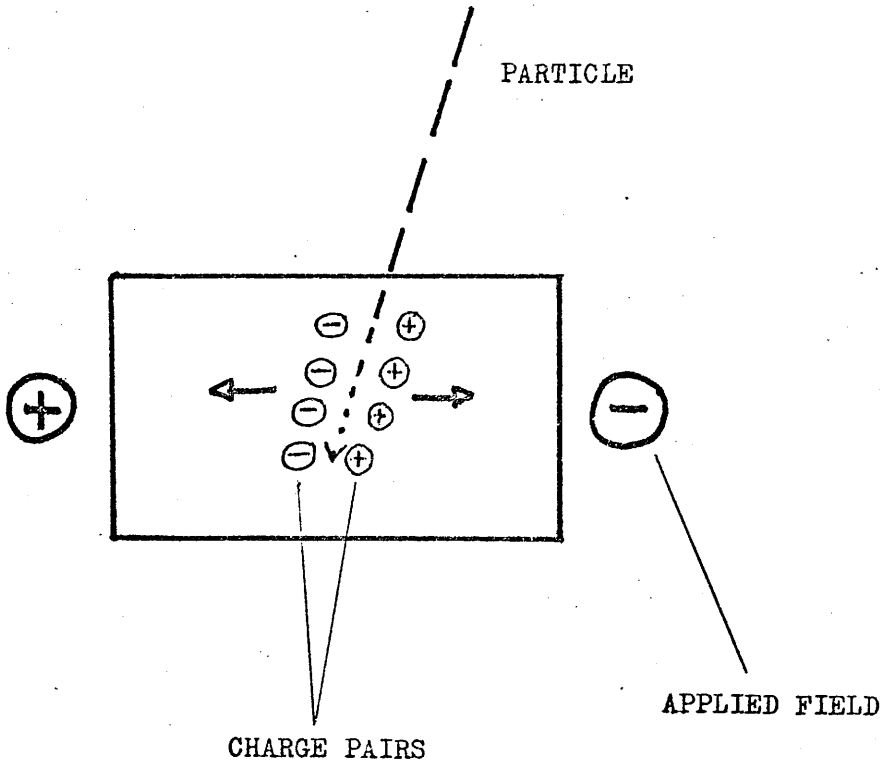

FIG. 3.15

being necessary to produce an ion pair in silicon. In germanium detectors the energy to produce an ion pair is even less and germanium detectors must be operated at low temperatures to reduce thermal noise to a satisfactory level.

The mounting of the detector, a Simtec L.C. 50-0.5-27, with an active area of 50 mm^2 and a depletion depth of 0.5 mm, is shown in fig. 3.16. It sits on a platform at the end of a copper tube which can slide up and down inside a second copper tube. The telescopic mount allows precise adjustment of the distance between target and detector, which is then locked in position using the grub screws. The tubes are necessary to form a co-axial shield round the detector against interference pick-up.(59) Of the two electrical leads to the detector one is provided via the copper mount. The other lead is a wire, insulated with ceramic beads, which passes down the centre of the tube to an insulated metal electrode, sealed through the copper base-plate by Araldite. Electrical joints to the counter are made with soft solder. If silver solder had been used there would have been a risk of heating the detector to a level at which its characteristics would have been permanently affected. The soft soldered joints were pared down so that they present a small surface area capable of being outgassed in vacuo. The copper base-plate has six holes on its circumference to allow it to be bolted to a 3" QVF flange. The inner surface of the copper base is plane and polished for good vacuum characteristics and sealing.

Fig. 3.17 shows in block form the linkage of the detector to the electronic equipment used in counting. In the early part of the work an Ecko Dynatron scaler was used instead of the Laben multi-scaler. The characteristics of the counter are shown in Appendix I. The Simtec solid-state detector, being light

FIG. 3.16

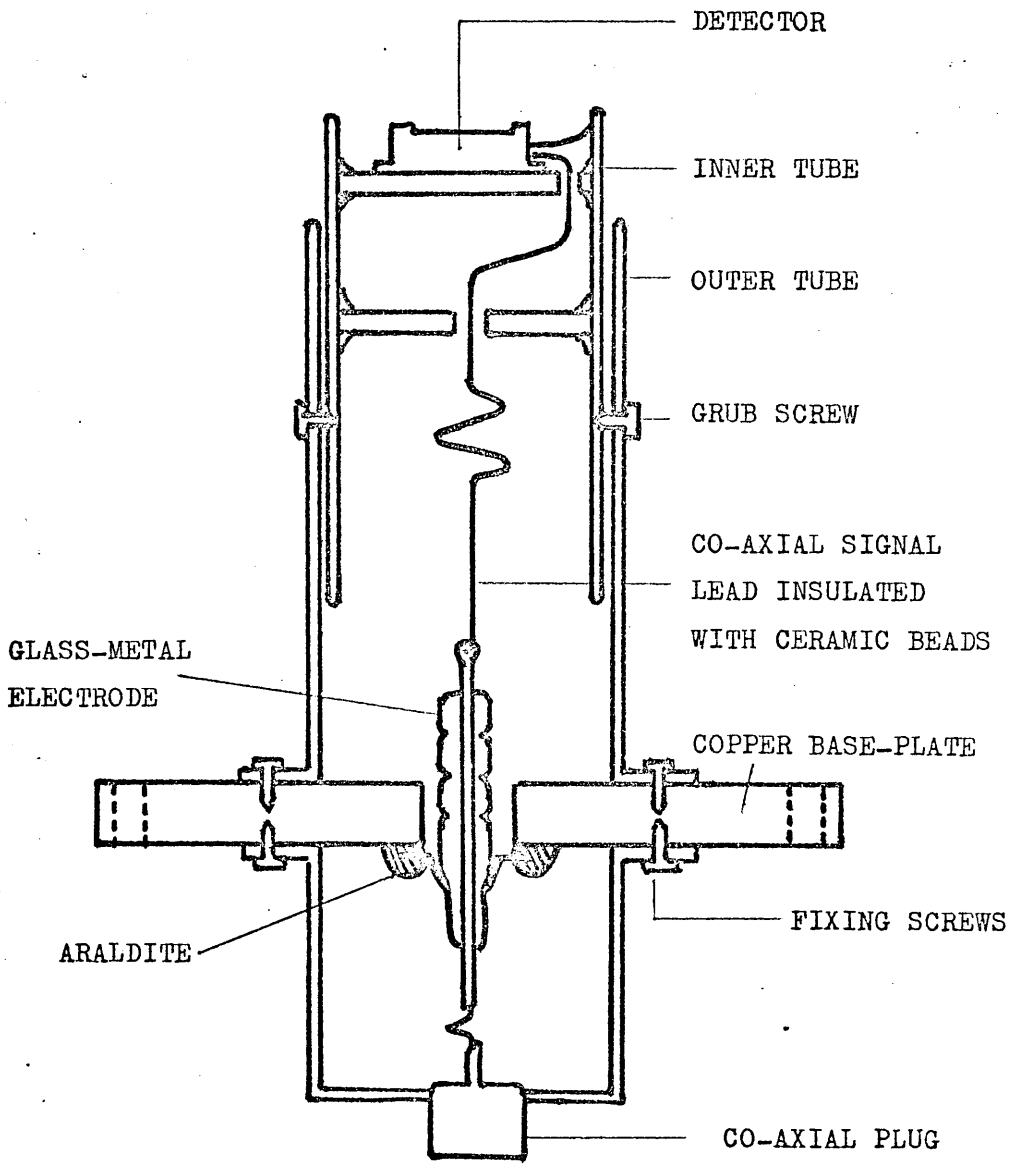
DETECTOR
INNER TUBE
OUTER TUBE
GRUB SCREW
CO-AXIAL SIGNAL
LEAD INSULATED
WITH CERAMIC BEADS
GLASS-METAL
ELECTRODE
COPPER BASE-PLATE
FIXING SCREWS
ARALDITE
CO-AXIAL PLUG

FIG. 3.17

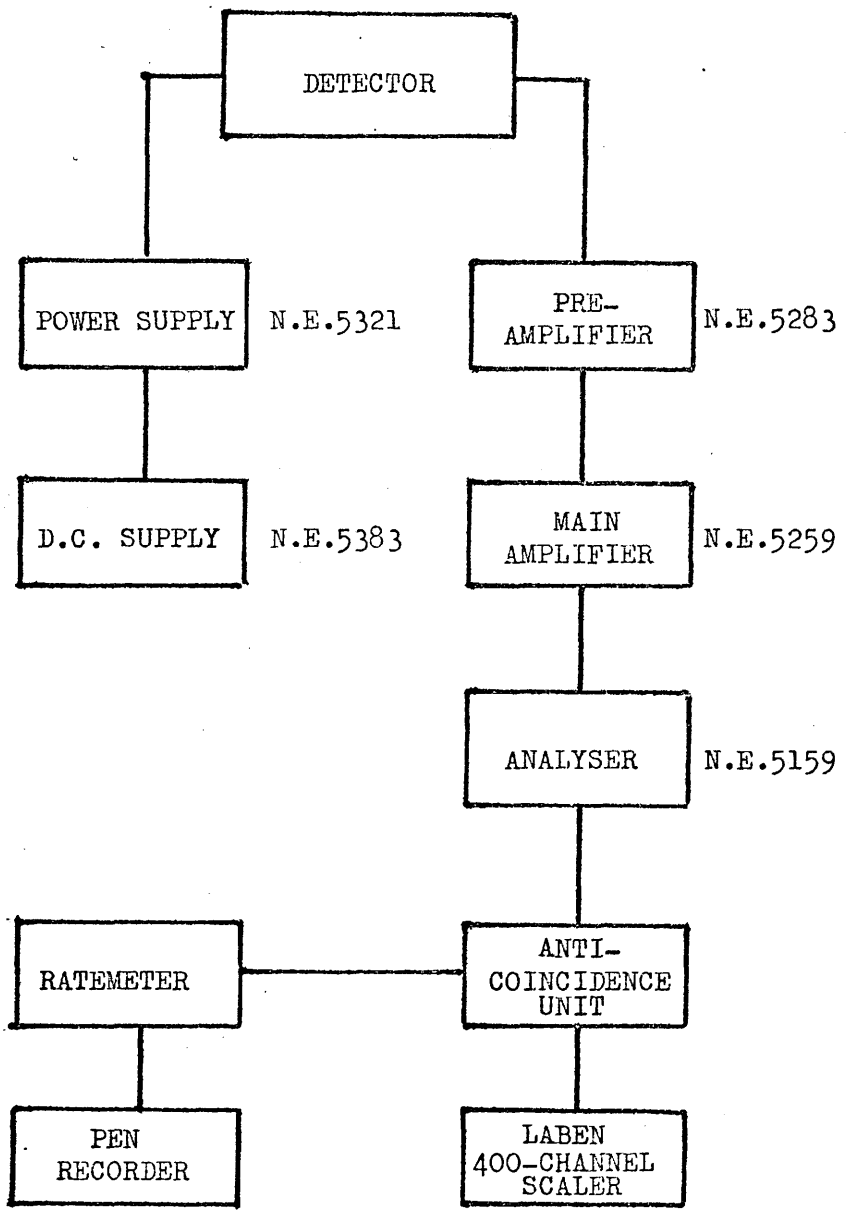
DETECTOR
POWER SUPPLY
N.E.5321
PRE-AMPLIFIER
N.E.5283
D.C. SUPPLY
N.E.5383
MAIN AMPLIFIER
N.E.5259
ANALYSER
N.E.5159
RATEMETER
ANTI-COINCIDENCE UNIT
PEN RECORDER
LABEN 400-CHANNEL SCALER

sensitive, was operated in a curtained room with a single red light providing illumination for manipulation of the apparatus.

During the testing of this equipment considerable trouble was experienced with pick-up of random impulsive interference. This was noted as a fluctuation in the background count between a normal 20-30 cpm and as much as 10,000 cpm, coinciding with the pick-up of static by a wireless receiver. When it is remembered that the count-level expected from the target face is several hundred cpm, it obviously would have been impossible to follow the behaviour of the system when such interference occurred.

Two types of interference were identified, using a portable wireless receiver to locate the sources. The first resulted from the normal operation of other instruments on the same power line. Examples of such instruments were spectrophotometers, variable speed electric motors, Tezla coils and R.F. heaters. Singly these could generate about 10^4 cpm. If one or more were running at the same time as much as 4×10^4 cpm could result. The occurrence of such high level interference during an experiment would have rendered it valueless.

In addition, a number of low level interference sources were identified. Examples of these were thermostats, electric light switching, lift switching, some types of adding machines and peripheral computing equipment. With this type of source one event could add from 1 to 10 cpm to the total. A combination of such sources could raise the background to as much as 400 cpm, capable of invalidating any experiment or at best obscuring a transitory point of interest.

There were two ways in which such interference could affect

the counter. It could have been by direct pick-up from the mains entering through the smoothing circuits or it could have been R.F. pick-up by the detector and/or the amplifier from pulses broadcast by mains cables in their vicinity - of which there were, of necessity, a good number. Measurements were made of these radiated pulses and amplitudes as high as 50 mV were detected 4 ft from the mains wiring.

The first attempt to overcome this problem involved fitting mains-suppressors to the power supplies of the counter unit and building a Faraday cage - an earthed close-meshed copper grid - round the detector and pre-amplifier. This had no effect, probably because the mains earth was in part at least responsible for broadcasting the interference and there was a short between the mains earth and the water pipes - to which the Faraday cage was earthed. Possibly the power of the interference rendered the Faraday cage useless in any case.

A novel method was then adopted to solve this problem. It was decided to pick up the interference pulses on another instrument, amplify them and use the amplified pulses to cancel the spurious pulses generated by the solid-state counter unit.(60) Fig. 3.18 shows the arrangement adopted in block diagram form. This has three channels capable of generating a cancelling pulse at the "and" gate whenever an interference pulse is received. Channel A is connected to an aerial. After amplification the interference pulse triggers a monostable circuit O.S.1, which is so connected that it closes the "and" gate on receiving a pulse. Channel B is connected through a small capacitor, 5 pfd, to the phase side of the mains supply. Mains borne pulses which are not radiated can be cancelled by this channel. Channel C is made available for use when a guard is needed against cosmic radiation. It was not used by us during this work. Channel D

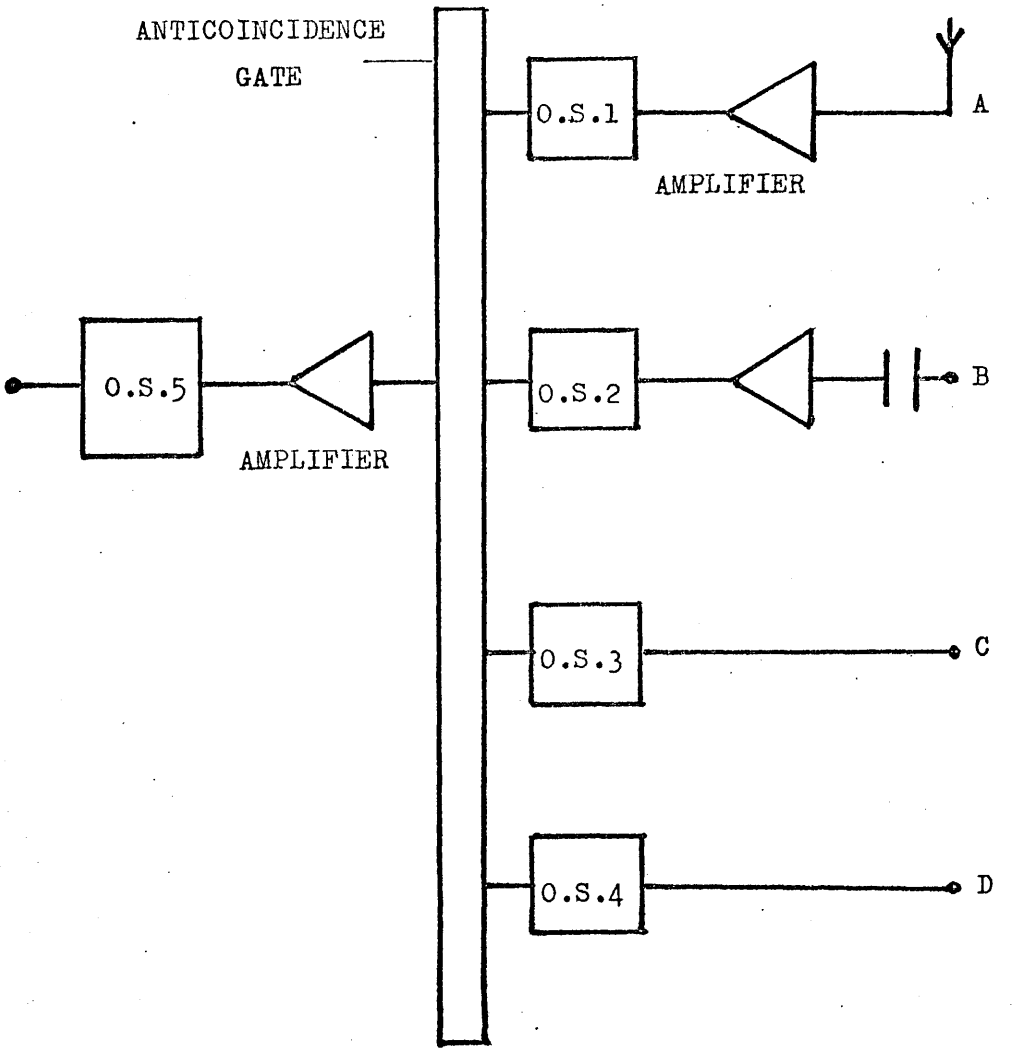
ANTICOINCIDENCE
GATE
O.S.1
AMPLIFIER
A
O.S.5
AMPLIFIER
O.S.2
B
O.S.3
C
O.S.4
D

FIG. 3.18

is fed from the Nuclear Enterprises amplifier and it triggers the monostable O.S.4 which is so connected that the "and" gate is normally closed and opens only when O.S.4 triggers. Fig. 3.19 shows details of the monostable circuits, all identical, the "and" gate and the amplifiers.

The pulse passing through the "and" gate when O.S.4 triggers (O.S.1, 2, 3 not triggering) is amplified and used to trigger O.S.5, the output of which is a negative going pulse of 50μ-sec duration available to drive a scaler or ratemeter. The paralysis time over-all is of the order 50μ-sec.

Without this anti-coincidence unit background counts varied from 20 cpm to well over 10,000 cpm. When the anti-coincidence unit was connected between the amplifier and the scaler or ratemeter the background, measured over 60 hours, did not rise above 30 cpm. Fig. 3.20 shows simultaneous ratemeter recordings before and after anti-coincidence for a period of one hour. The large increases in before anti-coincidence counts are not accompanied by an increase in after anti-coincidence counts. Leaving the pick-up from the mains supply disconnected, similar results were achieved, suggesting that the interference was caused purely by R.F. pick-up.

The performance of the three units - target, evaporator and counter were evaluated singly and together in vacuo in an apparatus (fig. 3.21) which was essentially that described before (fig. 3.4) with the addition of a 25 mm bore vacuum tap mounted with QVF flanges between the collimator chamber and the target chamber. The shields, which were no longer necessary, were deleted. The 3" QVF cross-piece carried target, evaporator and counter, as had the previous unit, till the special QVF five-armed unit previously described became available. This time, however,

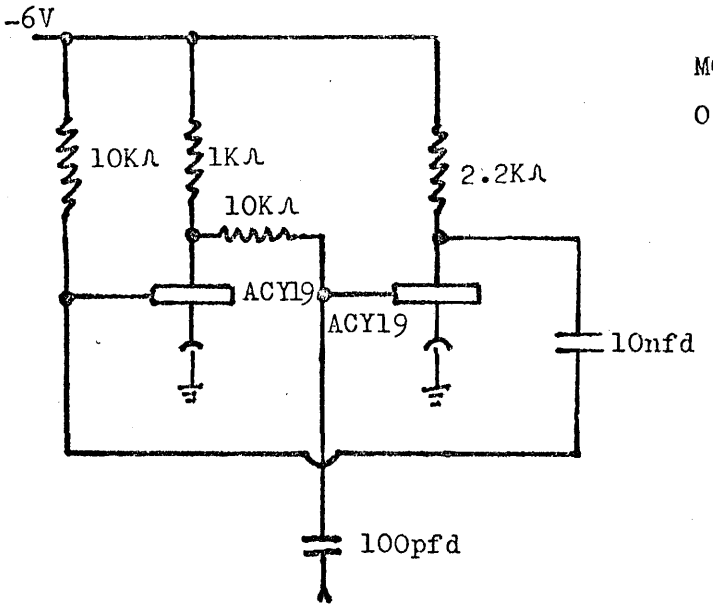

MONOSTABLE CIRCUIT
O.S. 1, 2, 3, 4, 5.

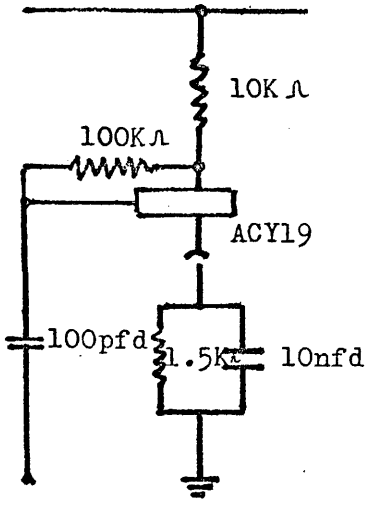

AMPLIFIER

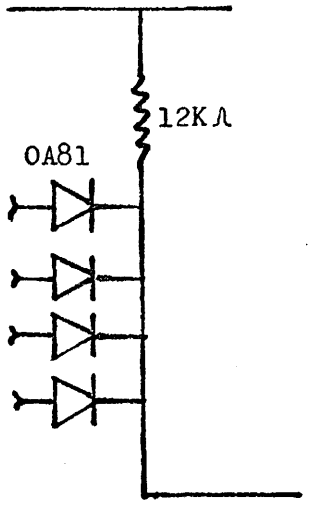

"AND" GATE

FIG. 3.19

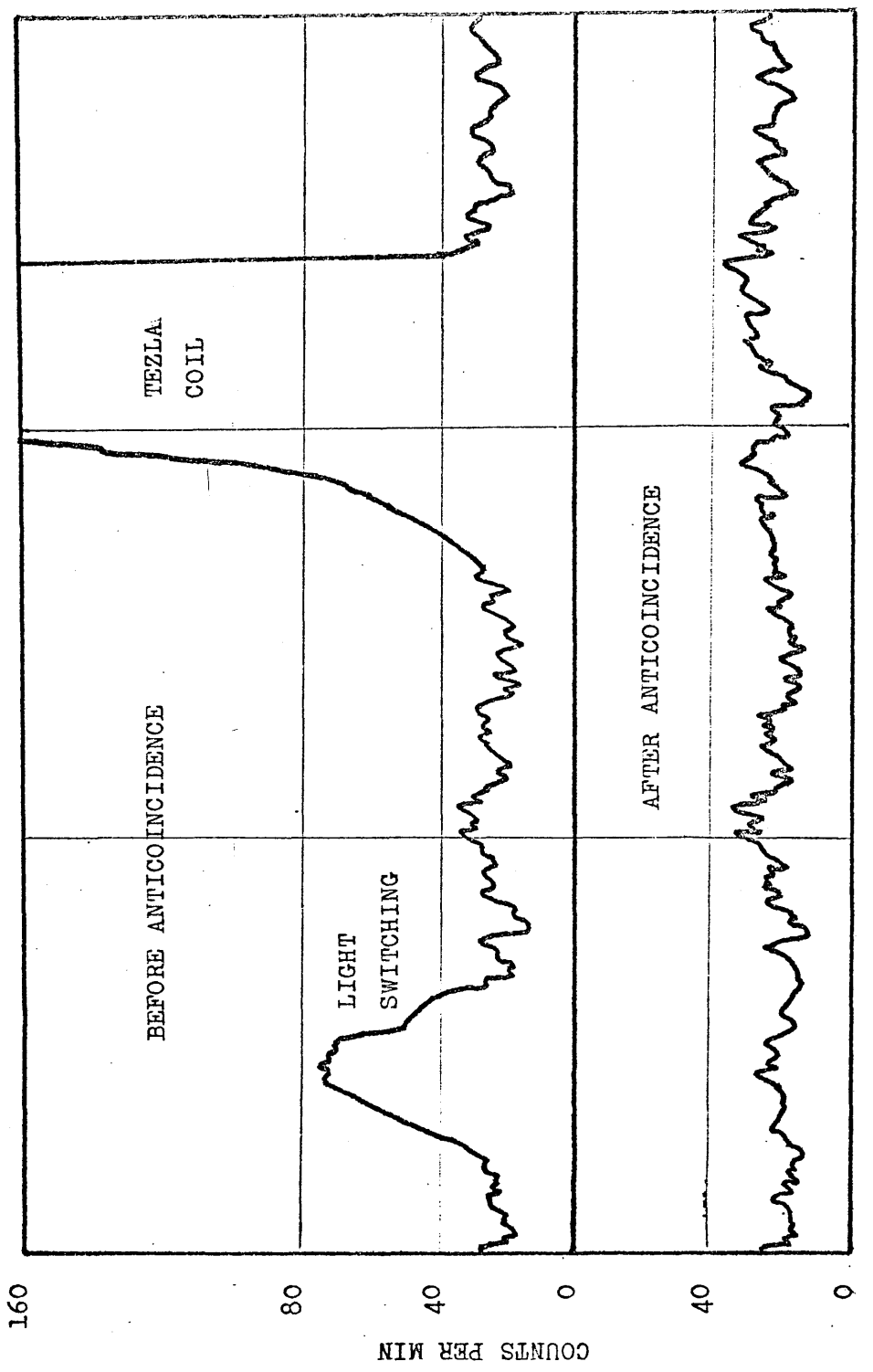
160
80
40
0
COUNTS PER MIN
BEFORE ANTICOINCIDENCE
LIGHT
SWITCHING
TEZLA
COIL
AFTER ANTICOINCIDENCE
40
0
0
20
40
60
TIME (MIN)

FIG. 3.20

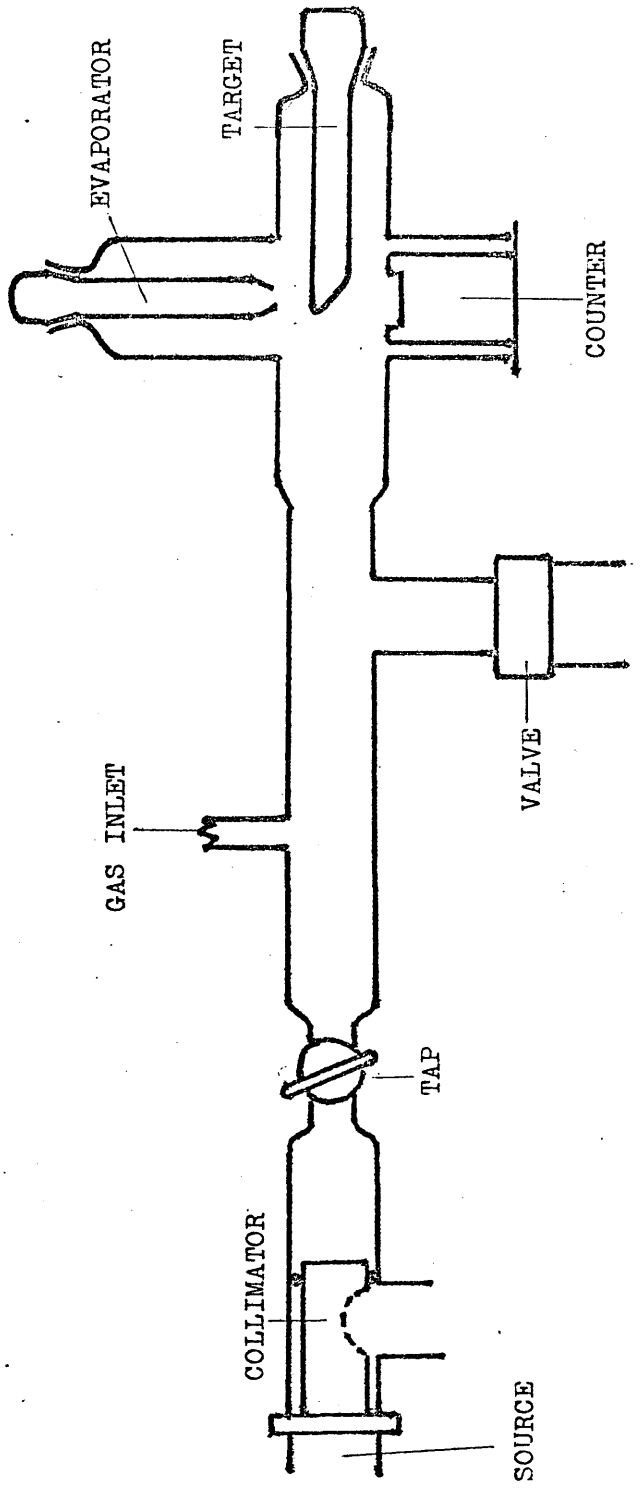
EVAPORATOR
TARGET
COUNTER
DIFF.
PUMP
VALVE
GAS INLET
TAP
COLLIMATOR
SOURCE

FIG. 3.21

the unit was laid horizontally, not vertically. With this arrangement the target chamber could be sealed off completely for adsorption of gases on metal films - which could not be done with the earlier apparatus.

The procedure used was to evacuate the chamber using the 2" oil diffusion pump until a pressure of approximately 2×10^{-6} torr was achieved. After the filament had been degassed during the pump-down period the film was thrown, the chamber valved off using the baffle valve, and ^{14}C ethylene introduced to the film. The gas was left in contact with the film for a few minutes and its pressure measured. The gas was then condensed back into the gas-inlet system for subsequent re-use and the chamber opened again to the diffusion pump.

With this apparatus and the above procedure (which will be described in the next chapter in greater detail) the bulk of the desorption studies involving ethylene on palladium was carried out.

Chapter 4

Apparatus for Molecular Beam Studies using Permanent Gases

(1) Design Considerations

It was essential that the eight requirements of section 4 of chapter 3 should be met, three of them - 5, 6, and 7 - having already been fulfilled. The first requirement for this apparatus was high speed pumping which could not be provided by liquid nitrogen traps as in the first apparatus. Two high speed diffusion pumps were available - an Edwards UHVM 2 mercury diffusion pump with a rated pump speed of 100 l/sec for air and an Edwards EO 4 4" air-cooled oil diffusion pump with a rated pump speed of 600 l/sec for air. The apparatus was designed around these two units.

The second requirement was one of the most critical, namely, the attainment of a beam : background flux ratio of 1 : 1 or better. Thus we endeavoured to design a system in which the distance between the source and the target was kept as small as possible. Experimental considerations dictated however that the target chamber had to be sealed off completely for preadsorption of gases on to the metal films. Thus there had to be a valve between source and target - a factor which caused a long source - target distance. The valve had to be of the "straight through" or "gate" type to allow free passage of the beam and it had to be compatible with QVF glass: otherwise there would have been adaptors and further lengthening of the beam path. Such a valve was found in the VAT N.W. series - Swiss made metal valves with a sliding metal gate - available in the U.K. from Vacuum Instruments and Products Ltd. The valve compatible with 3" QVF glassware is the VAT N.W.65 with a thickness of only 3 cm and, in

the stainless steel version, having an excellent ultimate vacuum capability.

A further design change was made to reduce background pressure by adopting a canal-type source instead of the slit used previously. The effect of this is illustrated in fig. 4.1. A slit source, provided it fulfils the requirements listed in section 3 of chapter 3, allows gas effusion to follow an almost perfect cosine distribution. If the thickness of the slit is increased the intensity of the gas effusing along the normal is unchanged, but the intensity and therefore the amount of gas effusing in other directions is reduced. Thus the amount of gas which could contribute to the background pressure is decreased.

The third requirement - that of good ultimate vacua - is fulfilled in part by the provision of high speed diffusion pumps. Thus any outgassing from materials in vacuo contributes less to the equilibrium pressure. The ultimate static pressure produced by these pumps must be as low as possible as the speed of the pump is reduced from its rated speed at its given working pressure unless its ultimate pressure is considerably less than its working pressure. The effective speed is given by:

$$S_E = S_R(1 - P_U/P_W)$$

where

S_E is the effective speed of the pump at its working pressure, in l/sec

S_R is the rated speed of the pump, in l/sec

P_U is the ultimate pressure of the pump in the system, in torr

P_W is the pressure achieved by the pump under its working load, in torr.

It was necessary therefore to reduce outgassing by careful choice

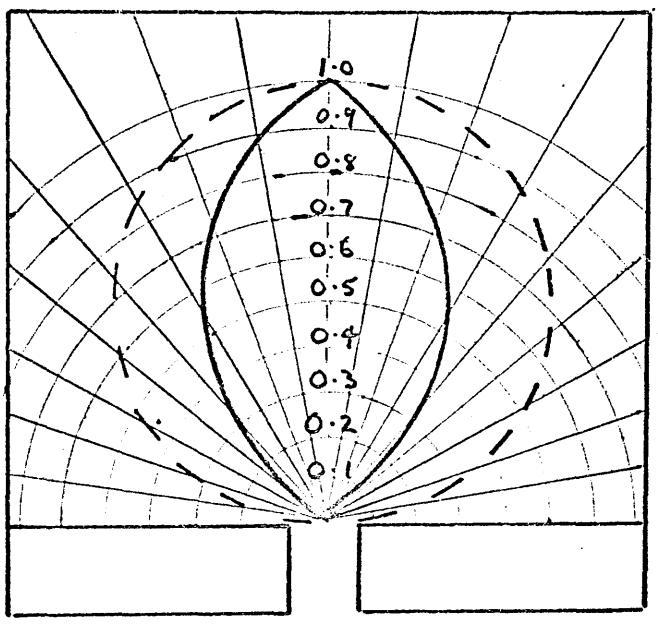

FIG. 4.1

The angular distribution of molecules effusing from a source. The dotted curve is for an aperture of negligible length. The full curve is for an aperture canal whose length is equal to its width.

of materials. In this respect the solid-state detector is much better than its predecessor, the scintillation unit, which had a layer of plastic incorporated in its structure. Mild baking of components in vacuo was carried out where possible after they had been carefully cleaned at the construction stage. The design of the pumps also contributes to the ultimate vacuum. Both diffusion pumps are stainless steel units and the UHVM 2 mercury diffusion pump is specifically designed to reach ultimate vacua, in fully baked apparati, of less than 10^{-10} torr. The EO 4 oil diffusion pump, when without the "in line" trap between it and the chamber to be evacuated, retains as much of its rated speed as possible; the trap has a conductance of 200 l/sec. To maintain a low ultimate pressure the pump fluid chosen was silicone 705 oil with a vapour pressure of 5×10^{-9} torr at room temperature and a liquid nitrogen trap is placed in the chamber which it pumps directly opposite the exit port to the pump: this catches as much of the backstreaming oil as possible and keeps the vapour pressure at a low level.

When considering pump speeds the question of ultimate vacua is a relative matter. An ultimate pressure of 5×10^{-9} torr would entail a speed loss of 50% at a working pressure of 10^{-8} torr: at a working pressure of 10^{-7} torr the speed loss is only 5% and this is tolerable for our purposes. These design features for achievement of good ultimate vacua naturally contribute towards the second requirement already discussed.

The requirement of pressure measurement in all sections meant measuring pressures in the range 10^{-6} - 10^{-9} torr. For this purpose Edwards Bayerd-Alpert ionisation gauges were proposed to supplement Pirani gauges already available for the range 5×10^{-4} torr - 5×10^{-1} torr.

The fifth, sixth and seventh requirements are met by the designs already discussed in section 5 of chapter 3. The eighth requirement, that concerning the source, is fulfilled by the design described in the next section, which permits source temperatures of 350°C to be attained.

To meet all of these varied requirements it is essential that none should be satisfied at the expense of any of the others. Thus in designing a target and evaporator which depend for their operation on greased ground glass joints, we must allow for the grease to be deliberately degassed over a period of time before good ultimate vacua are attained. Yet again the arrangement for retaining high pump speeds from the oil diffusion pump necessitate using silicone 705 oil and a well-positioned trap, otherwise ultimate vacua would be affected.

In the following sections we describe the permanent gas molecular beam apparatus and predict its performance, outline its construction and, finally, detail its operation and actual performance.

(2) Description and Calculation of Performance

The apparatus is shown in fig. 4.2 and 4.3. Fig. 4.2 shows the arrangement of the core of the apparatus. Two QVF units, a 3" cross-piece and the specially made five-armed unit, are clamped together, pinching a copper disc with the collimator hole and a VAT N.W.65 gate valve between them. The cross-piece forms the beam-source chamber, the five-armed unit the target chamber.

The EO 4 4" diffusion pump is connected to the source chamber by a tube, 12" long, whose diameter over the first 6" is 4", narrowing to 3" diameter for the rest of its length. This has a 3" QVF flange at one end and at the other is connected via a graded glass/Kovar seal to a stainless steel flange which mates to the top flange of the pump. One side arm on the tube allows attachment of an Edwards IG3G Bayerd-Alpert gauge. The other side arm is connected to the gas-handling lines for their evacuation. On the top of the cross-piece opposite the pump exit is mounted a liquid nitrogen trap.

The source, shown in detail in fig. 4.4, is carried on a detachable QVF 3" unit. A glass tube carries gas from the gas-handling lines (fig. 4.5) through the end of the QVF piece up to the source proper. This is a copper tube with an internal diameter of 1 cm connected to the gas inlet tube by a copper/glass Housekeeper seal silver soldered to the copper. The beam emerges from a circular canal 26 mm long and 2 mm in diameter. This end of the copper has been finned to remove excess copper and reduce weight. The copper unit was machined from a bar of solid copper. Wrapped around this copper tube is a sheet of mica, approximately 0.01 cm thick, which is held in place by thin

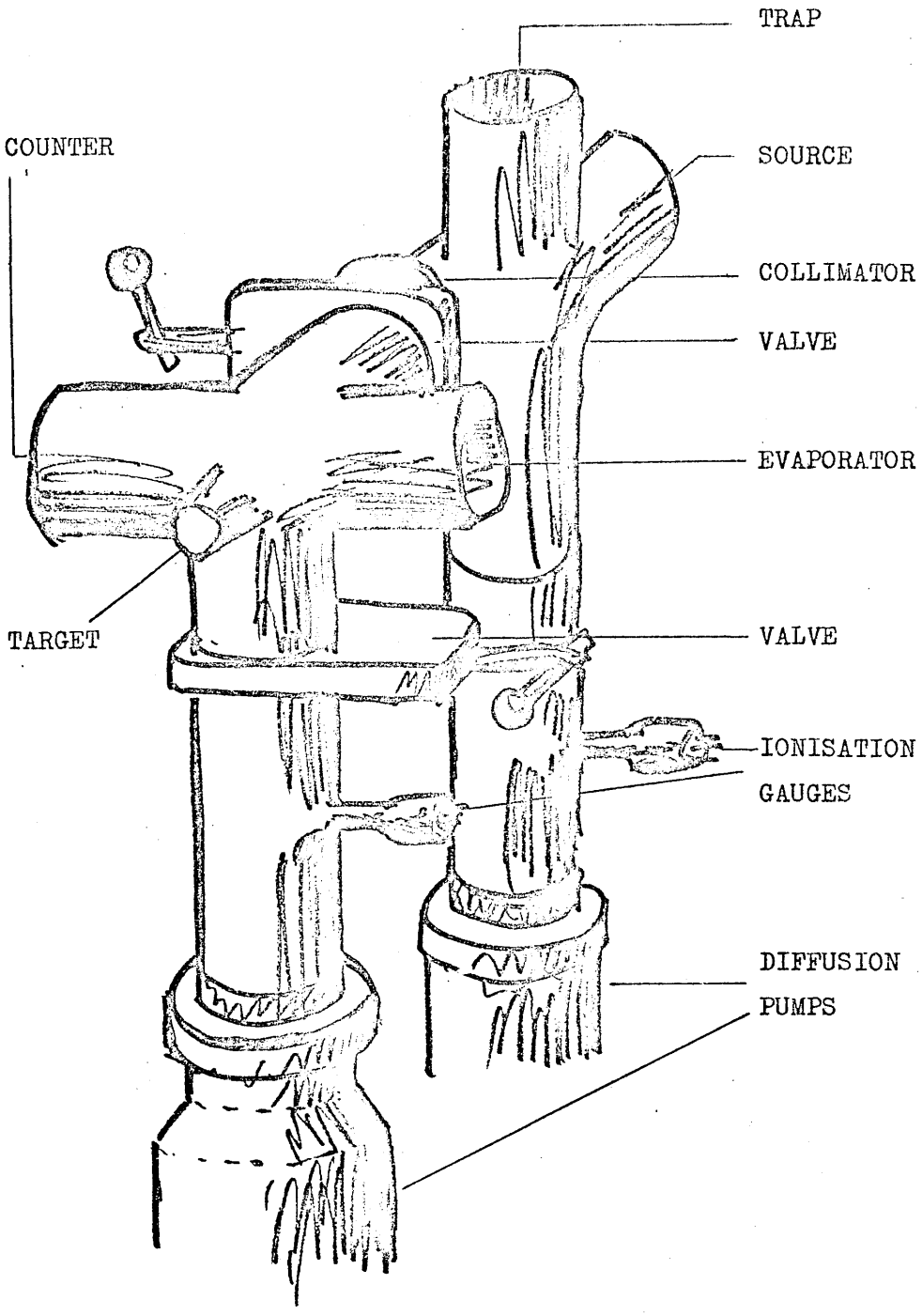
TRAP
COUNTER
SOURCE
COLLIMATOR
VALVE
EVAPORATOR
TARGET
VALVE
IONISATION
GAUGES
DIFFUSION
PUMPS

FIG. 4.2

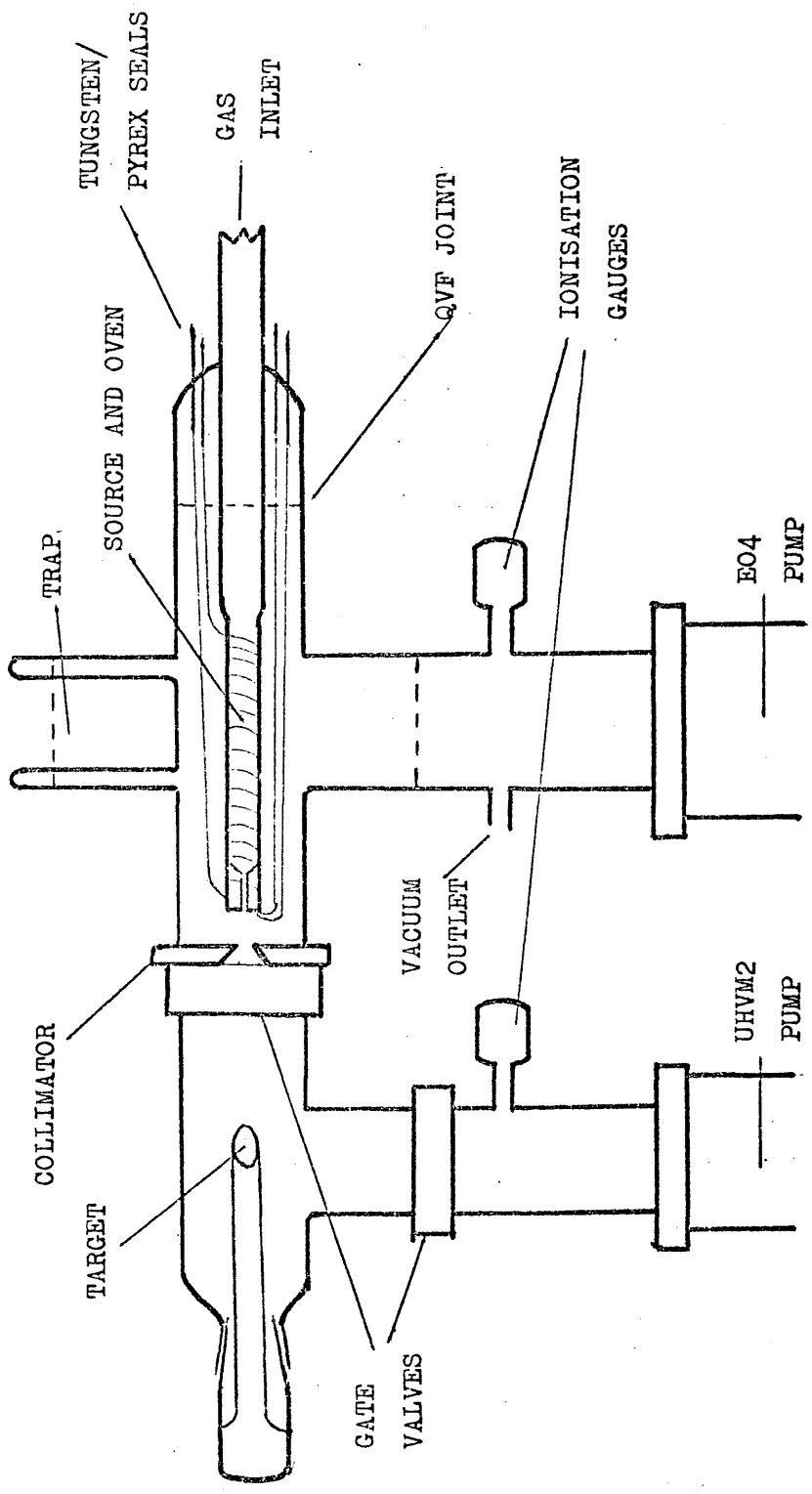
TUNGSTEN/
PYREX SEALS
GAS
INLET
QVF JOINT
IONISATION
GAUGES
SOURCE AND OVEN
TRAP
E04
PUMP
VACUUM
OUTLET
COLLIMATOR
UHVM2
PUMP
TARGET
GATE
VALVES

FIG. 4.3

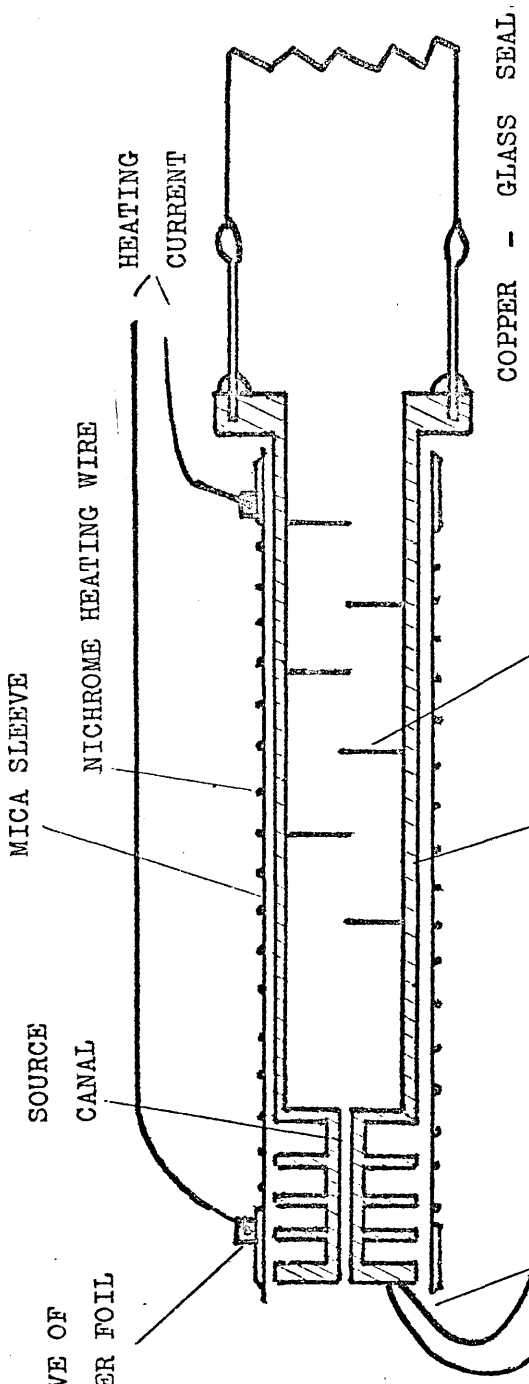
HEATING CURRENT
COPPER - GLASS SEAL
NICHROME HEATING WIRE
MICA SLEEVE
SOURCE CANAL
SLEEVE OF COPPER FOIL
HALF-MOON BAFFLE
COPPER SOURCE WALL
THERMOCOUPLE

FIG. 4.4

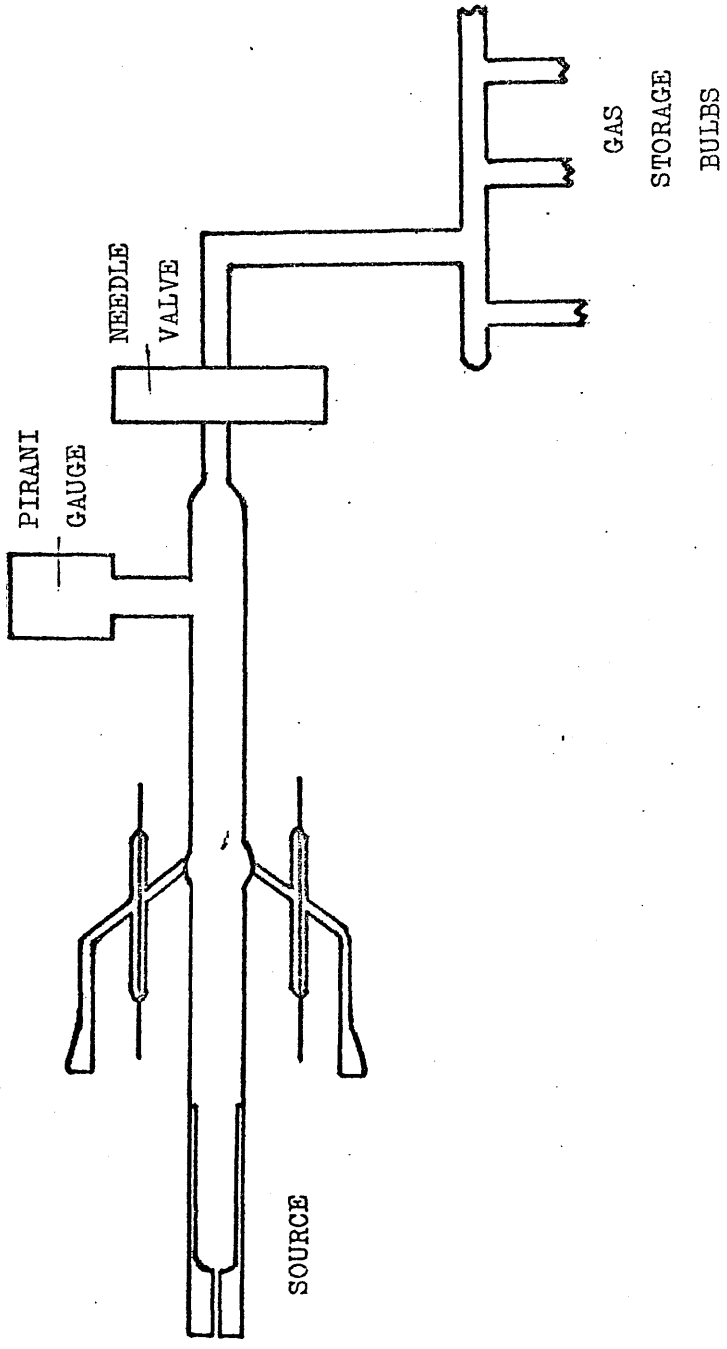

FIG. 4.5

bands of copper foil used as hose-clip type retainers. Between these two strips of copper foil is coiled Nichrome heating wire spot-welded to each foil. From each foil strip are led lengths of 16 gauge copper wire. These were silver soldered to tungsten/glass seals carried by the QVF unit. This mica/heating wire arrangement is used as an oven to heat the copper tube, current being fed through the tungsten/glass seals. To the front face of the tube, beside the beam exit canal, are silver soldered lengths of 32 gauge copper and Constantan wire. Connections to this copper/Constantan thermocouple are made via two more tungsten/glass seals. The tube is internally baffled with six half-moons of copper foil to ensure thermal equilibration of the beam gas. The thermocouple was calibrated in vacuo by sealing a thermometer into the gas inlet tube, with its bulb inside the inlet end of the copper tube, and heating the source. No variation from the expected e.m.f. of the thermocouple occurred up to 250°C, when a back e.m.f. caused by the connections to the tungsten/glass seals acting as thermocouples, with a hot junction inside the source chamber and a cold junction outside, was produced.

The source exit lies 3.4 cm from the collimator. This is a 6 mm diameter hole, with bevelled edges, in a $\frac{1}{4}$" thick copper plate. The collimator forms the beam, which then enters the target chamber through the gate valve, which is shown in detail in fig. 4.6. The gate-plate slides forward to fill the central opening and is then sprung to one side to clamp a Viton A O-ring it carries against the polished internal face of the valve. The outer faces of the valve carry two Viton A O-rings in grooves. One mates to the copper plate, both faces of which are plane and polished, the other to the ground glass 3" QVF flange of the target chamber. The other face of the copper is sealed by an indium O-ring to the QVF face of the source chamber.

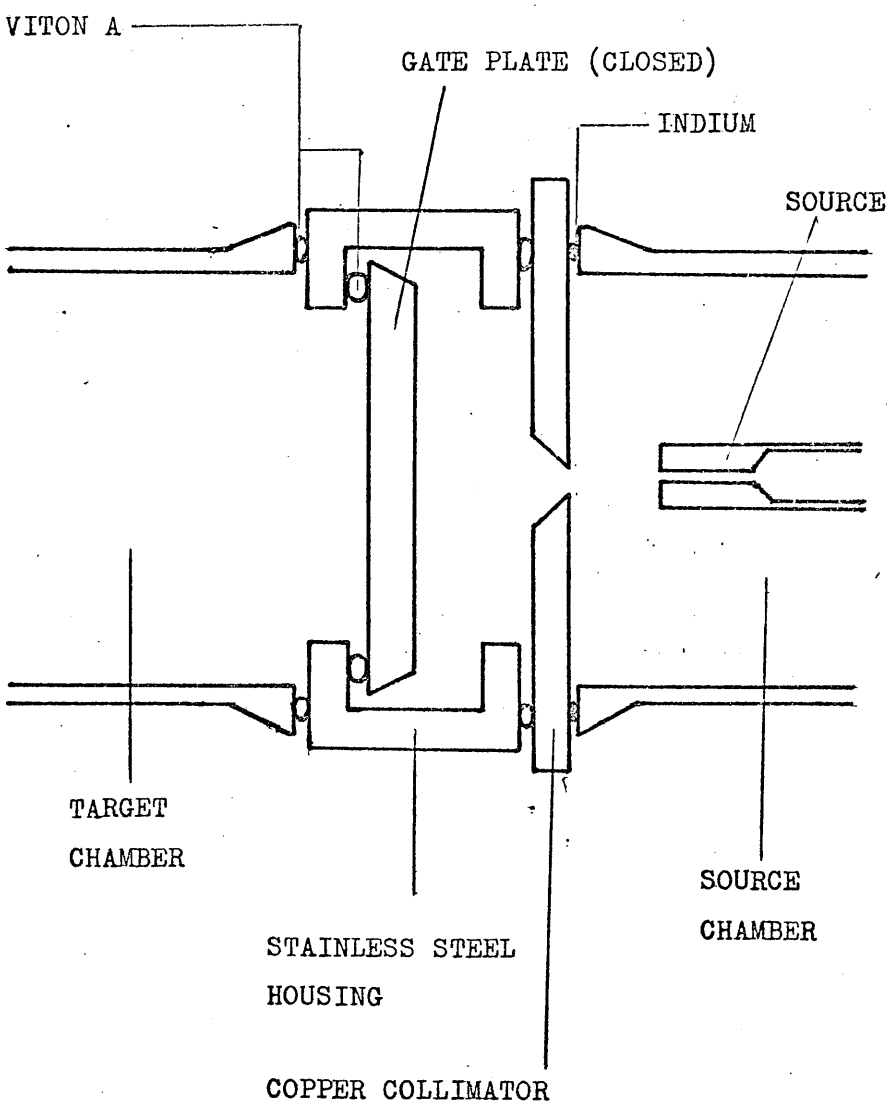
VITON A
GATE PLATE (CLOSED)
INDIUM
SOURCE
TARGET
CHAMBER
STAINLESS STEEL
HOUSING
COPPER COLLIMATOR
SOURCE
CHAMBER

FIG. 4.6

The UHV 2 mercury diffusion pump is coupled to the underside of the target chamber with a second VAT N.W.65 gate valve. This is held between the 3" QVF flange of the target chamber and a 3" QVF end of a tube similar to that connecting the oil diffusion pump to the source chamber. A side arm allows attachment of a second Edwards IG3G ionisation gauge. The pump has an integral liquid nitrogen trap and an integral Peltier cooled baffle. The arrangement of target, evaporator and counter has already been described in section 5 of chapter 3.

The system used for gas inlet to the beam source is, in essence, a number of gas reservoirs linked to the source via a variable leak needle valve. Gas pressures in the source are measured using an Edwards G5C2 Pirani gauge which can be used in the pressure range 10^{-4} torr to 5×10^{-1} torr, chosen to cover the range in which we are interested - about 2×10^{-3} torr (see later in this section).

Gas inlet to the target chamber is achieved via a large diameter greased tap from a boom carrying a reservoir, a sampling socket, a break-seal vial connection and a second Pirani gauge head. The two gas-inlet systems are interconnected and can be evacuated via the sidearm on the pump to the source chamber connecting tube.

Backing pumps used are, for the oil diffusion pump, an Edwards ES 150 rotary pump and, for the mercury diffusion pump, an Edwards ES 75 rotary pump, the numerals designating their speed in l/min. Both pumps incorporate safety valves so that, should the electricity supply fail, the valves close and no oil rises into the diffusion pumps. The water supply to the mercury diffusion pump has a pressure switch fitted to it so that, in the

event of water failure, the electricity supply to the pump is cut off. Both safety devices have operated satisfactorily on a number of occasions. As in earlier apparati, a blank flange is left in the pipeline-backing line for the connection of the leak-detector head.

Before the apparatus was built its performance was assessed by calculation using the equations employed in section 3 of chapter 3. The calculations which follow are for acetylene as the beam gas at a source temperature of $300^{o}K$. The highest source pressure that can be used is dictated by the requirement that the mean free path of the gas in the source must be equal to, or greater than, the length of the exit canal. For acetylene at $300^{o}K$ this pressure is 2×10^{-3} torr.

The total outflow of acetylene from the source is given by

$$Q = (1/K) \times 1.118 \times 10^{22} \times \pi \times p_S \times A_S / (M \times T)^{\frac{1}{2}} \text{ molecules/sec}$$

where $1/K$ expresses the effectiveness of the canal in reducing the total number of molecules emerging from the source and is, for a long cylindrical canal, equal to $8r/3l$[48] where r is the radius and l the length of the canal. In this case, with r = 1mm and l = 26 mm, $1/K = 1/10$.

Thus, with

$p_S = 2 \times 10^{-3}$ torr

$A_S = \pi \times 10^{-2}$ cm^2

$M = 26$

$T = 300^{o}K$:

$Q = 2.5 \times 10^{15}$ molecules/sec.

the pump speed available at this chamber is given by:

$1/S_E = 1/S_R + 1/C_1 + 1/C_2$ ..... as before.

The rated pump speed available is 600 l/sec. The connecting tube between pump and source chamber is 12" long, half of it 4" in diameter, the other half 3" in diameter. The conductances of the two sections are, respectively, 850 l/sec and 360 l/sec. Substituting these values in the pump speed equation we find that:

S_E = 180 l/sec.

This pump speed, acting on an inflow of 2.5×10^{15} molecules/sec produces a residual pressure, p_C, in the collimator chamber of 4.0×10^{-7} torr.

The inflow into the second chamber arises from two sources. Firstly, there is diffusion from the gas at a pressure of 4.0×10^{-7} torr in the collimator chamber, through the collimator hole. This amount is calculated from

$Q_1 = (1/K) \times 1.118 \times 10^{22} \times \pi \times p_C \times A_C / (M \times T)^{\frac{1}{2}}$ molecules/sec

as before. Here

$1/K = 1$ since the hole has bevelled edges and is not a canal

$p_C = 4 \times 10^{-7}$ torr

A_C = the area of the collimator hole

$= \pi \times (0.3)^2$ cm^2 (radius of the hole = 3 mm)

$M = 26$

$T = 300^{\circ}$K as before.

Thus,

$Q_1 = 4.4 \times 10^{13}$ molecules/sec.

The second inflow results from the direct input of the beam into the target chamber. This is given by

$Q_2 = 1.118 \times 10^{22} \times p_S \times A_S \times A_C / l_{SC}^2 \, (M \times T)^{\frac{1}{2}}$ molecules/sec

where p_S, A_S, A_C, M and T are as before and l_{SC} is the distance between source and collimator and is equal to 3.4 cm. Substituting numerical values in the above equation we obtain the value:

$Q_2 = 1.92 \times 10^{14}$ molecules/sec.

The total inflow to the target chamber is thus the sum of Q_1 and

Q_2 and is equal to 2.36×10^{14} molecules/sec.

The effective pump speed in the target chamber is given by a pump of rated speed 100 l/sec linked to the chamber by a tube 14" long and 3" in diameter, whose conductance is 155 l/sec. Thus, in this chamber,

$S_E = 60$ l/sec.

Acting on an inflow of 2.3×10^{14} molecules/sec this produces a pressure, in the target chamber, of 1.1×10^{-7} torr. The rate at which molecules in this residual vacuum strike unit surface area is calculated as 4.4×10^{13} molecules/cm^2/sec.

The beam intensity is given by:

$$I = 1.118 \times 10^{22} \times p_S \times A_S / l_{ST} (M \times T)^{\frac{1}{2}} \text{ molecules/cm}^2\text{/sec}$$

where p_S, A_S, M and T are as before and l_{ST} is the distance between source and target which in this case equals 15 cm. Substituting values in this equation gives:

$I = 3.7 \times 10^{13}$ molecules/cm^2/sec.

Thus the ratio of beam intensity : background flux on the target is as 3.7 : 4.1, i.e. as 1 : 1.1, which is sufficiently close to our proposed working ratio of 1 : 1 to be usable.

The beam formed by the collimator at a distance of 15 cm from the source exit will cover a circle with a diameter of 2.7 cm. The target spot has a diameter of 1 cm – much less than the beam spread. This was intended to ensure that the rough and ready collimation proposed would be effective.

To ensure that the maximum rated pump speeds could be used at the working pressures meant that the ultimate pressures achieved in each chamber (see section 1 of chapter 4) had to be at least an order of magnitude less than the working pressures. This was in fact achieved and the above pump speeds are applicable.

(3) Construction

Since this was the first working beam system the construction will be given in more detail than is perhaps usual. Pump exhausts were led out of a window to dispose of the small amounts of radioactive material used. To lessen vibration metal bellows units were included in the backing pipelines. Before assembly all units were washed, dried with acetone and heated to 150°C in air to ensure cleanliness, with the exception of the detector which was preserved in the clean state in which it was received until insertion into the apparatus. Heating or washing would have altered permanently the counter characteristics.

The method of construction, on a conventional island vacuum bench, was as follows. The two diffusion pumps were aligned roughly for height, the shorter 4" diffusion pump being raised and carried on two metal rods under its asbestos platform. The metal flange to glass flange connectors had already been bolted to the top flange of the diffusion pumps using indium O-rings. A VAT valve was placed on top of the mercury diffusion pump stack.

The five-armed unit and the cross-piece were then bolted together with the collimator plate and the second VAT valve between them, keeping the bottom flanges in the same plane by setting them against a wall. Only four bolts were used: the valve side housing meant that one bolt could not be used and the opposite bolt was also left out to keep the strain symmetrical. The copper collimator plate has six holes cut in its periphery to carry the bolts. Standing the assembly against the wall allowed the indium seal between the copper plate and the cross-piece to be made in a horizontal position - an easier task than with the indium in the vertical position. The nuts are always tightened

in the order shown in fig. 4.7, giving each nut half a turn each time. The twin unit was then turned on its side and the QVF/B34 socket unit to carry the evaporator and gas inlet bolted to the appropriate flange on the five-armed unit.

The assembly was then held again in a vertical position, with the gate valve open and the source unit bolted in with the source canal aligned by eye with the collimator hole. Several attempts were necessary as slight changes in position could occur during the tightening of the joint. It was feared that when the assembly was turned into the horizontal position the moment of the unsupported copper source at the end of the comparatively long glass tube would break the glass seal. This did not happen. A steel rod, which had been machined to fit into the source canal, was put in place through the collimator hole. The target was then placed into its B55 socket to ensure that the steel rod, which did not touch the sides of the collimator hole, pointed straight at the centre of the target face when the target face was pointed towards where the counter would be, i.e. in the position in which the beam would fall on it. This did not occur at first. The target was removed and the tube leading to the face was heated and the position of the face altered. Refitting and further adjustment of the position of the face were carried out until the target face was in position. As the collimator hole and the source to collimator distance had been chosen so that the beam would cover a greater area than necessary it was assumed that collimation had been accomplished. To confirm this, another rod with a rounded end was placed firmly against the source hole and moved around the edge of the collimator hole to ensure that the cone formed by the beam (and the rod) would cover the target.

The assembly was then placed on to a series of support rods on the framework and the support lowered until the source chamber

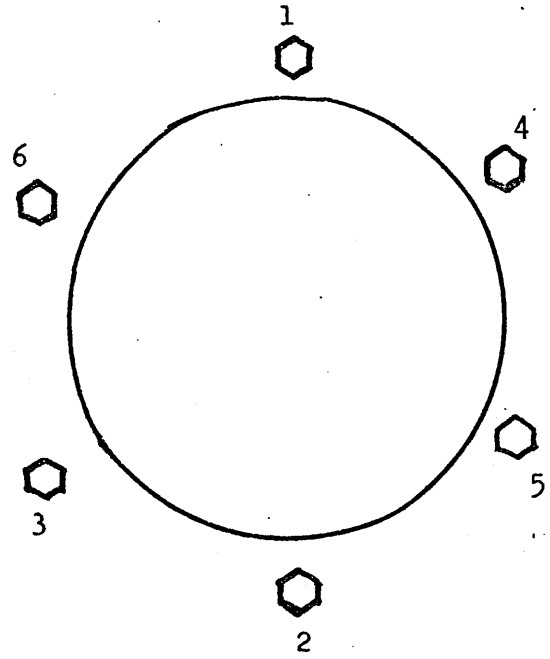

FIG. 4.7

could be bolted to the oil diffusion pump stack. The height and angle of the mercury diffusion pump stack were then adjusted to mate to the bottom flange of the five-armed unit, allowance being made for compression of the Viton A O-rings in the VAT valve.

The trap in the source chamber was then fitted. Gas inlets and gauges for the source and target chambers were blown on and the backing lines connected. The detector assembly was adjusted so that the detector was as close as possible to the target face and the unit was then put in place. The evaporator was fitted so that the hole which forms the film spot was pointing at the centre of the target face and scratches were made on the outside of the apparatus on the B34 cone and on the outside of the evaporator to ensure that the evaporator was always fitted in the correct position. Alignment scratches were similarly made on the internal B24 joint and on the target B55 joint. That the film spot was thrown in the right position was confirmed during the initial vacuum tests. It was also ensured that the target could be turned without touching the counter or the evaporator.

When the Simtec detector was used the windows were curtained off and a red light could be used to illuminate the gas-handling lines for their operation. When this detector eventually failed it was replaced by an Elliot lithium-drifted silicon detector, which had to be operated in complete darkness. The detector chamber was covered with black tape, a square of heavy cloth hung over it and the windows were blocked with hardboard. The scaler and rate-meter are placed outside the beam room.

(4) Operation and Performance

The apparatus was used to carry out sequences of from two to five runs. We shall describe the operation of the apparatus, starting from air pressure, during a typical experiment and show the preparation of a second run in the series. The actual performance of the apparatus is compared with the performance predicted in section 2 of this chapter. The run we describe involves the interaction of C-14 labelled ethylene, chemisorbed on a palladium film, with a beam of unlabelled acetylene. The film temperature is 25°C; the nominal beam temperature is 60°C.

Initially all taps are opened, with the exception of the two gate valves isolating the target chamber. The rotary pumps are used to evacuate the apparatus to a pressure of approximately 3×10^{-2} torr. At this point the cooling water flow to the mercury diffusion pump and the fan cooling the oil diffusion pump are switched on. The oil diffusion pump then evacuates the source chamber, the gas inlet systems and the target chamber - the last through the gas inlet systems. The target, evaporator and detector are already clean and mounted in the target chamber. The target chamber is evacuated in this way to ensure that no mercury vapour from the pump comes in contact with the detector, where it may affect the gold electrodes. Pressure in the source chamber drops to approximately 5×10^{-7} torr in two hours after switching on the oil diffusion pump. A U-tube trap before the target chamber prevents any contamination of it by pump oil. Oil does backstream from the pump, condensing on the walls of the target chamber. This condensate is removed by baking the chamber at 140°C using heating tape, at the same time heating the source oven to 200°C through a Variac. The ionisation gauge is baked separately at 250°C.

Simultaneously the connection between the mercury diffusion pump and the target chamber, the top of the pump flange and the closed gate valve leading to the target chamber are baked at 140°C. The ionisation gauge in this section is again baked separately at 250°C. During this baking procedure the integral trap is gradually filled with liquid nitrogen. After three hours the assembly is allowed to cool and pressure measurements taken after the gauge filament and electrodes have been degassed. The pressure reached in this section three hours after the end of baking is usually 3×10^{-9} torr. During baking cold water circulates through the copper cooling coils around the greased cone and socket joints on the target chamber to prevent binding of the joints which lie directly above the baked region. The cooling water is then turned off until degassing of the palladium filament is started. During this period the grease returns to room temperature and degassing occurs.

After twenty-four hours' pumping, with the target chamber being pumped through the gas inlet system and the mercury diffusion pump only evacuating up to the gate valve to the target chamber, this gate valve is opened and the gas inlet tap to this chamber closed. The source chamber is still being baked at 140°C and will remain so until immediately before the run proper is started. The pressure in the target chamber is at this moment about 5×10^{-8} torr and falls over the next twenty-four hours to about 5×10^{-9} torr. In this way any large amounts of condensable species in the target chamber are pumped away without being condensed on the integral trap in the target chamber pump stack, from where they could desorb back into the target chamber. The trap lifetime for liquid nitrogen is approximately eighteen hours which is just sufficient for it to be left unattended overnight.

The six-hour period after opening the target chamber to its own pump and before degassing of the palladium is used to carry out any gas handling which may be needed, to degas the greased cone and socket joints, and to check the counter characteristics. At the time the apparatus was built and tested the gas storage bulbs for the beam inlet were filled with ethylene and acetylene to a little less than one atmosphere pressure by admitting the appropriate gas, through the device shown in fig. 4.8, into the evacuated bulbs. The procedure used was to admit gas from British Oxygen cylinders into the vertical tube which is filled with mercury up to the sintered glass plug. This plug allows gas to pass but not liquid mercury. The gas then passes through an acetone/solid carbon dioxide trap, which condenses out mercury vapour, into the boom and storage bulb. As atmospheric pressure is approached inside the gas storage bulb the level of the mercury in the vertical tube drops below the glass sinter. The cylinder valve is then closed, as is the tap to the gas inlet system. The storage bulb is closed off and the gas handling boom is evacuated. The gas in the storage bulb, now at just under one atmosphere pressure, is then purified by condensing it into a cold finger on the bulb, allowing the condensate to evaporate and condensing the central fraction of the evaporating gas into a second gas storage bulb. The first and last fractions of gas are pumped away. This procedure is carried out several times. Gas samples are then withdrawn for mass spectrometric and G.L.C. analysis. Both the acetylene and the ethylene used have a purity greater than 99.5%. If fresh vials of ethylene C-14 are needed these are sealed on to the gas inlet line to the target chamber at this time. The ethylene C-14 is supplied by the Radiochemical Centre, Amersham and is 99% pure as ascertained by G.L.C. measurements.[61] The only impurity is ethane.

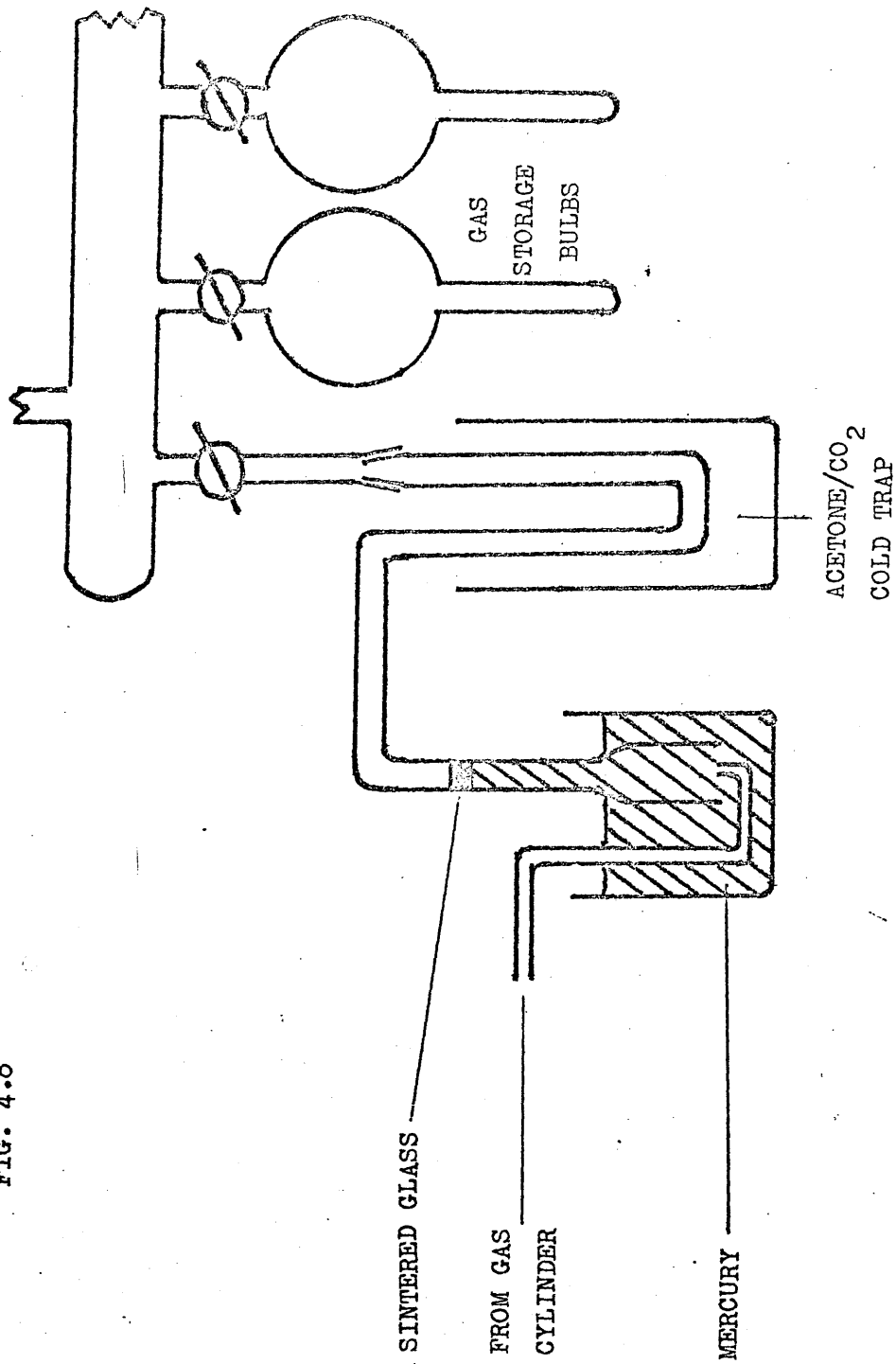
GAS
STORAGE
BULBS
ACETONE/CO_2
COLD TRAP
SINTERED GLASS
FROM GAS
CYLINDER
MERCURY

FIG. 4.8

At several times during this six-hour period the target and evaporator are turned in their cone and socket joints to degas the Apiezon N grease, as are any newly greased taps in the gas inlet systems. Each greased joint or tap is turned at least twenty times. At first bursts of gas are recorded as pressure rises by the ionisation gauges but these become progressively smaller until the effect is scarcely noticeable. Water is then passed through the cooling coils prior to the degassing of the palladium filament. Cooling the two cone and socket joints makes them stiff and turning the target then becomes slow and difficult. It has the advantage, however, of ensuring that no movement of the target or evaporator round their axes can occur. Movement of the target while counting is in progress would alter count geometry and the observed count rate from the surface. Movement of the evaporator could mean that the film is thrown on to the counter.

The level of background counts from the detector is also checked. These are due mostly to thermal production of ion pairs in the solid-state detector. The Simtec lithium-drifted silicon detector proved very stable over a six-month period until suddenly the background rose, over twelve hours, from about 30 c.p.m. to about 15,000 c.p.m. None of the remedies suggested by the manufacturers improved the situation. These included operating the detector with no bias voltage applied for forty-eight hours to eliminate any effects of current-produced defects and heating the detector to 100°C for twelve hours to ensure that the lithium was evenly distributed throughout the silicon sensing volume. Nor did the level of background counts fall after the detector had been left unused for a week. The failure of the detector has been ascribed to break-down of the electrical contacts, but it must be stressed that a great deal in the operation of solid-state

detectors and in the rectifying of their errant behaviour is guesswork, even on the part of the manufacturers. The height of the noise pulses, after the detector had deteriorated, observed on an oscilloscope, obscured the C-14 counts, though higher energy radiation, such as that from americium-241, was clearly observed. The difficulty arose from the fact that the low energy (150 keV) β-particles produced by carbon-14, gave pulses so small that they were indistinguishable from the rising background. Were higher energy particles being detected the effect of rising background would not have been noticed.

A second detector was then purchased, this time an Elliot Electronic Tubes Ltd. lithium-drifted silicon device, type SRD 15, with an area of 1.5 cm^2 and a depletion depth of 500 microns. This produced results similar to the Simtec device in terms of efficiency and background level for carbon-14. Its performance on test is described in Appendix 2. Changes in background level occurred with time. Typically, the count rate initially observed is 120 c.p.m. This drops, over a thirty minute period, to 70 c.p.m. If the device is operated for twenty-four hours the background then rises over a period of four hours to about 1,000 c.p.m. On switching off for a period of twenty-four hours the background again drops to 120 c.p.m. The first effect - that of falling background - is attributed to the discharge of thermally produced ion pairs until true equilibrium is reached. The second effect - the rise in background to high levels - is attributed to current production of ion pairs in the device after a period of time. A heavy duty cycle - greater than 50% on, 50% off - was avoided subsequent to this discovery. If the background level is lowered to 70 c.p.m., short "off" periods, up to four hours, do not increase the background level but longer periods do - after twelve hours the initial background observed is again 120 c.p.m.

While the counter is being operated the room is kept in total darkness with, as added precaution, black masking tape around, and heavy cloth draped over, the target chamber. It is usually run during most of the six-hour period prior to degassing the palladium: while the palladium filament is hot the counter cannot be used.

The palladium wire (grade: pure) for the filament is 0.020" thick, supplied by Johnson Matthey & Co. Ltd. The filament current used for evaporation is 6.8 - 7.0 amp. Degassing is thus carried out by passing 5.5 amp through the palladium for thirty minutes, then flashing the wire to 7.0 - 7.5 amp several times for about ten seconds. A further period of thirty minutes at 5.5 amp is then allowed before leaving the filament overnight with 4.0 amp passing through it. During degassing a light film deposits on the inside of the evaporator and on the target. Current is fed to the palladium from a step-down transformer whose input is controlled by a Variac. The target face is turned towards the evaporator during this period. The following morning the pressure in the target chamber, with the grease and the filament degassed, is usually 5×10^{-9} torr.

We have now reached the point at which the run proper may commence. The mild baking of the source chamber is halted and the trap in the source chamber filled with liquid nitrogen. The ionisation gauge on this chamber is degassed and thirty minutes after the end of baking the pressure recorded is usually about 5×10^{-9} torr. We have thus achieved, in both chambers, the ultimate vacua necessary for the pump speeds used in our calculations to be applicable. At this point the Variac controlling the heating of the source oven is switched on at a pre-calibrated setting which will result in a source temperature of approximately 60°C.

The tap water supply to the target is turned on. The thermostat bath is set to 25°C and switched on, with its connections to the target closed. The gauges and the filament are switched off, the room darkened and the counter switched on. The background level stabilises after thirty minutes and is recorded over the following thirty minutes. The counter is then switched off. By this time, the thermostat bath has reached 25°C and the source is at 60°C, as indicated by its thermo-couple. Any small adjustments to the source temperature are made by altering the Variac setting. Current to the palladium filament is switched on again.

All taps in the gas inlet system to the beam source are closed except those leading from the gas bulb of acetylene, through the needle valve, to the source. The needle valve is closed down to a level known to provide approximately the correct source pressure and the acetylene filled gas bulb opened. The needle valve is then adjusted until the source pressure is correct, as measured by the source Pirani gauge. In this case with a source temperature of 60°C the pressure in the source is adjusted to a true pressure of 2.1×10^{-3} torr to provide the same beam intensity as a source pressure of 2.0×10^{-3} torr at 25°C. The Pirani gauges had been calibrated beforehand, for air, acetylene and ethylene, against a McLeod gauge of known dimensions. The pressure recorded on the ionisation gauge in the source chamber for acetylene for this source pressure is 2×10^{-8} torr - an order of magnitude less than expected. This effect was not due to the trap pumping the acetylene, though the approximate value of the vapour pressure of acetylene at -196°C is 2.34×10^{-7} torr.[62] With the trap filled with an acetone/carbon dioxide slurry which could not contribute to the pumping of acetylene, a similar pressure in the source chamber was recorded. When air is used

as the source gas at 2×10^{-3} torr, the recorded pressures in the source and target chambers are 2.4×10^{-7} and 7.0×10^{-8} torr respectively, about one half of the values predicted in section 2 of this chapter - of 4.0×10^{-7} torr and 1.1×10^{-7} torr respectively. As the ionisation gauges are located approximately half-way between the pumps and the chambers, the pump speeds at the gauge heads will be approximately double those used in the calculations. The pressures recorded by the gauges should thus be approximately one-half of the pressures calculated for the source and target chambers proper. The pressures given by the ionisation gauges would thus indicate source and target chamber pressures in close agreement with the values predicted earlier. Acetylene should behave like air - having almost the same molecular weight as the effective molecular weight of air. The low pressures recorded on the ionisation gauges for acetylene must be due to a chemical interaction between the gauge filament and acetylene.

The gas inlet to the target chamber is now prepared. To obtain what is probably a monolayer coverage of the palladium film with ethylene we must have an ethylene pressure of at least 6.0×10^{-2} torr. (63, 64) In practice the pressure is kept between 8.0×10^{-2} torr and 10×10^{-2} torr. To obtain this pressure in the target chamber it is necessary to have a pressure in the gas-inlet reservoir of approximately 4×10^{-1} torr. This pressure of ethylene is a little more than that obtained from a single 0.5 mC vial of ethylene C-14 and a little inactive ethylene, obtained from the gas reservoir in the gas inlet system for the source, is added and time allowed for the gas to mix. The mixture is condensed into a separate side-arm, pumped on for five minutes, and then allowed to re-evaporate into the gas reservoir, closing the side-arm before any tail fractions can evaporate. This gas is used several times and the above procedure is followed to

separate out C_4 material which is discovered to be present in gas which has been in contact with the palladium film.

We are now at the stage where the target chamber gas inlet is ready and the molecular beam is ready and running, with all the gas emerging from the source being pumped away by the source chamber pump. The gate valve, which can admit the beam to the target, is still closed. The ionisation gauge on the target chamber is switched on, degassed, and the pressure again measured. The filament current is then increased to 6.8 - 7.0 amp to evaporate the palladium. The spot of film on the target face, which is maintained at 15°C by the flow of tap water through the target grows visibly thicker. Pressure measurements are recorded over the period of the evaporation. This lasts until the filament breaks - about fifteen minutes - during which time the pressure rises to approximately 3×10^{-7} torr. When the filament breaks the Variac controlling the evaporation is switched off, the gate valve in the target chamber pump stack is closed to seal off the target chamber and the gas inlet tap opened to admit the ethylene C-14. The equilibrium pressure of ethylene C-14 is recorded. No pressure change is noticed during a period of four minutes after which time the ethylene is condensed back into the gas inlet system for subsequent re-use. The room is darkened, the target chamber draped, the ionisation gauge switched off and the counter switched on to follow the removal of ethylene from the gas phase. This is also followed using the Pirani gauge in the gas inlet system. The count drops over a period of four minutes to about 2,000 c.p.m. At this point, the ethylene pressure is about 4×10^{-4} torr - its vapour pressure at -196°C. The gate valve to the pump stack is then opened, the gas inlet tap closed, and the residual ethylene pumped away. The count drops to background level immediately

and the ethylene C-14 which is chemisorbed on the palladium film is then in a vacuum environment where the pressure is approximately 1×10^{-8} torr.

The target is then turned in its B55 socket to present the C-14 covered surface to the counter. The count rate from the surface is followed, against time, for thirty minutes or longer to establish the count level from the surface at 15°C. This usually falls slowly during this period, though on some occasions rapid desorption of C-14 material is observed at 15°C, as will be seen in the next chapter. Once the count level has been established the tap water supply is turned off and the connections to the water bath opened to raise the target temperature to 25°C. Simultaneously the gate valve between the target and source chambers is opened and the beam falls on to the surface. The amount of C-14 on the surface is then followed against time using the scaler and ratemeter until no further change is observed in the count rate. At a later stage a Laben multi-channel analyser was used instead of the scaler. This was used in its multi-scaler mode, printing out the results at the end of the run. Hourly checks are made during the run on beam temperature and pressure, and the target chamber trap, which has a lifetime of approximately two and a half hours, is kept topped up with liquid nitrogen.

At the end of the run the counter is switched off and the needle valve controlling the beam pressure is closed. The unused beam material is condensed back into its storage bulb. The electrical supply to the source oven is switched off as is the thermostat bath, simultaneously closing its connections to the target. Both gate valves are closed to isolate the target chamber. With the ethylene C-14 safely back in its storage bulb the gas inlet system is used to admit air to the target chamber. The

evaporator and target are then removed for cleaning and filament replacement. The target is cleaned of grease and its film spot using a tissue soaked in ether. The detachable head of the evaporator is removed, cleaned of grease which it picks up being withdrawn through the B34 socket, immersed in aqua regia to remove its palladium film, washed in water, then acetone, and dried. A new filament is fitted into the screw connectors of the evaporator which also is cleaned of grease. The B55 and B34 sockets are cleaned with tissues soaked in ether. The evaporator head is replaced. The palladium filament position is adjusted so that it lies centrally in the evaporator, with the scratches on the B24 cone and socket, by which the evaporator head is attached, aligned. The B34 and B55 cones are greased and the evaporator and target replaced in the target chamber which is again evacuated, through the gas inlet system, by the oil diffusion pump.

The sequence of events described above is then repeated, with the exception that the connection between the mercury-diffusion pump and the target chamber need not be baked. The following morning the target chamber is opened to its own pump stack. The sequence of events normally runs as follows:

Day 1 : start from air pressure, baking the pump connection to the target chamber, evacuating the target chamber through the gas inlet system.

Day 2 : morning:
open the target chamber to its own pump, carrying out gas handling, counter checks and grease degassing, until -
evening:
degas filament

Day 3 : morning:
run proper
evening:
finish run and prepare second
Day 4 : as Day 2
Day 5 : as Day 3.

Chapter 5
Results

(1) Introduction

The studies carried out fall into four categories:

1) vacuum desorption studies of ethylene from palladium;
2) displacement of pre-adsorbed ethylene on palladium by a beam of acetylene;
3) displacement of pre-adsorbed ethylene on palladium by a beam of ethylene;
4) miscellaneous displacement and condensation reactions and mass spectrometric analysis of the ethylene which had been in contact with the film to form the monolayer studied.

The results of the first vacuum desorption experiment will be fully explained, showing the processing of the primary data to yield the final answers. Thereafter, only the primary data and the final answers, together with the necessary graphs, will be shown. The spectrum of results produced will then be collated and discussed and their relation to other work examined.

(2) Vacuum Desorption of Ethylene from Palladium

The first vacuum desorption experiments, at surface temperatures of 25°C and 60°C, were carried out using the intermediate apparatus on which development of target and counter systems was performed. The vacuum desorption study at 15°C and 70°C surface temperatures was performed with the permanent gas molecular beam apparatus, as were all the displacement reactions.

(a) Vacuum Desorption - Surface Temperature 60°C

Table 1 shows the surface count (in cpm) versus time; a count taking place, for example, from 6.50 min to 11.50 min is recorded at 9.00 min. The third column shows the log of the surface count. The background count has been subtracted from each of the count figures. Fig. 5.1 shows the plot of count versus time; fig. 5.2 shows the plot of log count versus time.

From these two plots it was at once apparent that three distinct phases were visible in the desorption. These were:

1. a fast desorption phase - the α phase;
2. a slow desorption phase - the β phase;
3. a retained phase - whose value corresponds to the count level after 20 hours.

Furthermore, fig. 5.2 suggested that each of the two desorbing phases - α and β - followed first order kinetics. To examine this point the value of the retained phase was subtracted from the counts recorded and the log values of these counts again plotted against time. Table 2 shows the values and fig. 5.3 the plot. This procedure is necessary since the retained species produces a count which does not vary with time - in effect, an addition to the background count. The resulting graph is now compared with the graph of the simultaneous decay of two radioactive isotopes in fig. 5.4.[65] The similarity of the two led us to believe that both α and β phases did indeed display first order kinetics with respect to desorption. This picture was confirmed over the range of vacuum desorptions studied and, indeed, in the displacement reactions carried out, as will be shown later. Consequently, the results have been analysed by a computed best straight line least squares analysis of each section - using the log figures obtained after subtracting the value of the

retained species. Firstly the β phase is analysed, selecting a range of points starting after the α phase desorption is complete and before the values at the end become statistically meaningless. These last points are the difference between two values which are close to each other and which have a certain statistical error. The error in the resulting difference is thus comparatively large and the computer programme used (Appendix 3) would treat such points as being equal in weight to the statistically more accurate early points, which have a similar error but in a much larger value. Thus, points with a large possible error have been discarded.

The best straight line thus produced gives us the intercept of the β phase on the y-axis - enabling us to estimate the percentage of β phase present - and the slope. From the slope value the time for the β phase to fall from its initial concentration to one-half of that value - the $t_{\frac{1}{2}}$ characteristic of the desorption for that temperature - is obtained. The intercept also defines the limit of the α phase, the value being subtracted from the initially observed count rate, and the slope enables values of the corrections to be applied to the counts obtained while the α phase is desorbing. This correction is necessary since the count observed during the α phase desorption is the sum of the residual α phase, the residual β phase and the retained phase. Thus the log values at each time at which counts have been recorded during the α phase desorption are calculated, converted back into counts and subtracted from the counts obtained. The counts of the α phase are then again converted into logarithms, (Table 3), replotted and the best straight line computed for these values - resulting in a $t_{\frac{1}{2}}$ characteristic of the α phase desorption at that temperature. Fig. 5.5 shows the plot obtained for the desorption of the α phase at $60^{\circ}C$. A more convincing demonstration of first order kinetics for the α phase will be shown

later. The final results for each run thus consist of the $t_{\frac{1}{2}}$ values for each phase and the percentage values of the α, β and retained phases - each value being quoted as a percentage of the count initially observed at a surface temperature of 15°C.

The percentages of α, β and retained species in the vacuum desorption at 60°C are as follows:

α phase = 11.5%

β phase = 17.2%

retained phase = 71.3%

The $t_{\frac{1}{2}}$ values are:

$$\alpha t_{\frac{1}{2}} = 15.2 \text{ min} \pm 5 \text{ min}$$

$$\beta t_{\frac{1}{2}} = 101.8 \text{ min} \pm 15 \text{ min.}$$

The errors expressed are given by the errors in intercept and gradient produced by the final best straight line least squares programme used. In this the error results from the statistical variation of the counts and is reduced by using a large number of points. The error in any one point can be large - in the case of the α phase the error is the sum of the errors in the initial count, the background count, the estimated value of the retained species and the error in the calculated β phase. The error in this is in turn dependent on the first three values named, although less so since the values used are computed from a greater number of points and the error is proportionally reduced. This single point error is, however, meaningless when discussing the error in the final values of phase percentage and $t_{\frac{1}{2}}$ obtained, since each is computed using a number of points - which in some later runs is very large.

When describing later runs we shall give the primary data - counts against time, the corrected count, and the log of the

corrected count, together with plots of log observed count against time and log corrected count against time. The final results consist of the percentage of each phase, expressed relative to the initially observed count rate at a surface temperature of $15^{o}C$, and the $t_{\frac{1}{2}}$ values for each phase.

We do not consider that the α and β phases desorb consecutively. If they did we would expect a sharp break to be observed in the plot of log count versus time. In some cases (e.g. vacuum desorption at $70^{o}C$) there is no such break - simply a picture closely resembling that of fig. 5.4 - which would indicate concurrent desorption. Both cases, concurrent and consecutive, were further tested by synthesising curves with typical $t_{\frac{1}{2}}$ values to test the validity of treating the results. These synthesised curves were then compared to the results and it was apparent that concurrent desorption was taking place. The above procedure, which treats the results as if concurrent desorption takes place, has thus been applied.

Table 1

Vacuum Desorption at 60°C

Time (min)	Count (cpm)	log count
3.50	348	2.5441
9.00	320	2.5051
17.00	325	2.5119
27.50	312	2.4942
38.50	302	2.4800
49.00	292	2.4654
62.00	284	2.4533
73.00	288	2.4594
84.00	278	2.4440
95.50	284	2.4533
107.50	274	2.4378
124.00	274	2.4378
154.00	269	2.4298
202.00	258	2.4116
20 hours	248	= value of retained species

Table 2

Vacuum Desorption at 60°C

Counts Corrected by Subtracting Value of Retained Species

Time (min)	Corrected Count (cpm)	log Corrected Count
3.50	100	2.0000
9.00	72	1.8573
17.00	77	1.8865
27.50	64	1.8062
38.50	54	1.7324
49.00	44	1.6435
62.00	36	1.5563
73.00	40	1.6021
84.00	30	1.4771
95.50	36	1.5563
107.50	26	1.4150
124.00	26	1.4150
154.00	21	1.3222
202.00	10	1.0000

Table 3

Vacuum Desorption at 60°C

Corrected ∝ Phase Values

Time (min)	∝ Phase Count (cpm)	log Count
3.50	42	1.6232
9.00	16	1.2041
17.00	24	1.3802
27.50	15	1.1761
38.50	8	.9031

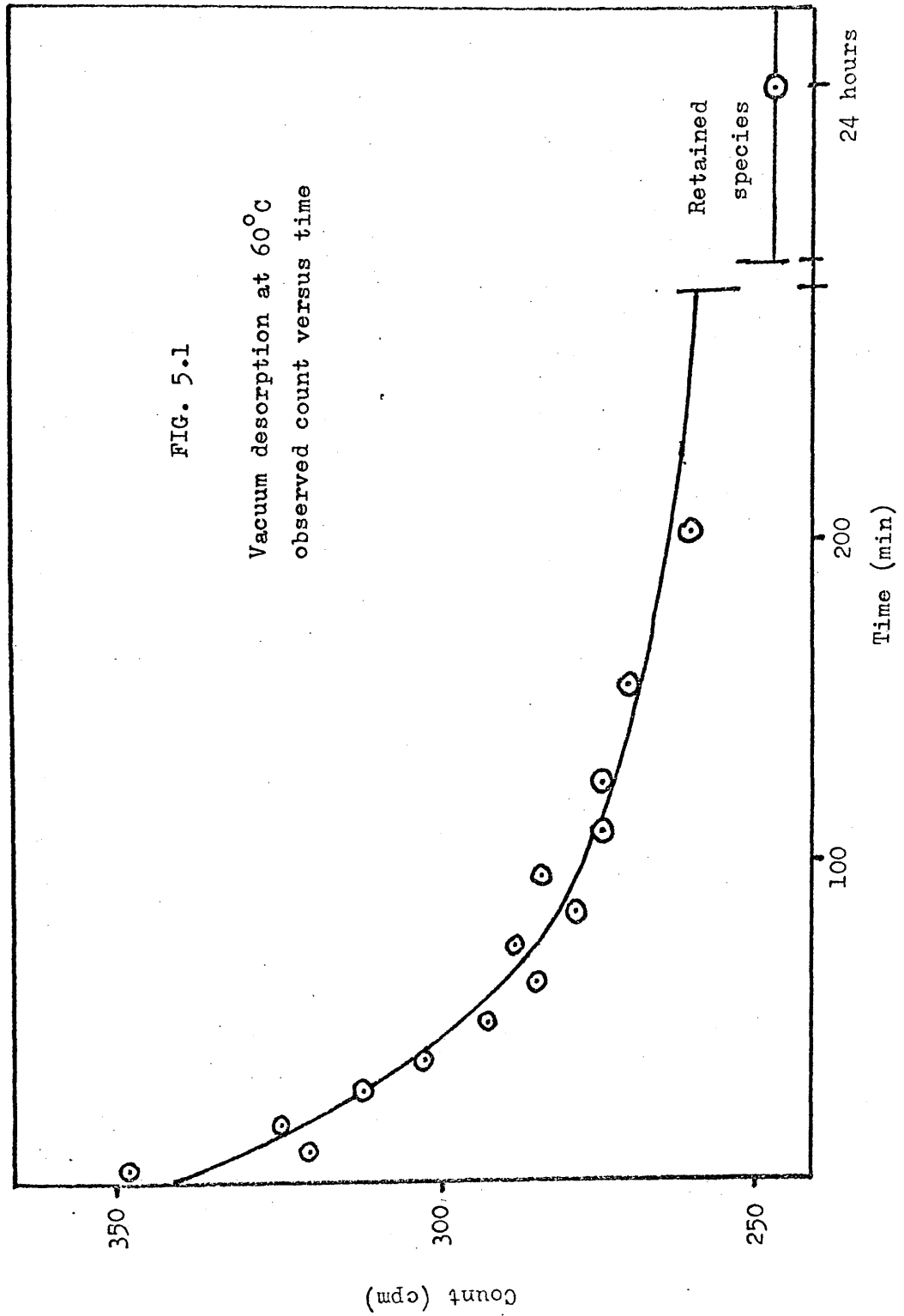

FIG. 5.1

Vacuum desorption at 60°C
observed count versus time

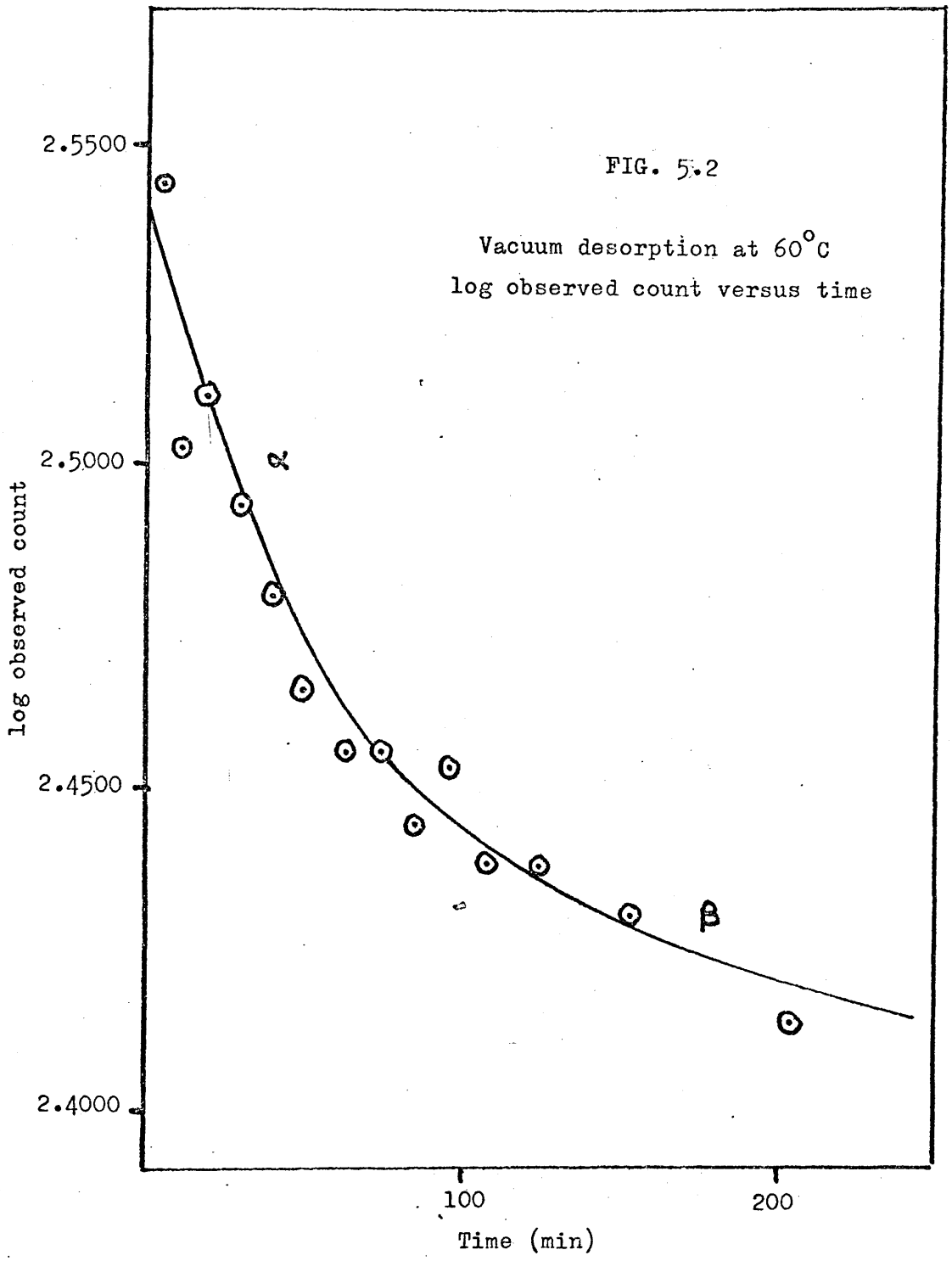

FIG. 5.2

Vacuum desorption at 60°C
log observed count versus time

FIG. 5.3

Vacuum desorption at 60°C
log corrected count versus time

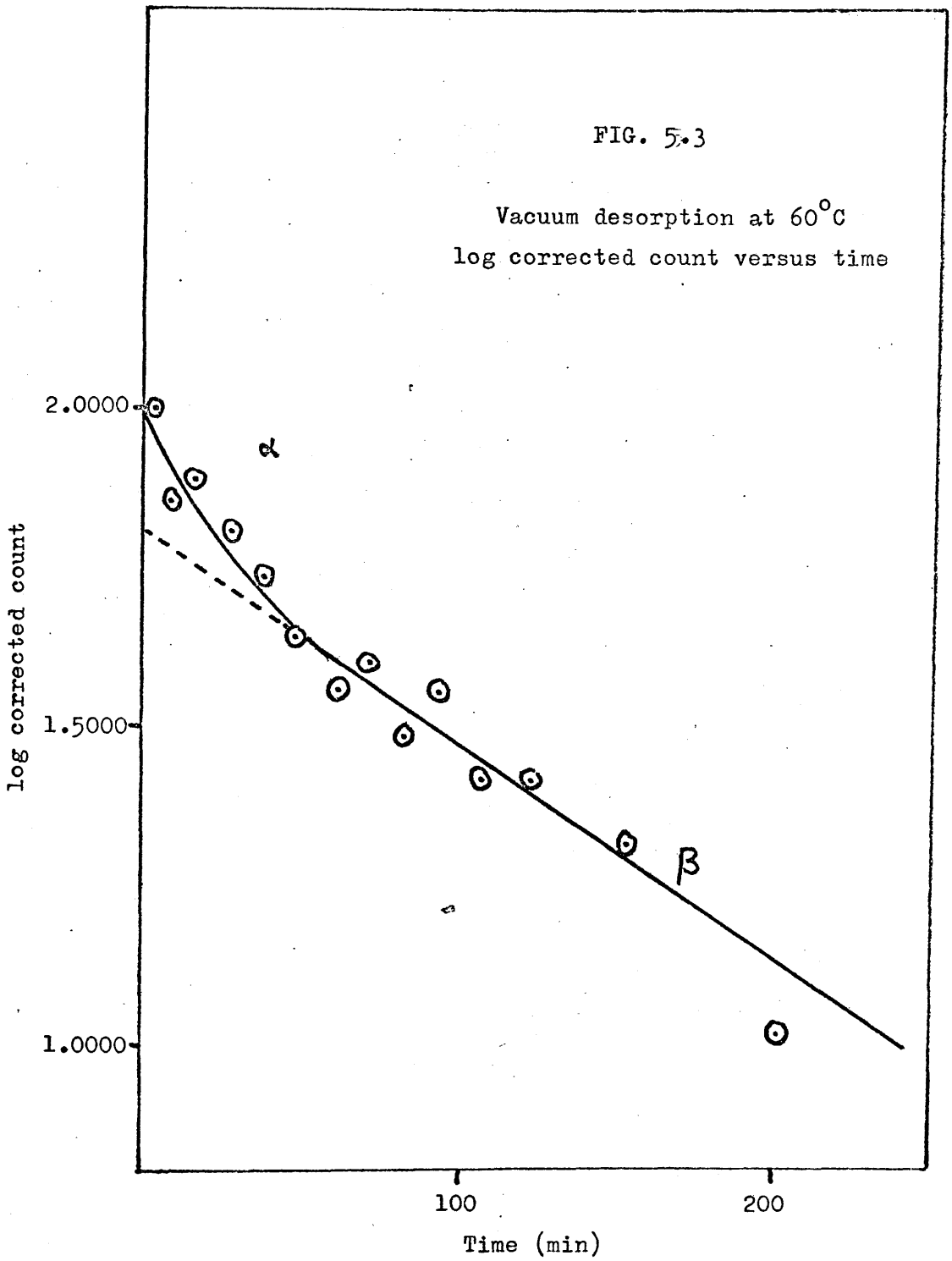

FIG. 5.4

Analysis of composite decay curve

(a) composite decay curve

(b) longer-lived component ($t_{\frac{1}{2}}$ = 8.0 hr.)

(c) shorter-lived component ($t_{\frac{1}{2}}$ = 0.8 hr.)

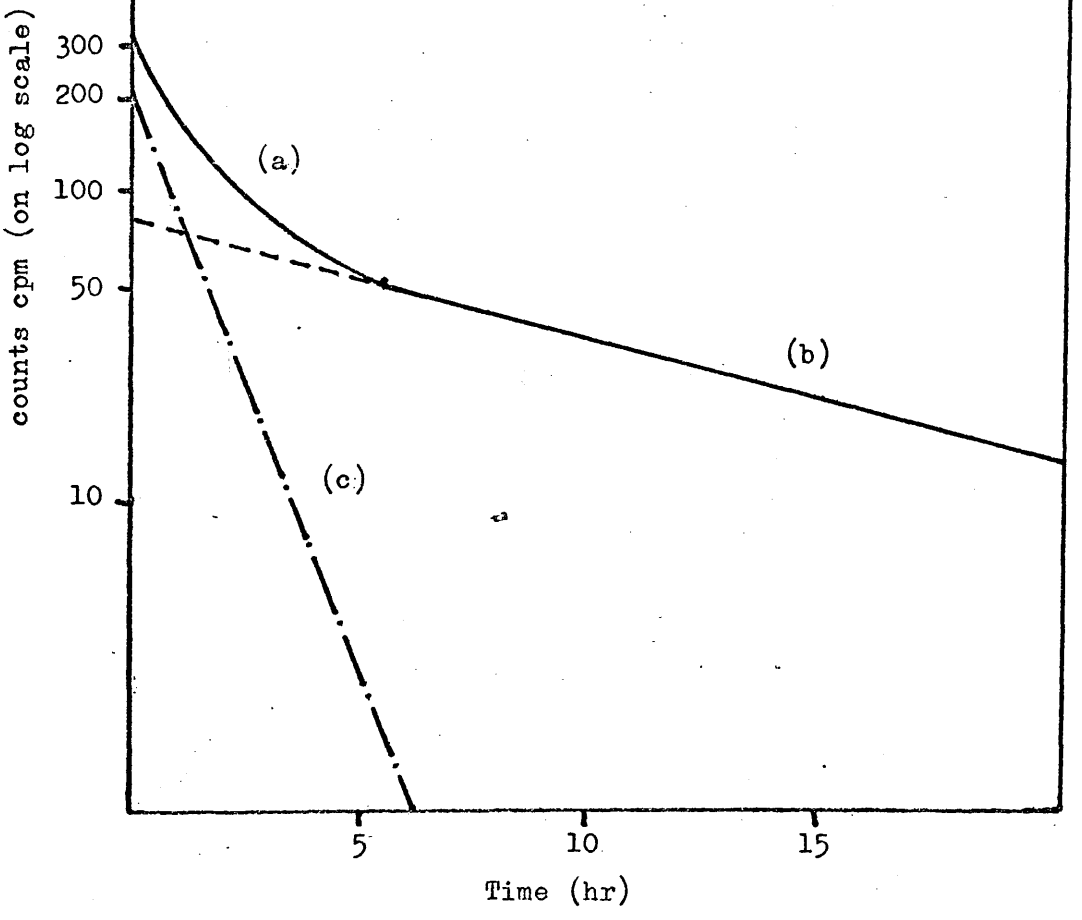

FIG. 5.5

Vacuum desorption at 60°C
log corrected ∝ phase count
versus time

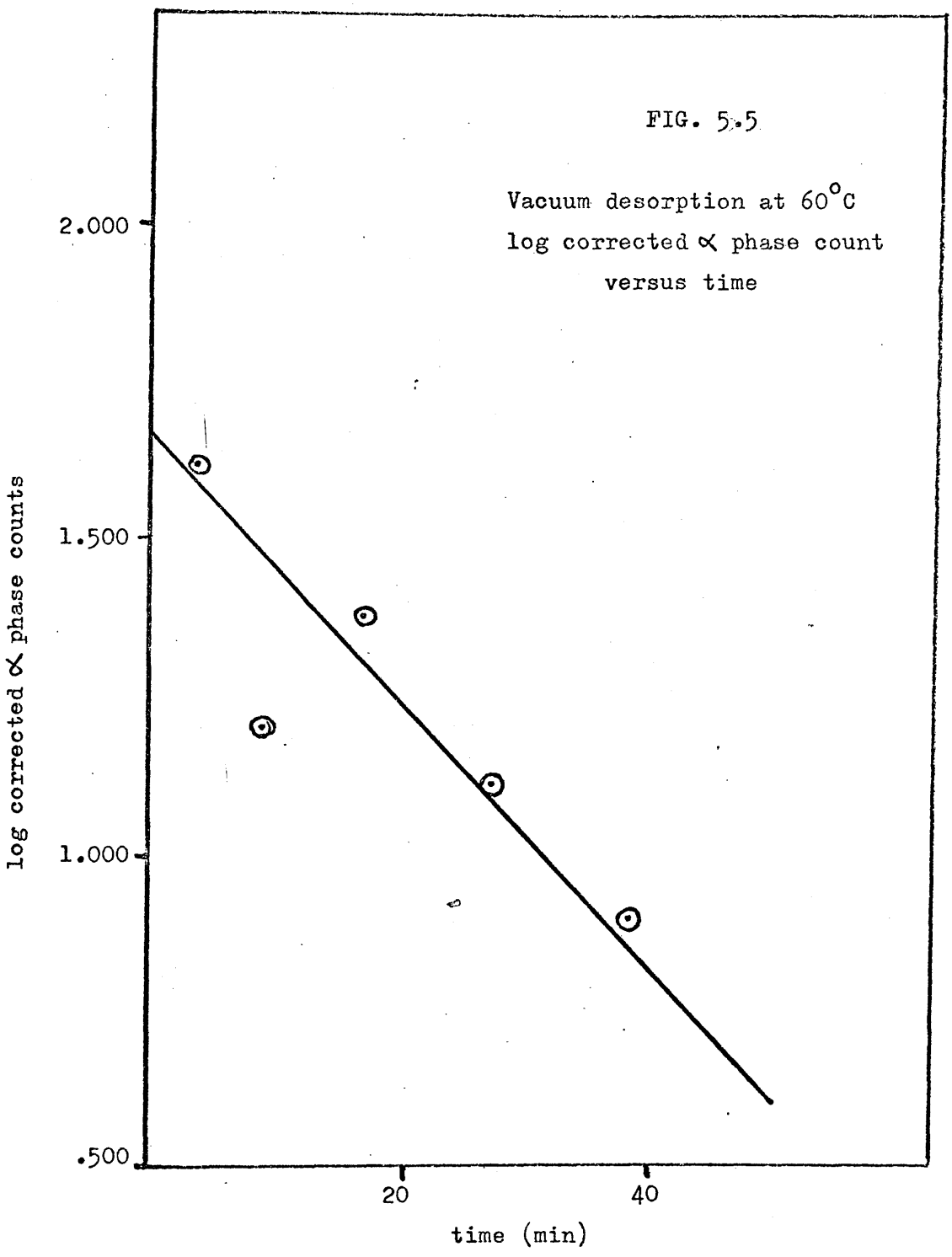

(b) Vacuum Desorption - Surface Temperature 25°C

Table 4 shows the counts recorded against time, the corrected counts after subtracting the retained species and the log of the corrected count. Fig. 5.6 shows the plot of log observed count versus time and fig. 5.7 the plot of log corrected count versus time. Table 5 shows the corrected α phase counts. The results obtained were:

α phase = 7.5%

β phase = 22.0%

retained phase = 70.5%

$\alpha t_{\frac{1}{2}}$ = 18.2 min $\pm$ 4 min

$\beta t_{\frac{1}{2}}$ = 251.2 min $\pm$ 25 min

Table 4

Vacuum Desorption at 25°C

Time (min)	Count (cpm)	Corrected Count (cpm)	log Corrected Count
5.00	362	106	2.0253
18.50	339	83	1.9191
29.00	343	87	1.9395
39.50	327	71	1.8513
50.00	335	79	1.8976
65.50	325	69	1.8388
93.00	319	63	1.7993
124.50	309	53	1.7243
154.00	311	55	1.7404
195.00	303	47	1.6721
245.50	292	36	1.5563
289.00	290	34	1.5315
342.00	289	33	1.5185
403.00	283	27	1.4314
455.00	274	18	1.2553
545.00	264	8	.9031
20 hours	256	= value of retained species	

Table 5

Vacuum Desorption at 25°C

Time (min)	Corrected α Phase Count (cpm)	log Count
5.00	28	1.4472
18.50	7	.8451
29.00	14	1.1461
39.50	0	0
50.00	10	1.0000

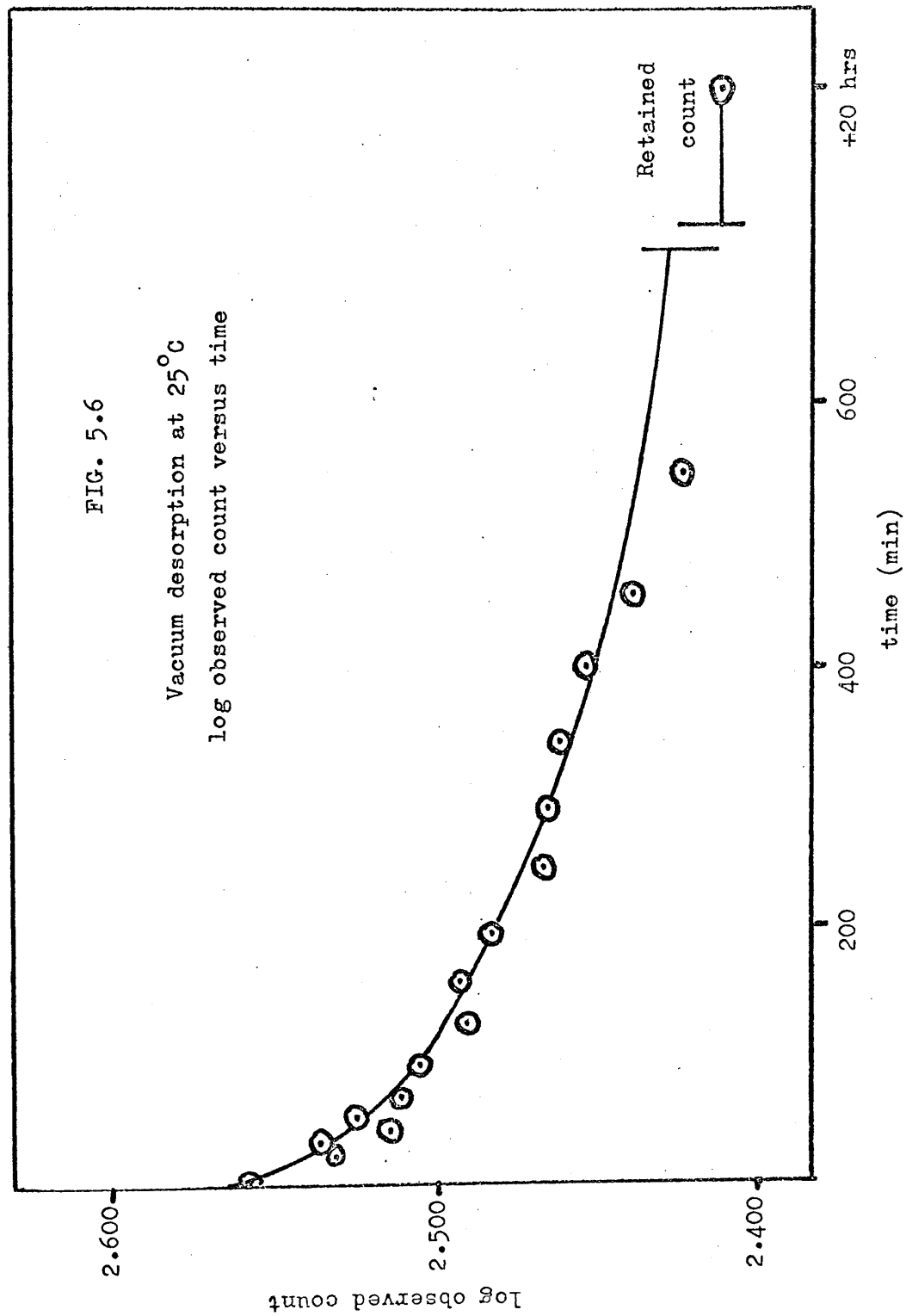

FIG. 5.6

Vacuum desorption at 25°C

log observed count versus time

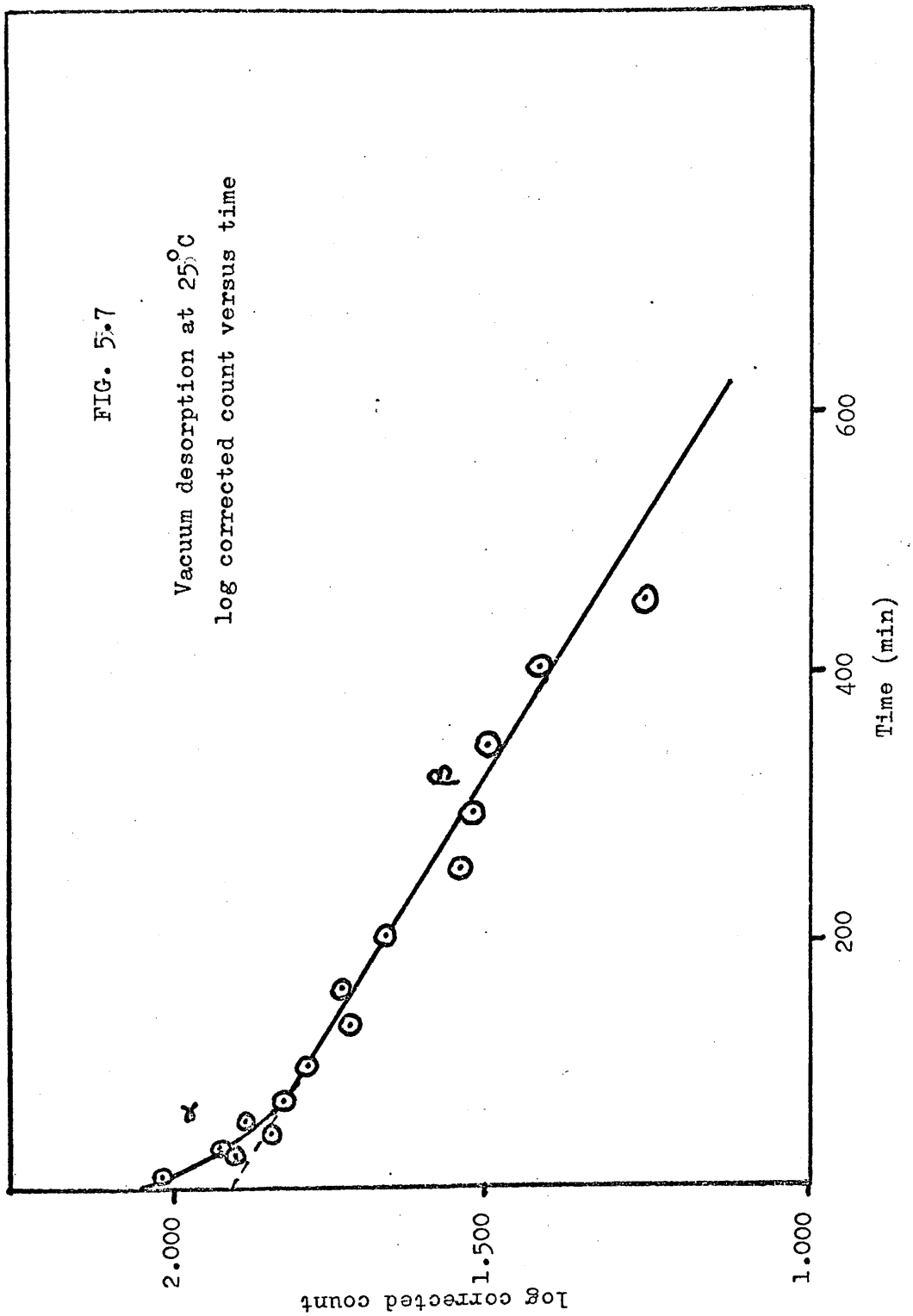

FIG. 5.7

Vacuum desorption at 25°C

log corrected count versus time

(c) Vacuum Desorption - Surface Temperatures 15°C and 70°C

This experiment was carried out later than the others in this series. At the time we were interested in the effect of increasing the rate of evaporation of palladium on the amounts of each of the phases. The evaporation was carried out at 7.1 amp evaporating current, higher than the usual 6.8 amp. The high count rate observed, initially about 5,000 cpm, is due probably in part to the increased amount of α and β phases found. In part also it was due to a particularly low level of background given by the Elliot detector - which enabled us to lower the discriminator level on the pulses obtained to include more of the pulses produced by the lower energy C-14 β-particles. The high count rate reduces the possible statistical error in the count obtained - this being proportional to the square root of the count.

Counts were recorded on a Laben multi-scaler. This accepts counts for a given preset time, storing them in a count channel. At the end of the preset time this channel is closed and pulses produced during the next preset time interval are stored in the next channel. 400 such channels are available. The waiting or off time between channels is always zero. The channel width used here was 200 sec.

In addition to a simple vacuum desorption at a surface temperature of 70°C, the initial vacuum desorption at 15°C was followed for some time. After some desorption of the β phase at 70°C, a beam of ethylene from a source at 15°C, in which the ethylene pressure was 2.0×10^{-3} torr, was introduced to the surface, which was kept at 70°C. The sequence of events was thus:

channel no. 1 - 10 : vacuum desorption at 15°C;
channel no. 11 - 27 : vacuum desorption at 70°C;
channel no. 28 - end: ethylene displacement at 70°C.

Table 6 shows the values of time channel and count, the corrected count after subtraction of the retained phase and the log of this corrected count. Fig. 5.8 shows the plot of count observed versus time, fig. 5.9 the plot of log observed count versus time and fig. 5.10 the plot of log corrected count versus time. Table 7 shows the corrected α phase counts and their log values and fig. 5.11 the plot of the log of these α phase counts against time. The α phase values during the period when the surface was at 15°C were calculated assuming that there was negligible loss of β phase at this temperature.

The values obtained were:

α phase = 40.8%

β phase = 40.7%

retained phase = 18.5%

$\alpha t_{\frac{1}{2}}$ (15°C vacuum desorption) = 52.6 min $\pm$ 12 min

$\alpha t_{\frac{1}{2}}$ (70°C vacuum desorption) = 5.1 min $\pm$ 1.5 min

$\beta t_{\frac{1}{2}}$ (70°C vacuum desorption) = 57.4 min $\pm$ 14 min

$\beta t_{\frac{1}{2}}$ (70°C ethylene displacement) = 26.5 min $\pm$ 3 min

Fig. 5.10 shows clearly the first order kinetics of the β phase desorption and displacement, with the break corresponding to the introduction of the beam clearly visible. Fig. 5.11 shows clearly the first order kinetics of the α phase desorption.

A second value of the $\alpha t_{\frac{1}{2}}$ (15°C vacuum desorption), obtained in the course of a later displacement reaction, was 31.7 min $\pm$ 3 min. This run will be described later. This second value resulted from the observation of the desorption of an α phase over a longer period of time. Many more points were recorded and the resulting value is consequently more accurate. This second value will thus be used in our discussion of the vacuum desorption results which now follows.

Table 6

Vacuum Desorption at 70°C

Time Channel	Count	Corrected Count	log Corrected Count
1	16813	13693	4.1364
2	16615	13495	4.1303
3	16426	13306	4.1245
4	16141	13021	4.1145
5	16088	12968	4.1130
6	15459	12339	4.0913
7	15241	12121	4.0835
8	15262	12142	4.0842
9	14772	11652	4.0664
10	13595	10475	4.0200
11	12832	9712	3.9873
12	11147	8027	3.9046
13	9948	6828	3.8343
14	9639	6519	3.8142
15	9203	6083	3.7841
16	8786	5666	3.7533
17	8696	5576	3.7464
18	8149	5029	3.7015
19	8098	4978	3.6971
20	7856	4736	3.6754
21	7096	3976	3.5996
22	6875	3755	3.5758
23	6652	3532	3.5480
24	7210	4092	3.6119
25	6523	3403	3.5319
26	6170	3050	3.4857
27	5824	2704	3.4319

Table 6 (contd.)

Time Channel	Count	Corrected Count	log Corrected Count
28	5562	2442	3.3876
29	5463	2343	3.3695
30	5200	2080	3.3181
31	4870	1750	3.2430
32	4960	1840	3.2648
33	4766	1646	3.2164
34	4673	1553	3.1911
35	4389	1269	3.1035
36	4377	1257	3.0997
37	4263	1143	3.0580
38	4099	979	2.9908
39	3954	834	2.9212
40	3996	876	2.9425
41	3900	780	2.8921
42	3814	694	2.8414
43	3728	608	2.7839
44	3691	571	2.7566
45	3717	597	2.7760
46	3705	585	2.7672
47	3456	336	2.5263
48	3591	471	2.6730
49	3374	254	2.4048
50	3344	224	2.3502
51	3435	315	2.4983
52	3412	292	2.4654
53	3248	128	2.1072
54	3213	93	1.9685
55	3194	74	1.8692

Table 6 (contd.)

Time Channel	Count	Corrected Count	log Corrected Count
56	3078	-42	-
57	3135	15	1.1761
58	3156	36	1.5563
59	3193	73	1.8633
60	3156	36	1.5563
61	3117	-3	-
62	3146	26	1.4150
63	3134	14	1.1461
64	3167	47	1.6721
65	3033	-87	-
66	3151	31	1.4914
67	3121	1	.0000
68	3109	-11	-
69	3038	-82	-

Channel width = 200 seconds

Table 7

Vacuum Desorption at 70°C

Corrected ∝ Phase Counts

Time (min)	Corrected Count (cpm)	log Corrected Count
1	6852	3.8358
2	6654	3.8231
3	6465	3.8105
4	6180	3.7910
5	6127	3.7873
6	5498	3.7402
7	5280	3.7226
8	5301	3.7244
9	4811	3.6822
10	3634	3.5604
11	3133	3.4959
12	1707	3.2322
13	758	2.8797
14	687	2.8370
15	481	2.6821
16	285	2.4548

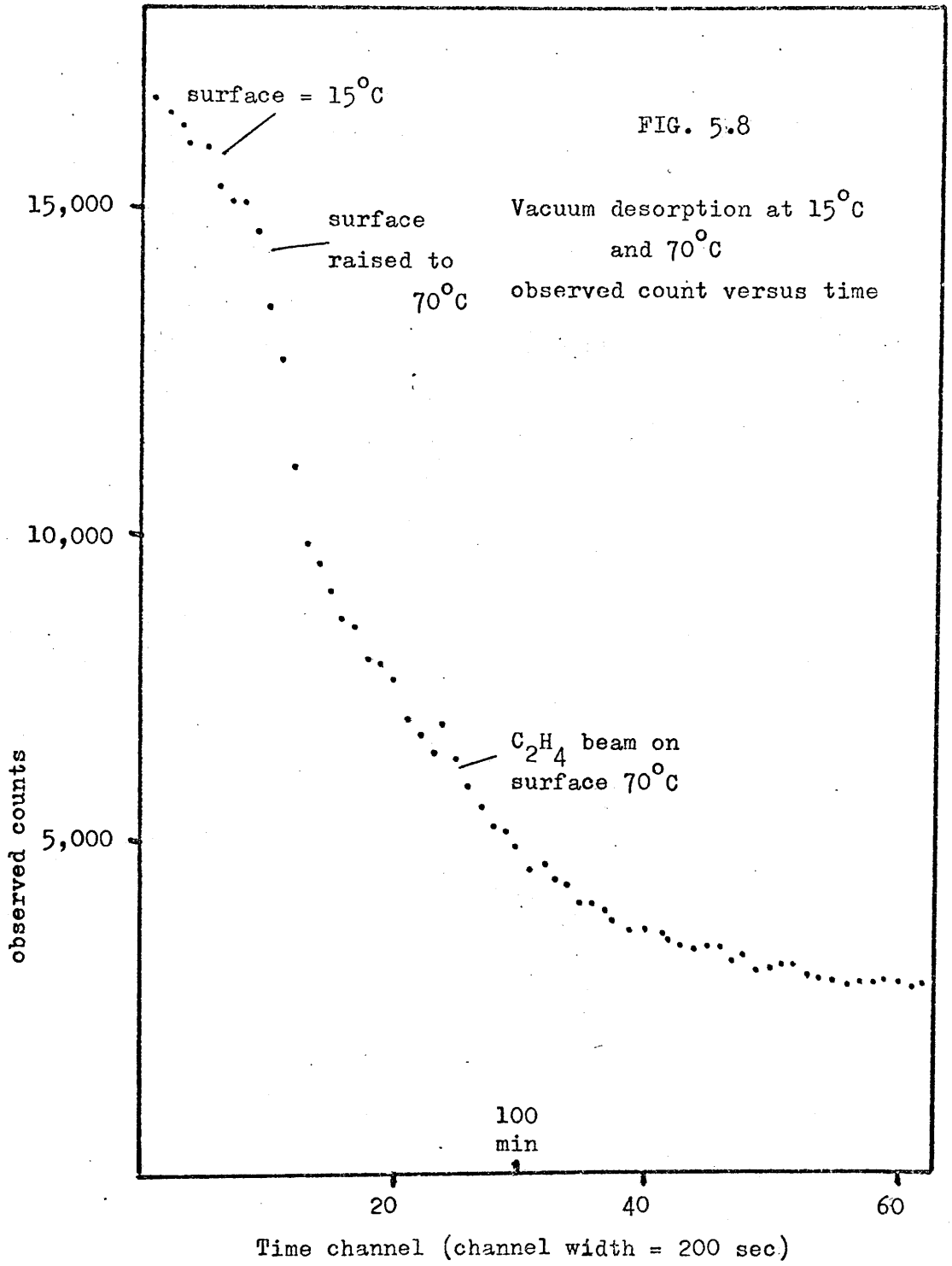

FIG. 5.8

Vacuum desorption at 15°C and 70°C observed count versus time

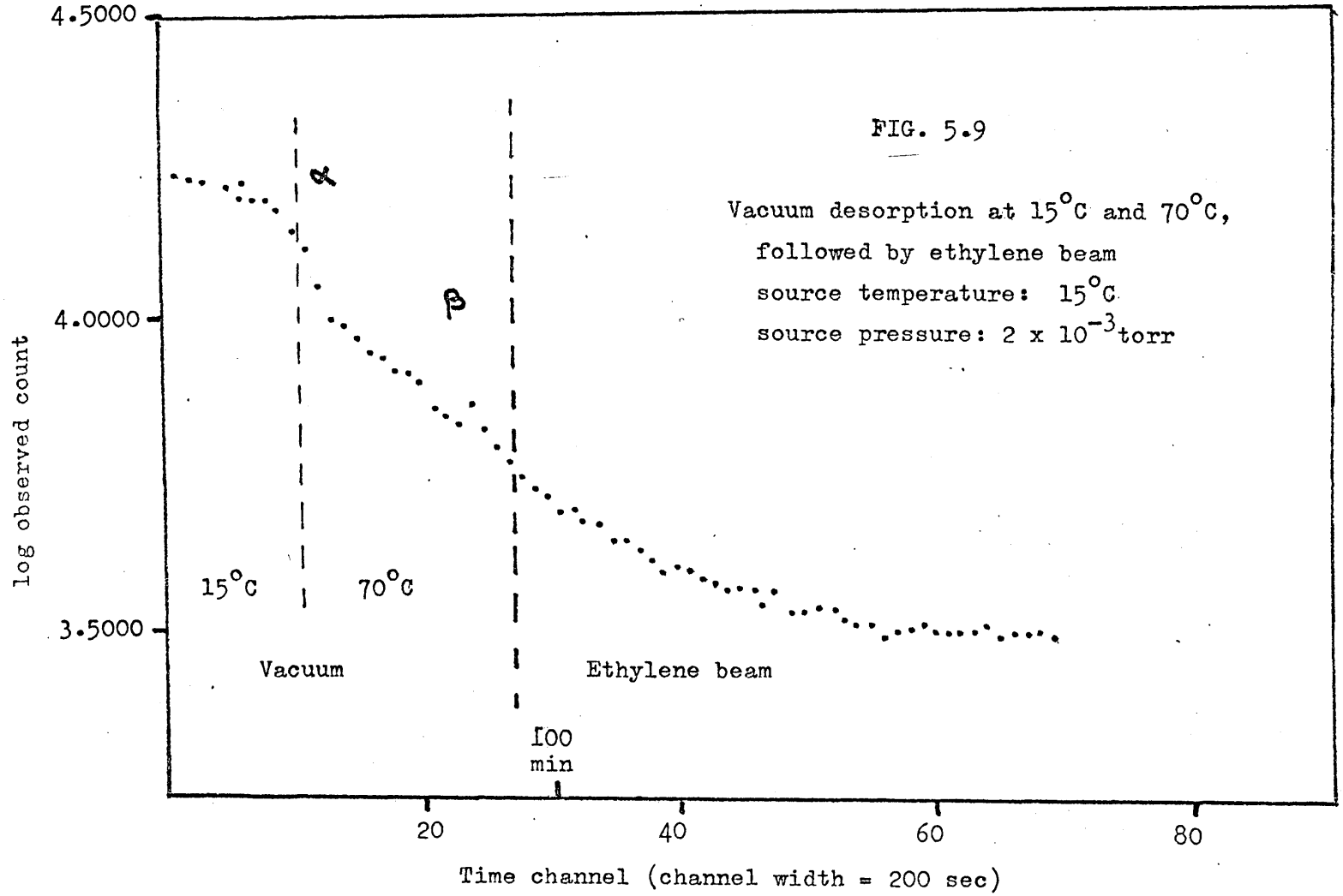

FIG. 5.9

Vacuum desorption at 15°C and 70°C,
followed by ethylene beam
source temperature: 15°C
source pressure: 2×10^{-3} torr

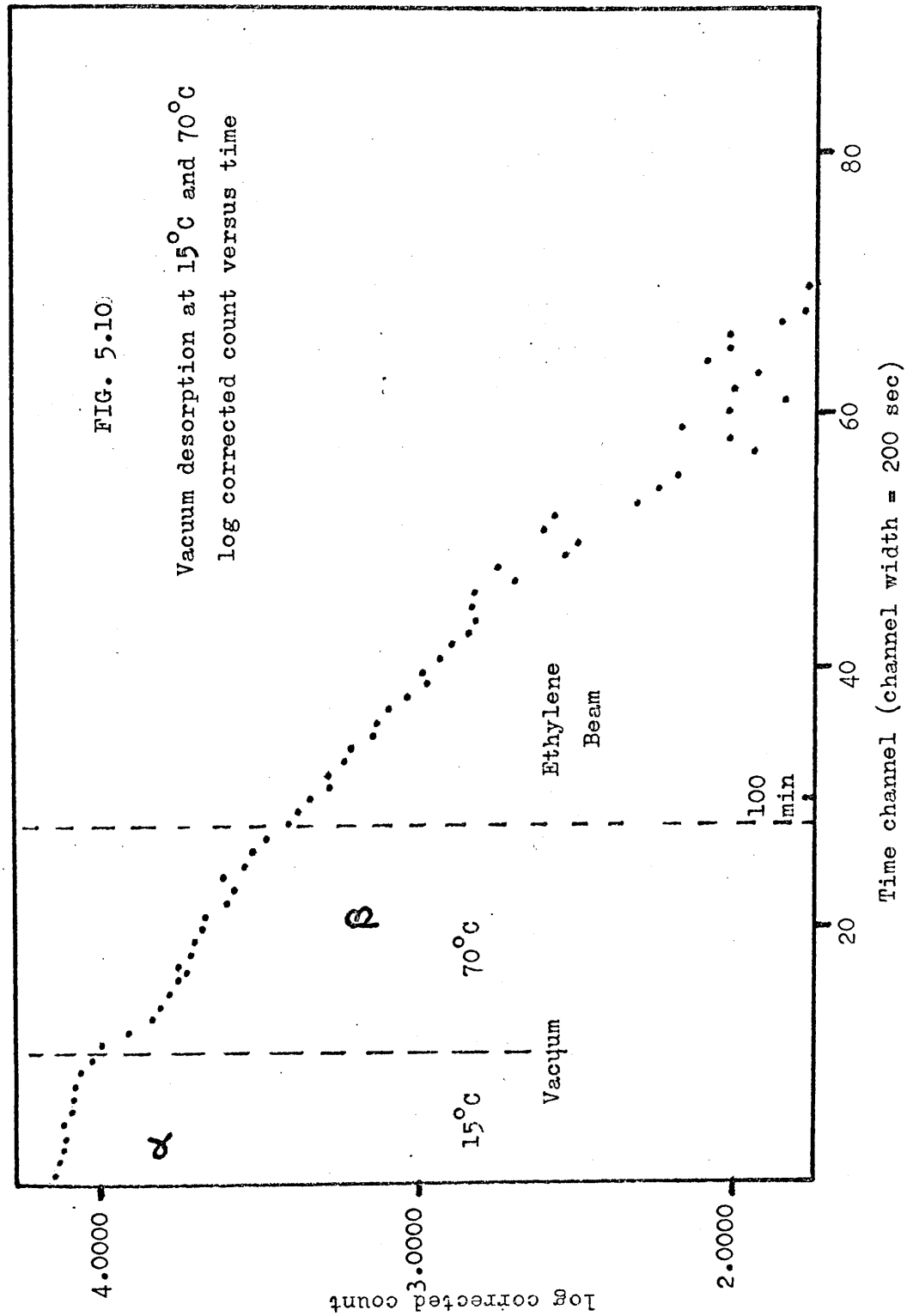
FIG. 5.10
Vacuum desorption at 15°C and 70°C
log corrected count versus time
log corrected count
4.0000
3.0000
2.0000
α
β
15°C
Vacuum
70°C
Ethylene
Beam
100
min
20
40
60
80
Time channel (channel width = 200 sec)

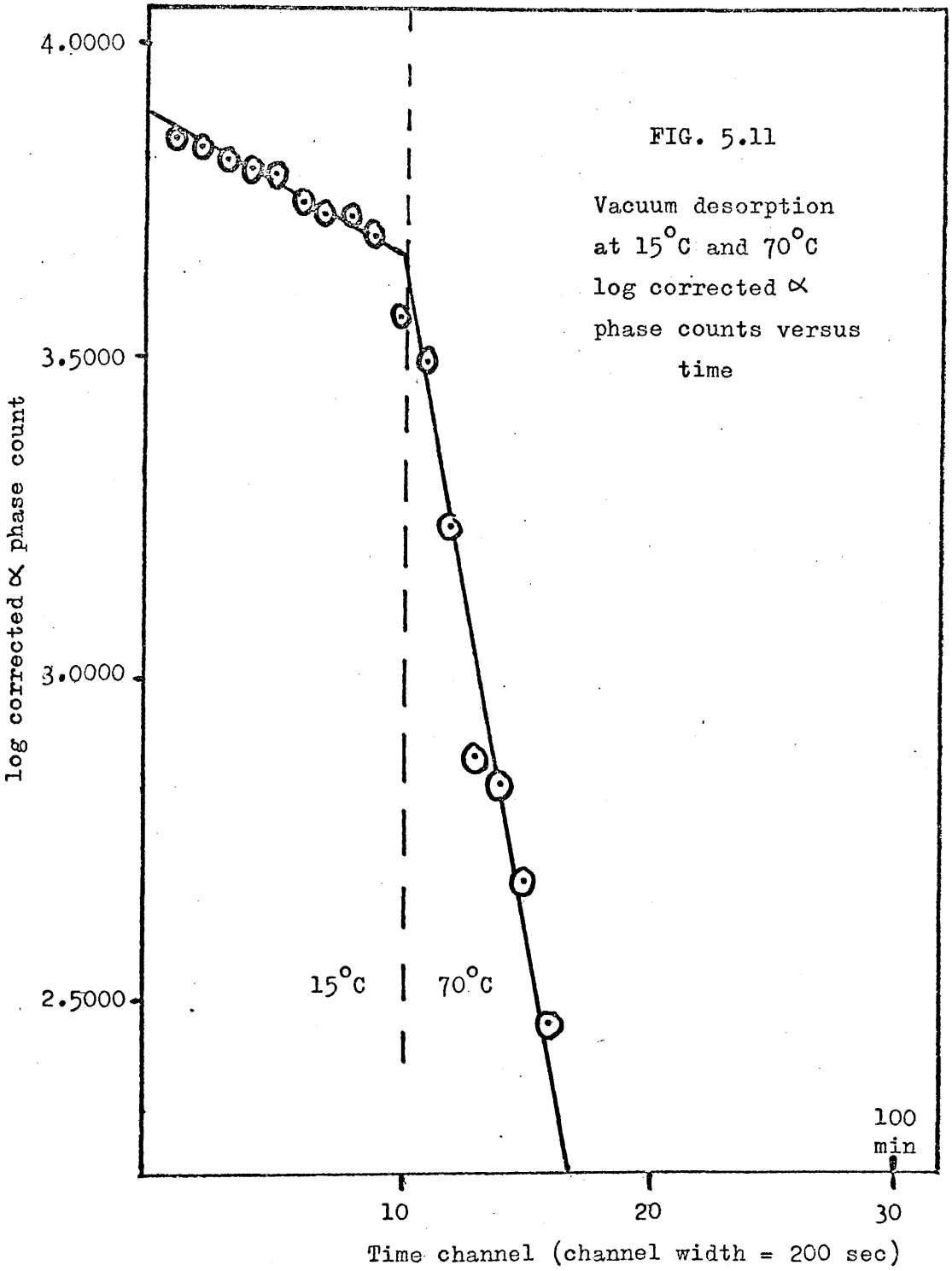

FIG. 5.11

Vacuum desorption at 15°C and 70°C log corrected ∝ phase counts versus time

(d) Conclusion to Vacuum Desorption Experiments

Since both the α and β phases display first order kinetics for the desorption process in these studies, we can estimate approximately the activation energies for these desorption processes.

The rate constant at a given temperature T_1 is given by:

$$k_1 = A \times e^{-E_A/RT_1}$$

thus: $\ln k_1 = -E_A/RT_1 + \ln A$

and: $\ln k_2 = -E_A/RT_2 + \ln A$

by subtraction $\ln k_1/k_2 = E_A/RT_2 - E_A/RT_1$

$$= \frac{E_A}{R}\left[\frac{T_1 - T_2}{T_1T_2}\right]$$

thus: $$E_A = \ln \frac{k_1}{k_2} \times R \times \left[\frac{T_1T_2}{T_1 - T_2}\right]$$

$$= 2.303 \log \frac{k_1}{k_2} \times R \times \left[\frac{T_1T_2}{T_1 - T_2}\right]$$

Since the rate constant, k, is the slope of our plot of log count versus time, and since the $t_{\frac{1}{2}}$ values which we use to express our results are inversely proportional to k, we may restate the equation as:

$$E_A = 2.303 \log \frac{t_{\frac{1}{2}}(2)}{t_{\frac{1}{2}}(1)} \times R \times \left[\frac{T_1T_2}{T_1 - T_2}\right]$$

If R is taken in cal/deg/mole, the value of E_A is then in cal/mole.

Using the $t_{\frac{1}{2}}$ values obtained, we can calculate the approximate values for the activation energies of the two desorption phases. The following are the collected $t_{\frac{1}{2}}$ values for vacuum desorption:

$T^{o}C$	α	β
15	31.7 min	-
25	18.2 min	251.2 min
60	15.2 min	101.8 min
70	5.1 min	57.5 min.

The six values of activation energy resulting from the α phase desorption are: 6.5; 3.1; 9.5; 5.8; 1.0 and 24.8 k cal/mole. Excluding the highest and the lowest the average value is:

$$E_A\ (\alpha) = 6.1 \text{ k cal/mole.}$$

The three values obtained for the β phase are: 5.1; 6.7 and 13.0 k cal/mole. The average value is:

$$E_A\ (\beta) = 8.3 \text{ k cal/mole.}$$

We can thus say that both phases desorb with low activation energy.

(3) Displacement of Pre-adsorbed Ethylene on Palladium by Beams of Acetylene.

These fall into four sections:

(a) maximum beam intensity with source at 15°C and target temperatures of 25°C and 60°C;

(b) maximum beam intensity with source at 60°C and a target temperature of 25°C;

(c) one-half maximum beam intensity from a source at 15°C and target temperatures of 25°C and 60°C;

(d) interrupting the beam during a displacement for a short interval.

By maximum beam intensity is meant a source pressure of 2.0×10^{-3} torr, giving a flux of 3.5×10^{13} molecules/cm^2/sec at the target distance; since the target is mounted at 45° to the beam direction the effective beam intensity is $(1/\sqrt{2}) \times 3.5 \times 10^{13}$ molecules/cm^2/sec; i.e. 2.5×10^{13} molecules/cm^2/sec. At this intensity the background flux is approximately 4.1×10^{13} molecules/cm^2/sec. One-half of this beam intensity is obtained with a source pressure of 1.0×10^{-3} torr and correspondingly reduced beam and background fluxes. The effective beam temperature from a source at 15°C is 388°K or 115°C; from a source at 60°C it is 449°K or 176°C. The background flux, thermalised by collisions with the walls of the vessel, is at room temperature, about 23°C.

(a) Acetylene Displacement - Source Temperature 15°C, Source Pressure 2 x 10^{-3} torr.

1. Surface temperature 25°C

The surface was held in vacuo at 15°C before the run started and the initial count rate was 470 cpm. The values of count against time are listed in Table 8, together with the corrected values after subtraction of the retained phase and the log values of the corrected counts. Fig. 5.12 shows the plot of the log of the observed count against time and fig. 5.13 the plot of log corrected count versus time. Insufficient first phase was visible to obtain data on the kinetics of α phase desorption - which in any case would have been too rapid to be followed.

The results were:

α phase = 6.4%

β phase = 25.5%

retained phase = 68.1%

$\beta\, t_{\frac{1}{2}}$ (acetylene displacement) = 61.0 min $\pm$ 12 min

Table 8

Acetylene Displacement

Surface Temperature: 25°C

Source Temperature: 15°C

Source Pressure: 2×10^{-3} torr

Time (min)	Count (cpm)	Corrected Count	log Corrected Count
2.00	446	126	2.1004
4.25	432	112	2.0492
6.50	433	113	2.0899
8.75	418	98	1.9912
11.00	425	105	2.0212
13.25	413	93	1.9685
15.50	414	94	1.9731
17.75	422	102	2.0086
20.00	423	103	2.0128
22.25	406	86	1.9345
24.50	416	96	1.9823
26.75	440	120	2.0792
29.00	413	93	1.9685
31.25	410	90	1.9542
33.50	400	80	1.9031
35.75	412	92	1.9638
38.00	391	71	1.8513
43.00	377	57	1.7559
47.00	394	74	1.8692
49.25	396	76	1.8808
51.75	401	81	1.9085
54.00	369	49	1.6902
56.25	392	72	1.8573
58.50	405	85	1.9294

Table 8 (contd.)

Time (min)	Count (cpm)	Corrected Count	log Corrected Count
60.75	410	90	1.9542
64.00	419	99	1.9956
66.25	395	75	1.8751
72.50	388	68	1.8325
83.50	377	57	1.7559
102.00	368	48	1.6812
119.00	357	37	1.5682
135.00	377	57	1.7559
147.50	368	48	1.6812
172.00	304	-	-
200.00	260	-	-
211.50	338	18	1.2553
222.00	345	25	1.3979
244.00	339	19	1.2788
282.00	329	9	.9542
305.00	317	-	-
315.00	327	7	.8451
325.00	323	3	.4771
335.00	307	-	-

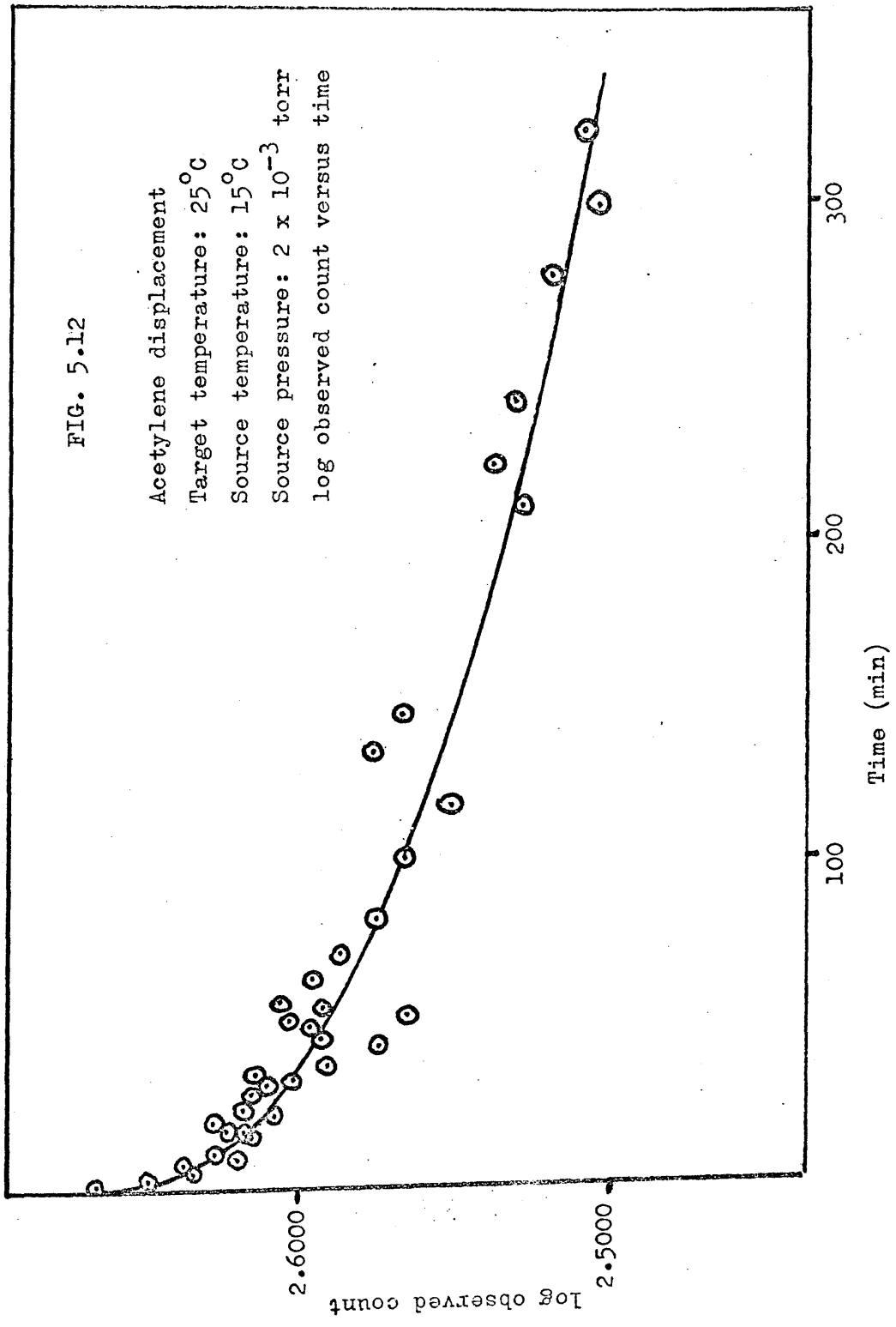
Acetylene displacement
Target temperature: 25°C
Source temperature: 15°C
Source pressure: 2 x 10⁻³ torr
log observed count versus time
log observed count
2.6000
2.5000
100
200
300
Time (min)

FIG. 5.12

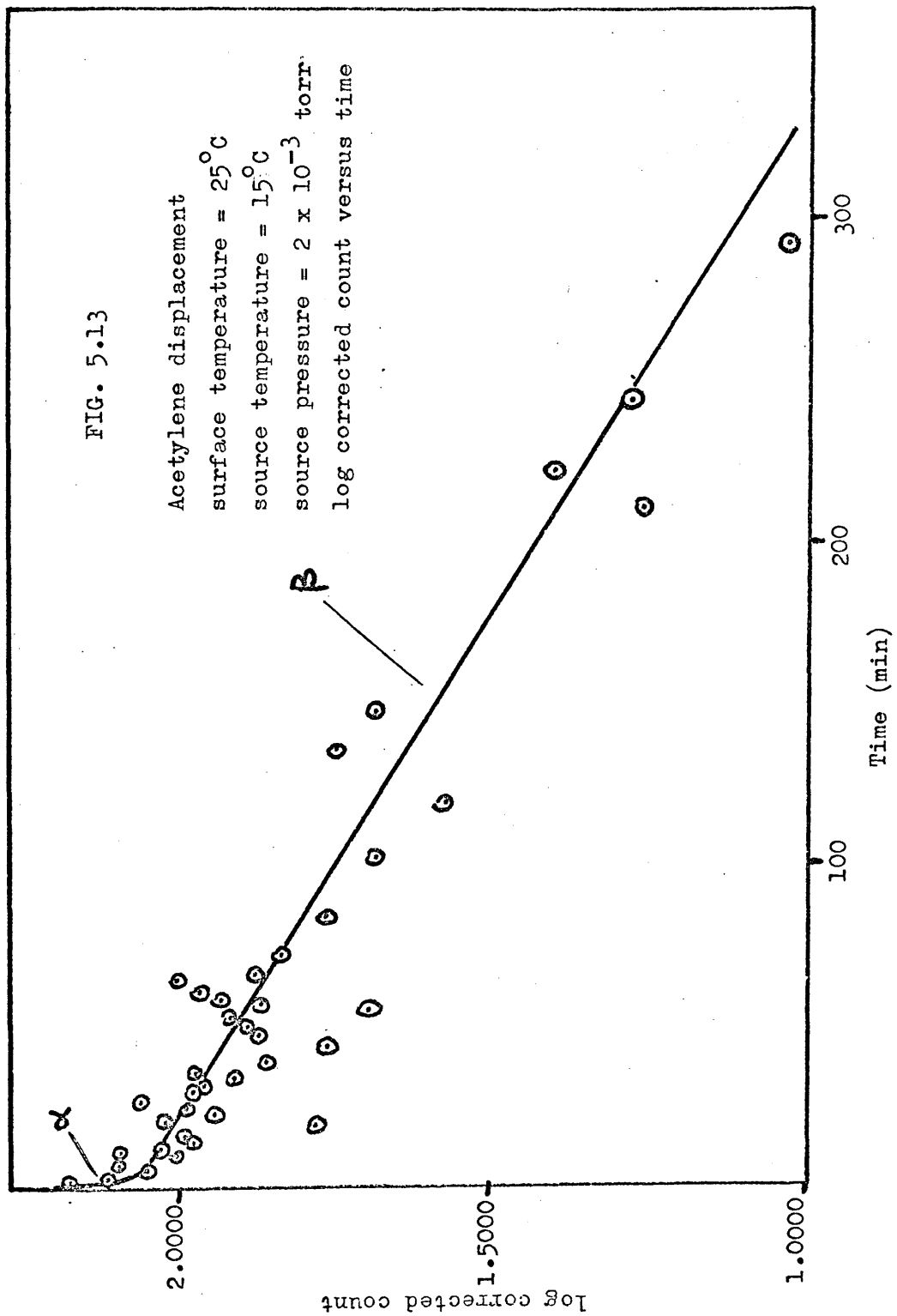
FIG. 5.13
Acetylene displacement
surface temperature = 25°C
source temperature = 15°C
source pressure = 2 x 10⁻³ torr
log corrected count versus time
A
B
2.0000
1.5000
1.0000
log corrected count
100
200
300
Time (min)

2. Surface temperature 60°C

Table 9 shows the usual data of time, count, corrected count and log of corrected count. Fig. 5.14 shows the plot of log of observed count versus time and fig. 5.15 the plot of log corrected count versus time. Here again the target was held at 15°C for some time before starting the run and some α phase desorption was seen. This data was not processed as much better data became available shortly afterwards. The initial surface count rate was 499 cpm. The rate of displacement of the α phase at 60°C was such that only two or three counts could be made while it was proceeding. No attempt has been made to evaluate these.

The values obtained were:

α phase = 18.0%

β phase = 25.5%

retained phase = 56.5%

β $t_{\frac{1}{2}}$ (acetylene displacement) = 18.3 min $\pm$ 4 min

Table 9

Acetylene Displacement

Surface Temperature: 60°C

Source Temperature: 15°C

Source Pressure: 2×10^{-3} torr

Time (min)	Count (cpm)	Corrected Count	log Corrected Count
1.30	431	149	2.1732
3.45	405	123	2.0899
6.00	402	120	2.0792
8.15	372	90	1.9542
10.30	359	77	1.8865
12.45	370	88	1.9445
15.00	353	71	1.8513
17.15	353	71	1.8513
19.30	367	85	1.9294
21.45	334	52	1.7160
24.00	322	40	1.6021
26.15	317	35	1.5441
28.30	327	45	1.6532
30.45	331	49	1.6902
33.00	316	34	1.5315
35.15	308	26	1.4150
37.30	302	20	1.3010
39.45	318	36	1.5563
42.00	285	3	.4771
44.15	293	11	1.0414
48.15	273	-	-
50.45	279	-	-
54.30	284	2	.3010

FIG. 5.14

Acetylene displacement
surface temperature = 60°C
source temperature = 15°C
source pressure = 2×10^{-3} torr
log observed count
versus time

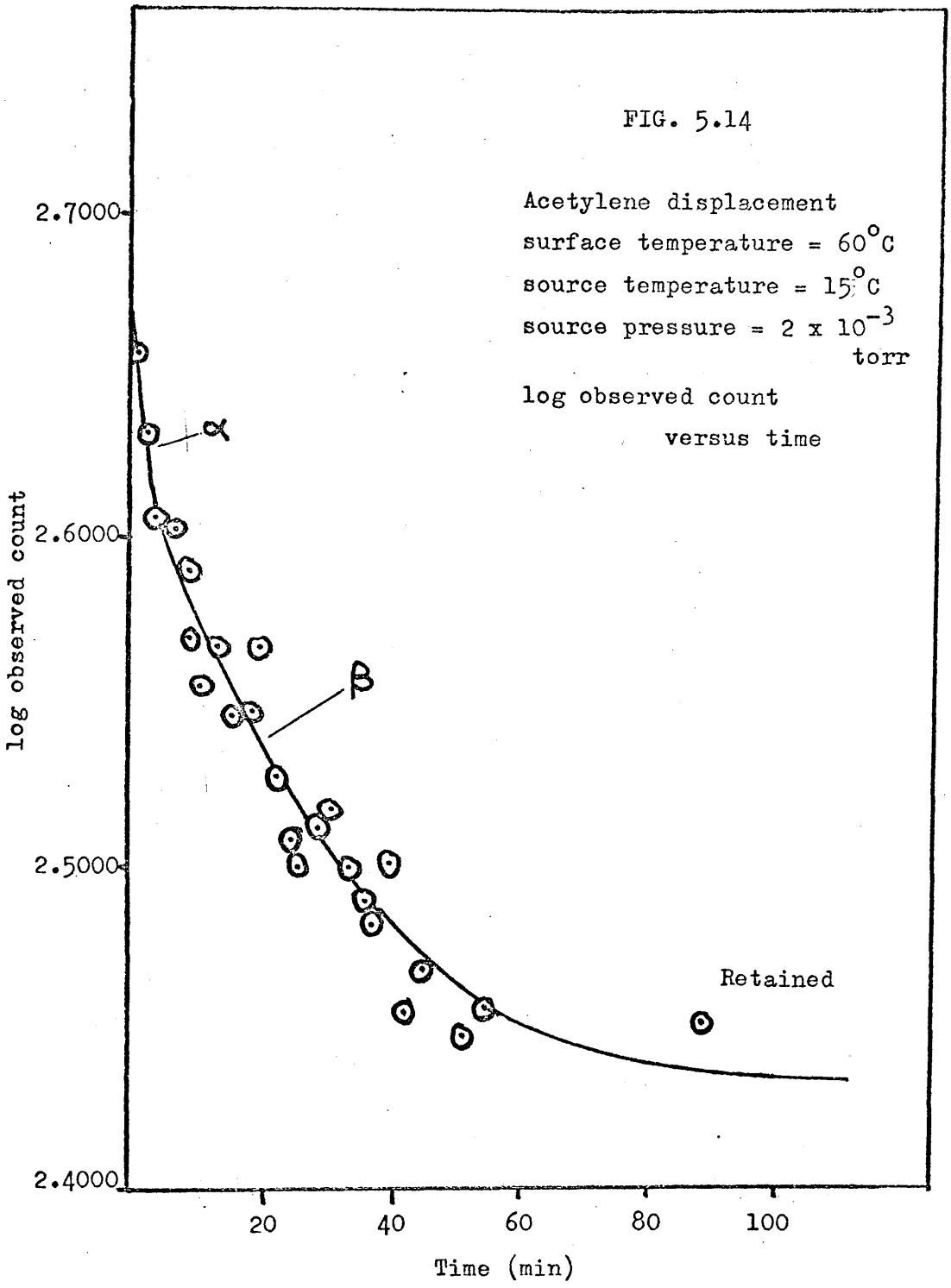

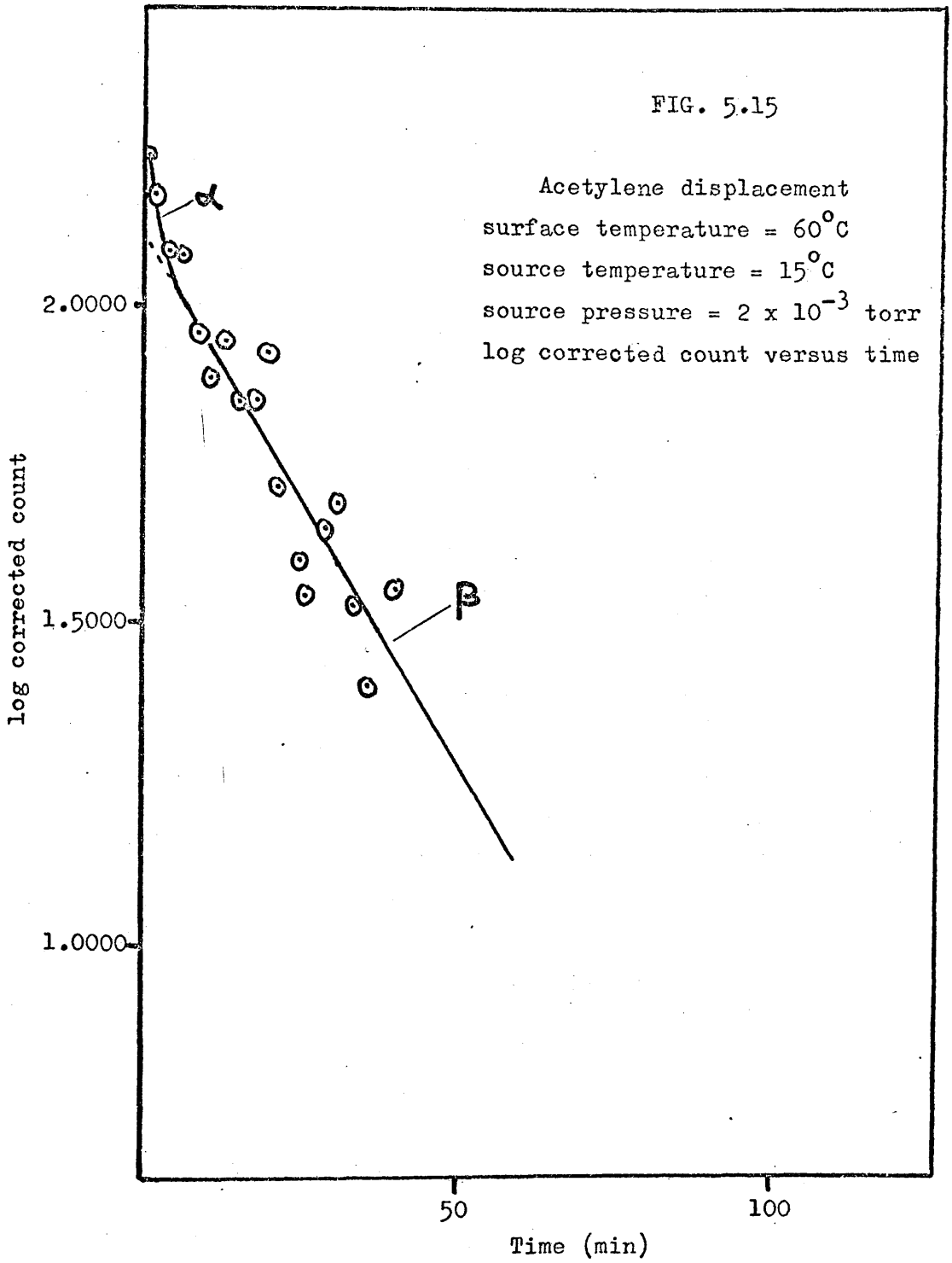

FIG. 5.15

Acetylene displacement
surface temperature = 60°C
source temperature = 15°C
source pressure = 2×10^{-3} torr
log corrected count versus time

(b) Acetylene Displacement - Surface Temperature 25°C, Source Temperature 60°C, Source Pressure 2 x 10^{-3} torr.

Here malfunction of the beam gas inlet prevented introduction of the beam till 40 minutes after evacuation of residual gas. Since only the α phase desorbs noticeably at 15°C and since the α displacement was already too rapid to measure in the previous runs the run was allowed to proceed. The initial surface count was 410 cpm. Table 10 shows the usual data, fig. 5.16 the plot of log observed count versus time and fig. 5.17 the plot of log corrected count versus time.

The values obtained were:

α phase = 9.8%

β phase = 33.4%

retained phase = 56.8%

$\beta\, t_{\frac{1}{2}}$ (acetylene displacement) = 43.4 min $\pm$ 10 min.

Table 10

Acetylene Displacement

Surface Temperature: 25°C

Source Temperature: 60°C

Source Pressure: 2×10^{-3} torr

Time (min)	Count (cpm)	Corrected Count	log Corrected Count
41.45	384	151	2.1790
44.00	355	122	2.0864
46.15	344	111	2.0453
48.30	360	127	2.1038
50.45	334	101	2.0043
53.00	324	91	1.9590
60.15	341	108	2.0334
71.30	324	91	1.9590
82.00	314	81	1.9085
92.30	304	71	1.8513
105.30	282	49	1.6902
125.30	262	29	1.4624
142.00	252	19	1.2788
152.30	248	15	1.1761
165.00	259	26	1.4150
177.00	255	22	1.3424
242.00	233	0	0
305.00	217	-	-

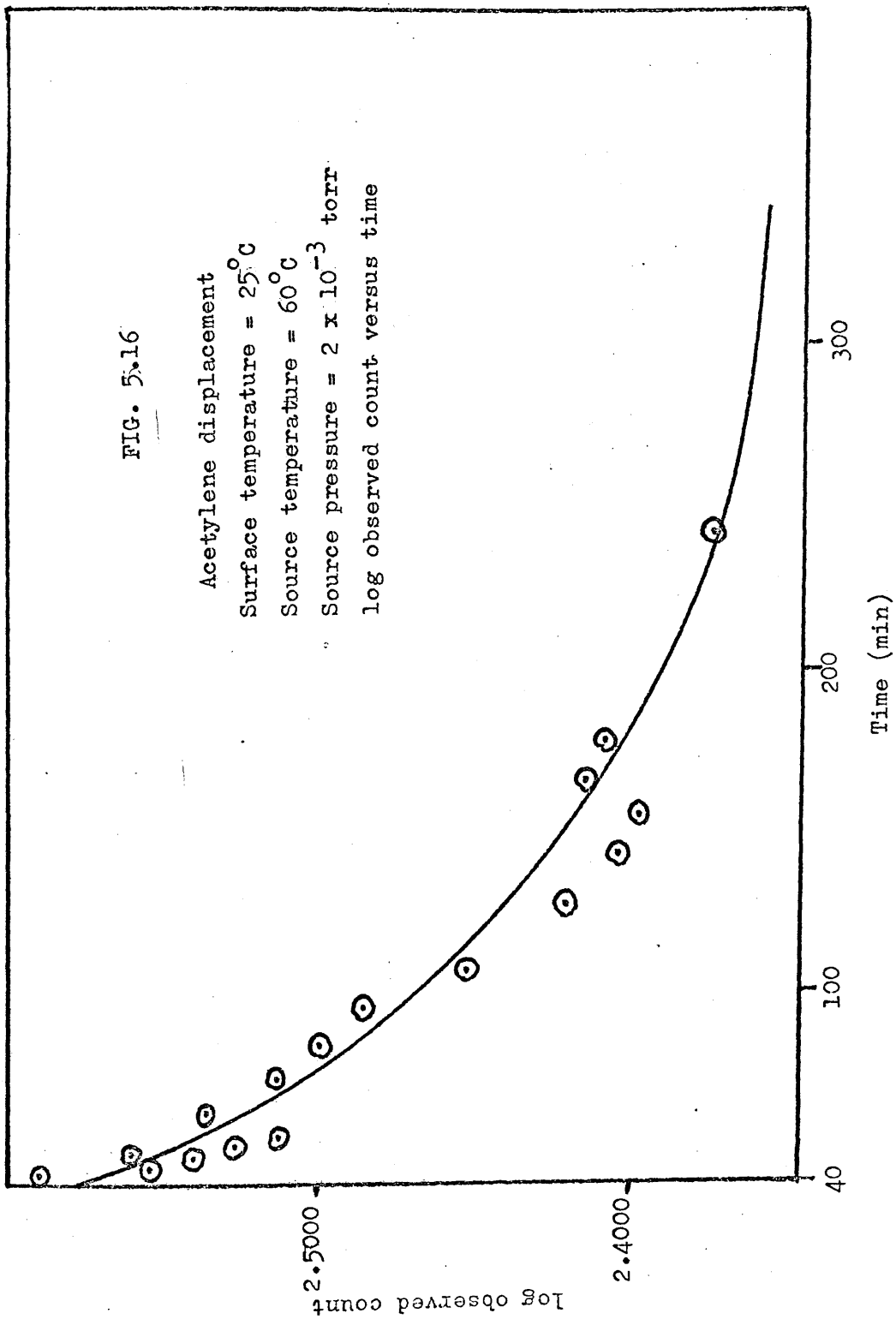
Acetylene displacement
Surface temperature = 25°C
Source temperature = 60°C
Source pressure = 2 x 10⁻³ torr
log observed count versus time
log observed count
2.5000
2.4000
40
100
200
300
Time (min)

FIG. 5.16

FIG. 5.17

Acetylene displacement
surface temperature: 25°C
source temperature: 60°C
source pressure: 2×10^{-3} torr
log corrected count versus time

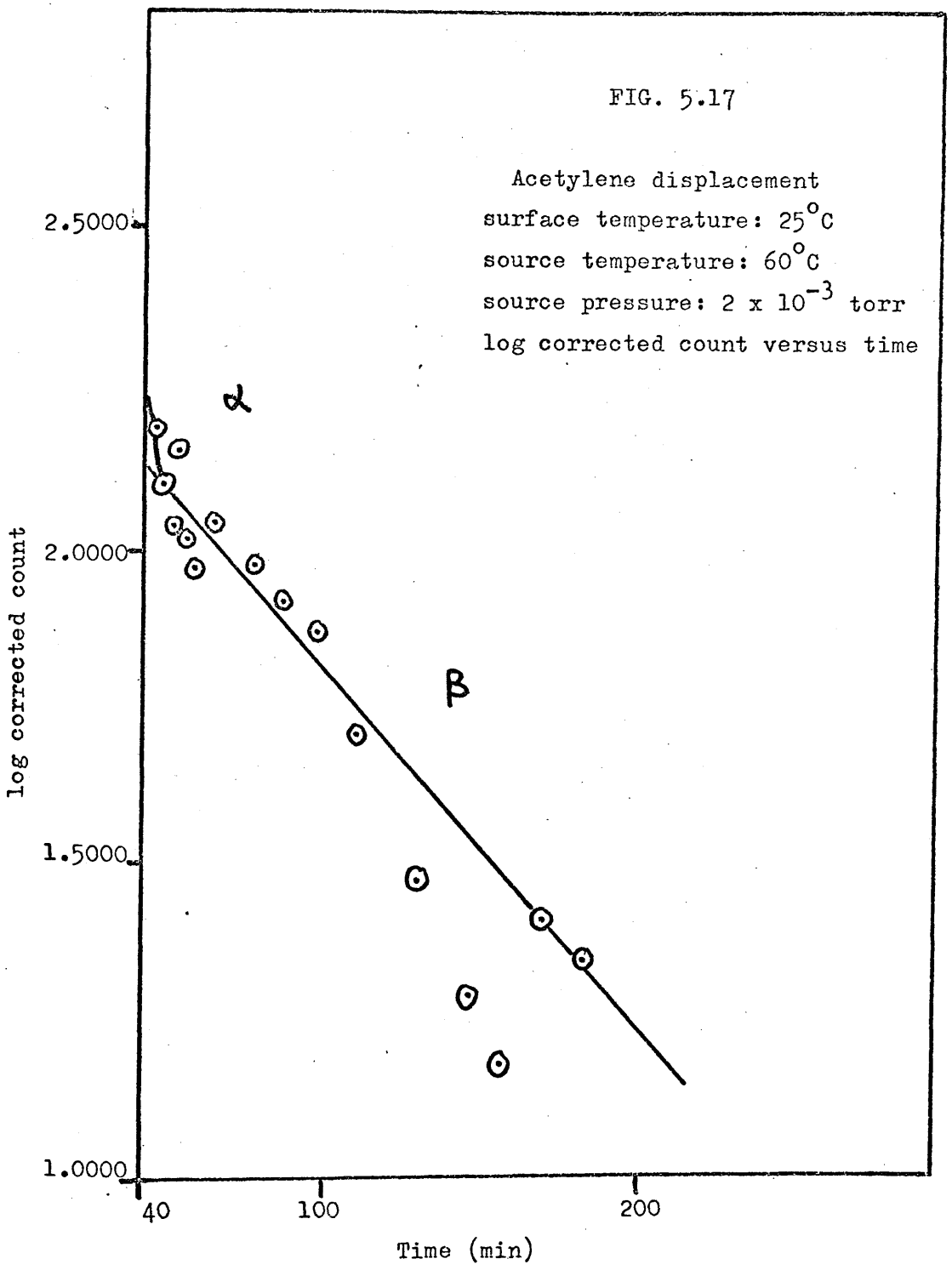

(c) Beam Intensity Half Maximum

1. Surface temperature 25°C, source temperature 15°C, source pressure 1 x 10^{-3} torr

Here the count rate initially observed was 8102 cpm and a small amount of first phase desorption was followed for 30 minutes. Table 11 shows the results from starting the beam, fig. 5.18 the plot of the log of the observed count versus time and fig. 5.19 the plot of log corrected count versus time. The rate of desorption was noticeably slower both for the α phase and the β phase and this time an $\alpha t_{\frac{1}{2}}$ could be measured. The corrected α values are shown in Table 12.

The values obtained were:

α phase = 15.2%

β phase = 23.2%

retained phase = 61.6%

$\alpha t_{\frac{1}{2}}$ (acetylene displacement) = 3.1 min $\pm$ 1.5 min

$\beta t_{\frac{1}{2}}$ (acetylene displacement) = 59.1 min $\pm$ 3 min.

Table 11

Acetylene Displacement

Surface Temperature: 25°C

Source Temperature: 15°C

Source Pressure: 1×10^{-3} torr

Time (min)	Count (cpm)	Corrected Count (cpm)	log Corrected Count
2.00	7458	2446	3.3885
4.25	7436	2424	3.3845
6.50	7245	2233	3.3489
8.50	6849	1837	3.2642
11.00	6656	1644	3.2159
13.25	6652	1640	3.2148
15.50	6648	1636	3.2138
17.75	6546	1534	3.1858
20.00	6482	1470	3.1673
22.75	6397	1385	3.1415
25.50	6419	1407	3.1483
27.75	6395	1383	3.1409
31.75	6351	1339	3.1268
37.00	6393	1381	3.1402
42.25	6133	1121	3.0496
47.50	6038	1026	3.0112
53.50	5996	984	2.9930
59.00	5950	938	2.9722
65.50	5901	889	2.9489
70.50	5829	817	2.9122
77.50	5787	775	2.8893
86.00	5483	471	2.6730
94.00	5465	453	2.6561
102.00	5350	338	2.5289
133.50	5157	145	2.1614

Table 12

Acetylene Displacement

Surface Temperature: 25°C

Source Temperature: 15°C

Source Pressure: 1 x 10^{-3} torr

Time (min)	Corrected ∝ Phase Count (cpm)	log Corrected Phase Count
2.00	598	2.7767
4.25	624	2.7952
6.50	480	2.6812
8.50	125	2.0969
11.00	-	-
13.25	20	1.3010
15.50	58	1.7634

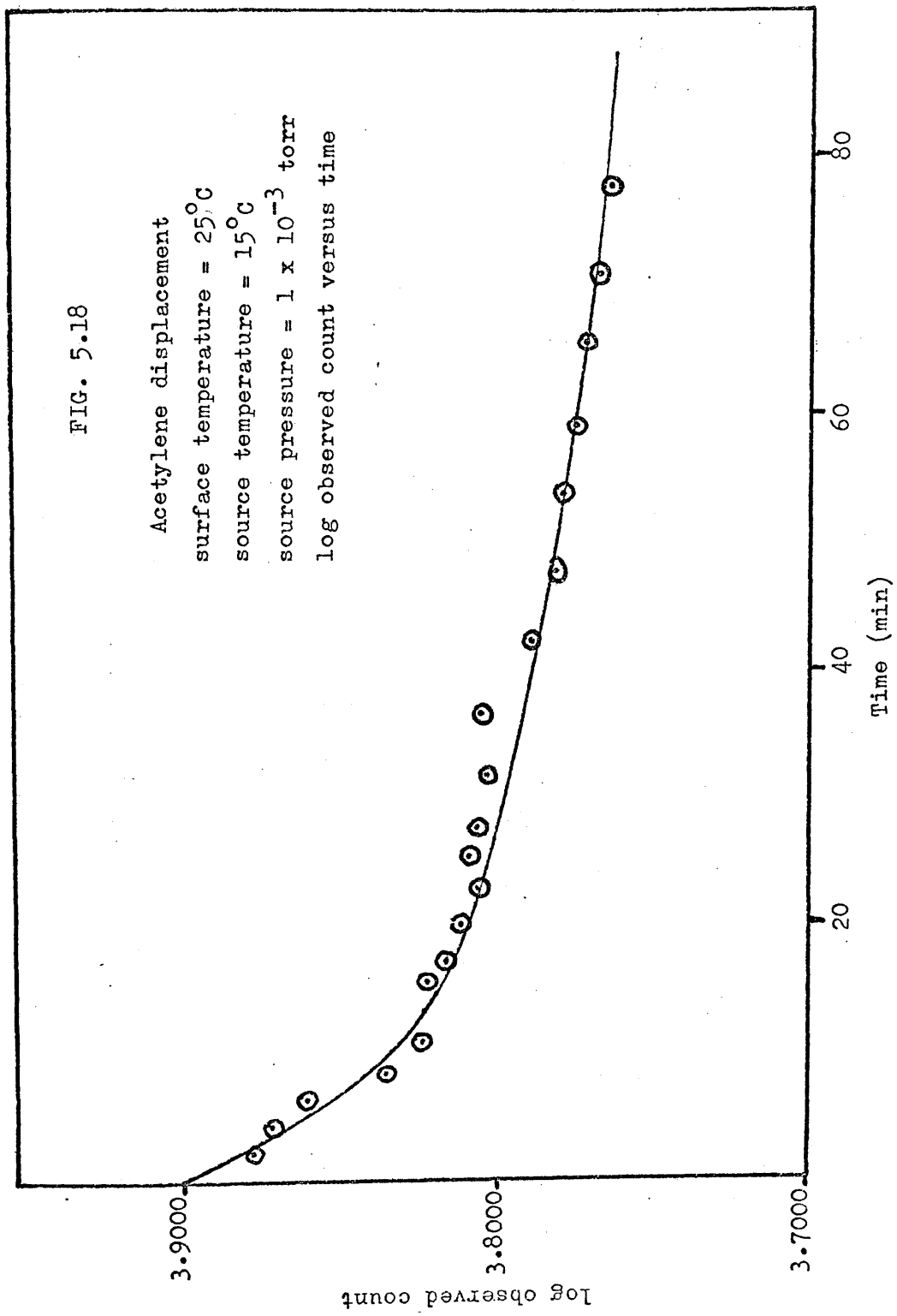
Acetylene displacement
surface temperature = 25°C
source temperature = 15°C
source pressure = 1 x 10⁻³ torr
log observed count versus time
3.9000
3.8000
3.7000
log observed count
20
40
60
80
Time (min)

FIG. 5.18

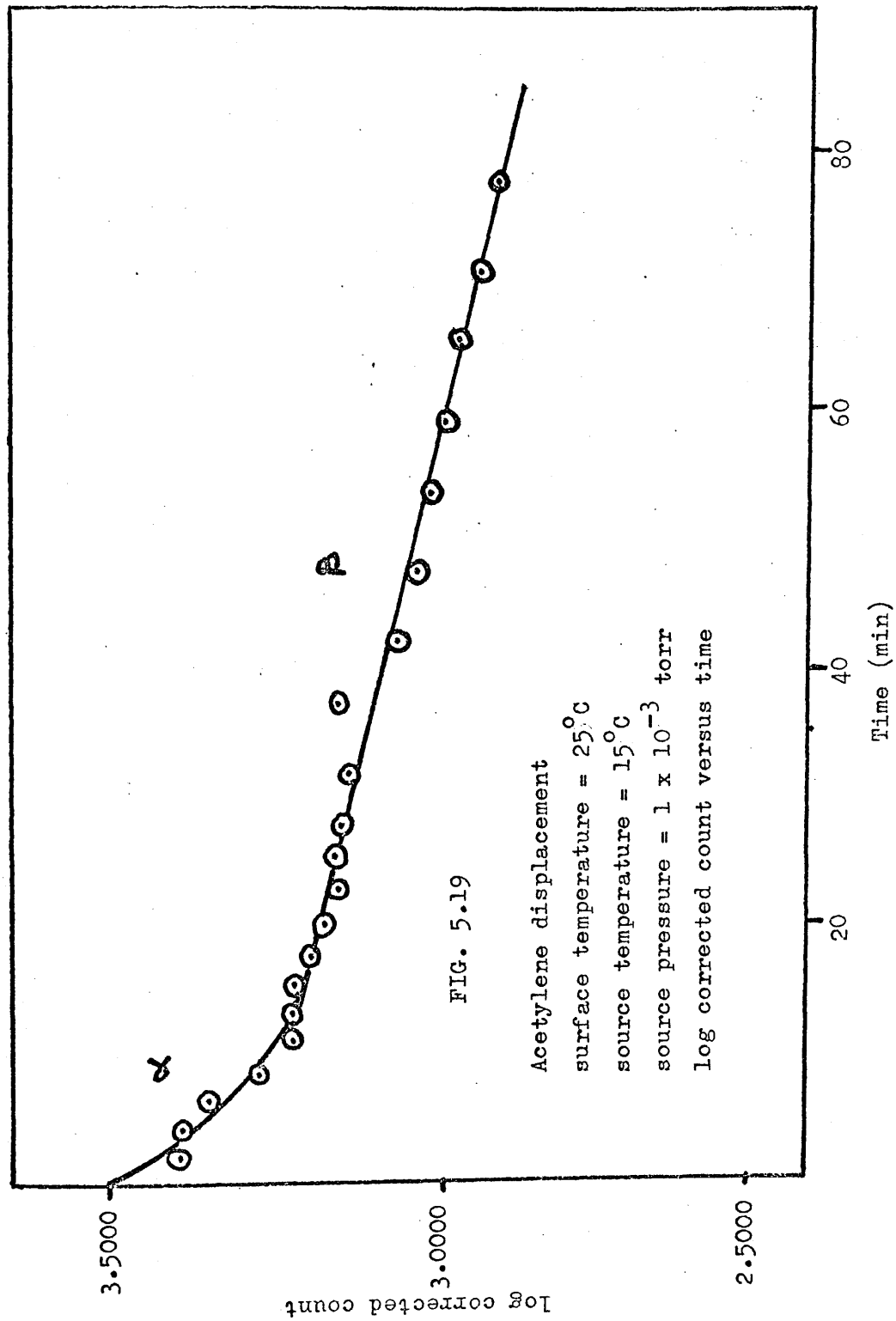
3.5000
3.0000
2.5000
log corrected count
20
40
60
80
Time (min)
Acetylene displacement
surface temperature = 25°C
source temperature = 15°C
source pressure = 1 x 10⁻³ torr
log corrected count versus time

FIG. 5.19

2. Surface temperature 60°C, source temperature 15°C, source pressure 1 x 10^{-3} torr

Here the initial vacuum desorption at 15°C was large and has been used to estimate the vacuum desorption $\alpha t_{\frac{1}{2}}$ at 15°C. The Laben multi-scaler was used to record counts. The time values listed are count channels 100 sec wide, with zero waiting time between them. Table 13 lists the usual primary data for the run, fig. 5.20 shows the plot of log of observed count versus time and fig. 5.21 the plot of log corrected count versus time. Table 14 lists the corrected α phase count versus time. The accompanying graph fig. 5.22 shows the first order kinetics of the α phase. The surface temperature was raised to 60°C and the beam admitted to the surface at the end of channel 49. Again faster evaporation of the palladium was carried out.

The values found were:

α phase = 52.7%

β phase = 10.3%

retained phase = 37.0%

$\alpha t_{\frac{1}{2}}$ (vacuum desorption at 15°C) = 31.7 min $\pm$ 3 min

$\alpha t_{\frac{1}{2}}$ (acetylene displacement) = 4.1 min $\pm$ 1 min

$\beta t_{\frac{1}{2}}$ (acetylene displacement) = 53.1 min $\pm$ 5 min.

Table 13

Acetylene Displacement

Surface Temperature: 60°C

Source Temperature: 15°C

Source Pressure: 1×10^{-3} torr

Time Channel	Count	Corrected Count	log Corrected Count
1	1813	1143	3.0580
2	1793	1123	3.0503
3	1624	954	2.9795
4	1690	1020	3.0086
5	1630	960	2.9823
6	1584	914	2.9609
7	1474	804	2.9053
8	1394	724	2.8597
9	1362	692	2.8401
10	1352	682	2.8331
11	1426	756	2.8785
12	1526	856	2.9325
13	1577	907	2.9576
14	1546	876	2.9425
15	1439	769	2.8859
16	1535	865	2.9370
17	1448	778	2.8910
18	1426	756	2.8785
19	1459	789	2.8971
20	1421	751	2.8756
21	1344	674	2.8287
22	1218	548	2.7388
23	1220	550	2.7404
24	1195	525	2.7202

Table 13 (contd.)

Time Channel	Count	Corrected Count	log Corrected Count
25	1156	486	2.6866
26	1206	536	2.7292
27	1200	530	2.7243
28	1225	555	2.7443
29	1170	500	2.6990
30	1143	473	2.6749
31	1132	462	2.6646
32	1217	547	2.7380
33	1122	452	2.6551
34	1095	425	2.6284
35	1113	443	2.6464
36	1129	459	2.6618
37	1054	384	2.5843
38	1067	397	2.5988
39	1154	484	2.6848
40	1101	431	2.6345
41	1011	341	2.5328
42	1054	384	2.5843
43	1071	401	2.6031
44	987	311	2.4928
45	1043	373	2.5717
46	1060	390	2.5911
47	995	325	2.5119
48	1072	402	2.6042
49	1023	353	2.5478
50	963	293	2.4669
51	966	296	2.4713

Table 13 (contd.)

Time Channel	Count	Corrected Count	log Corrected Count
52	929	259	2.4133
53	921	251	2.3997
54	862	192	2.2833
55	882	212	2.3263
56	870	200	2.3010
57	857	187	2.2718
58	835	165	2.2175
59	867	197	2.2945
60	827	157	2.1959
61	827	157	2.1959
62	791	121	2.0828
63	819	149	2.1732
64	874	204	2.3096
65	843	173	2.2380
66	843	173	2.2380
67	753	83	1.9191
68	807	137	2.1367
69	744	74	1.8692
70	758	88	1.9445
71	839	169	2.2279
72	813	143	2.1553
73	773	103	2.0128
74	800	130	2.1139
75	738	68	1.8325
76	789	119	2.0755
77	788	118	2.0719
78	810	140	2.1461

Table 13 (contd.)

Time Channel	Count	Corrected Count	log Corrected Count
79	724	54	1.7324
80	785	115	2.0607
81	709	39	1.5911
82	769	99	1.9956
83	777	107	2.0294
84	789	119	2.0755
85	759	89	1.9494
86	734	64	1.8062
87	749	79	1.8976
88	762	92	1.9638
89	728	58	1.7634
90	759	89	1.9494
91	760	90	1.9542
92	760	90	1.9542
93	723	53	1.7243
94	726	56	1.7482
95	743	73	1.8633
96	765	95	1.9777
97	707	57	1.7559
98	728	58	1.7634
99	766	96	1.9823
100	689	19	1.2788
101	702	32	1.5051
102	784	114	2.0569
103	749	79	1.8976
104	746	76	1.8808
105	702	32	1.5051
106	673	3	.4771

Table 13 (contd.)

Time Channel	Count	Corrected Count	log Corrected Count
107	642	-	-
108	695	25	1.3979
109	755	85	1.0374
110	693	23	1.3617
111	682	12	1.0792
112	679	9	.9542
113	714	44	1.6435
114	721	51	1.7076
115	702	32	1.5051
116	685	15	1.1761
117	667	-	-
118	688	18	1.2553
119	702	32	1.5051
120	654	-	-
121	680	10	1.0000
122	682	12	1.0792
123	713	43	1.6355
124	731	61	1.7853
125	655	-	-
126	712	42	1.6232
127	699	29	1.4624
128	681	11	1.0414
129	710	40	1.6021
130	691	21	1.3222
131	685	15	1.1761
132	688	18	1.2553
133	730	60	1.7782

Table 13 (contd.)

Time Channel	Count	Corrected Count	log Corrected Count
134	712	42	1.6232
135	655	-	-
136	677	7	.8451
137	660	-	-
138	693	23	1.3617

Channel width = 100 seconds

Table 14 (a)

Vacuum Desorption of ∝ Phase

Surface Temperature: 15°C

Time Channel	Corrected ∝ Phase Count	log Corrected ∝ Phase Count
1	957	2.9809
2	937	2.9717
3	768	2.8854
4	833	2.9206
5	774	2.8887
6	728	2.8621
7	618	2.7910
8	538	2.7308
9	506	2.7042
10	496	2.6955
11	570	2.7559
12	670	2.8261
13	721	2.8579
14	690	2.8388
15	583	2.7657
16	679	2.8319
17	592	2.7723
18	570	2.7559
19	603	2.7803
20	565	2.7520
21	488	2.6884
22	362	2.5587
23	364	2.5611
24	339	2.5302
25	230	2.4771

Table 14 (a) (contd.)

Time Channel	Corrected ∝ Phase Count	log Corrected ∝ Phase Count
26	350	2.5441
27	344	2.5366
28	369	2.5670
29	314	2.4969
30	287	2.4579
31	276	2.4409
32	361	2.5575
33	266	2.4249
34	239	2.3784
35	257	2.4099
36	273	2.4362
37	198	2.2967
38	211	2.3243
39	298	2.4742
40	245	2.3892
41	155	2.1903
42	198	2.2967
43	215	2.3324
44	125	2.0969
45	187	2.2718
46	204	2.3096
47	139	2.1430
48	217	2.3365
49	167	2.2227

Channel width = 100 seconds

Table 14 (b)

Acetylene Displacement of α Phase

Surface Temperature: $60^{\circ}C$

Source Temperature: $15^{\circ}C$

Source Pressure: 1×10^{-3} torr

Time Channel	Corrected α Phase Count	log Corrected α Phase Count
50	107	2.0294
51	114	2.0569
52	81	1.9085
53	77	1.8865
54	21	1.3222
55	45	1.6532
56	37	1.5682
57	27	1.4314
58	8	.9031

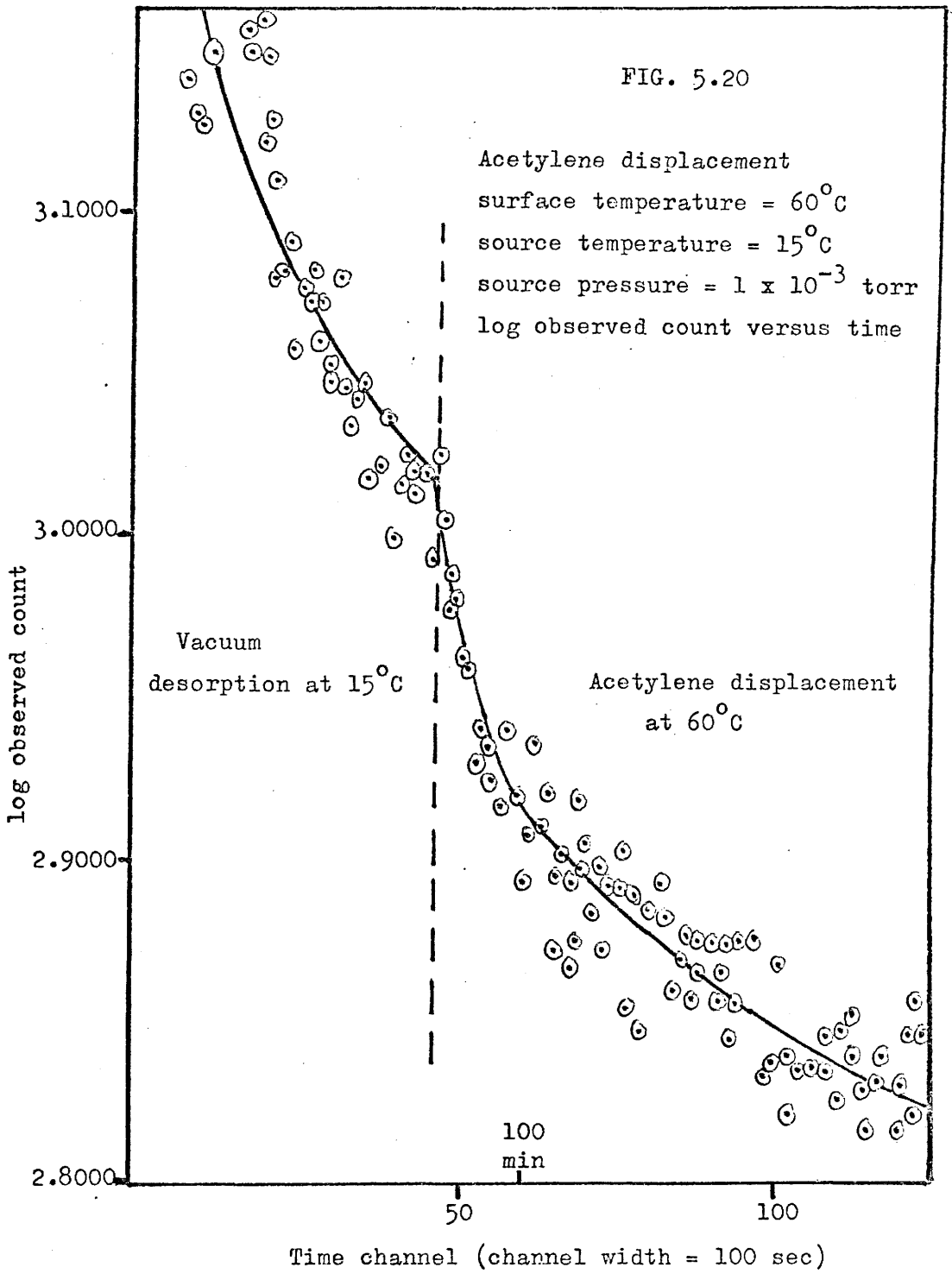
FIG. 5.20
Acetylene displacement
surface temperature = 60°C
source temperature = 15°C
source pressure = 1 x 10⁻³ torr
log observed count versus time
3.1000
3.0000
2.9000
2.8000
log observed count
Vacuum
desorption at 15°C
Acetylene displacement
at 60°C
100
min
50
100
Time channel (channel width = 100 sec)

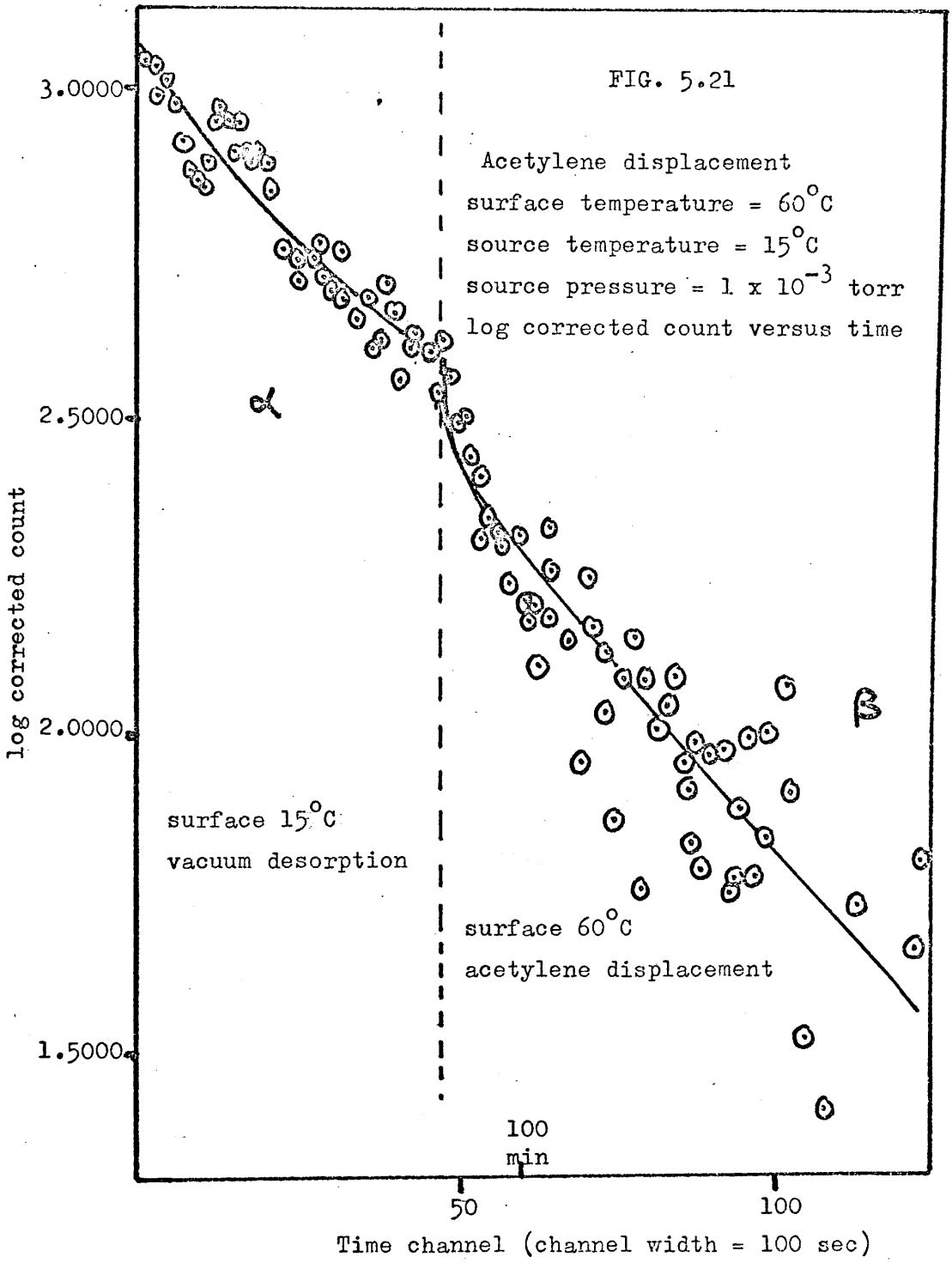
FIG. 5.21
Acetylene displacement
surface temperature = 60°C
source temperature = 15°C
source pressure = 1 x 10⁻³ torr
log corrected count versus time
3.0000
2.5000
2.0000
1.5000
log corrected count
α
β
surface 15°C
vacuum desorption
surface 60°C
acetylene displacement
100
min
50
100
Time channel (channel width = 100 sec)

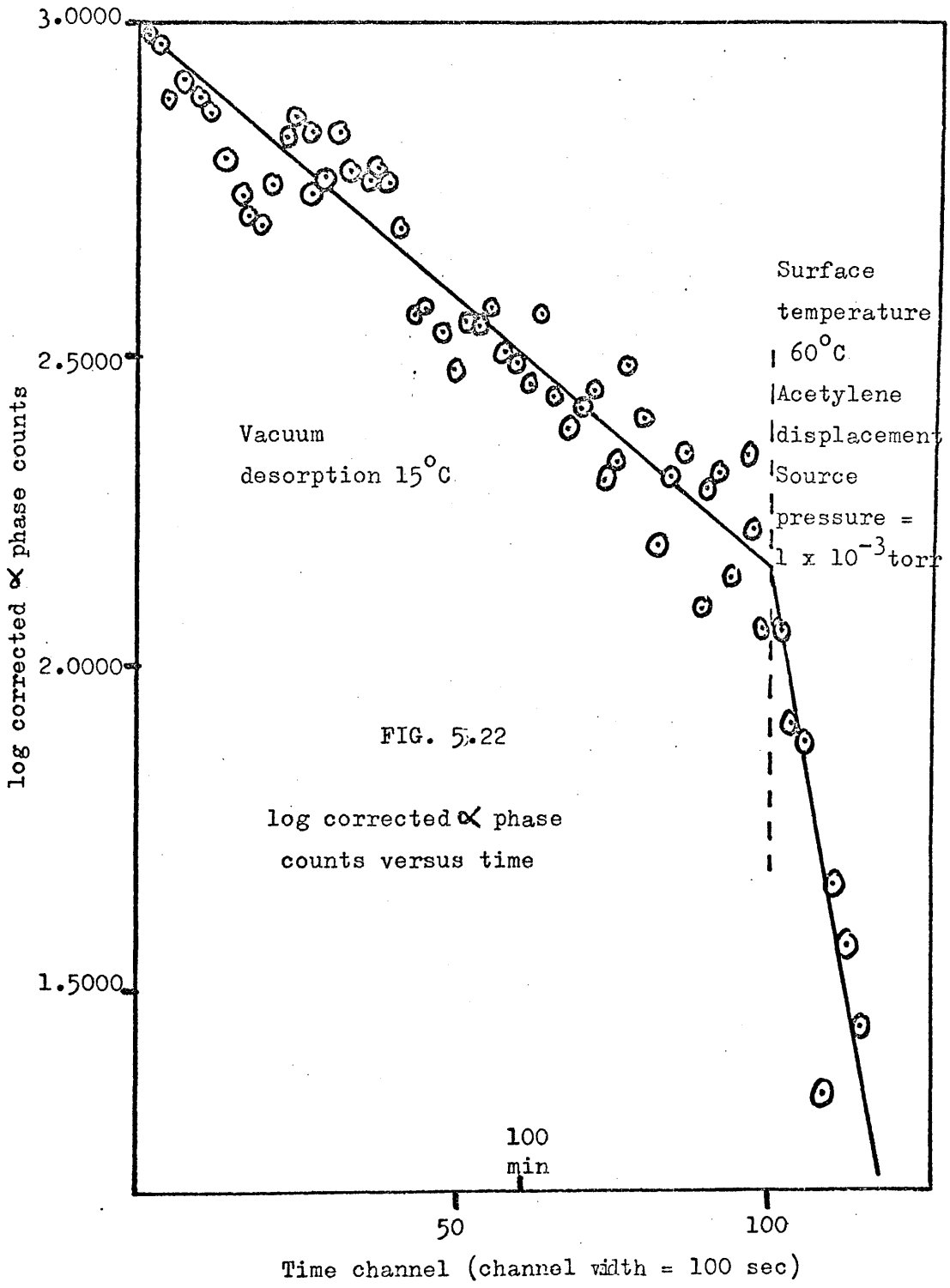

FIG. 5.22

log corrected ∝ phase counts versus time

(d) Beam Interruption - Surface Temperature 25°C, Source Temperature 15°C, Source Pressure 2 x 10^{-3} torr

Here the displacement at a surface temperature of 25°C by a beam of acetylene, of maximum intensity, was chosen to be interrupted. Table 15 lists the usual data and fig. 5.23 is the plot of log corrected count versus time. The initial surface count was 579 cpm. The best straight lines for the initial acetylene displacement, for the period of interruption and for the period after restarting the beam, were calculated. The slopes were, respectively, -61.3, -10.1 and -72.1, indicating that the displacement had ceased immediately the beam was stopped - as is evident from fig. 5.15. From the slopes could be calculated the $t_{\frac{1}{2}}$ values for desorption. These were:

$\beta t_{\frac{1}{2}}$ (initial acetylene displacement) = 49.7 min $\pm$ 5 min

$\beta t_{\frac{1}{2}}$ (beam off) = 299 min $\pm$ 100 min

$\beta t_{\frac{1}{2}}$ (final acetylene displacement) = 42.1 min $\pm$ 5 min.

The percentages for each phase were:

α phase = 11.0%

β phase = 22.0%

retained phase = 67.0%

The $\beta t_{\frac{1}{2}}$ displacement values are used later in calculations of the activation energy for the displacement reaction. The $\beta t_{\frac{1}{2}}$ value obtained when the beam was off is close to the vacuum desorption $\beta t_{\frac{1}{2}}$ (251 min) obtained at this temperature.

Table 15

Interrupted Acetylene Displacement

Surface Temperature: 25°C

Source Temperature: 15°C

Source Pressure: 2×10^{-3} torr

Time (min)	Count (cpm)	Corrected Count (cpm)	log Corrected Count
1.50	464	134	2.1761
3.75	427	97	1.9868
6.00	412	87	1.9395
8.15	423	93	1.9685
10.50	425	95	1.9777
12.75	439	109	2.0374
15.00	415	85	1.9294
17.25	428	98	1.9912
19.50	426	96	1.9823
21.75	393	63	1.7993
24.00	412	83	1.9191
26.25	423	93	1.9685
28.50	394	64	1.8062
30.75	393	63	1.7993
33.00	409	73	1.8633
35.25	390	60	1.7782
	Beam off		
38.25	404	74	1.8692
40.50	386	56	1.7482
42.75	374	34	1.5315
45.00	386	56	1.7482
47.25	392	62	1.7924
49.50	383	53	1.7243

Table 15 (contd.)

Time (min)	Count (cpm)	Corrected Count (cpm)	log Corrected Count
51.75	392	62	1.7924
54.00	386	56	1.7482
56.25	405	65	1.8129
58.50	389	59	1.7709
60.75	399	69	1.8388
63.00	367	37	1.5682
65.25	376	46	1.6628
67.50	394	64	1.8062
69.75	392	62	1.7924
72.00	376	46	1.6628
74.25	382	52	1.7160
78.50	377	47	1.6721
80.75	380	50	1.6990
83.00	389	57	1.7559
	Beam on		
86.75	361	31	1.4914
89.00	382	52	1.7160
91.25	381	51	1.7076
93.50	380	50	1.6990
95.75	333	3	.4771
98.00	373	43	1.6335
100.25	367	47	1.6721
102.50	373	43	1.6335
107.50	366	36	1.5563
109.75	364	34	1.5315
112.00	360	30	1.4771
114.25	357	27	1.4314

Table 15 (contd.)

Time (min)	Count (cpm)	Corrected Count (cpm)	log Corrected Count
116.50	332	2	.3010
118.75	349	19	1.2788
121.00	359	29	1.4624
123.25	383	53	1.7243
125.50	361	31	1.4914
127.75	369	39	1.5911
132.00	354	24	1.3802
134.25	355	25	1.3979
136.50	344	14	1.1461
147.50	359	29	1.4624
158.25	353	23	1.3617
168.25	353	23	1.3617
181.00	343	13	1.1139
213.00	343	13	1.1139

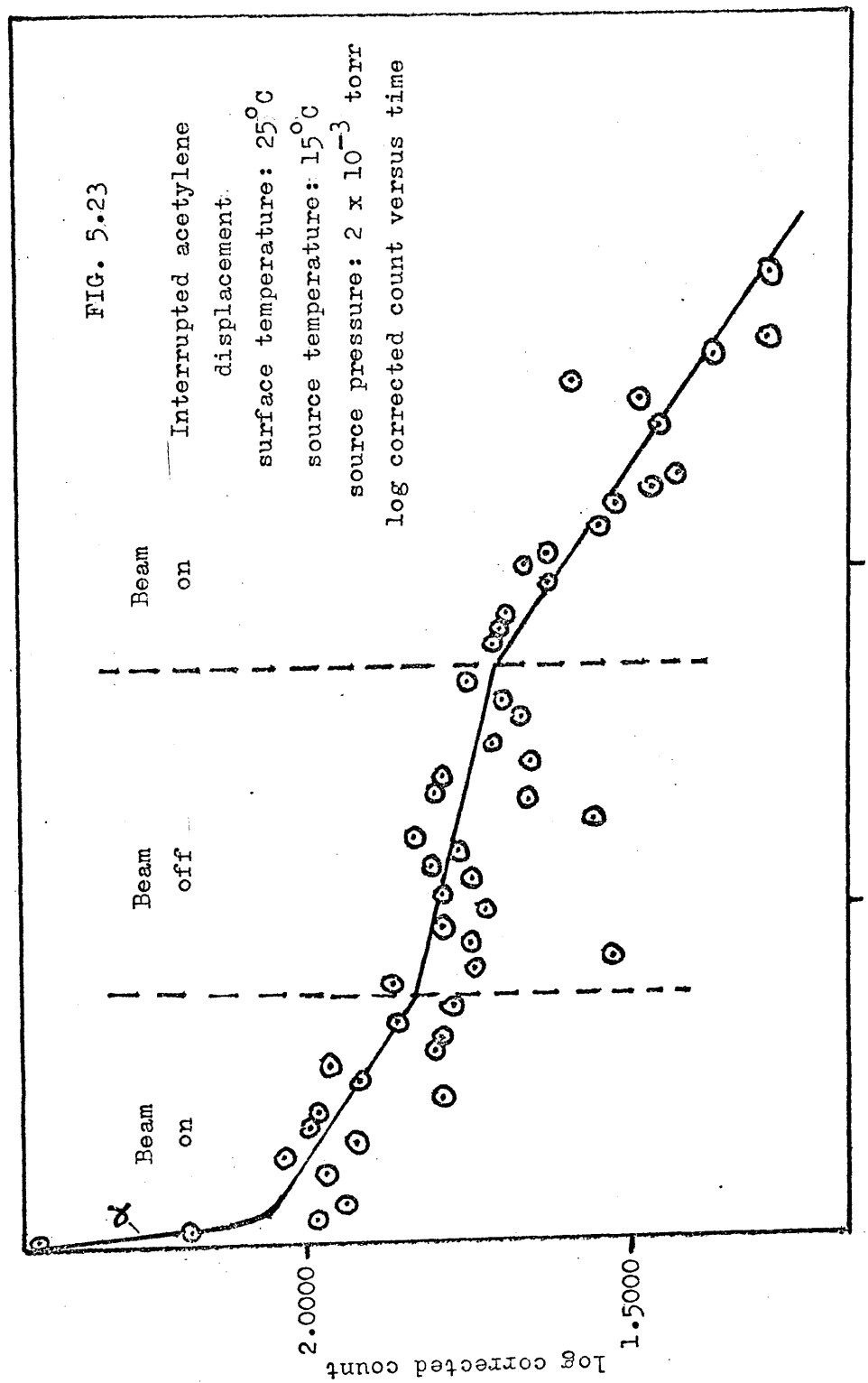
FIG. 5.23
Interrupted acetylene displacement
surface temperature: 25°C
source temperature: 15°C
source pressure: 2 x 10⁻³ torr
log corrected count versus time
Beam on
Beam off
Beam on
2.0000
1.5000
log corrected count
50
100
Time (min)

(e) Conclusions to Acetylene Displacement Reactions

In these experiments two phases in the removal of the C-14 from the surface are observed. The rates of removal involved are much faster than those for the corresponding vacuum desorption of each of the phases. We can thus say that displacement of surface species by beams of acetylene is taking place.

The α phase displacement at any surface temperature is much faster than the corresponding vacuum desorption for a beam flux of 2.5×10^{13} molecules/cm^2/sec - which corresponds to a source pressure of 2×10^{-3} torr. At half this beam flux the displacement rate is less, but a figure cannot be given for the activation energy for the process. The $t_{\frac{1}{2}}$ values observed for α phase displacement show the rate of displacement decreasing with increasing surface temperature, but the possible error in each determination is large.

The β phase displacements again follow first order kinetics and the activation energy can be calculated for this displacement using the $t_{\frac{1}{2}}$ values for displacements by the higher intensity beams at 25°C and 60°C surface temperatures. The value obtained is:

$$E_A = 5.4 \text{ k cal/mole.}$$

Three values of the $\beta t_{\frac{1}{2}}$ for acetylene displacement at 25°C surface temperature have been used - arising from the run whose purpose was solely to follow this displacement, from the run in which interruption of the beam was carried out and from the run, which is described later, in which a beam of acetylene was introduced to a surface after a beam of ethylene had failed to cause displacement. The average figure for this $t_{\frac{1}{2}}$ value - $\beta t_{\frac{1}{2}}$ at 25°C - is 48.0 min. The possible error in this activation energy

is large but one can say that the activation energy for the displacement of the β phase by acetylene is low. A picture also emerges of decreasing rate of displacement with decreasing beam intensity - suggesting that the rate of displacement is proportional to the beam intensity.

The most striking feature of the acetylene displacements is the lack of effect of changing the source temperature on the rate of displacement. The displacement produced by a beam, from a source whose temperature is 15°C and whose pressure is 2×10^{-3} torr, reacting with a target at 25°C proceeds with an average $t_{\frac{1}{2}}$ value of 48 min; the result from an experiment where the only difference is that the source temperature is 60°C is a $t_{\frac{1}{2}}$ value of 43.4 min, little different from that produced by the lower temperature beam. The effect of increasing the target temperature produces a striking increase in rate from a $t_{\frac{1}{2}}$ value at 25°C of 48 min to a $t_{\frac{1}{2}}$ value at 60°C of 18.3 min.

That we are, in fact, displacing the β phase is shown in the interrupted beam experiment where the rate of loss of C-14 from the surface, while the beam is off, is close to the rate at which vacuum desorption of the β phase at that temperature takes place. The result also shows that the displacement ceases immediately the beam is stopped.

(4) Displacement of Pre-adsorbed Ethylene on Palladium by Beams of Ethylene

All the ethylene beams used were produced by a source whose temperature was 15°C and whose pressure was 2×10^{-3} torr. The first study attempted was of the displacement of ethylene at a surface temperature of 25°C. No displacement apparently occurred. The run in which the surface temperature was 60°C was then carried out and displacement was found to occur. The 25°C surface temperature run was then repeated and again no displacement was noticed. The same surface was then exposed to a beam of acetylene, to ensure that the pre-adsorbed ethylene could be replaced. Displacement did occur as expected.

Two displacement reactions at 70°C were then carried out. In the first a vacuum desorption at 70°C was allowed to proceed till about one-half of the β phase had desorbed. The surface was then exposed to a beam of ethylene of maximum intensity from a source at 15°C which displaced the rest of the β phase. This has already been described in the vacuum desorption section. This was followed by a displacement experiment at 70°C surface temperature in which there was no preliminary vacuum desorption. The beam of ethylene ran from the start of the experiment. No displacement occurred. In this part of the study no effects of changing beam intensity or temperature have been attempted.

These experiments will now be described. As the first experiment was duplicated, only the second experiment, where an acetylene beam was subsequently introduced to the surface, will be described.

(a) Interaction of Pre-adsorbed Ethylene on Palladium, at a Surface Temperature of 25°C, with a Beam of Ethylene and Subsequently with a Beam of Acetylene.

Here again the Laben multi-scaler was used to record counts in 100 sec channels. The usual values are recorded in Table 16, the plot of the log of the observed count against time is shown in fig. 5.24 and that of the log corrected count against time in fig. 5.25. From the acetylene desorption figures a $t_{\frac{1}{2}}$ value for acetylene displacement of the β phase was found which was used in the discussion of acetylene displacements. The slow desorption of the α phase at 25°C, which was not found, would not have been noticed and presumably did occur. The acetylene beam was introduced at channel 71.

The percentages were:

α and β phases (total) = 33.2%

retained phase = 66.8%

β $t_{\frac{1}{2}}$ (acetylene displacement, surface temperature 25°C, source temperature 25°C, source pressure 2×10^{-3} torr) = 39.4 min $\pm$ 6 min.

Table 16

Ethylene Displacement

Surface Temperature: 25°C

Source Temperature: 15°C

Source Pressure: 2×10^{-3} torr

Time Channel	Count	Corrected Count	log Corrected Count
1	821	353	2.5478
2	854	386	2.5866
3	889	421	2.6243
4	799	331	2.5198
5	781	313	2.4955
6	830	362	2.5587
7	869	401	2.6031
8	877	409	2.6117
9	811	343	2.5353
10	781	313	2.4955
11	771	303	2.4814
12	817	349	2.5428
13	821	353	2.5478
14	835	367	2.5647
15	761	393	2.5944
16	829	361	2.5575
17	866	398	2.5999
18	886	418	2.6212
19	888	420	2.6232
20	803	335	2.5250
21	926	458	2.6609
22	799	331	2.5198
23	862	394	2.5955

Table 16 (contd.)

Time Channel	Count	Corrected Count	log Corrected Count
24	820	352	2.5465
25	873	405	2.6075
26	888	420	2.6232
27	907	439	2.6425
28	806	338	2.5289
29	796	328	2.5159
30	926	458	2.6609
31	865	397	2.5988
32	827	359	2.5551
33	875	407	2.6096
34	796	328	2.5159
35	845	377	2.5763
36	719	251	2.3997
37	892	424	2.6274
38	845	377	2.5763
39	853	385	2.5855
40	842	374	2.5729
41	797	329	2.5172
42	825	357	2.5527
43	848	380	2.5798
44	813	345	2.5378
45	842	374	2.5729
46	861	393	2.5994
47	863	395	2.5966
48	856	388	2.5888
49	847	379	2.5786
50	824	356	2.5514

Table 16 (contd.)

Time Channel	Count	Corrected Count	log Corrected Count
51	813	345	2.5378
52	793	325	2.5119
53	788	320	2.5051
54	829	361	2.5575
55	813	345	2.5378
56	829	361	2.5575
57	819	351	2.5453
58	808	340	2.5315
59	717	249	2.3962
60	751	283	2.4518
61	748	280	2.4472
62	760	292	2.4654
63	772	304	2.4829
64	773	305	2.4843
65	724	256	2.4082
66	774	306	2.4857
67	820	352	2.5465
68	795	327	2.5145
69	750	282	2.4502
70	844	376	2.5752
71	792	324	2.5105
72	783	315	2.4983
73	787	319	2.5038
74	823	355	2.5502
75	757	289	2.4609
76	756	288	2.4594
77	776	308	2.4886
78	827	359	2.5551

Table 16 (contd.)

Time Channel	Count	Corrected Count	log Corrected Count
79	791	323	2.5092
80	842	374	2.5729
81	793	325	2.5119
82	743	275	2.4393
83	778	310	2.4914
84	796	328	2.5159
85	756	288	2.4594
86	718	250	2.3979
87	688	220	2.3434
88	760	292	2.4654
89	765	297	2.4728
90	732	264	2.4216
91	717	249	2.3962
92	697	229	2.3598
93	615	147	2.1673
94	662	194	2.2878
95	585	117	2.0682
96	588	120	2.0792
97	656	188	2.2742
98	645	177	2.2480
99	660	192	2.2833
100	551	83	1.9191
101	571	103	2.0128
102	618	150	2.1761
103	607	139	2.1430
104	584	216	2.3345
105	599	131	2.1173
106	597	129	2.1106

Table 16 (contd.)

Time Channel	Count	Corrected Count	log Corrected Count
107	598	130	2.1139
108	582	114	2.0569
109	604	136	2.1335
110	572	104	2.0170
111	592	124	2.0934
112	525	57	1.7559
113	573	105	2.0212
114	558	90	1.9542
115	527	59	1.7709
116	534	66	1.8195
117	604	136	2.1335
118	615	147	2.1673
119	527	59	1.7709
120	521	53	1.7243
121	483	15	1.1761
122	434	-34	-
123	488	20	1.3010
124	452	-16	-
125	493	25	1.3979
126	503	35	1.5441
127	521	53	1.7243
128	490	22	1.3424
129	530	62	1.7924
130	512	44	1.6435
131	469	1	.0000
132	486	18	1.2553
133	540	72	1.8573
134	482	14	1.1461

Table 16 (contd.)

Time Channel	Count	Corrected Count	log Corrected Count
135	474	6	.7782
136	496	28	1.4472
137	526	108	2.0344
138	488	20	1.3010
139	533	65	1.8129
140	480	12	1.0792
141	491	23	1.3617
142	540	72	1.8573
143	563	95	1.9777
144	568	100	2.0000
145	508	40	1.6021
146	528	60	1.7782
147	492	24	1.3802
148	504	36	1.5563
149	457	-11	-

Channel width = 100 seconds

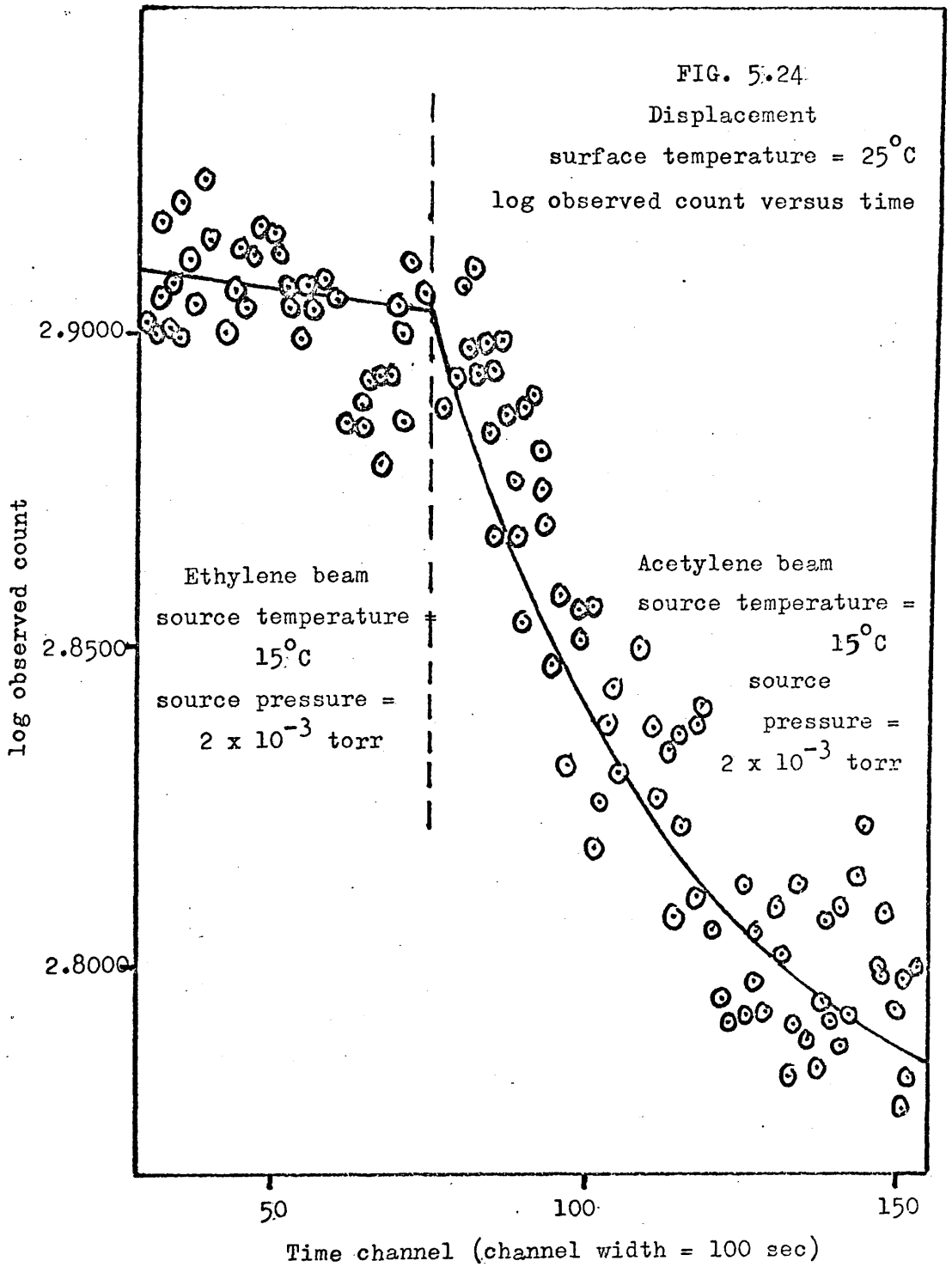
FIG. 5.24
Displacement
surface temperature = 25°C
log observed count versus time
2.9000
2.8500
2.8000
log observed count
Ethylene beam
source temperature = 15°C
source pressure = 2 x 10⁻³ torr
Acetylene beam
source temperature = 15°C
source pressure = 2 x 10⁻³ torr
50
100
150
Time channel (channel width = 100 sec)

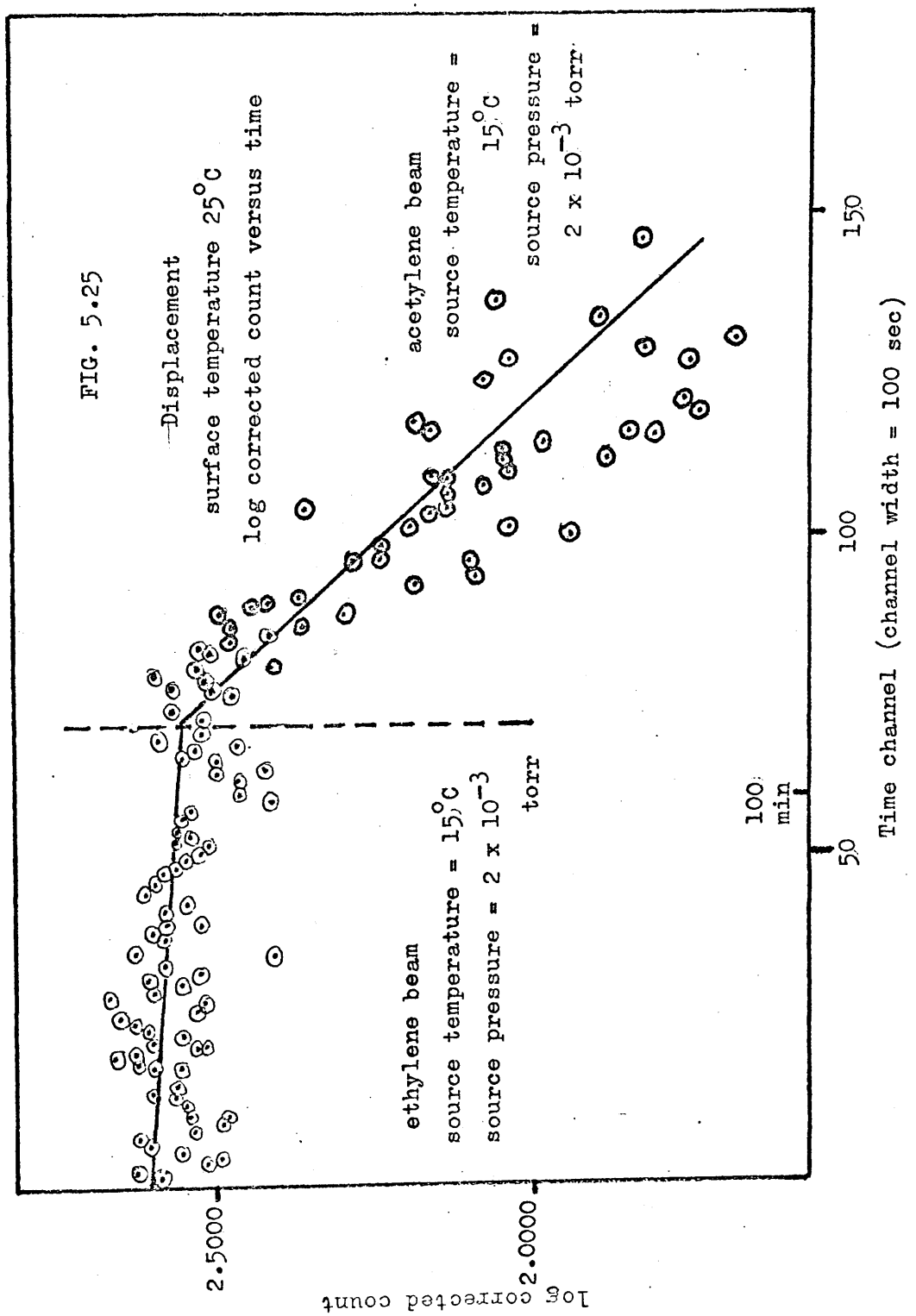
FIG. 5.25
Displacement
surface temperature 25°C
log corrected count versus time
ethylene beam
source temperature = 15°C
source pressure = 2 x 10⁻³ torr
acetylene beam
source temperature = 15°C
source pressure = 2 x 10⁻³ torr
100 min
2.5000
2.0000
log corrected count
50
100
150
Time channel (channel width = 100 sec)

(b) Ethylene Displacement - Surface Temperature 60°C, Source Temperature 15°C, Source Pressure 2 x 10^{-3} torr

Table 17 shows the data produced. Fig. 5.26 shows the plot of log observed count versus time and fig. 5.27 the plot of log corrected count versus time. There was very fast removal of the α phase: on the simultaneous rate-meter recording there appeared to be an immediate accommodation by the rate-meter to a new, lower count rate, corresponding to the instantaneous removal of part of the surface species. No value of the $\alpha t_{\frac{1}{2}}$ can thus be produced. The initially observed surface count rate was 648 cpm.

The values obtained were:

α phase = 28.2%

β phase = 15.7%

retained phase = 56.1%

$\beta t_{\frac{1}{2}}$ (ethylene displacement) = 36.0 min $\pm$ 7 min.

Table 17

Ethylene Displacement

Surface Temperature: 60°C

Source Temperature: 15°C

Source Pressure: 2×10^{-3} torr

Time (min)	Count (cpm)	Corrected Count (cpm)	log Corrected Count
1.50	537	174	2.2405
3.75	493	130	2.1139
6.00	471	108	2.0334
8.25	442	79	1.8976
10.50	453	90	1.9542
12.75	485	122	2.0864
15.00	444	81	1.9085
17.25	450	87	1.9395
19.50	400	37	1.5682
21.75	417	54	1.7324
24.00	429	66	1.8195
26.25	414	51	1.7076
28.50	418	55	1.7404
30.75	403	40	1.6021
33.00	416	53	1.7243
35.75	441	78	1.8921
39.00	422	59	1.7709
42.25	401	38	1.5798
45.75	414	51	1.7076
49.00	366	3	.4771
53.25	386	23	1.3617
58.50	368	5	.6990
63.75	365	2	.3010

Table 17 (contd.)

Time (min)	Count (cpm)	Corrected Count (cpm)	log Corrected Count
69.00	368	5	.6990
74.50	366	3	.4771
82.50	368	5	.6990
93.00	367	4	.6021

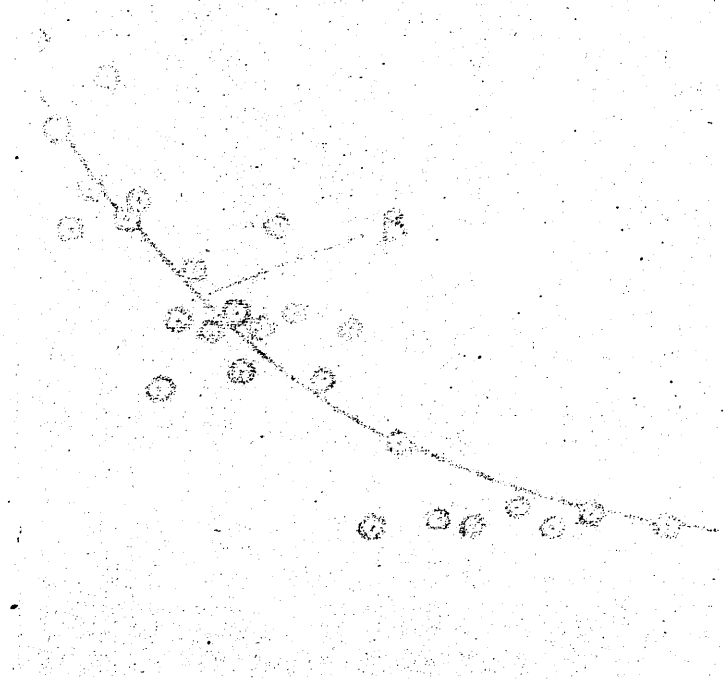

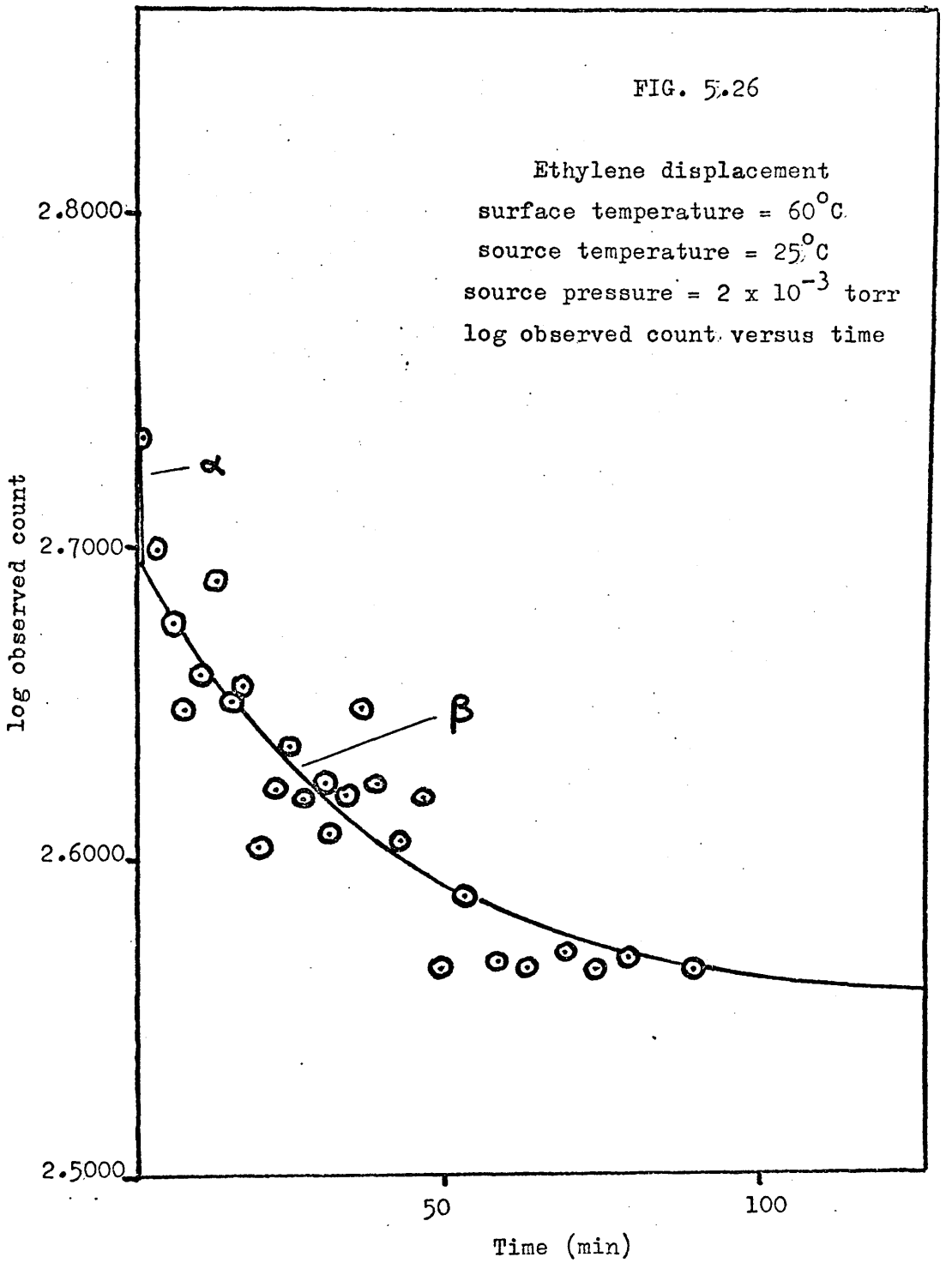

FIG. 5.26

Ethylene displacement
surface temperature = 60°C
source temperature = 25°C
source pressure = 2×10^{-3} torr
log observed count versus time

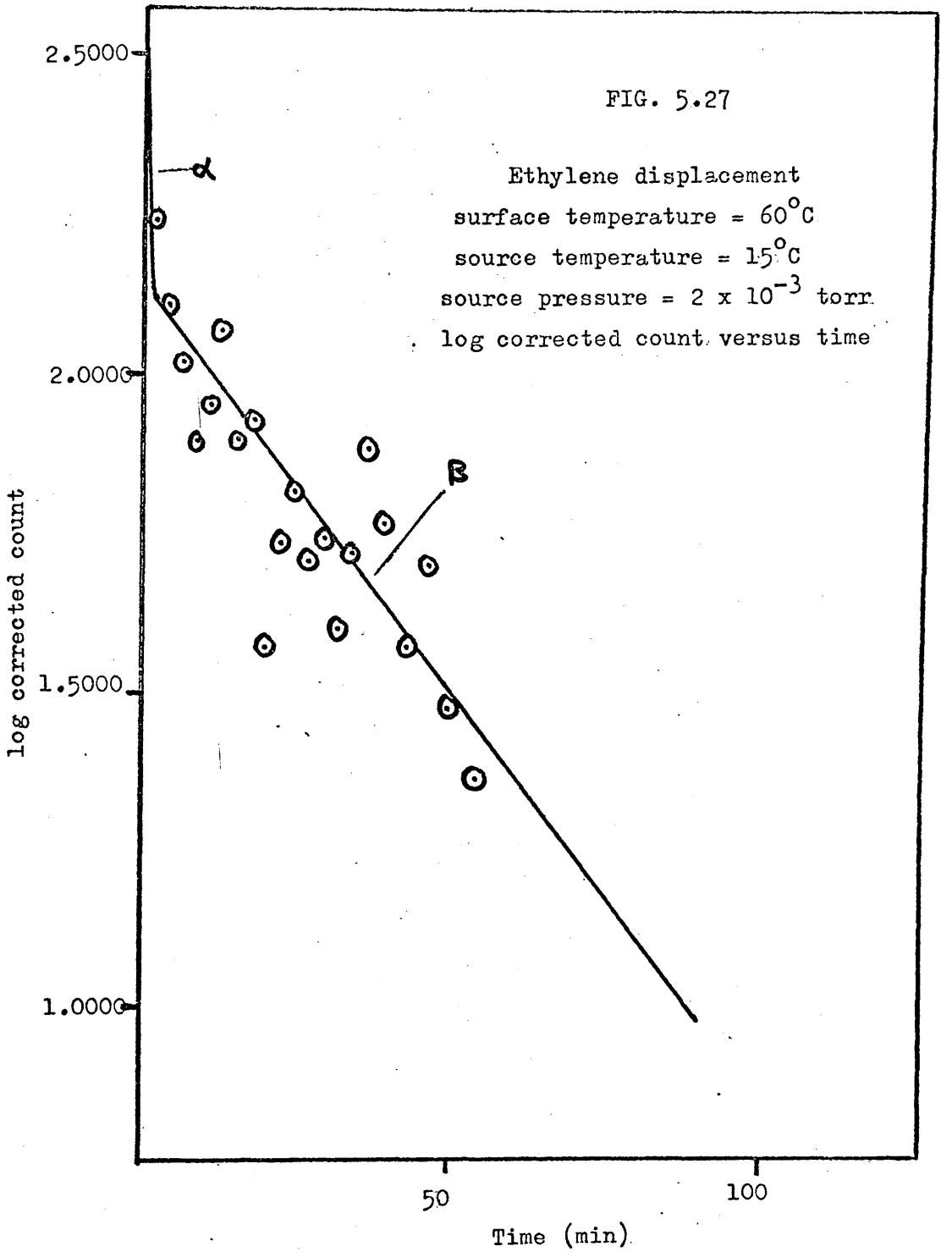

FIG. 5.27

Ethylene displacement
surface temperature = 60°C
source temperature = 15°C
source pressure = 2×10^{-3} torr
log corrected count versus time

(c) Ethylene Displacement - Surface Temperatures $40^{\circ}C$ and $55^{\circ}C$, Source Temperature $15^{\circ}C$, Source Pressure 2×10^{-3} torr

While no displacement by ethylene beams was observed at $25^{\circ}C$, a rapid displacement was seen at $60^{\circ}C$. The present experiments were designed to fill this gap in temperature. Again the Laben multi-scaler was used to record results, each channel being 200 sec wide. Until channel 11 the surface is at $15^{\circ}C$ in vacuo. From channel 12 to channel 84 the surface is at $40^{\circ}C$ with a beam of ethylene running. From channel 85 onwards the surface temperature is $55^{\circ}C$, still with an ethylene beam running. Table 18 shows the data; fig. 5.28 shows the plot of log observed count versus time and fig. 5.29 the plot of log corrected count versus time. Table 19 shows the corrected α phase counts.

The results produced were:

α phase = 15.2%

β phase = 23.3%

retained phase = 61.5%

$\alpha\ t_{\frac{1}{2}}$ ($40^{\circ}C$ ethylene displacement) = 19.1 min $\pm$ 5 min

$\beta\ t_{\frac{1}{2}}$ ($40^{\circ}C$ ethylene displacement) = 562 min $\pm$ 150 min

$\beta\ t_{\frac{1}{2}}$ ($55^{\circ}C$ ethylene displacement) = 86.2 min $\pm$ 15 min.

Table 18

Ethylene Displacement

Surface Temperature: $40^{\circ}C/55^{\circ}C$

Source Temperature: $15^{\circ}C$

Source Pressure: 2×10^{-3} torr

Time Channel	Count	Corrected Count	log Corrected Count
1	1938	758	2.8797
2	1905	725	2.8603
3	1933	753	2.8768
4	1878	698	2.8439
5	1903	723	2.8591
6	1981	801	2.9036
7	1934	754	2.8774
8	1899	719	2.8567
9	1910	730	2.8633
10	1975	795	2.9004
11	1891	711	2.8519
12	1838	658	2.8182
13	1797	617	2.7903
14	1788	608	2.7839
15	1839	659	2.8189
16	1738	558	2.7466
17	1737	557	2.7459
18	1716	536	2.7292
19	1671	491	2.6911
20	1711	531	2.7251
21	1705	525	2.7202
22	1693	513	2.7101
23	1647	467	2.6693

Table 18 (contd.)

Time Channel	Count	Corrected Count	log Corrected Count
24	1593	413	2.6160
25	1594	414	2.6170
26	1672	492	2.6920
27	1675	495	2.6946
28	1591	411	2.6138
29	1633	453	2.6561
30	1697	517	2.7135
31	1600	420	2.6232
32	1635	455	2.6580
33	1551	371	2.5694
34	1645	465	2.6675
35	1617	437	2.6405
36	1606	426	2.6296
37	1544	364	2.5611
38	1599	419	2.6222
39	1582	402	2.6042
40	1576	396	2.5977
41	1558	398	2.5999
42	1502	322	2.5079
43	1561	381	2.5809
44	1441	261	2.4166
45	1542	362	2.5587
46	1531	351	2.5453
47	1596	416	2.6191
48	1553	373	2.5717
49	1526	346	2.5391
50	1580	400	2.6021
51	1603	423	2.6263

Table 18 (contd.)

Time Channel	Count	Corrected Count	log Corrected Count
52	1555	375	2.5740
53	1561	381	2.5809
54	1640	460	2.6628
55	1513	333	2.5224
56	1571	391	2.5922
57	1474	294	2.4683
58	1603	423	2.6263
59	1585	405	2.6075
60	1646	466	2.6684
61	1549	364	2.5611
62	1531	351	2.5453
63	1590	410	2.6128
64	1577	397	2.5988
65	1552	372	2.5705
66	1478	298	2.4742
67	1553	373	2.5717
68	1570	390	2.5911
69	1553	373	2.5717
70	1567	387	2.5877
71	1588	408	2.6107
72	1513	333	2.5224
73	1514	334	2.5237
74	1560	380	2.5798
75	1468	288	2.4594
76	1545	365	2.5623
77	1442	262	2.4183
78	1548	368	2.5658

Table 18 (contd.)

Time Channel	Count	Corrected Count	log Corrected Count
79	1450	270	2.4314
80	1494	314	2.4969
81	1524	344	2.5366
82	1513	333	2.5224
83	1519	339	2.5302
84	1503	323	2.5092
85	1480	300	2.4771
86	1446	266	2.4249
87	1448	268	2.4281
88	1477	297	2.4728
89	1512	332	2.5211
90	1404	224	2.3502
91	1439	259	2.4133
92	1491	311	2.4914
93	1518	338	2.5289
94	1435	255	2.4065
95	1445	265	2.4232
96	1430	250	2.3979
97	1505	325	2.5119
98	1389	204	2.3096
99	1416	236	2.3729
100	1449	269	2.4298
101	1416	236	2.3729
102	1445	265	2.4232
103	1425	245	2.3892
104	1418	238	2.3766
105	1328	148	2.1703

Table 18 (contd.)

Time Channel	Count	Corrected Count	log Corrected Count
106	1380	200	2.3010
107	1421	241	2.3820
108	1444	264	2.4216
109	1274	94	1.9731
110	1361	181	2.2577
111	1350	170	2.2304
112	1321	141	2.1492
113	1321	141	2.1492
114	1310	130	2.1139
115	1296	116	2.0645
116	1338	158	2.1987
117	1359	179	2.2529
118	1296	116	2.0645
119	1277	97	1.9868
120	1348	168	2.2253
121	1255	75	1.8751
122	1284	104	2.0170
123	1279	99	1.9956
124	1307	127	2.1038
125	1288	108	2.0334
126	1211	31	1.4914
127	1259	79	1.8976
128	1302	122	2.0864
129	1314	134	2.1271
130	1346	166	2.2201
131	1275	95	1.9777
132	1340	160	2.1206
133	1223	43	1.6335

Table 18 (contd.)

Time Channel	Count	Corrected Count	log Corrected Count
134	1269	89	1.9494
135	1283	103	2.0128
136	1230	50	1.6990
137	1325	145	2.1614
138	1229	49	1.6902
139	1317	137	2.1367
140	1273	93	1.9685
141	1250	70	1.8451
142	1316	136	2.1335
143	1346	166	2.2201
144	1240	60	1.7782
145	1266	86	1.9345
146	1297	117	2.0682
147	1258	78	1.8921
148	1263	83	1.9191
149	1217	37	1.5682
150	1236	56	1.7482
151	1249	69	1.8388
152	1253	73	1.8633
153	1320	140	2.1461
154	1216	36	1.5563
155	1216	36	1.5563
156	1233	53	1.7243
157	1308	128	2.1072
158	1226	46	1.6628

Channel width = 200 seconds

Table 19

Ethylene Displacement of α Phase

Surface Temperature: $40^{\circ}C$

Source Temperature: $15^{\circ}C$

Source Pressure: 2×10^{-3} torr

Time Channel	Corrected α Phase Count	log Corrected α Phase Count
1	310	2.4914
2	277	2.4425
3	305	2.4843
4	250	2.3979
5	275	2.4393
6	353	2.5478
7	306	2.4857
8	271	2.4330
9	282	2.4502
10	347	2.5403
11	263	2.4200
12	210	2.3222
13	173	2.2380
14	167	2.2227
15	220	2.3424
16	121	2.0828
17	121	2.0828
18	102	2.0086
19	59	1.7709
20	101	2.0043
21	96	1.9823
22	86	1.9345
23	42	1.6232

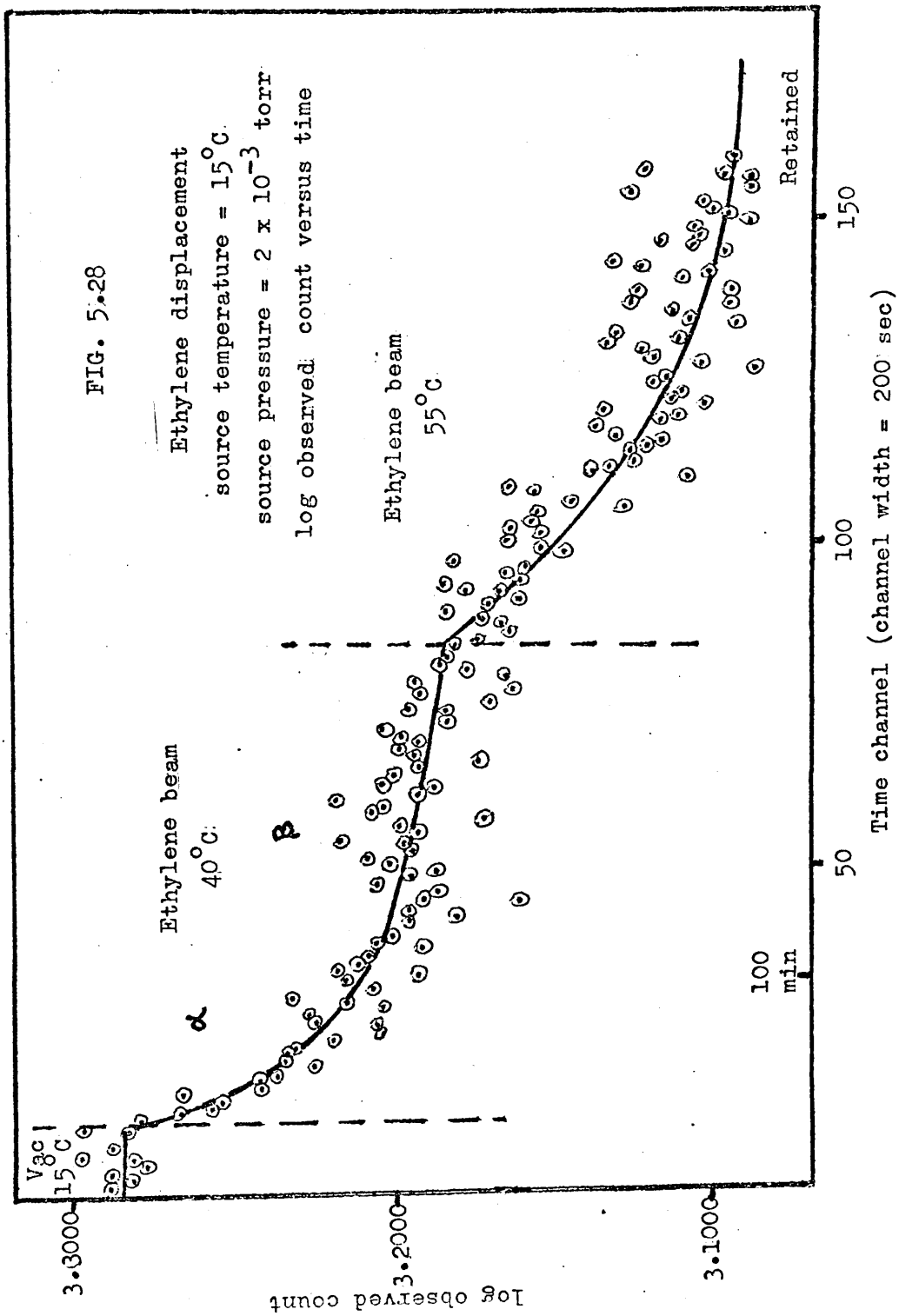
FIG. 5.28
Ethylene displacement
source temperature = 15°C.
source pressure = 2 x 10⁻³ torr
log observed count versus time
Ethylene beam
40°C.
Ethylene beam
55°C
Vac
15°C
α
β
Retained
100
min
3.3000
3.2000
3.1000
log observed count
50
100
150
Time channel (channel width = 200 sec)

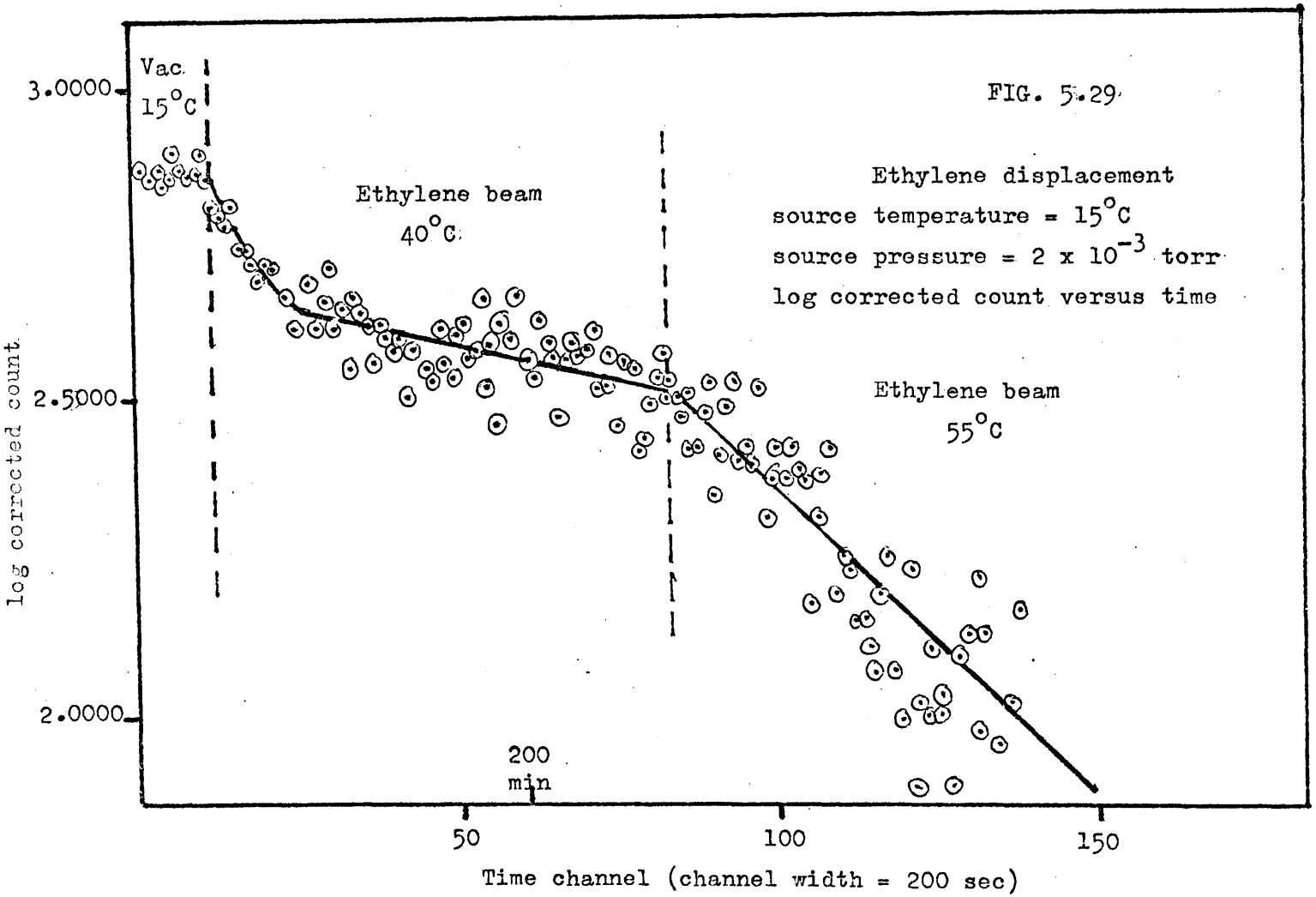

FIG. 5.29

Ethylene displacement
source temperature = 15°C
source pressure = 2×10^{-3} torr
log corrected count versus time

(d) Ethylene Displacement - Surface Temperature 70°C, Source Temperature 15°C, Source Pressure 2 x 10^{-3} torr

Again the Laben multi-scaler was used to record the results with a channel width of 30 sec. Table 20 shows the usual figures, fig. 5.30 the plot of log observed count versus time and fig. 5.31 the plot of log corrected count versus time. Until channel 55 the surface is at 15°C in vacuo. From channel 56 onwards the surface is at 70°C with a beam of ethylene running. The α phase was again removed almost instantaneously by the ethylene beam.

The figures resulting were:

α phase = 21.8%

β phase = 53.3%

retained phase = 24.9%

$\beta t_{\frac{1}{2}}$ (ethylene displacement) = 82.5 min $\pm$ 15 min.

The evaporation of the palladium filament was again carried out faster than usual - using an evaporation current of 7.1 amp.

The $\beta t_{\frac{1}{2}}$ figure can be compared with that produced ($\beta t_{\frac{1}{2}}$ = 26.5 min) by the admission of an ethylene beam to the β phase after partial vacuum desorption, as already described.

Table 20

Ethylene Displacement

Surface Temperature: 70°C

Source Temperature: 15°C

Source Pressure: 2×10^{-3} torr

Time Channel	Count	Corrected Count	log Corrected Count
1	3376	2525	3.4023
2	3411	2560	3.4082
3	3431	2580	3.4116
4	3286	2485	3.3954
5	3150	2299	3.3615
6	3348	2497	3.3974
7	3324	2473	3.3932
8	3193	2342	3.3696
9	3217	2366	3.3740
10	3257	2406	3.3813
11	3152	2301	3.3619
12	3109	2258	3.3537
13	3004	2153	3.3330
14	3136	2285	3.3589
15	3089	2238	3.3498
16	3075	2224	3.3472
17	3139	2288	3.3594
18	3050	2199	3.3422
19	2959	2108	3.3238
20	2999	2148	3.3320
21	3000	2149	3.3322
22	2951	2100	3.3222
23	3032	2181	3.3387

Table 20 (contd.)

Time Channel	Count	Corrected Count	log Corrected Count
24	2890	2039	3.3094
25	2987	2136	3.3296
26	3064	2213	3.3450
27	2985	2134	3.3292
28	2884	2033	3.3081
29	2919	2068	3.3155
30	2916	2065	3.3150
31	2952	2101	3.3224
32	2945	2094	3.3209
33	2850	1999	3.3008
34	2790	1939	3.2876
35	2819	1968	3.2940
36	2926	2075	3.3171
37	2912	2061	3.3141
38	2852	2001	3.3012
39	2920	2069	3.3158
40	2815	1964	3.2931
41	2867	2016	3.3045
42	2923	2072	3.3164
43	2874	2023	3.3060
44	2877	2026	3.3067
45	2903	2052	3.3122
46	2902	2051	3.3120
47	2975	2124	3.3271
48	2826	1975	3.2956
49	2868	2017	3.3047
50	2854	2003	3.3016
51	2926	2075	3.3171

Table 20 (contd.)

Time Channel	Count	Corrected Count	log Corrected Count
52	2779	1928	3.2851
53	2779	1928	3.2851
54	2812	1961	3.2925
55	2838	1987	3.2982
56	2727	1876	3.2732
57	2571	1720	3.2355
58	2566	1715	3.2343
59	2605	1754	3.2440
60	2550	1699	3.2302
61	2626	1775	3.2492
62	2565	1714	3.2340
63	2570	1719	3.2353
64	2600	1749	3.2428
65	2562	1711	3.2333
66	2490	1639	3.2146
67	2603	1752	3.2435
68	2601	1750	3.2430
69	2490	1639	3.2146
70	2540	1689	3.2276
71	2673	1822	3.2606
72	2478	1627	3.2114
73	2607	1756	3.2445
74	2516	1665	3.2214
75	2414	1563	3.1939
76	2578	1727	3.2373
77	2440	1589	3.2012
78	2501	1650	3.2175

Table 20 (contd.)

Time Channel	Count	Corrected Count	log Corrected Count
79	2388	1537	3.1867
80	2414	1563	3.1939
81	2505	1654	3.2185
82	2379	1528	3.1841
83	2411	1560	3.1931
84	2462	1611	3.2071
85	2439	1588	3.2009
86	2480	1629	3.2119
87	2422	1571	3.1962
88	2446	1595	3.2028
89	2322	1471	3.1676
90	2281	1430	3.1553
91	2362	1511	3.1793
92	2389	1538	3.1870
93	2385	1534	3.1858
94	2354	1503	3.1770
95	2443	1592	3.2020
96	2408	1557	3.1922
97	2350	1499	3.1758
98	2427	1576	3.1976
99	2350	1469	3.1670
100	2321	1470	3.1673
101	2262	1411	3.1495
102	2234	1383	3.1409
103	2381	1530	3.1847
104	2339	1488	3.1726
105	2243	1392	3.1437

Table 20 (contd.)

Time Channel	Count	Corrected Count	log Corrected Count
106	2338	1487	3.1723
107	2207	1356	3.1322
108	2221	1370	3.1367
109	2363	1512	3.1796
110	2338	1487	3.1723
111	2338	1487	3.1723
112	2279	1428	3.1548
113	2191	1340	3.1271
114	2199	1348	3.1297
115	2243	1392	3.1437
116	2420	1569	3.1956
117	2325	1474	3.1685
118	2252	1401	3.1464
119	2318	1467	3.1664
120	2214	1363	3.1345
121	2318	1457	3.1634
122	2191	1340	3.1271
123	2278	1427	3.1545
124	2273	1422	3.1529
125	2198	1347	3.1294
126	2188	1337	3.1262
127	2204	1353	3.1313
128	2155	1304	3.1152
129	2228	1377	3.1389
130	2232	1381	3.1402
131	2241	1390	3.1430
132	2157	1306	3.1158

Table 20 (contd.)

Time Channel	Count	Corrected Count	log Corrected Count
133	2183	1332	3.1245
134	2085	1234	3.0913
135	2159	1308	3.1165
136	2158	1307	3.1162
137	2129	1278	3.1065
138	2136	1285	3.1089
139	2107	1256	3.0989
140	2012	1161	3.0649
141	2252	1401	3.1464
142	2138	1287	3.1096
143	2172	1321	3.1209
144	2058	1207	3.0817
145	2086	1235	3.0917
146	2106	1255	3.0986
147	2093	1242	3.0941
148	2124	1273	3.1048
149	2039	1188	3.0748
150	2137	1286	3.1092
151	2024	1173	3.0693
152	2135	1284	3.1086
153	2240	1389	3.1428
154	2285	1434	3.1565
155	2151	1300	3.1139
156	2140	1289	3.1103
157	2128	1277	3.1062
158	2168	1317	3.1196
159	2101	1250	3.0969
160	2238	1387	3.1421

Table 20 (contd.)

Time Channel	Count	Corrected Count	log Corrected Count
161	2123	1272	3.1045
162	2076	1225	3.0882
163	2099	1248	3.0962
164	2158	1307	3.1162
165	2194	1343	3.1281
166	2016	1165	3.0663
167	2091	1240	3.0934
168	2161	1310	3.1173
169	2164	1313	3.1183
170	2105	1254	3.0983
171	2081	1230	3.0899
172	1970	1119	3.0488
173	2120	1269	3.1035
174	2035	1184	3.0734
175	1987	1136	3.0554
176	2008	1157	3.0633
177	1992	1141	3.0573
178	2050	1199	3.0788
179	1891	1040	3.0170
180	1819	968	2.9859
181	1818	967	2.9854
182	1944	1093	3.0386
183	1960	1109	3.0449
184	1941	1090	3.0374
185	1911	1060	3.0253
186	1865	1014	3.0060
187	1898	1047	3.0200

Table 20 (contd.)

Time Channel	Count	Corrected Count	log Corrected Count
188	1945	1094	3.0390
189	1946	1095	3.0394
190	1995	1144	3.0585
191	1947	1096	3.0398
192	1934	1083	3.0346
193	1826	975	2.9890
194	2026	1175	3.0700
195	1901	1050	3.0212
196	1931	1080	3.0334
197	1923	1072	3.0302
198	1850	999	2.9996
199	1858	1007	3.0030
200	1806	955	2.9800
201	1811	960	2.9823
202	1770	919	2.9633
203	1881	1030	3.0128
204	1885	1034	3.0145
205	1821	970	2.9868
206	1904	1053	3.0224
207	1845	994	2.9974
208	1910	1059	3.0248
209	1845	994	2.9974
210	1812	961	2.9827
211	1863	1012	3.0052
212	1798	947	2.9763
213	1859	1008	3.0034
214	1885	984	2.9930

Table 20 (contd.)

Time Channel	Count	Corrected Count	log Corrected Count
215	1859	1008	3.0034
216	1805	954	2.9795
217	1790	939	2.9727
218	1813	962	2.9832
219	1903	1052	3.0220
220	1804	953	2.9791
221	1732	881	2.9450
222	1842	991	2.9961
223	1878	1027	3.0116
224	1771	920	2.9638
225	1701	850	2.9294
226	1789	938	2.9722
227	1721	870	2.9395
228	1796	945	2.9754
229	1745	894	2.9513
230	1664	813	2.9101
231	1678	827	2.9175
232	1755	904	2.9562
233	1762	911	2.9595
234	1675	824	2.9159
235	1619	768	2.8854
236	1574	723	2.8591
237	1675	824	2.9159
238	1560	709	2.8506
239	1542	691	2.8395
240	1592	741	2.8698
241	1642	791	2.8982

Table 20 (contd.)

Time Channel	Count	Corrected Count	log Corrected Count
242	1584	733	2.8651
243	1597	746	2.8727
244	1593	742	2.8704
245	1521	670	2.8261
246	1572	721	2.8579
247	1631	780	2.8921
248	1571	720	2.8573
249	1613	762	2.8820
250	1701	850	2.9294
251	1728	877	2.9430
252	1636	785	2.8949
253	1632	781	2.8927
254	1619	768	2.8854
255	1684	833	2.9206
256	1637	786	2.8954
257	1604	753	2.8768
258	1560	709	2.8506
259	1636	785	2.8949
260	1577	726	2.8609
261	1555	704	2.8476
262	1628	777	2.8904
263	1549	698	2.8439
264	1527	676	2.8299
265	1608	757	2.8791
266	1541	690	2.8388
267	1512	661	2.8202
268	1637	786	2.8954

Table 20 (contd.)

Time Channel	Count	Corrected Count	log Corrected Count
269	1554	703	2.8470
270	1579	728	2.8621
271	1686	835	2.9217
272	1617	766	2.8842
273	1590	739	2.8686
274	1553	702	2.8463
275	1631	780	2.8921
276	1523	672	2.8274
277	1489	638	2.8048
278	1592	741	2.8698
279	1578	727	2.8615
280	1623	772	2.8876
281	1570	719	2.8567
282	1508	657	2.8176
283	1540	689	2.8382
284	1504	653	2.8149
285	1510	659	2.8189
286	1565	714	2.8537
287	1484	633	2.8014
288	1397	546	2.7372
289	1404	553	2.7427
290	1501	650	2.8129
291	1480	629	2.7987
292	1475	624	2.7952
293	1396	545	2.7364
294	1425	574	2.7589
295	1430	579	2.7627

Table 20 (contd.)

Time Channel	Count	Corrected Count	log Corrected Count
296	1365	514	2.7110
297	1413	562	2.7497
298	1450	599	2.7774
299	1431	580	2.7634
300	1436	585	2.7672
301	1458	607	2.7832
302	1390	539	2.7316
303	1468	617	2.7903
304	1436	585	2.7672
305	1446	595	2.7745
306	1466	615	2.7889
307	1408	557	2.7459
308	1385	534	2.7275
309	1450	599	2.7774
310	1423	572	2.7574
311	1367	516	2.7126
312	1374	523	2.7185
313	1449	598	2.7767
314	1415	564	2.7513
315	1304	453	2.6561
316	1378	527	2.7218
317	1575	724	2.8597
318	1477	626	2.7966
319	1570	719	2.8567
320	1348	497	2.6964
321	1313	462	2.6646
322	1248	397	2.5988

Table 20 (contd.)

Time Channel	Count	Corrected Count	log Corrected Count
323	1338	487	2.6875
324	1417	566	2.7528
325	1297	446	2.6493
326	1255	404	2.6064
327	1225	374	2.5729
328	1372	521	2.7168
329	1395	544	2.7356
330	1322	476	2.6776
331	1342	491	2.6911
332	1248	397	2.5988
333	1210	359	2.5551
334	1268	417	2.6201
335	1373	522	2.7177
336	1292	441	2.6444
337	1362	511	2.7084
338	1335	484	2.6848
339	1213	362	2.5587
340	1303	452	2.6551
341	1235	384	2.5843
342	1216	365	2.5623
343	1318	467	2.6693
344	1246	395	2.5966
345	1267	416	2.6191
346	1212	351	2.5453
347	1230	379	2.5786
348	1246	395	2.5966
349	1378	527	2.7218
350	1245	394	2.5955

Table 20 (contd.)

Time Channel	Count	Corrected Count	log Corrected Count
351	1258	407	2.6096
352	1213	362	2.5587
353	1188	337	2.5276
354	1209	358	2.5539
355	1176	325	2.5119
356	1175	324	2.5105
357	1222	371	2.5694
358	1217	366	2.5635
359	1201	350	2.5441
360	1218	367	2.5647
361	1190	339	2.5302
362	1284	433	2.6365
363	1229	378	2.5775
364	1318	467	2.6693
365	1214	363	2.5599
366	1272	421	2.6243
367	1317	456	2.6590
368	1355	504	2.7024
369	1388	537	2.7300
370	1320	469	2.6712
371	1285	434	2.6375
372	1314	463	2.6656
373	1216	365	2.5623
374	1247	396	2.5977
375	1299	448	2.6513
376	1329	478	2.6794
377	1314	463	2.6656

Table 20 (contd.)

Time Channel	Count	Corrected Count	log Corrected Count
378	1234	383	2.5832
379	1271	420	2.6232
380	1293	442	2.6454
381	1118	267	2.4265
382	1125	274	2.4378
383	1081	230	2.3617
384	1150	299	2.4757
385	1181	330	2.5185
386	1190	339	2.5302
387	1174	323	2.5092
388	1181	330	2.5185
389	1176	325	2.5119
390	1142	291	2.4639
391	1102	251	2.3997
392	1112	261	2.4166
393	1128	277	2.4425
394	1104	253	2.4031
395	1130	279	2.4456
396	1110	259	2.4133
397	1114	263	2.4200
398	1048	197	2.2945
399	1102	251	2.3997
400	1074	223	2.3483
431	994	143	2.1553
432	969	118	2.0719
433	963	112	2.0492
434	1032	181	2.2577
435	1072	221	2.3444

Table 20 (contd.)

Time Channel	Count	Corrected Count	log Corrected Count
436	1108	257	2.4099
437	1212	361	2.5575
438	1146	295	2.4698
439	1167	316	2.4997
440	1082	231	2.3636
441	1138	287	2.4579
442	1053	182	2.2601
443	1087	236	2.3729
444	971	120	2.0792
445	1005	154	2.1875
446	1067	216	2.3345
447	1051	206	2.3139
448	1157	306	2.4857
449	1156	305	2.4843
450	1049	198	2.2967
451	1050	199	2.2989
452	1036	185	2.2672
453	1011	160	2.2041
454	1088	237	2.3747
455	980	129	2.1106
456	1080	229	2.3598
457	1088	237	2.3747
458	1127	276	2.4409
459	1100	249	2.3962
460	1012	161	2.2068
461	1049	198	2.2967
462	1000	149	2.1732

Table 20 (contd.)

Time Channel	Count	Corrected Count	log Corrected Count
463	932	81	1.9085
464	943	92	1.9638
465	1079	228	2.3579
466	1035	184	2.2648
467	1070	219	2.3404
468	1080	229	2,3598
469	1054	203	2.3075
470	1013	162	2.2095
471	1048	197	2.2945
472	998	147	2.1673
473	1023	172	2.2355
474	1008	157	2.1959
475	1031	180	2.2553
476	1050	199	2.2989
477	1024	173	2.2380
478	918	67	1.8261
479	1167	316	2.4997
480	980	129	2.1106
481	966	115	2.0607
482	1055	204	2.3096
483	1056	205	2.3118
484	985	134	2.1271
485	1081	230	2.3617
486	1027	176	2.2455
487	1103	252	2.4014
488	1067	216	2.3345
489	1122	271	2.4330

Table 20 (contd.)

Time Channel	Count	Corrected Count	log Corrected Count
490	1116	265	2.4232
491	992	191	2.2810
492	1025	174	2.2405
493	1049	198	2.2967
494	1008	157	2.1959
495	1009	158	2.1987
496	895	44	1.6435
497	1105	254	2.4048
498	912	61	1.7853
499	975	124	2.0934
500	995	144	2.1584
501	947	96	1.9823
502	1034	183	2.2625
503	925	74	1.8692
504	984	133	2.1239
505	994	143	2.1553
506	972	121	2.0828
507	1020	169	2.2279
508	1064	213	2.3284
509	939	88	1.9445
510	1025	174	2.2405
511	849	-2	-
512	911	60	1.7782
513	874	23	1.3617
514	857	6	.7782
515	819	-32	-
516	941	90	1.9542

Table 20 (contd.)

Time Channel	Count	Corrected Count	log Corrected Count
517	906	85	1.9294
518	974	123	2.0899
519	857	6	.7782
520	952	101	2.0043
521	987	136	2.1335
522	966	115	2.0607
523	945	94	1.9731
524	998	147	2.1673
525	999	148	2.1703
526	878	27	1.4314
527	891	40	1.6021
528	958	107	2.0294
529	941	90	1.9542
530	942	91	1.9590
531	942	91	1.9590
532	870	19	1.2788
533	904	53	1.7243
534	909	58	1.7634
535	899	48	1.6812
536	911	60	1.7782
537	929	78	1.8921
538	919	68	1.8325
539	858	7	.8451
540	926	75	1.8751
541	782	-69	-
542	963	112	2.0492
543	925	74	1.8692

Table 20 (contd.)

Time Channel	Count	Corrected Count	log Corrected Count
544	909	58	1.7634
545	917	66	1.8195
546	894	40	1.6021
547	852	1	.0000
548	953	102	2.0086
549	905	54	1.7324
550	851	-	-
551	902	51	1.7076
552	834	-17	-
553	881	30	1.4771
554	904	53	1.7243
555	819	-32	-
556	930	79	1.8976
557	812	-39	-
558	892	41	1.6128
559	891	40	1.6021
560	822	-29	-
561	924	73	1.8633
562	940	89	1.9494
563	936	85	1.9294
564	990	179	2.2529
565	896	45	1.6532
566	960	109	2.0374
567	995	144	2.1584
568	922	71	1.8513
569	938	87	1.9395
570	835	-16	-

Table 20 (contd.)

Time Channel	Count	Corrected Count	log Corrected Count
571	917	66	1.8195
572	974	123	2.0899
573	960	109	2.0374
574	884	33	1.5185
575	1020	169	2.2279
576	936	85	1.9294
577	912	61	1.7853
578	922	71	1.8513
579	848	-3	-
580	884	33	1.5185
581	970	119	2.0755
582	897	46	1.6628
583	947	96	1.9823
584	1020	169	2.2279
585	886	35	1.5441
586	935	84	1.9243
587	853	2	.3010
588	885	34	1.5315
589	915	64	1.8062
590	846	-5	-
591	1001	150	2.1761
592	912	61	1.7853
593	914	63	1.7993
594	905	54	1.7324
595	831	-20	-
596	1034	183	2.2625
597	907	56	1.7482
598	893	42	1.6232

Table 20 (contd.)

Time Channel	Count	Corrected Count	log Corrected Count
599	1037	186	2.2695
600	929	78	1.8921
601	955	104	2.0170
602	949	98	1.9912
603	849	-2	-
604	889	38	1.5798
605	915	64	1.8062
606	832	-19	-
607	961	110	2.0414
608	892	41	1.6128
609	911	60	1.7782
610	985	134	2.1271
611	879	28	1.4472
612	997	146	2.1644
613	937	86	1.9345
614	871	20	1.3010
615	928	77	1.8865
616	872	21	1.3222
617	806	-45	-
618	898	47	1.6721

Channel width = 30 seconds

FIG. 5.30

Ethylene displacement
surface temperature = 70°C
source temperature = 15°C
source pressure = 2×10^{-3} torr
log observed count versus time

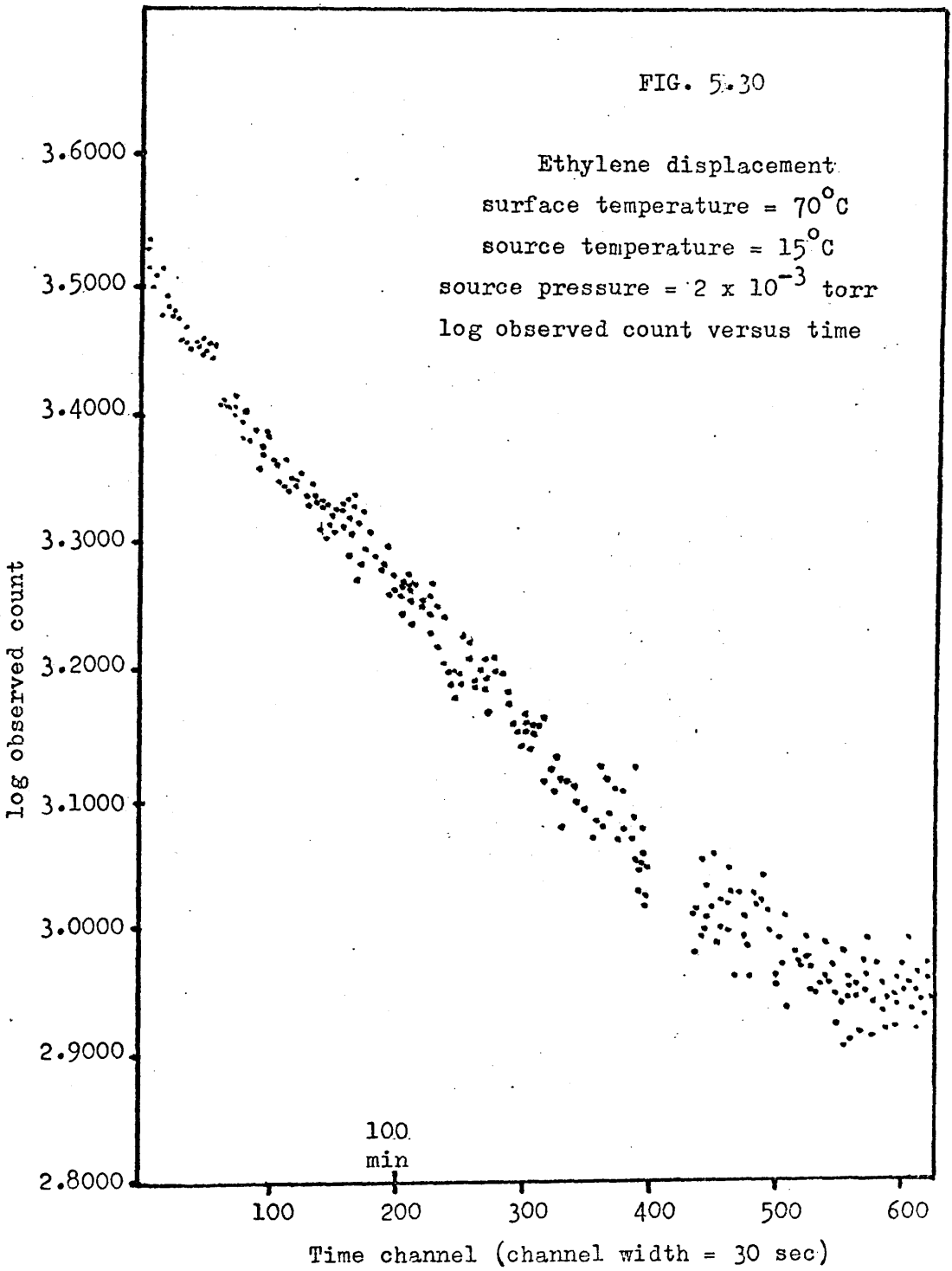

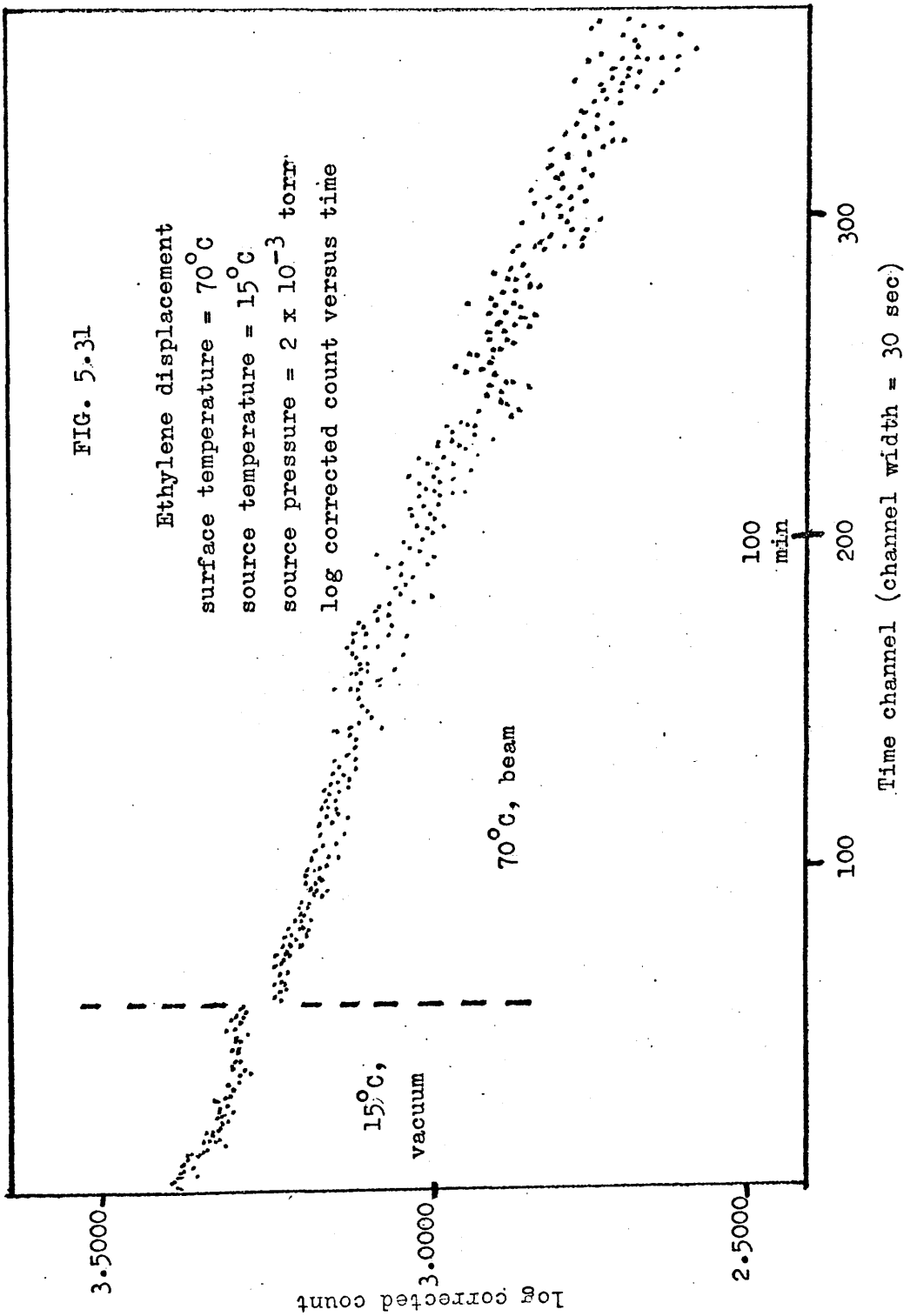
FIG. 5.31
Ethylene displacement
surface temperature = 70°C
source temperature = 15°C
source pressure = 2 x 10⁻³ torr
log corrected count versus time
15°C, vacuum
70°C, beam
100 min
3.5000
3.0000
2.5000
log corrected count
100
200
300
Time channel (channel width = 30 sec)

(e) Conclusions to the Ethylene Displacement Experiments

These experiments, at first sight, are contradictory. At 25°C, while the β phase is still on the surface - as shown by its subsequent displacement by acetylene - no displacement occurs. At 60°C displacement of the α phase occurs almost instantaneously and of the β phase quickly ($\beta t_{\frac{1}{2}}$ = 36.0 min). At the intermediate temperature of 40°C no displacement of the α or β phase apparently occurs, the respective $t_{\frac{1}{2}}$ values of 19.1 min and 562 min being equal to or greater than those which could be expected from vacuum desorption alone. The $\beta t_{\frac{1}{2}}$ value for 55°C is 86.2 min - about that expected for vacuum desorption alone, ($\beta t_{\frac{1}{2}}$ vacuum desorption at 60°C = 101 min), within experimental error. If the introduction of the beam, in the experiments at surface temperature of 70°C, is delayed until most of the α and β surface material has desorbed, rapid displacement of the remaining β phase occurs ($\beta t_{\frac{1}{2}}$ = 26.5 min). If, however, the beam is introduced after only a little material has desorbed, the $\beta t_{\frac{1}{2}}$ obtained is 82.5 min, which is greater than the $\beta t_{\frac{1}{2}}$ for vacuum desorption (57 min) at this temperature.

If we then re-examine the displacement at 60°C, we find that the total amount of α and β phase corresponded to 285 cpm and that an amount corresponding to 111 cpm was allowed to desorb before the beam was introduced to the surface. In the experiment at 40°C and 55°C, the amount allowed to desorb corresponded to about 38 cpm whilst the total amount of α and β phase corresponded to 758 cpm. At 25°C surface temperature, where no displacement was observed, the ethylene beam was introduced before any desorption could occur at all.

We thus obtain a view of the ethylene displacement reactions that, if the beam is allowed to impinge on the surface before little, if any, vacuum desorption takes place, the loss of C-14

from the surface proceeds at the same rate, or slower, than in normal vacuum desorptions. If, on the other hand, a large amount of the total α and β phase desorption has taken place, rapid displacement of the remaining β phase is witnessed.

(5) Miscellaneous Runs

Into this category fall a number of experiments in which a very small proportion of displaced or desorbed material was recorded and which were not used to provide kinetic evidence. These experiments fall into two categories:

1. where a given sample of ethylene C-14 had been used for several previous adsorptions to form a monolayer;
2. where vacuum conditions were poor, e.g. where the film was unavoidably left for several minutes or more before admission of ethylene C-14 to form a monolayer.

In the first case it was suspected that, although the pressure of ethylene was apparently high enough to give monolayer coverage, this recorded pressure also included a substantial quantity of ethane which could not be separated from ethylene. Mass spectrometric analysis of the residual gas taken back from the target chamber after formation of a monolayer had been attempted revealed the presence of 2 - 5% of C_4 material and about 10% or greater of ethane. The figures are obscure due to the presence of C-14 and C-12 isotopes. The instrument used, an A.E.I. M.S.10.C.1. could not distinguish, for example, between $^{12}CH_2 \equiv ^{14}CH_2$ and $^{12}CH_3 - ^{12}CH_3$. What could be detected with certainty was $^{14}CH_3 - ^{14}CH_3$.

The second category includes, in addition to the already described experiment, two runs in which the pressure during evaporation of palladium rose to between 1 and 3 x 10^{-5} torr due to streaking of the gas inlet greased tap. Again a very high percentage of retained material was observed (95%).

In addition to runs in these two categories, there was one run, for which no detailed figures were recorded, in which, inadvertently, the valve to the target chamber pump stack was

left open when ethylene C-14 was admitted to form the monolayer. A surface count was, however, obtained in spite of the pressure of ethylene being probably about 10^{-2} torr for only a few seconds. This surface material was not removed by an acetylene beam at a surface temperature of 25°C, but 90% of it was removed by subsequent vacuum desorption at a surface temperature of 60°C - as shown by a ratemeter recording trace.

Again, into the general category of miscellaneous experiments fall two attempts to adsorb a beam firstly of ethylene C-14 on to a bare palladium surface at 60°C and secondly a beam of acetylene C-14 on to a palladium film covered with the unlabelled products of ethylene self-hydrogenation. In the first case the expected monolayer count rate was about 1000 cpm. The count rate rose from an initial background count of 100 cpm to about 180 cpm, corresponding to less than 10% of monolayer coverage, and dropped back to 100 cpm over a period of 2 hours. No weight is placed on the result, except that, obviously, little of the beam material adsorbed on to the bare palladium film.

In the second case the results were disappointing. The activity of the acetylene C-14 used was low compared with that of the ethylene C-14 used (10 mC/mM versus 50 mC/mM). The experiment was carried out against a falling background and only a hump, corresponding to a possible surface count rate of about 20 cpm is seen in a graph of count rate versus time. Again no weight can be placed on the result.

Estimates of the film weight were made on a number of occasions. The weight loss of the filament used was found and, knowing the area of the film spot produced and its distance from the filament, the solid angle occupied by the film was calculated. The film weights found were between 0.1 mg and 0.2 mg.

(6) Over-all Conclusion to the Results

In both the displacement and the desorption experiments carried out, we have observed that the surface species resulting from the interaction of ethylene with a palladium film is heterogeneous in nature. Part is reactive - as demonstrated by the displacement reactions observed - and part - the retained phase - is inactive. Furthermore, the active fraction of the surface species is itself heterogeneous in nature - two active phases being clearly discernible. Each of the two active phases displays first order kinetics with respect to the surface concentration of that phase in all cases where the order of reaction can be discerned.

The relative amounts of retained and active phases appears to be affected by the contamination of the film before adsorption of ethylene on to the film is brought about. In the three cases where a rapid evaporation of the film has been carried out the relative percentages of the three phases were:

α	40.8	52.7	21.8
β	40.7	10.3	53.5
retained	18.5	37.0	24.9

Here, since the film was formed rapidly, there was relatively less chance of contamination by vacuum residual gases. The bulk of our experiments, where "normal" evaporation of the palladium was carried out resulted in the following distribution of phases:

α	11.5	7.5	6.4	18.0	9.8	15.2	11.0	28.2	15.2	
β	17.2	22.0	25.5	25.5	33.4	23.2	22.0	15.7	23.3	33.2
retained	71.3	70.5	68.1	56.5	56.8	61.6	67.0	56.1	61.5	66.8

The average value of the retained phase in these ten experiments was 63.6%. This resulted when evaporation was slower than in the

first set described. The surface was thus exposed to a residual gas pressure of up to 3×10^{-7} torr for a longer period. The probability of gas contamination in these circumstances would have been greater than in those which displayed low retentions. In the few cases where serious contamination of the film is thought to have occurred in poor vacuum conditions the percentage of the retained phase is between 95% and 100%.

A picture can be drawn of progressively better vacuum conditions producing progressively less retained species. This is best explained by assuming that a high percentage of retained phase is caused by absence of the active phases - which would have adsorbed on sites occupied by adsorption of residual gases in the system. This preferential poisoning of sites on which α and β phase adsorption can occur suggests that these sites causing active and inactive adsorption are fundamentally different. This difference may result from the different crystal faces displayed by the palladium or it may be the result of localised defects in the surface.

The corollary to the above is that the cases to be considered when we discuss the results are primarily those in which low retention of the surface species is evidenced, these cases representing more accurately the basic nature of the surface interaction with ethylene.

Chapter 6
Discussion

(1) Introduction

It was the stated intention at the outset of this work to design and build an apparatus with which the molecular beam method could be employed to study systems of interest in the catalytic field and to demonstrate its potential as a method of investigating surface/gas systems. It is therefore relevant, before discussing the results, to examine the final characteristics of the molecular beam apparatus.

In the apparatus for permanent gas molecular beam studies, a surface can be exposed to a beam flux of up to 3.7×10^{13} molecules/cm^2/sec, if the surface is at right angles to the beam, with a background flux of scattered beam material of 4.1×10^{13} molecules/cm^2/sec. It can produce beams of any gas or vapour except those which will corrode the source, such as mercury. The source temperature may be varied at will between 15°C and 350°C. The vacuum achieved in the target chamber is about 5×10^{-9} torr, which enables relatively clean films to be prepared for study and the target temperature may be varied between 15°C and 90°C with the present water-bath used. With slight modification the range of target temperatures could be extended to 200°C or greater.

Two detection systems capable of observing low energy radioactive particles arising from the target inside the beam system have been studied. One, the scintillation unit originally used, was found lacking in both its vacuum properties and its counting characteristics. The second, the solid-state detector system, was found to be excellent in its vacuum properties and sufficiently

stable and efficient in its counting characteristics to follow the behaviour of as little as 1 x 10^{15} molecules in detail.

The use of indium-sealed QVF units as building units has enabled us to build a system which is both robust and flexible. The solid-state counter and the greased joints in our target chamber have prevented the attainment of pressures below 5 x 10^{-9} torr by baking the target area. Nevertheless by careful selection of components and by providing high speed pumping to both chambers this value of 5 x 10^{-9} torr, usually incompatible with unbaked systems containing greased joints, is obtained rapidly and reproducibly.

We had thus constructed an apparatus capable of investigating the type of system which we wished to investigate - which was in particular the displacement of the surface species produced by the interaction of ethylene with palladium films. We have carried out the following studies of the system:

(1) the desorption of the surface species as a precursor to the molecular beam studies we wished to perform. No previous studies of the desorption of this surface species have appeared in the literature;

(2) a dynamic study of the removal of the surface species by displacement with beams of acetylene and ethylene. Displacement is observed in spite of the low beam fluxes used and would in conventional systems with higher pressures of gas have been too rapid to follow. The use of the beam technique, which provides a constant gas flux on the target, has simplified the understanding of the results and enabled us to vary separately target and beam temperature in the case of the acetylene displacements. It has in addition prevented the complication of the species

displaced from the surface interacting with the surface for a second time.

What emerges from the vacuum desorption and replacement studies is a picture of three-fold heterogeneity of the surface species produced by the interaction of ethylene with palladium. The picture of two phases desorbing, each with first order kinetics, from the palladium surface is strikingly similar to that found by Crowell and Matthews [66] for the desorption of carbon monoxide from molybdenum, although they can distinguish five phases of desorption. What we can also say is that the use of the molecular beam method has allowed us to confirm that the two phases evidenced in vacuum desorption are also evidenced in replacement by acetylene and ethylene and that first order kinetics are displayed in the β phase displacement.

We can also say that in the displacement by beams of acetylene, increasing the surface temperature produces a marked increase in the rate of replacement whilst increasing the beam temperature produces no such increase. The inference that we may draw from this is that the acetylene must be adsorbed in some way on to the palladium film before it can replace the surface species already there. This last observation is one which could never have been obtained in a conventional system. It is also believed that first order kinetics would not have been observed in a conventional displacement experiment where a given amount of gas causing the displacement is introduced to a species adsorbed on a metal film. The pressure of the displacing gas is bound to change through interaction with the film and any material desorbed could produce displacement in its own right. Diffusion through the gas phase to and from the surface will similarly obscure any kinetic treatment of the system.

From this kinetic angle it must be admitted that the

radiochemical method is not the most suitable if one wishes to follow in great detail the type and rate of process which we have been observing. No one count can represent the true state of the system at any one time due to the statistical fluctuations in the decay of any radioactive isotope. An interrogatory method, which could provide an accurate measure of the desired parameter of a chemical system and with which measurements could be made at frequent intervals, would have served our purpose better. No such method is however available. Nevertheless we have obtained a picture of the processes occurring which gives us approximate values of the rates of desorption and displacement, of the activation energies for these processes and a fairly precise measure of the amounts of each of the three phases α, β and retained which we find.

The retained phase which is observed can be compared with the retention of hydrocarbons resulting from ethylene adsorption on metals found by Beeck [67], Stephens [64], Trapnell [68], Cormack, Thomson and Webb [54], and others. This product cannot be removed from the surface in our desorption and displacement experiments, in complete accord with the retained species seen by these other studies.

It would be wrong not to speculate on what the three species which we observe are. In this we are hampered by not knowing the identity of the surface species in our system, nor being able to draw directly on the work of other people for this information. No such desorption of these species in vacuo has been observed in the past and thus the information we seek does not exist. What we can do is combine the information we have obtained using the combination of the molecular beam method and radiochemical labelling with what other workers have found in other ways for similar and related systems. The resulting model of the surface

we construct is thus a tentative one in that sufficient evidence is available to allow us to speculate as to the nature of the chemical system and its interactions but not enough to allow us to be sure of our conclusions. Following this we shall discuss further the displacement reactions seen in this work and then link the picture of heterogeneity obtained with the picture of surface heterogeneity as a whole.

(2) The Nature of the Surface Species

When ethylene is admitted to the clean surface of many metals, including palladium, ethane is produced, with the simultaneous formation on the metal surface of adsorbed, dehydrogenated hydrocarbon, commonly referred to as an "acetylenic complex". This process is known as self-hydrogenation. The only study of the self-hydrogenation of ethylene on palladium films was carried out by Stephens [64]. In his studies, performed at 0°C and -78°C, he finds an average composition of the residual species of C_2H_2, resulting from a reaction with the stoichiometry:

$$2C_2H_4\ (gas) \longrightarrow C_2H_2\ (adsorbed) + C_2H_6\ (gas)\ ;$$

which proceeds until the available surface is completely covered by the residual species. A similar picture of ethylene reaction on nickel has been presented by Beeck [67], Jenkins and Rideal [69], McKee [70] and Hirota and Teratani [71,72] and for other metals by Beeck [67], Trapnell [68] and others.

The method which we use to pre-adsorb a species on the surface of our palladium (by admitting ethylene to a pressure of 10^{-1} torr for four minutes) together with the mass spectrometric analysis of the gas withdrawn from the surface (showing ethane and C_4 hydrocarbons) leads us to believe that some, perhaps a considerable amount, of self-hydrogenation has occurred on the palladium surface. Thus the surface species we are studying may well be the "acetylenic complex" produced by self-hydrogenation.

In most reactions studied by others part of the surface species cannot be removed by reaction. Stephens, for example, finds that 20% of the acetylenic complex remains on the surface after prolonged reaction with hydrogen. This would accord with the values which we observe in two experiments where we attempted to prepare films by faster than usual evaporation and thus more cleanly.

Stephens' work was carried out in u.h.v. conditions, whose threshold we approach, and his films can therefore be considered as being clean. Cormack, Thomson and Webb [54] find that the amount of retained species on palladium supported catalysts is 60% when their pre-adsorbed ethylene residues are involved in exchange and hydrogenation reactions. This value would correspond to the majority of our cases in which normal evaporation of palladium was carried out - in what we believe are less clean conditions. Cormack et al. also report that the retention figure is almost 100% when oxygen is admitted to the catalyst before ethylene admission. This corresponds to the cases of contamination of our surface, before forming an adsorbed species, which we observe - where the retention is about 95%. This high retention corresponds to poisoning of those sites for ethylene adsorption which are active in the exchange experiments carried out. Stephens postulates that the retained species is polymerised and possibly a surface carbide.

The other picture invariably produced by self-hydrogenation studies is the fast adsorption of the initial aliquots admitted to the surface under study. Stephens reported an initial coverage of 70%, with very little residual gas pressure. Each molecule of ethylene admitted up to this coverage was adsorbed and from the immediate production of ethane in the gas phase after 70% coverage has been attained this adsorption was presumed to be dissociative:

$$C_2H_4\ (gas) \longrightarrow C_2H_2\ (adsorbed) + 2H\ (adsorbed);$$

ethylene adsorbed above 70% coverage was hydrogenated by the adsorbed hydrogen. Self-hydrogenation ceases when all hydrogen produced by dissociative adsorption has been removed from the surface. Presumably ethylene can still adsorb on to the surface but cannot either dissociate or be hydrogenated to ethane. From Stephens' data only part of the dissociatively adsorbed species forms the retained species.

These findings for palladium are closely paralleled by the other work already mentioned on nickel and tungsten. For the self-hydrogenation of ethylene on nickel Hirota and Teratani[71] have advanced a theory to explain the effects of partial poisoning by carbon dioxide and acetylene. They postulate two separate regions on the nickel surface: the S region on which ethylene dissociates to acetylenic complexes and adsorbed hydrogen; and the W region where associatively adsorbed ethylene is hydrogenated using the hydrogen produced on the S region which can migrate through the metal. In our case two phases of desorption and reaction can be distinctly seen, together with an inactive retained phase. The retained phase, which can occur even when the surface is contaminated by oxygen, we believe to be on a separate set of sites from our α and β phases which are not observed when the surface is thus poisoned. The α and β phases may occur on different sites, but we have no evidence to suggest that this is so. Both, or neither, have always been seen on any one surface. We must assume therefore that the α and β phases occupy the same type of surface site.

Working essentially from the above information and assuming that the ethylene in our system has undergone partial, if not complete, self-hydrogenation, we have constructed the following model of the surface species and reaction. To this model we shall fit the results of our beam displacement reactions and then compare our ideas with the evidence found by other workers in the catalytic field.

The retained phase is a carbide species which results from the dissociative adsorption of ethylene on a particular set of sites, akin to the S region postulated by Hirota and Teratani. This carbide is unreactive at the temperatures at which our studies were carried out although it may be removed from the surface at

high temperatures by hydrogen, as surface carbides on other metals can be removed [73]. During the carbiding process, hydrogen is released, which can migrate across the palladium to sites where it is employed in hydrogenation.

To maintain an average surface species composition of about C_2H_2 we must assume that the β phase species, which can comprise up to 50% of the total surface species, is essentially C_2H_2. Thus:

$$C_2H_4 \text{ (gas)} \longrightarrow C_2H_2 \text{ (adsorbed)} + 2H \text{ (adsorbed)}.$$

In the later stages of β phase adsorption (corresponding to a point at about 70% surface coverage) some ethylene molecules can adsorb on to the surface only in the associated form, neighbouring sites being filled. Though it cannot dissociate, it can react with adsorbed hydrogen to form ethane and desorb to the gas phase. Thus:

$$C_2H_4 \text{ (gas)} \longrightarrow C_2H_4 \text{ (adsorbed)} \xrightarrow{+H} C_2H_5 \text{ (adsorbed)}$$

$$\downarrow +H$$

$$C_2H_6 \text{ (gas)}$$

The vacant sites left by hydrogen and ethylene thus combining enable further ethylene molecules to adsorb. These may either dissociate or by hydrogenated in turn. Eventually, when essentially all the hydrogen has been removed from the surface, no further reaction of ethylene, already adsorbed in the associated form can occur. This associatively adsorbed ethylene would then constitute our α phase.

We thus have a surface covered by the phase species:

α : C_2H_4 (adsorbed);

β : C_2H_2 (adsorbed);

retained : carbide;

with the α and β phases occupying one set of sites and the retained phase a separate set of sites. The over-all surface species (for the limiting case of 25% α, 50% β and 25% retained phases) is thus C_2H_2, and the over-all reaction that has occurred is:

$$2C_2H_4\ (gas) \longrightarrow C_2H_2\ (adsorbed) + C_2H_6\ (gas).$$

The α phase species could then desorb from the surface in two ways - as ethylene itself or as ethane. To desorb as ethane would require the interaction of surface ethylene with surface hydrogen and it is to be doubted whether this process would follow first order kinetics - which α phase desorption does - though Stephens has observed a slow evolution of ethane from a palladium surface on which an incomplete self-hydrogenation has been carried out. The first order kinetics, together with the low activation energy of about 6 k cal/mole observed for this desorption lead us to believe that the process is the desorption of adsorbed associated ethylene to the gas phase:

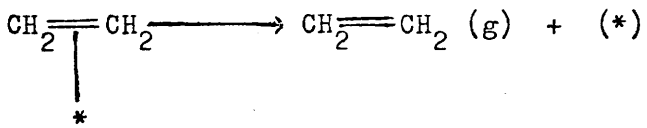

This single site adsorption, involving an ethylene to palladium π-bond would be in keeping with the relatively high α to β phase ratio at times observed, higher than is probably for two site adsorption if, as we have postulated, the ethylene results from the terminal adsorption on to sites from which reaction and desorption have taken place. In common with many others we shall signify associative adsorption of both ethylene and acetylene in this discussion by such π-bonded species. This species can be involved in other equilibria on the surface, e.g:

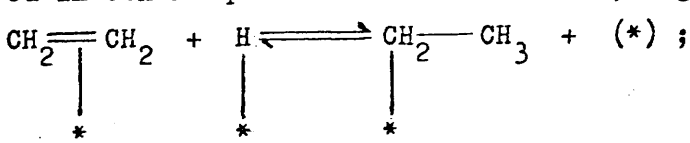

and:

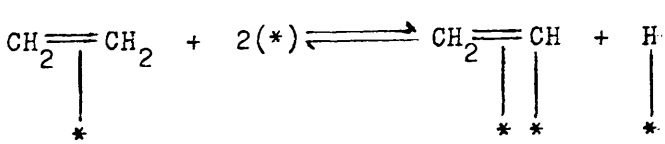

There is now the problem of defining the species being desorbed as the β phase. The high activation energy of adsorption of acetylene on to metal surfaces and the surety that the energy of desorption would be even higher makes it unlikely that the β species is, in fact, acetylene. No evidence has been found of the desorption of acetylene adsorbed on metal surfaces. Where exchange occurs between acetylene and acetylene-d_2 on nickel [74] this can be explained as exchange of hydrogen and deuterium between one species chemisorbed on the surface, the other physically adsorbed. There is almost certainly insufficient hydrogen in the system to allow us to postulate that the β phase species is removed as ethylene and certainly insufficient to allow us to postulate it as ethane. The prolonged outgassing of the palladium wire before film evaporation was carried out is felt to have removed any hydrogen which may have been dissolved in the wire.

Bond and Wells [75] have observed, in the hydrogenation of acetylene over supported palladium the presence of butenes, 1:3-butadienes and trace amounts of hexenes in their gaseous reaction products. These could only have been formed on the surface and the total amounts of polymer formed are large: for reactions at 16°C, polymer formation accounts for some 37% of the acetylene consumed in the reaction. A similar result, again for the hydrogenation of acetylene on palladium, has been reported by Kabe and Yasumori [76]. These observations, found in the presence of hydrogen would suggest that polymeric, unsaturated hydrocarbons could well be formed in our system and that these can desorb as such. These materials could be formed by the following processes, originally postulated by Sheridan [77]:

firstly formation of a vinyl radical (A):

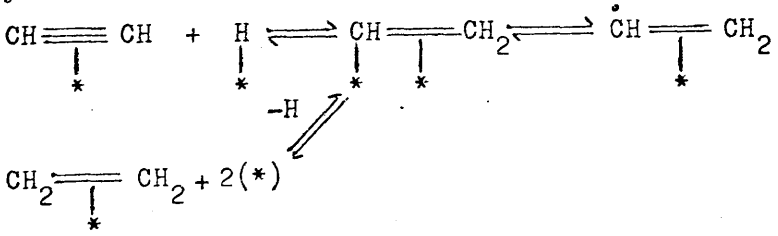

(A)

this radical can then polymerise by the following route:

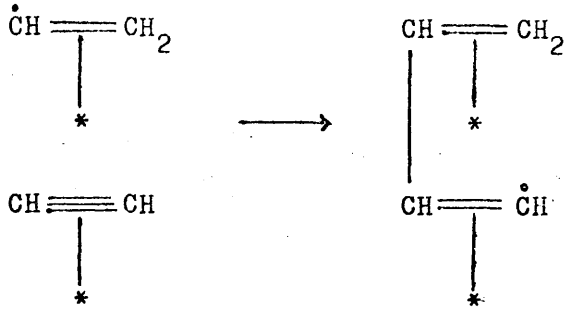

with chain termination as:

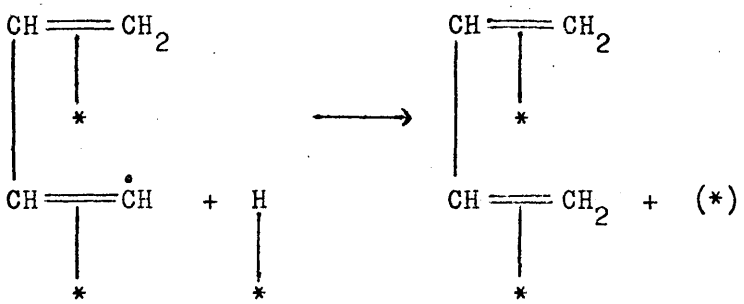

A second intermediate polymerisation step could result in hexatriene, which can be postulated to be in the adsorbed state as:

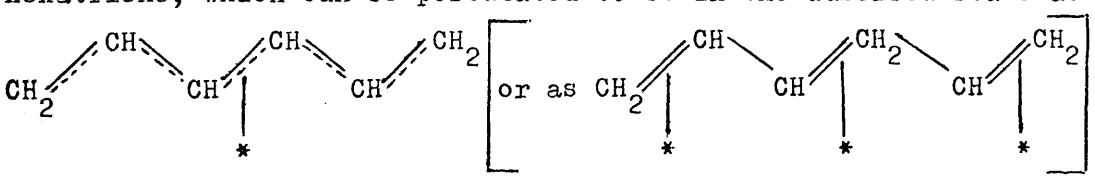

with a single π bond from the conjugated triene to the surface.

Yet another possible surface species would be vinylacetylene ($CH_2 = CH - C \equiv CH$) or even benzene which could be formed by:

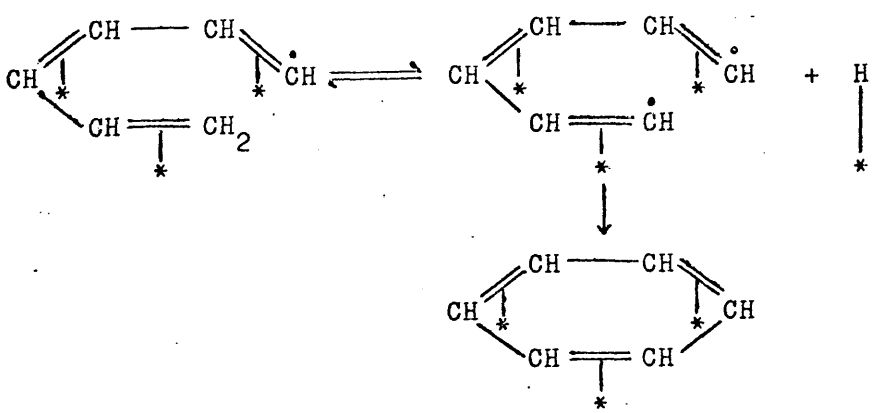

which can be represented as:

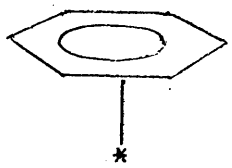

From Bond and Wells' study of acetylene hydrogenation on palladium we think it not at all unlikely that, in the absence of hydrogen, hexatriene could be the species seen as our β phase desorption, although this is merely a choice from among several possibilities. We may thus postulate our three phases as:

α : $CH_2=CH_2$ (*)

β : $CH_2-CH-CH-CH-CH-CH_2$ (*)

retained : surface carbide.

The selection of hexatriene as the β species does not imply that certain amounts of other C_4 or C_6 polymers are not present in this phase. The amounts of minor polymers may be small compared to the major component and these lesser amounts might not affect the kinetics of β phase desorption. The first order kinetics displayed in this phase do suggest that there is one major component and that no change in composition of the β phase takes place with time during vacuum desorption. If a change did take place the rate of removal of the new product would almost certainly differ from that of the initial product and no such change in rate was detected.

An alternative explanation of the two phases α and β, which should be mentioned, is that they may be two polymers, with the α phase, let us say, not ethylene but butadiene, and the β phase

hexatriene or benzene, or vice versa. Such an explanation cannot be discounted, though we consider the above scheme to be more likely.

One result in particular is of interest when discussing the surface species present. The percentage of each phase in the experiment studying the displacement of surface species by a beam of acetylene of half intensity at a surface temperature of 25°C was: α, 52.7%; β, 10.3%; retained, 37.0%. The five to one ratio of α and β phases is far in excess of that found in any other experiment. The cause of it must thus have been a unique occurrence. If the sites responsible for α and β phase adsorption are indeed different then selective poisoning of the β phase sites by a contaminant present in that case alone could have occurred. Alternatively, it may have been that the film was thrown in such a way that relatively more α than β sites were formed. Another explanation could be that, if the α and β phases are both polymeric in nature, one polymer was formed preferentially. If the underlying reason for this abnormally high α:β population ratio were known our understanding of the system might be greater.

We shall now discuss the displacement reactions carried out in relation to this scheme.

(3) Displacement of Surface Species by Beams of Acetylene

In the case of the α phase displacement this was observed to be rapid, though no definite assignment of first order kinetics can be made. It can be formulated as:

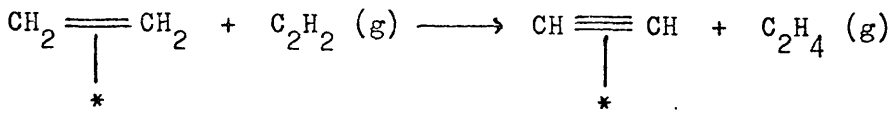

The β phase displacement is observed to display first order kinetics with respect to the surface concentration of the β phase. The rate of displacement is also observed to be proportional to the concentration of gas phase acetylene (i.e. the beam flux). The rate would be given by:

$$r = k\,[C_2H_2\ (g)\ ][\beta(ads)]\ .$$

Since the concentration of gas phase (beam) acetylene is constant this reduces to:

$$r = k_1\,[\beta\,(ads)]$$

where $k_1 = k\,[C_2H_2\ (g)]$.

The over-all rate would thus be first order. The order with respect to acetylene need not be unity. If $[C_2H_2]$ is constant then $[C_2H_2]^n$ is also constant and n may be fractional or greater than unity.

Increasing the beam temperature does not produce the same marked effect as increasing the surface temperature which increases the rate of displacement markedly, suggesting that acetylene does not displace the surface species directly from the gas phase. It would seem likely that the initial step involved in any chemisorption process is the thermal accommodation of the incident gas molecule by the surface. This picture emerges from studies of the interaction of molecular beams of argon with surfaces [35,78]. The process can be interpreted as being essentially one of physical adsorption and that the molecule, once thermally accommodated, can

either react chemically with the surface or be desorbed with a velocity distribution different from that of the incident gas beam and controlled by the temperature of the surface. The displacement reaction of ethylene can then be expressed as:

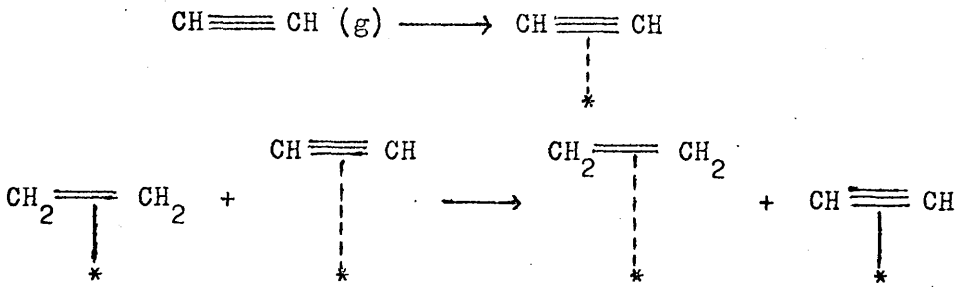

and the ethylene formed in the "physically adsorbed" state could then undergo desorption. A similar mechanism could be used to explain the β phase displacement. The immediate halt in the displacement process which was observed when a beam of acetylene, which was displacing the β phase from the surface, was stopped, can be ascribed to the short residence time (possibly of the order of milliseconds) characteristic of such a thermally accommodated molecule - as has been seen for other systems [35,78].

The case of the single experiment, mentioned in section 5 of chapter 5, in which only partial coverage of the surface was obtained, must be considered here. No displacement by an acetylene beam was recorded though subsequent vacuum desorption at 60°C was achieved. In this case we feel that at such a low coverage the dissociated ethylene was unable to polymerise to any great extent and existed mainly as adsorbed acetylene and hydrogen. This adsorbed acetylene cannot be displaced by a beam of acetylene. Increasing the temperature to 60°C could then have resulted in migration of the surface species to adjacent sites where formation of a polymer which could have been desorbed would have resulted.

(4) Displacement of Surface Species by Ethylene

The β phase is only displaced at a more rapid rate than is observed in vacuum desorption if a large proportion of non-retained species has already been desorbed from the surface, suggesting that the adsorption of ethylene on to sites where it can dissociate contributes to the removal. The view we have is that hydrogen from the dissociative adsorption of such ethylene is involved in hydrogenation of our surface species to another species, which may either be desorbed at a faster rate, or can be displaced by ethylene reacting from the gas phase or from a transitory "physically adsorbed" state. Thus:

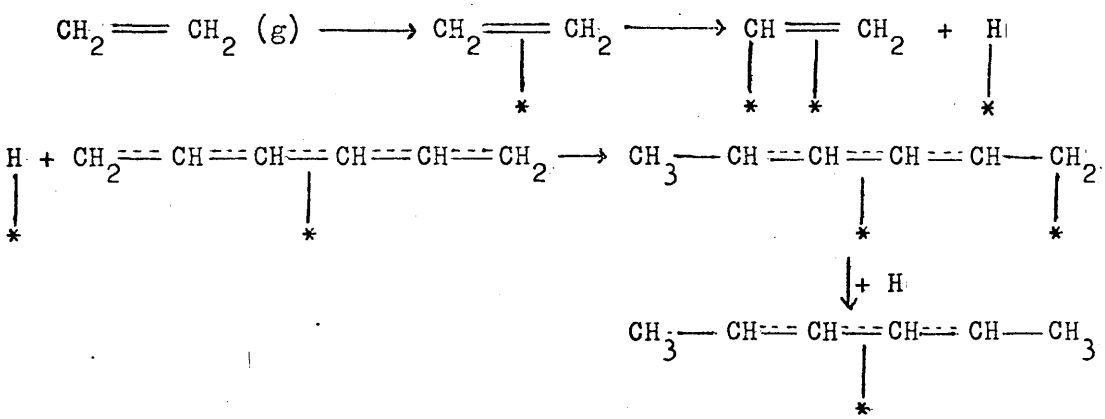

in a 1, 6 addition to form hexa-2:4-diene (or, if the surface species were buta-1:3-diene, conversion to butenes).

If ethylene, on the other hand, adsorbs on the few sites left vacant by desorption of a small amount of ethylene from the α phase, it will not dissociate to a sufficient extent to provide hydrogen which can change the β species to one which can be replaced by ethylene.

It may, on the other hand, release sufficient hydrogen to preferentially remove the remaining α species. At 25°C and at 40°C practically no α phase was desorbed from the surface before it

was exposed to an ethylene beam - and little or no displacement of the α phase was observed. At 60°C and 70°C, however, a large fraction of the α phase was desorbed before the beam was introduced. The remainder of the α phase was instantly displaced. At 60°C, in addition, sufficient hydrogen could have been released to remove the β phase. This mechanism could only apply if the α phase were polymeric in nature.

The alternative explanation of the α phase displacement, which would be in keeping with the postulate of the α phase being associatively adsorbed ethylene, is that the activation energy for displacement of the α species is large, say, 40-50 k cal/mole. A 20 Centigrade degree change in temperature would thus increase the rate of displacement markedly - in keeping with our results of no displacement at 40°C and 25°C but clearly visible displacement at 60°C and 70°C.

We now turn to a comparison with work carried out by others.

(5) Examination of the Surface Species in Regard to Other Works

Stephens [64], in the only direct examination of the self-hydrogenation of ethylene on palladium films, using mass spectrometry, finds results which are mostly in agreement with our own. Hydrogenation of the residual species, for example, results in an initial rapid removal of the surface complex, followed by a slow removal, with 20% being retained on the surface. The rapid removal would correspond to our α phase, the slow removal to the β phase. The products of hydrogenation are, however, mostly ethane - while we find it impossible to imagine the presence of C_2 hydrocarbon units in our system in the β phase.

The products of hydrogenation of the residual surface species resulting from ethylene self-hydrogenation on nickel are variously reported as pure ethane [69] or 90 % polymeric saturated hydrocarbons and 10% ethane [67]. The polymeric hydrocarbons are C_4, C_6, C_8 and higher. In both cases 20% of the acetylenic complex is removed in about one hour. Depending on the amounts of α and β phase material present, if both phases are exhibited by nickel, both results seem feasible to use, for the removal of such a low percentage.

Little, Sheppard and Yates [73] have studied the infra-red adsorption spectra of acetylene and ethylene on silica supported palladium. They conclude that the spectrum of surface species resulting from the adsorption of ethylene on palladium displays large amounts of olefinic and small amounts of paraffinic groupings on the surface. Furthermore when the surface complex is hydrogenated a surface species with the structure

$$Pd \text{——} (CH_2)_3 \text{——} CH_3$$

results.

With acetylene only olefinic hydrogen stretching frequencies are observed and on hydrogenation the spectrum obtained corresponds to the structure

$$Pd\text{——}(CH_2)_5CH_3$$

These infra-red results seem to be much in accord with our own view of the surface species. The presence of $(CH_3—)$ groupings for ethylene adsorbed on palladium could be attributed to isolated ethylene molecules undergoing half-hydrogenation by:

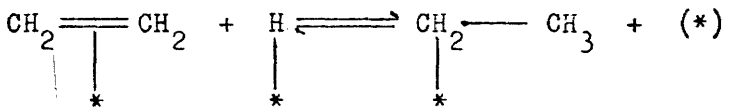

As their results were for palladium produced by reduction it is possible that small amounts of hydrogen may have been retained by the metal. These could assist in the above reaction and could also terminate the polymerisation of ethylenic species at C_4 hydrocarbons.

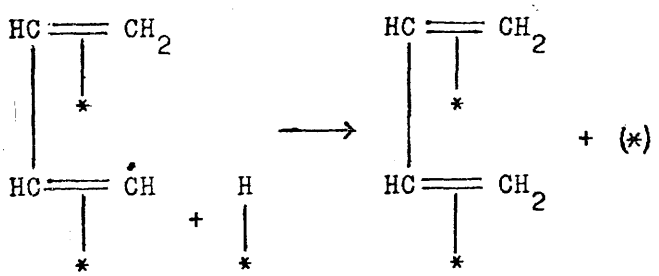

With acetylene the polymerisation could continue to produce C_6 hydrocarbons with any adsorbed hydrogen being used to form the initial vinyl radical needed to initiate the polymerisation.

Thus:

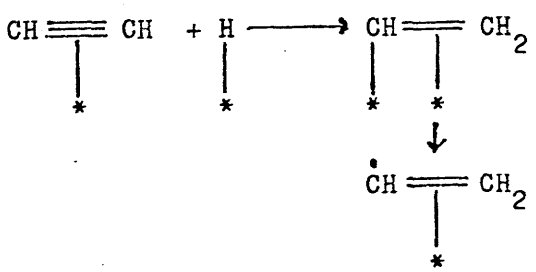

Eischens and Pliskin [79] observe an olefinic species adsorbed on bare nickel - in accord with our views for palladium-but do not speculate on the detailed structure of the adsorbed species. They comment that "the carbon-hydrogen ratio will depend on the severity of the dehydrogenation conditions" without defining these conditions precisely.

The direct view of the surface with infra-red spectroscopy would thus seem to be in agreement with the definitions of the surface species we have proposed.

The exchange of ethylene with ethylene d_4, although on other metals than palladium, produces results which are compatible with our own. Flanagan and Rabinovitch [80], for example, studying this exchange over nickel films at room temperature showed complete equilibration to occur in less than an hour - in keeping with the rapid displacement and presumably replacement of the α phase by a beam of ethylene. The mechanism would be by a hydrogen transfer:

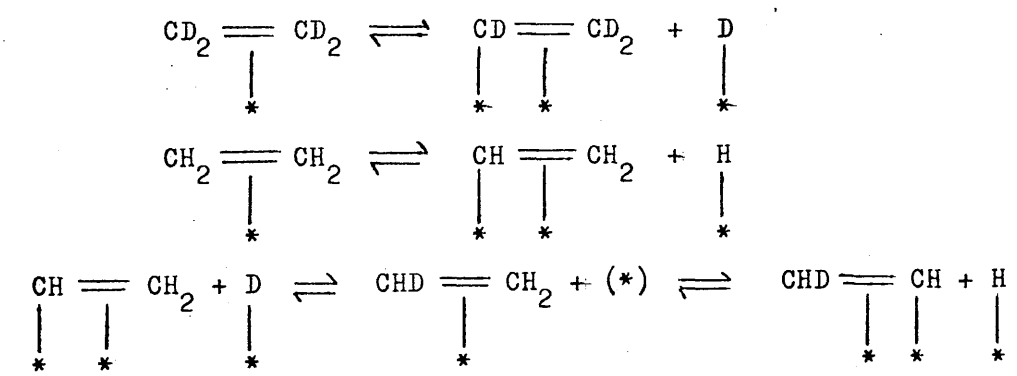

with the π-bonded ethylene or deutero-ethylene being replaced by the gas phase ethylene to appear in the gas phase. A similar mechanism would explain the isomerisation of trans ethylene-d_2, observed by Douglas and Rabinovitch [81].

The reaction of ethylene with deuterium over nickel wire [82] results in the production of both deutero-ethylenes and

deutero-ethanes. The partial pressure of ethylene-d_1, the main initial olefin product, passes through a maximum and the concentrations of the successively higher deutero-ethylenes increases slowly until they are consumed in the deuteration to ethanes. The formation of ethylene-d_1 as the main initial olefin product would be expected from the above reaction scheme - with its appearance in the gas phase caused by rapid displacement by gas phase ethylene. The chief initial products of ethane formation are ethane d_o and ethane d_1 - supporting the view of dissociative adsorption providing the bulk of the initial hydrogen to saturate the ethylene although this explanation is unnecessary in the case of these results. Similar high initial concentrations of ethane-d_o are found by Addy and Bond [83] for palladium on pumice at 50°C, though no ethane-d_o is recorded by Turkevich et al.[82] at -78°C with palladium on silica and palladium on charcoal - suggesting that little dissociative adsorption of ethylene occurs at this temperature. The production of the higher deutero-ethanes is believed to be brought about by the redistribution reaction among the deutero-ethylenes before they are deuterated to, for example, ethane-d_6.

(6) Surface Heterogeneity

As one of the most obvious features of the results obtained was the display of three-fold heterogeneity of a palladium surface in its interaction with ethylene, we feel we must place this feature in context by examining the place of surface heterogeneity in the field of catalysis. The question of surface heterogeneity has almost certainly been the prime cause of our lack of a clear understanding of even the simplest reactions.

For a surface to participate in a reaction one or more types of gas molecules must physically or chemically interact with it. Any one such substrate material can display a variety of surfaces, differing principally in their crystallographic orientation, towards the gas phase. It is to be expected that the different crystal faces will differ in the manner of their interaction with the gas phase.

The first postulates of surface heterogeneity by Constable[84] and Taylor [85] were made to explain changes in heats of chemisorption with coverage. On a heterogeneous surface the more active sites are covered first, and as coverage increases less active sites are filled, so that the heat of adsorption continually decreases. The early work of Pease and Stewart [86], who found that a 1% coverage of copper powder by carbon monoxide reduced its activity by a factor of 9 for ethylene hydrogenation, lent support to these ideas. Beeck and his co-workers[67,87] have shown that nickel films with preferentially exposed (110) crystal surfaces display a five-fold greater activity for ethylene hydrogenation over randomly oriented films.

Nichols [88] showed that certain properties of crystal

surfaces, notably the work function, depend on the orientation of the crystal surface. This fact is the basis of the field emission and field ion microscopes. By this method preferential adsorption of gases on different crystal faces has been demonstrated by, among others, Muller [89], Becker [90] and Gomer [91] for such simple systems as hydrogen and nitrogen on tungsten and nickel. Recently Arthur and Hansen [92] demonstrated preferential adsorption of ethylene on iridium by this method.

Low energy electron diffraction work has shown the (111) face of nickel to be active in benzene hydrogenation but not the (110) face [93], whilst X-ray reflection has linked the dehydrogenation of cyclohexene to the (111) face of nickel [94]. Attempts have been made by Gwathmey and Cunningham [95] to demonstrate the difference in the rates of ethylene hydrogenation on different crystal faces of nickel. Rhodin [96] has used a micro-balance to demonstrate rates of adsorption varying with crystal face. In all of these cases the heterogeneity found has been tied to the crystallographic orientation of the metal surface under study. Other cases have been noted where no such correlation has been attempted.

Desorption studies by Ehrlich [97] and Redhead [98] of carbon monoxide from tungsten filaments have shown evidence of heterogeneity, with two main phases α and β. The β phase can be further subdivided in three sub-phases. The heterogeneity in desorption is presumed to arise from adsorption on different crystal planes. Ehrlich [99] has studied the flash desorption of nitrogen from tungsten. His results suggest the presence of three adsorbed phases, with one phase, the γ phase, displaying first order kinetics with respect to the surface concentration and that the relative population of the three phases varies with

surface conditions. Hickmott [100], using the same technique, suggested two binding states of hydrogen on tungsten surfaces to explain his results. The results found by Crowell and Matthews[66] for the desorption of carbon monoxide from molybdenum showed multiple heterogeneity of desorption from the surface. Each desorbing phase, like ours, follows first order kinetics and they find five such phases. The resolution of their method, the radiochemical labelling of carbon monoxide, is such that the results are demonstrably not in accord with a picture of continuously varying heat of desorption with coverage. Sharp breaks between each of the phases can be seen.

The differential isotope method of Roginskii and Keier[101] has produced conflicting results. The theory behind this is simple: the gas, adsorbed first on the most active sites, should desorb last. If isotopic labelling of the fractions of gas admitted to a surface is carried out then the first gas to desorb should be seen to be the last to adsorb - if the surface is heterogeneous. With deuterium labelled hydrogen on charcoal this was observed, as it was in the carbon monoxide/promoted iron system studied by Kummer and Emmett[102]. Schuit[103], however, observed a result suggesting homogeneity in hydrogen adsorption on nickel - silica catalysts. This result can be explained in terms of surface mobility of the adsorbed species since the desorption was carried out at high temperatures.

Heterogeneity of the adsorbed species has been shown by infra-red spectroscopy measurements. In addition to the work of Little, Sheppard and Yates[73] and Eischens[79], which have already been discussed, Yates and Lucchesi[104] find two forms of acetylene and methyl acetylene on alumina. Carbon monoxide has been shown[105] to be adsorbed in two forms, which are inter-connected by pressure changes.

Most of these observations of surface heterogeneity, as distinct from those mentioned earlier where direct observation of different crystal faces was possible, are inferred from data of a secondary nature. For example, in the infra-red spectroscopy of adsorbed hydrocarbons the metal to carbon bond cannot be observed. Deductions are made almost entirely from observation of the carbon to hydrogen bond frequencies which are not directly affected by the metal surface. The observations above come mainly from chemisorption studies. Studies of the effect of surface heterogeneity in actual catalytic systems are less common. Selwood [106] has followed the change in magnetic properties when ethylene is adsorbed on to nickel - silica catalysts and has found that 46% of the adsorbed hydrocarbon produced could not be removed by hydrogen. Tamaru [107] showed that the decomposition of formic acid on silver, copper and nickel catalysts was accompanied by adsorption on only 10% of the available surface, while Thomson and his co-workers [108] have shown that in the Rosenmund reaction and in the hydrogenation of vinylacetic and crotonic acids the active area of the catalyst was only a small percentage of the adsorbing area. Cranstoun and Thomson [56] have shown that only part of a pre-adsorbed layer of hydrogen on nickel films can be displaced by mercury while Thomson and Wishlade [55] found that only 40% of an evaporated nickel film was active for ethylene hydrogenation. The work of Cormack, Thomson and Webb [54], Hirota and Teratani [71], Beeck [67] and others has already been mentioned.

The postulate of surface heterogeneity which we have made is, as in most cases, an inferred postulate as against the type of data already mentioned which is derived from studies involving particular crystal faces. We presume that the carbide species results from adsorption on a different set of sites. Whether these sites are present due to the presence of physical surface

defects, such as grain boundaries, we cannot say. In this connection it should be noted that Shirasaki et al.[109] have linked the carbiding of ethylene on nickel to the metallographic structure of the clean nickel plate.

What we can say is that the desorption reactions do not come about by the adsorbed surface species migrating across the surface to one particular surface site from which desorption occurs. This situation, typified by the report by Hall and Rase[110] that the rate of dehydrogenation of ethanol on lithium fluoride is proportional to the number of dislocations in the surface, would have resulted in zero order kinetics of desorption since the rate would be proportional to the constant number of such active sites. Zero order kinetics are not observed in our systems.

(7) Conclusion

We feel that we have thus fulfilled the goal which we set ourselves at the outset. We have built a system which demonstrates the applicability of the molecular beam method to problems in surface chemistry. In particular it has demonstrated certain facets of the reaction of the surface residues resulting from the interaction of ethylene with palladium which would not have been observed in a static adsorption or reaction system. One can imagine the difficulties of interpretation presented by such a static system in the displacement of these pre-adsorbed species by acetylene. If ethylene is displaced, it could have again interacted with the surface - perhaps on different sites from which it could have perpetrated an entirely different displacement reaction. The separation of the α and β phases kinetically would have been most difficult if not impossible in such a system. The results produced, though lacking in refinement, have clearly revealed the extent of the surface which is active in catalytic reactions and the heterogeneity of the catalytically active fraction itself.

Chapter 7
Future Experiments

The problems raised by the work are many in number. They fall into two categories:

(a) those which can be looked at by the present apparatus or after modifications thereof, i.e. by the molecular beam method;

(b) those which need entirely different systems to explore their secrets.

The first problem is the refinement of the kinetics of the desorption of the α and β phases. The only solution, since we cannot use either a much larger film area or more active ethylene C-14, lies in improving the counting system used. Solid-state detectors are excellent in their vacuum characteristics, but room-temperature operation does not take best advantages of their high potential detection efficiency. A detector cooled to $-25^{\circ}C$ by a Peltier cooled copper rod, or placed inside a coil cooled by the circulation of a refrigerant such as acetone to even lower temperatures, would reduce noise background to very low levels. Such an arrangement would enable detectors of larger surface area, say 10 cm^2, to be used. At room temperature the noise characteristics of such a large crystal are poor, due to the difficulties of making large crystals of low conductance, free from impurities and evenly compensated for intrinsic defects. The combination of high surface area and low background - which enables relatively more of the C-14 β spectrum to be seen - should be capable of producing about 50,000 cpm in our system. The gain in resolution in such a system would be enormous.

The evaporator arrangements could also be changed. The amount of gas produced during the evaporation of the palladium wire

is inconsistent with the pressure rises seen by other workers. The gas is almost certainly being produced by the desorption of molecules, probably mostly water vapour, from the walls of the evaporator tube. This could be prevented by wrapping a mica core furnace - similar to that used to heat the beam source - round the evaporator tube and baking the evaporating unit in vacuo while the filament is being degassed. This would certainly result in less contamination of the films.

The vacuum arrangements in the source chamber could be improved by mating the diffusion pump to the gate valve by a simple adaptor flange thus eliminating the length of 3" diameter tubing at present used between target chamber and pump. If the target chamber pump were changed to, say, a trapped 6" diffusion pump, pump speeds in excess of 300 l/sec should be attained in the target chamber - with consequent lowering of the static residual pressure to about 1×10^{-9} torr. The ionisation gauge would then need to be placed in the target chamber - perhaps on an arm coming from the top of the present five-armed target chamber. More accurate readings of target chamber pressure would then result. A similar pump arrangement could be adopted in the source chamber.

The ultimate molecular beam system which would result is of course a fully bakeable u.h.v. system, with very high speed diffusion pumps, of, say, 30,000 l/sec speed, with a maximum beam intensity of about 10^{16} molecules/cm^2/sec. A variety of interrogatory methods could be employed simultaneously in such a system. The target surfaces could be single crystals, enabling low energy electron diffraction to look at the surface and a mass spectrometer could be used to examine desorbed or displaced material. A u.h.v. system would also enable condensation experiments to be carried out - the surface could be kept in a clean state for sufficiently long periods in such a system.

The range of experiments which could be tackled by the molecular beam method encompasses the whole of gas/solid catalysis. The method we have used is limited to the study of those substances which have radioactive isotopes. This need not always be the case. One could study the decomposition of hydrocarbons on metal foils, using a mass spectrometer to analyse the products, the effect of changing beam and target temperature and the effect, for example, of surface contamination on the system. Any system involving decomposition of vapours on metals could be similarly studied.

The "spot" nature of a beam could be used to study surface diffusion. Radioactive material deposited at one area of a film could migrate across the surface under observation by a position sensitive radiation detector - several varieties of which already exist. Dalins is attempting the study of the diffusion of caesium on tungsten by depositing caesium from a molecular beam on to one side of a field emission microscope tip. The molecular beam method is the only method by which one can place molecules on a certain area of a surface in vacuo - i.e. on clean surfaces.

We now turn to the catalytic problems revealed in the study. Foremost among these is the identification of the species leaving the surface. This would be difficult though not impossible in a molecular beam apparatus but should be a comparatively simple matter in a conventional apparatus. It would appear from the literature that this has not been attempted in the past. Again the theory that the initially adsorbed ethylene contributes the initial hydrogen for self-hydrogenation while it, itself, is polymerised and carbided could be tested by C-14 labelling the ethylene adsorbed before hydrogenation takes place, then allowing only unlabelled ethylene to adsorb on to the surface. Only or mainly unlabelled ethane should appear in the gas phase. Subsequent hydrogenation or exchange reactions should then remove

the polymerised residues rapidly leaving the carbided C-14 residue as the only radioactive surface species.

We have not been able to distinguish whether the α and β phases are adsorbed on similar sites. A selective poison to differentiate between such sites could be sought, though this aspect could more easily be studied by following the rate of desorption of ethylene C-14 from different crystal faces by examination of single crystals. It may even be possible to relate each of the three phases to a particular crystal face.

These are some of the experiments suggested by this work. We feel that it has already shown promise in that it has allowed us to see aspects of surface behaviour previously hidden.

Appendix 1

Performance of the Simtec Solid-State Detector

Fig. A.1 and A.2 show the variation in observed count with discriminator setting for carbon-14 and background. The carbon-14 was in the form of a sheet of methyl methacrylate C-14 obtained from the Radiochemical Centre, Amersham.

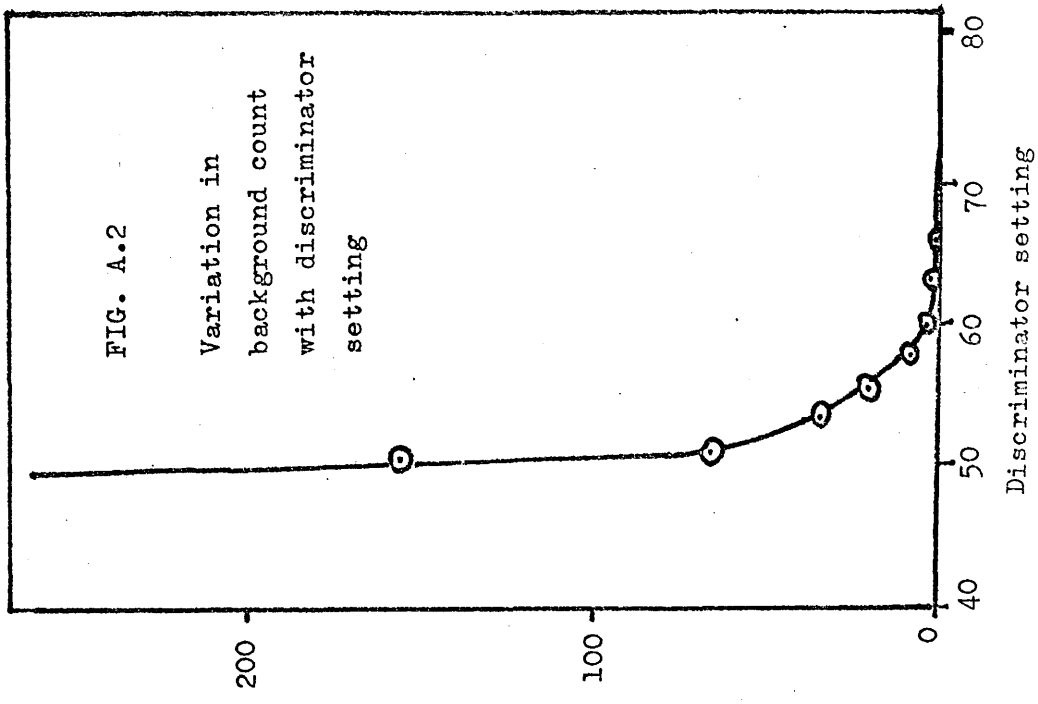
FIG. A.2
Variation in background count with discriminator setting
cpm
200
100
0
40
50
60
70
80
Discriminator setting

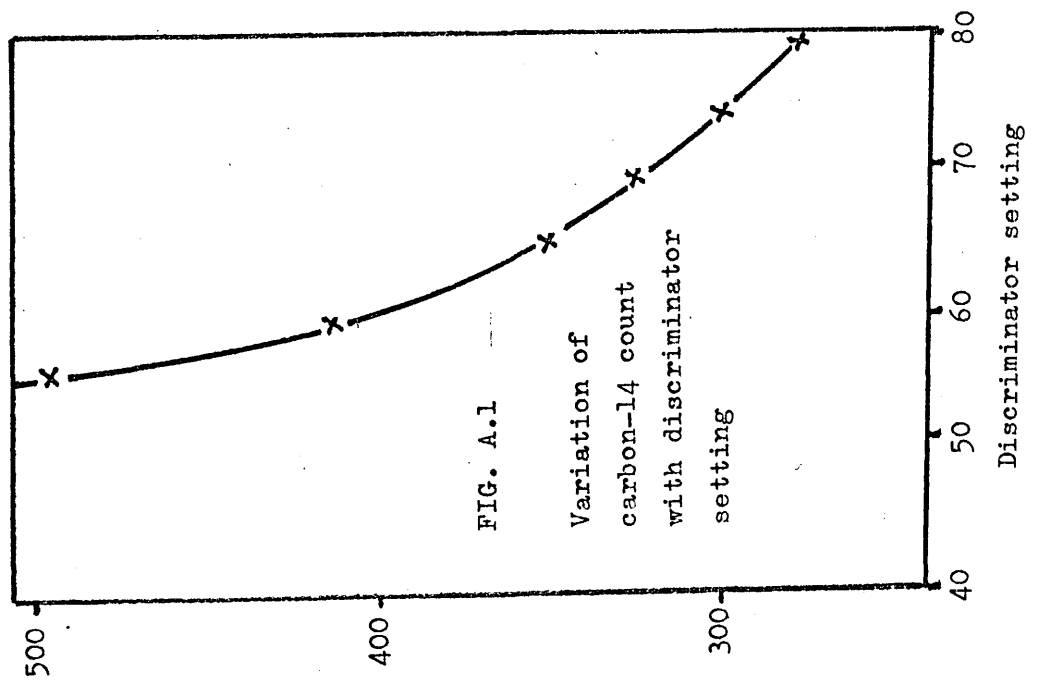
FIG. A.1
Variation of carbon-14 count with discriminator setting
cpm
500
400
300
40
50
60
70
80
Discriminator setting

Appendix 2

Performance of the Elliot Solid-State Detector

Fig. A.3 shows the variation in observed count with discriminator setting for background and carbon-14 detection.

Fig. A.4 and A.5 show the variation in observed count with applied voltage for carbon-14 and background respectively.

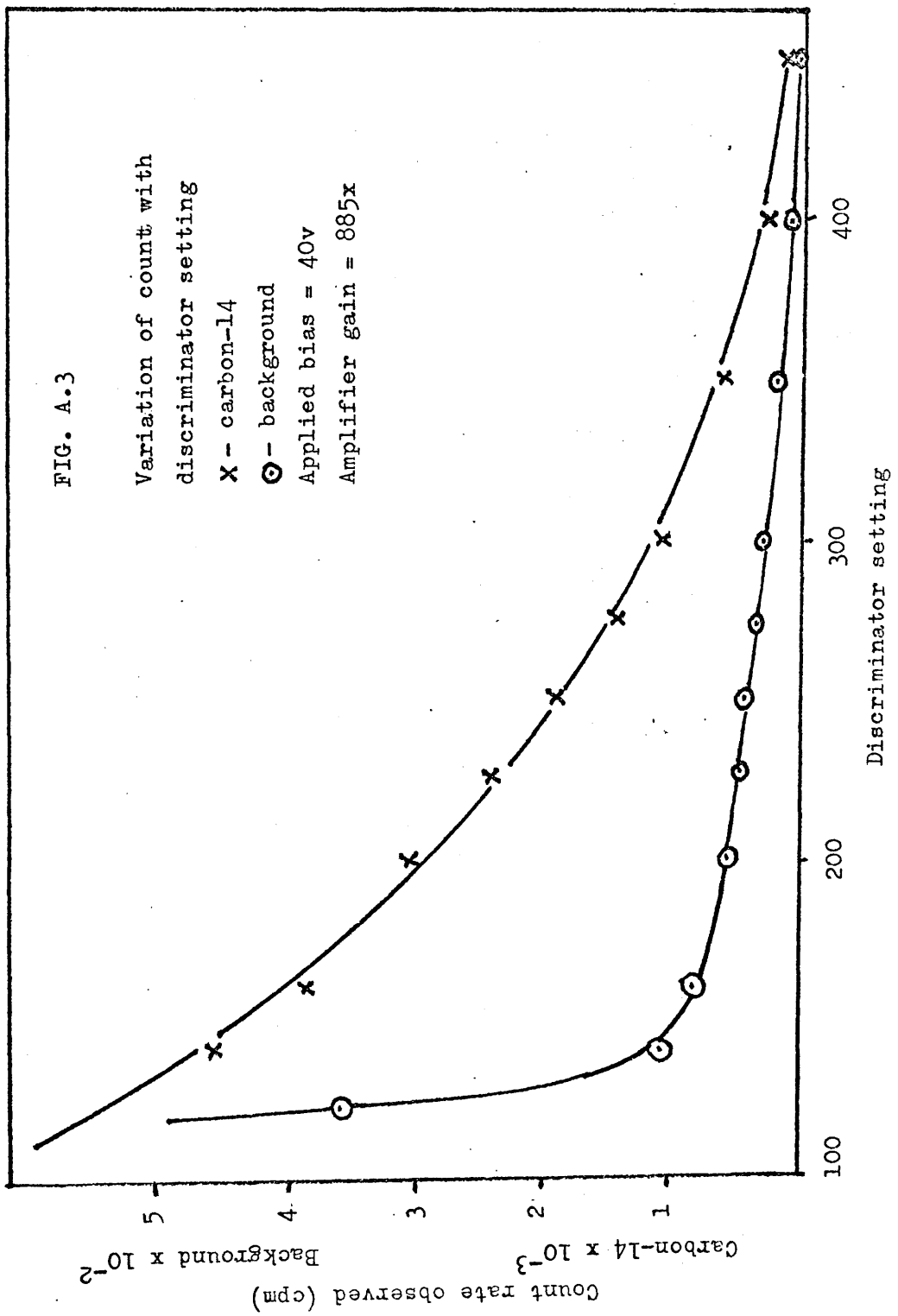
FIG. A.3
Variation of count with discriminator setting
X - carbon-14
⊙ - background
Applied bias = 40v
Amplifier gain = 885x
Count rate observed (cpm)
Carbon-14 x 10⁻³
Background x 10⁻²
1
2
3
4
5
100
200
300
400
Discriminator setting

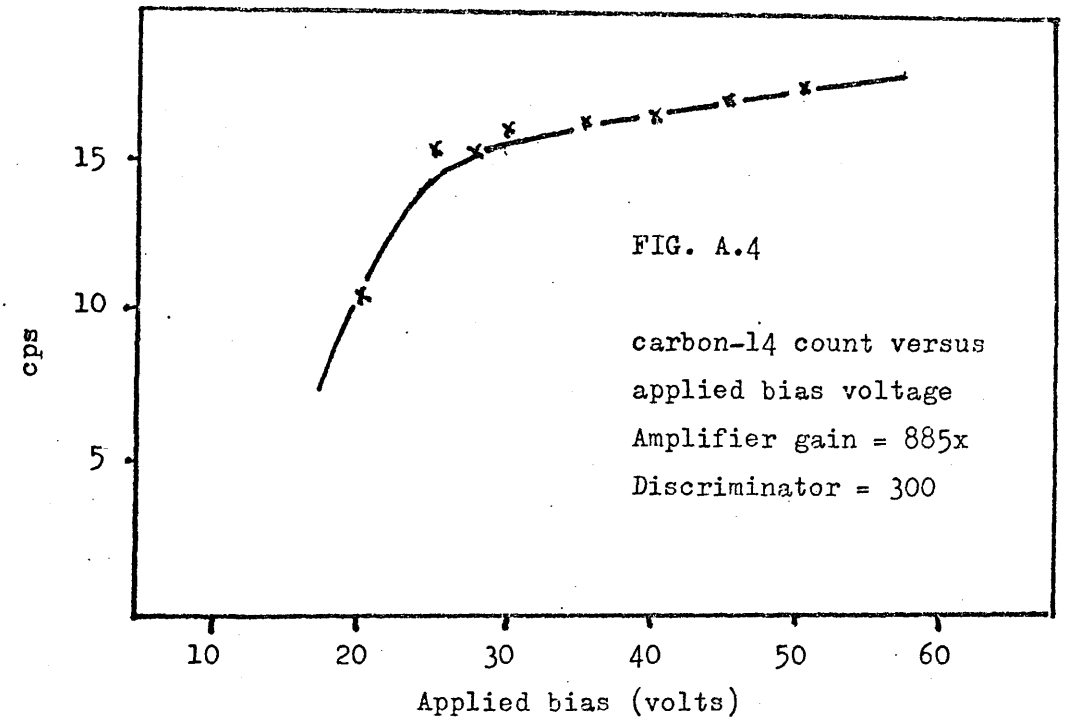

FIG. A.4

carbon-14 count versus
applied bias voltage
Amplifier gain = 885x
Discriminator = 300

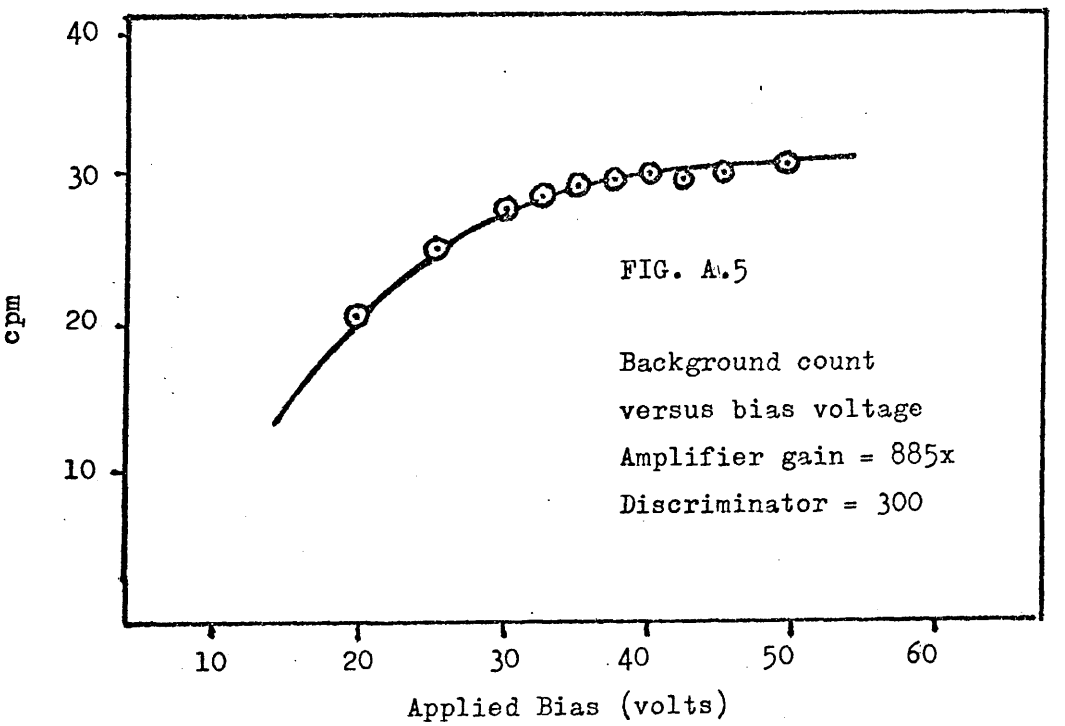

FIG. A.5

Background count
versus bias voltage
Amplifier gain = 885x
Discriminator = 300

Appendix 3

Straight Line Least Squares Programme Used
Language: K.D.F.9 Algol

```
DD122L600WPU+T0300481PST→
begin comment STRAIGHT LINE LEAST SQUARES;
real A,B,C,D,a0,b0,a,b,d,R,S,RE,Pm,Pb;
real array X[1:1000],Y[1:1000],F1[1:1000],G[1:1000],Y1[1:1000],
d1[1:1000];
integer i,r,P,n,F;
open(10);open(20);
F:=format([s+nddddd.dddddddcc]);
P:=read(20);for r:=1 step 1 until P do begin
write text(10,[Cycle*Number*]);write(10,format([sndcc]),r);
a0:=read(20);b0:=read(20);n:=read(20);
for i:=1 step 1 until n do begin
X[i]:=read(20);Y[i]:=read(20);
d:=Y[i]-X[i]xa0-b0;
F1[i]:=X[i]xd;
G[i]:=dend;
A:=0;B:=0;C:=0;D:=0;
for i:=1 step 1 until n do begin
A:=A+X[i]↑2;B:=B+X[i];C:=C+F1[i];D:=D+G[i]end;
a:=a0+(Cxn-BxD)/(nxA-B↑2);
b:=b0+D/n-Bx(Cxn-BxD)/(nx(nxA-B↑2));
write(10,F,a);write(10,F,b);
for i:=1 step 1 until n do begin
Y1[i]:=axX[i]+b;write(10,F,Y1[i]);
d1[i]:=Y[i]-Y1[i]end;
R:=0;for i:=1 step 1 until n do R:=R+d1[i]↑2;
S:=nxA-B↑2;
```

```
RE:=0.6745xsqrt(R/(n-2));
Pm:=RExsqrt(n/S);Pb:=RExsqrt(A/S);
write text(10,[PROBABLE*ERRORS*]);
write(10,F,Pm);write(10,F,Pb);
end;close(10);close(20)end→
```

References

1. Dunoyer: Comptes Rendus 152 594 (1911)
2. Gerlach and Stern: Z. Physik. 8 110 (1922)
   Z. Physik. 9 349, 353 (1922)
3. Stern: Z. Physik. 3 49, 417 (1920)
4. Yang, Simnad and Pound: Acta. Met. 2 470 (1954)
5. Goodman and Wexler: Phys. Rev. 99 192 (1955)
6. Bellamy and Smith: Phil. Mag. 44 33 (1953)
7. Taylor: Z. Physik. 57 242 (1929)
8. Kerschbaum: Ann. Physik. 2 201 (1929)
9. Simons and Glasser: J. Chem. Phys. 8 547 (1940)
10. Knauer and Stern: Z. Physik. 53 779 (1929)
11. Johnson: Phys. Rev. 31 1122 (1928)
12. Kerschbaum: Ann. Physik. 2 219 (1929)
13. Estermann and Stern: Z. Physik. 61 95 (1930)
14. Estermann, Frisch and Stern: Z. Physik. 73 348 (1931)
15. Crews: J. Chem. Phys. 37 2004 (1962)
16. Crews: Personal Communication
17. Smith: J. Chem. Phys. 40 2520 (1964)
18. Smith and Fite: J. Chem. Phys. 37 898 (1962)
19. Smith and Saltzburg: J. Chem. Phys. 40 3585 (1964)
20. Datz, Moore and Taylor: in "Rarefied Gas Dynamics" 1 347
    Academic Press, New York (1963)
21. Moore, Datz and Taylor: J. Catalysis 5 218 (1966)
22. McFee and Marcus: Proc. Atomic Mol. Beam Conf.,
    Univ. of Denver, June 1960.
23. Estermann: Z. Physik. 33 320 (1925)
24. Cockroft: Proc. Roy. Soc. (London) A.119 295 (1928)
25. Frauenfelder: Helv. Phys. Acta. 23 347 (1950)
26. Sears and Cahn: J. Chem. Phys. 33 494 (1960)
27. Rapp, Hirth and Pound: Can. J. Phys. 38 709 (1960)
28. Shade: J. Chem. Phys. 40 915 (1964)

29. Pound, Simnad and Yang: J. Chem. Phys. 22 1215 (1954)
30. Frenkel: Z. Physik. 26 1117 (1924)
31. Goodman: J. Phys. Chem. Solids 23 1269 (1962)
32. Wexler: Rev. Mod. Phys. 30 402 (1958)
33. Holst and Clausing: Physica 6 48 (1926)
34. Veszi: Z. Physik. Chem. B 11, 211 (1930)
35. Leonas: Heat and Mass Transfer (Rus) 3 540 (1963)
36. Dewing and Robertson: Proc. Roy. Soc. A 240 423 (1957)
37. Goeler and Peacock: J. Chem. Phys. 39 169 (1963)
38. Goeler and Luscher: J. Phys. Chem. Solids 24 1217 (1963)
39. Godwin and Luscher: Surface Science 3 42 (1965)
40. Scheer and Fine: J. Chem. Phys. 39 1752 (1963)
41. McKinley: J. Phys. Chem. 66 554 (1962)
42. Anderson and Boudart: J. Catalysis 3 216 (1964)
43. Madix and Boudart: J. Catalysis 7 240 (1967)
44. Hollister, Brackman and Fite: J. Chem. Phys. 34 1872 (1961)
45. Hollister, Brackman and Fite: Planet-Space Sci. 3 162 (1961)
46. Beeck: J. Chem. Phys. 4 680 (1936)
J. Chem. Phys. 5 268 (1937)
47. Dalins: Personal Communication
48. Ramsey: "Molecular Beams", Clarendon Press, London. (1956)
49. Leonas: Soviet Physics Uspekhi 7 121 (1964)
50. Bersey and Simpson: Chem. Rev. 30 234 (1942)
51. Fraser: "Molecular Beams", Methuen, London. (1937)
52. Ross, ed.: Molecular Beams, Adv. in Chem. Phys. 10 (1966)
53. Fite and Datz: Ann. Rev. Phys. Chem. 14 61 (1963)
54. Cormack, Thomson and Webb: J. Catalysis 5 224 (1966)
55. Thomson and Wishlade: Trans. Far. Soc. 58 1170 (1962)
56. Cranstoun and Thomson: Trans. Far. Soc. 59 2403 (1963)
57. Turnbull: "An Introduction to Vacuum Technique", Newnes, (1962)
58. Dushman: "Vacuum Technique", Chapman and Hall, (1949)
59. Dr. Hogg: Personal Communication

60. Hardy and McCarroll: J. Sci. Instr. 44 792 (1967)
61. G. F. Taylor: Personal Communication
62. Liang: J. Phys. Chem. 56 660 (1952)
63. D. Cormack: Ph.D. Thesis, University of Glasgow, (1964)
64. Stephens: J. Phys. Chem. 62 714 (1958)
65. Friedlander, Kennedy and Miller: "Nuclear Chemistry", Wiley, (1964).
66. Crowell and Matthews: Surface Science 7 79 (1967)
67. Beeck: Disc. Far. Soc. 8 118 (1950)
68. Trapnell: Trans. Far. Soc. 48 160 (1952)
69. Jenkins and Rideal: J. Chem. Soc. 2490, 2496 (1955)
70. McKee: J.A.C.S. 84 1109 (1962)
71. Hirota and Teratani: Z. Physik. Chem. 48 66 (1966)
72. Hirota and Teratani: Sci. Pap. Inst. Phys. Chem. (Tokyo) 57 206 (1963)
73. Little, Sheppard and Yates: Proc. Roy. Soc. A259 242 (1960)
74. Bond, Sheridan and Whiffen: Trans. Far. Soc. 48 715 (1952)
75. Bond and Wells: J. Catalysis 5 65 (1966)
76. Kabe and Yasumori: J. Chem. Soc. Japan 85 410 (1964)
77. Sheridan: J. Chem. Soc. 133, 301 (1945)
78. Hagena: App. Phys. Letters 9 385 (1966)
79. Eischens and Pliskin: Advances in Catalysis 10 1 (1958)
80. Flanagan and Rabinovitch: J. Phys. Chem. 60 724, 730 (1956)
81. Douglas and Rabinovitch: J.A.C.S. 74 2486 (1952)
82. Turkevich et al.: Disc. Far. Soc. 8 352 (1950)
83. Addy and Bond: Trans. Far. Soc. 53 377 (1957)
84. Constable: Proc. Roy. Soc. A108 355 (1925)
85. Taylor: Proc. Roy. Soc. A108 105 (1925)
86. Pease and Stewart: J.A.C.S. 47 1235 (1925)
87. Beeck: Adv. Catalysis 2 151 (1950)
88. Nichols: Phys. Rev. 57 297 (1940)
89. Muller: Ergeb. Exact. Naturw. 27 290 (1953)

90. Becker: Adv. Catalysis 7 135 (1955)
91. Gomer: Adv. Catalysis 7 93 (1955)
92. Arthur and Hansen: J. Chem. Phys. 36 2062 (1962)
93. Sachtler, Dorgelo and Van der Knapp: J. Chim. Phys. 51 491 (1954)
94. Rubinstein, Shuikin and Minachev: Doklady. Akad. Nauk., S.S.S.R., 67 287 (1948)
95. Gwathmey and Cunningham: Adv. Catalysis 10 57 (1958)
96. Rhodin: J.A.C.S. 72 5102 (1950)
97. Ehrlich: J. Chem. Phys. 34 39 (1961)
98. Redhead: Trans. Far. Soc. 57 641 (1961)
99. Ehrlich: J. Chem. Phys. 34 29 (1961)
100. Hickmott: J. Chem. Phys. 32 810 (1960)
101. Roginskii and Keier: Doklady. Akad. Nauk., S.S.S.R. 57 151 (1947)
102. Kummer and Emmett: J.A.C.S. 73 2886 (1951)
103. Schuit: Proc. Intern. Symp. React. Solids, Gothenburg, 1954
104. Yates and Lucchesi: J. Chem. Phys. 35 243 (1961)
105. O'Neill and Yates: J. Phys. Chem. 65 901 (1961)
106. Selwood: J.A.C.S. 83 2853 (1961)
107. Tamaru: Bull. Chem. Soc. Japan 31 666 (1958)
Trans. Far. Soc. 55 824, 1191 (1959)
108. Affrossman and Thomson: J. Chem. Soc. 2024 (1962)
Affrossman, Cormack and Thomson: J. Chem. Soc. 3217 (1962)
109. Shirasaki et al.: Kogyo Kagaku Zasshi 68 2300 (1965)
110. Hall and Rase: Nature 199 585 (1963)

is available to drive a scaler or ratemeter. The paralysis time is of the order of 50 μsec.

3. Results

Without the anti-coincidence unit, background counts varied from 20 to 6000 counts per min. When the anti-coincidence unit was connected the background measured over sixty hours did not rise above 20 counts per min. Ratemeter recordings before and after coincidence are shown in figure 2. The large increase in before-anti-coincidence counts is not accompanied by an increase in the after-anti-coincidence counts.

The authors thank Dr. S. J. Thomson for his encouragement and helpful suggestions during the investigation, and Mr. L. Crickmore for carrying out the constructional work.